Mathematical programming for the support of river water management: water allocation and reservoir location

Jaime Eduardo VEINTIMILLA REYES

Supervisors:
Prof. dr. ir. Jos Van Orshoven
Prof. dr. ir. Dirk Cattrysse
Prof. dr. ir. Felipe Cisneros (University of Cuenca)
Prof. dr. ir. Pablo Vanegas (University of Cuenca)

Members of the Examination Committee:
Prof. dr. ir. Herman Ramon (chair)
Prof. dr. ir. Guido Wyseure
Prof. dr. ir. Patrick Willems
Dr. ir. Annelies De Meyer (Vito)
Dr. ir. Stefaan Dondeyne (UGent)
Prof. dr. Kenneth Sörensen (UAntwerpen)

Dissertation presented in partial fulfilment of the requirements for the degree of Doctor of Bioscience Engineering (PHD)

February 2022

Doctoraatsproefschrift nr. 1424 aan de faculteit Bio-ingenieurswetenschappen van de KU Leuven

Acknowledgements

Pursuing and obtaining a PhD degree is not the work of only one person. In this section, I would like to express my gratitude to all the people and institutions that contributed to this research.

Thanks to the Secretaría de Educación Superior, Ciencia, Tecnología e Innovación (SENESCYT) of the Ecuadorian government, which granted me a scholarship in 2013. Thanks to the University of Cuenca for supporting this endeavor and to the University of Leuven (KU Leuven) for hosting me to pursue a PhD.

I want to take this opportunity to express my gratitude to the members of my Examination Committee for their valuable contribution to improve the quality of this dissertation.

Thanks Prof. Guido Wyseure for your time and efforts during our meetings to discuss the progress of my research. I really enjoyed your course “Hydrological Processes”, and all the anecdotes and memories you told us about my hometown.

Thanks Dr. Annelies De Meyer for helping me find my way in the Operations Research world and for your recommendation on how to tackle the optimization problem I addressed during my PhD.

Thanks Prof. Kenneth Sörensen for your time and for your feedback to improve the manuscript. Thanks Dr. Stefaan Dondeyne for your valuable recommendations to improve the chapter 5 of my PhD manuscript.

Thanks Prof. Patrick Willems. Your recommendations about the LP-model were very useful. I also thank you for your course “Systems Approach to Water Management”, which made water management systems understandable for a computer engineer.

Thanks Prof. Felipe Cisneros for all the support you gave me since I was working on my engineering thesis. You gave me the opportunity to involve myself in the research world by participating in several projects at PROMAS. I also want to express my gratitude for your help throughout my PhD studies and for providing the datasets of the Machángara river basin.

Thanks Prof. Pablo Vanegas for your guidance and support during the last 20 years, since I was a computer engineering student until the end of my PhD research project. I also thank you for your friendship and for encouraging me to pursue a PhD.

Thanks Prof. Dirk Cattrysse for all your support and the time you invested in our monthly meetings. When I had a problem with the optimization models, you always came up with an immediate solution.

Thanks Prof. Jos Van Orshoven for the help you have provided me with ever since we met in a summer course back in 2008. I am grateful that I have had the opportunity to work under your supervision; first, during a research project; later, during a summer course in 2014; and, finally, throughout this PhD research. I express my gratitude to you for your help and efforts

to guide me through this research even beyond the responsibilities and obligations of a PhD promoter.

I thank all my colleagues from the LandInforMan group, especially Sam, Stien, Ine, Bianca, Anicet, Michiel, Karen and Mulenga. A special acknowledgement to Ann Cuppens, whose MSc. thesis I had the opportunity to supervise, which in turn became the basis for the chapter 5 of my PhD manuscript. Special thanks to my colleagues at PROMAS: Diego Mora, Eduardo Tacuri, Marco Ramírez and Vicente Íñiguez, who contributed in many ways to this dissertation.

My gratitude to René Estrella, my friend since we were children. Thanks for all your support since secondary school until now that I am finishing my PhD. I also thank all the "Cuencanos" in Leuven who became a family to me: Paola and Andrés, Iván and Elina, Juan and Carolina, Paúl and Lorena, Edgardo and Mónica, Peter and Fernanda, Geovanny and Miriam, Hernán and Paty, Gaby and Pepe, Mary, Olga, Loli, Vladimiro and Armando.

Thanks Danielle Van der Weën and Frank. You made our stay in Belgium more pleasant from the moment we arrived. Thank you for all the trips to special parts of the city and the country. In general, thanks for sharing your time and kindness with my family.

Special thanks to my family: Jaime, Mimi, Marcelo, Chabe, Edgar, Fanny, Adri, Gus, Feli, Xime, Belén, Analiz, Anisabel, Daniel and David, which with their support and love helped me coping with the distance. I also thank my mother Martha, who always wanted me to succeed in the academic field.

Finally, I thank my wife Fernanda, who was always ready to join me in every endeavor, since I was an undergraduate student until now that I am finishing my PhD studies. I really appreciate your strength and love. Thanks to my children Sofía and Martín for your understanding and efforts to adapt to a new country, new friends and a new language. Finally, I thank Mateo, my youngest son, for bringing me new joy.

Table of contents

Summary

Surface and ground water availability is variable in space and time and the spatio-temporal pattern of this variability often does not match with the distributed use pattern of sectors and individual consumers. This mismatch can become controversial when overall water availability decreases, e.g., due to climate change, and competition for water increases. It is in this context that the so called WEF-nexus between water for human consumption and industrial use, water for Energy (hydropower) and water for Food (irrigated agriculture) (WEF) has gained increasing attention in research, business and policy spheres, especially in regions with more arid climate. An additional dimension of this nexus is the water required for sustainable functioning of ecosystems in general and wetlands in particular.

Allocation of scarce water has challenged water managers for decades. The construction and operation of reservoirs is the typical solution put forward. In this research we addressed the optimization of the allocation of water available in a river-with-reservoir system towards multiple users as a network flow optimization (NFO) problem. There are two classes of methods to tackle NFO problems: heuristic models and mathematical models. Heuristic models are able to provide a feasible solution within reasonable computation time whereas mathematical models are able to come up with the optimal solution but often requiring longer computation times. Since for strategic decisions computation times are less crucial, the latter, i.e. linear programming (LP) models and mixed integer linear programming (MILP) models were the subject of this research. LP and MILP models were formulated to optimize the flow and storage of water through Water Supply Networks (WSN) created from geographic information describing the river basin under study. A WSN encompasses a set of oriented lines connected in georeferenced nodes whereby the lines represent river segments and the nodes represent reservoirs, natural water bodies, inflow points and abstraction points. Whereas inflow and abstraction points are characterized by time series of incoming and required water volumes, the water volume available in river segments, reservoirs and other water bodies, each having predetermined capacities, is updated throughout the simulation period.

The LP- and MILP-models were first formulated and evaluated for hypothetical river basins characterized by artificial time series. In a next step two real world basins were considered: the Machángara River Basin, located in the Andes region of Ecuador and the Omo River Basin, located in Ethiopia, Kenya and South Sudan. Since for the latter the required time series of water discharge were not operationally available a semi-spatially distributed hydrological model (ARCSWAT) was used to generate the time series based on meteorological archives, digital elevation models and soil and landcover maps.

The resulting NFO-LP model is meant to optimize water allocation to the different demand nodes assuming that water takes one time step to flow from one node to the next one and that water losses, temporal delays in water availability and water lost during a flood are represented by fixed fractions. The objective function –to be minimized– expressed the sum of monetary penalties related to not meeting or to exceeding the demands, to not meeting the minimum amount of water required to be available in reservoirs and river segments and to the flooding of reservoirs and segments.

The LP model was the basis for an NFO-MILP to find the optimal location of reservoirs in the WSN. To this end, all nodes present in the WSN are considered to be candidate reservoirs of a predefined capacity. With the MILP model every candidate reservoir is evaluated individually and in combination with other reservoirs in terms of its contribution to the objective function, i.c. the minimization of the considered penalties. Four scenarios were considered: Adding additional reservoirs to the network with the pre-existing reservoirs whereby the reservoirs are either pre-filled or initially empty, and evaluating all nodes for the construction of a reservoir, including those where a reservoir is already present, again prefilled or initially empty.

The NFO-LP model was found to allow for a quick evaluation of a given water supply network (WSN). With the NFO-MILP it could be verified whether existing reservoirs are located at the most optimal location and whether their capacity is sufficient. Also, the potential location of new reservoirs can be screened. Herewith the huge building and maintenance costs of reservoirs dominate the penalty costs related to the (non-)adequate allocation of water.

Both the LP and MILP-models can be extended with additional constraints to enhance their real-world application potential. The huge spatio-temporal data requirements remain a hurdle though.

Samenvatting

De beschikbaarheid van oppervlakte- en grondwater is variabel in ruimte en tijd en deze beschikbaarheidspatronen komen in vele gevallen niet overeen met de noden van maatschappelijke sectoren en individuele consumenten. Dit gebrek aan overeenkomst wordt problematisch wanneer de waterbeschikbaarheid daalt, bv. t.g.v. veranderend klimaat, en/of de competitie voor het beschikbare water tussen de gebruikers toeneemt. Het is in deze context dat de interesse in het concept WEF-nexus is gegroeid in onderzoek, bij maatschappelijke actoren en in het beleid. 'WEF-nexus' verwijst naar de situatie waarbij onvoldoende water beschikbaar is om ten allen tijde de vraag naar water voor energieproductie enerzijds en voor voedselproductie anderzijds te voldoen, en is vooral van toepassing in regio's met meer aride klimaatcondities of met uitgesproken afwisseling van droge en natte seizoenen. In de nexus worden bovendien de vraag naar water door industrie, huishoudens en voor het duurzaam functioneren van ecosystemen meegenomen.

Het toewijzen van het schaarse beschikbare water doorheen ruimte en tijd aan diverse gebruikers is een uitdaging van formaat voor waterbeheerders. De typische ingenieurtechnische oplossing bestaat in het bouwen en beheren van reservoirs. In dit doctoraatsonderzoek behandelden we de toewijzing van water beschikbaar doorheen de tijd in een systeem van rivieren met reservoirs, aan concurrentiële gebruikers, als een optimalisatieprobleem van stroming in netwerken (NFO). De literatuur beschrijft twee groepen van methodes om dergelijk NFO-probleem aan te pakken. De eerste groep omvat de heuristische modellen terwijl de tweede gebaseerd is op wiskundige modellen. Heuristische modellen beogen het leveren van haalbare en aanvaardbare oplossingen binnen redelijke rekentijden. Wiskundige modellen kunnen optimale oplossingen leveren maar vergen dikwijls aanzienlijke rekentijden. Aangezien de rekentijd voor strategische beslissingen minder cruciaal is werd in dit onderzoek geopteerd voor de ontwikkeling van wiskundige modellen van het type 'Lineaire Programmering (LP)' en 'Gemengde Geheeltallige Lineaire Programmering (MILP)'.

LP en MILP-modellen werden geformuleerd om de stroming en opslag van water in open waterdistributienetwerken (WSN) te optimaliseren waarbij de WSN beschreven werden o.b.v. geografische informatie over het bestudeerde stroombekken. Een WSN is geconcipiëerd als een verzameling van vectoren geconnecteerd in knooppunten waarbij de vectoren riviersegmenten voorstellen en de knooppunten reservoirs, natuurlijke waterlichamen als meren en inlaatpunten en uitvoerpunten. De inlaat- en uitvoerpunten worden gekarakteriseerd door tijdseries van inkomend en gevraagde watervolumes. De volumes water aanwezig in de riviersegmenten, reservoirs en de andere waterlichamen, die elk vooraf vastgestelde opslagcapaciteiten hebben, worden geactualiseerd doorheen de modellering.

De LP- en MILP-modellen werden eerst geformuleerd, geparameteriseerd en geëvalueerd voor hypothetische stroombekkens gekarakteriseerd door artificiële tijdseries. Vervolgens werden echte bekken beschouwd: het Machangarabekken gelegen in de Andes regio in Ecuador en het grotere Omo-bekken gelegen op het grondgebied van Ethiopië, Kenya en Zuid-Soedan. Omdat voor beide bekkens tijdseries van inkomende watervolumes niet beschikbaar zijn werden deze gesimuleerd via het semi-ruimtelijke gedistribueerde neerslag-afvoermodel

ArcSWAT met tijdseries van geobserveerde meteorologische variabelen, een digitaal hoogtemodel en bodem- en landgebruik-geodatasets als input.

Het resulterende NFO-LP-model is bedoeld om de toewijzing van water aan de vraag-knooppunten te optimaliseren veronderstellend dat water van het ene naar het volgende knooppunt stroomt in één tijdstap en dat watervolumes die verloren gaan door evaporatie en infiltratie, overstroming van riviersegmenten en van reservoirs en door vertraging in de waterstroming, als vaste fracties beschreven kunnen worden. De –te minimaliseren- doelfunctie van het NFO-LP-model kwantificeert de som van de boetes die verband houden met het niet voldoen of overmatig voldoen aan de vraag van de vraagknooppunten, het niet voldoen van het minimum volume water dat geacht wordt in reservoirs en riviersegmenten aanwezig te zijn en met de volumes water die betrokken zijn bij overstromingen van segmenten en reservoirs.

Het LP-model werd vervolgens uitgebreid tot een NFO-MILP-model om de optimale locatie te vinden van reservoirs in de WSN. Hiertoe worden alle knooppunten aanwezig in de WSN beschouwd als kandidaat-reservoirs met een voorafbepaalde capaciteit. Met het MILP-model wordt elk kandidaat-reservoir geëvalueerd zowel apart als in combinatie met andere reservoirs wat betreft zijn bijdrage aan de doelfunctie, i.c. het minimaliseren van de som van de boetes. Vier scenario's werden bestudeerd: Het toevoegen van reservoirs, hetzij leeg hetzij gevuld, aan de WSN met de bestaande reservoirs en het evalueren van alle knooppunten in de WSN m.i.v. deze waar een reservoir reeds aanwezig is, opnieuw veronderstellend dat de reservoirs leeg of reeds gevuld zijn.

Met het NFO-LP-model kan een snelle evaluatie gemaakt worden van elke WSN terwijl het met het NFO-MILP-model mogelijk was te evalueren of bestaande reservoirs zich op de optimale locatie bevinden en of hun capaciteit voldoende groot is. Ook kunnen de potentiële locaties van nieuwe reservoirs gescreend worden. Hierbij domineren de zeer grote bouw- en onderhoudskosten de boetes die het gevolg zijn van de sub-adequate toewijzing van water. Zowel het LP- als het MILP-model kunnen uitgebreid worden met bijkomende beperkingen om hun gehalte aan realisme en toepassingsbereik te vergroten. De zeer grote spatio-temporele datavereisten blijven een obstakel voor toepassing.

List of abbreviations

ArcSWAT	ArcGiS - ArcView extension for SWAT
CFSR	Climate Forecast System Reanalysis
DSS	Decision Support Systems
GWD4S	Global Weather Dataset for SWAT
GA	Genetic Algorithms
HBV	Hydrologiska Byrans Vattenbalansavdelning model
HRU	Hydrological Response Units
ILP	Integer Linear Programming
LP	Linear Programming
MCFP	Minimum Cost Flow Problem
MILP	Mixed Integer Linear Programming
MINLP	Mixed Integer Non-linear Programming
NCEP	National Centers for Environmental Prediction
NFO-LP	Network Flow Optimization – Linear Programming model
NFO-MILP	Network Flow Optimization – Mixed Integer Linear Programming model
NFO-P	Network Flow Optimization Problem
NFP	Network Flow Programming model
NLP	Non-Linear Programming models
ORSTOM	Office de la Recherche Scientifique et Technique d'Outre-Mer
PSO	Particle Swarm Optimization
RMSD	Root Mean Square Deviation
SC	Supply Chain
SCO	Supply Chain Optimization
SDG	Sustainable Development Goals
SWAT	Soil and Water Assessment Tool
UNDP	United Nations Development Programme
WEF-nexus	Water, Energy and Food Nexus
WRM	Water Resources Management
WSN	Water Supply Network

List of tables

List of figures

Chapter 1
Context, objectives and outline of manuscript

1.1. WEF (Water Energy Food) – Nexus

According to the Cambridge dictionary (Cambridge Dictionary, 2019) the meaning of the word "Nexus" is "An important connection between the parts of a system or a group of things". The "nexus" between water, energy and food (WEF) has gained increasing attention in research, business and policy spheres (Leck et al., 2015). Water, energy and food are closely linked. A correct access to and effective management of these resources underpins development progress (FAO, 2014; Kurian, 2017; Pittock et al., 2013).

In recent years, profiling the interlinkages between availability of water, energy and food as a nexus has been strongly promoted on the global research agenda and has influenced the emerging development paradigm. At the core of nexus debates are natural resource scarcities and the recognition that water, energy, food and other resources are interlinked in a web of complex relations where resource use and availability are interdependent (Dupar & Oates, 2012; Hoff, 2011). Furthermore, as a result of those dependencies, decision makers from all sectors try to establish synergies and potential trade-offs between food, energy, water and environment at multiple spatial and temporal scales (Howells & Rogner, 2014).

The World Economic forum was the first organization that invested in research regarding the WEF-nexus and at the same time to make people aware of the implications of an inappropriate management as well as of the processes to tackle development challenges. At the 2008 World Economic Forum's annual meeting in Greece, water security was addressed together with energy, food and other sectors (Smajgl et al., 2016). There was certain criticism about the idea of establishing water as a main component, since it contradicts a cross-sectorial approach that should substitute the traditional sectorial approaches (Smajgl et al., 2016). Additionally, there are other external impacts (physical, social, chronic and acute) that can complicate the performance of the nexus system (C. Zhang et al., 2018). Among physical impacts we can mention climate change, which might affect the water, energy and food supply. Among social impacts we count the political aspect, which might affect resources management. External impacts can be related to the occurrence time (acute) where the nexus can be affected in a short period of time (natural hazards), whereas other external impacts (chronic) might take more time to be notorious (population growth) (C. Zhang et al., 2018). All these external impacts are shown in Figure 1.1 along two axes: physical-social and chronic-acute.

Accounting for the external impacts there is an opportunity to connect the nexus with broader development planning (Entholzner & Reeve, 2016). Additionally, the United Nations Development Programme (UNDP) considered the WEF-nexus as one of the main rationales to set the Sustainable Development Goals (SDGs), which incorporate the sustainable use of natural resources (Benson et al., 2015; Brouwer et al., 2018). The main WEF-nexus-related SDGs identified by (Brouwer et al., 2018) are the following:

- SDG-2: End hunger and promote sustainable food production systems as well as agricultural systems;
- SDG-6: Ensure access to clean water and sanitation for all;
- SDG-7: Everyone should have access to modern energy services that are reliable,

affordable and produced in a sustainable manner;

- SDG-13: Alleviate climate change and its impacts by taking urgent action.

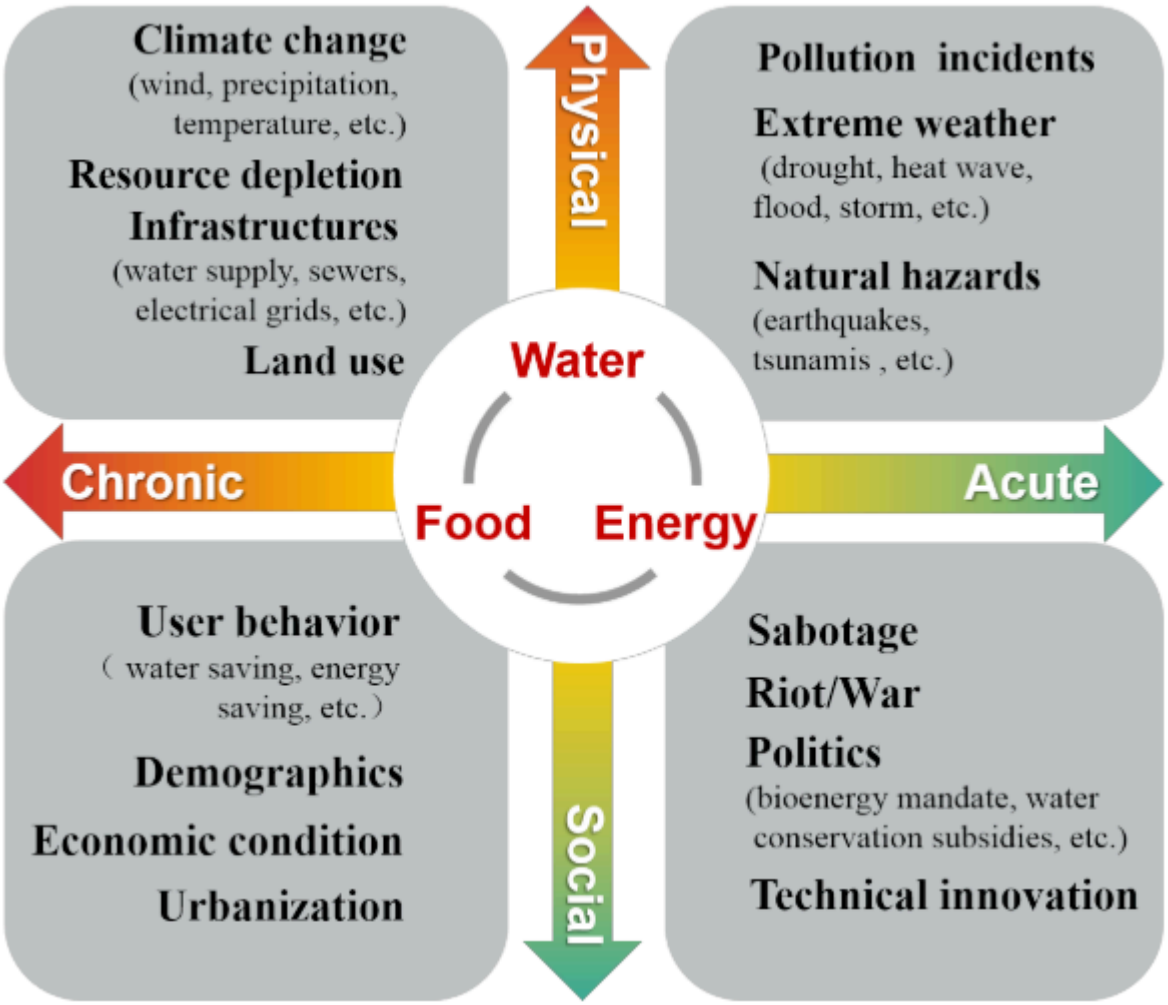

Figure 1.1. Classification of external factors that have an impact on the WEF nexus (C. Zhang et al., 2018)

The nexus approach takes into account multiple, often contradictory, dimensions of a problem. In this context, (Smajgl et al., 2016) established a dynamic nexus approach to identify the interactions between the components (water, energy and food) as well as the interaction between the components and the nexus core. There are three possible classes of policy interventions that can be envisaged: a) sector specific; b) intersectorial links and c) change of the nexus core drivers. The first one is the most typical and results into a high risk of unintended side effects and adverse sectorial trade-offs. In Figure 1.2, a diagram of the cross-sectorial connections is presented.

From Figure 1.2, we can infer that for a decision about whether or not to increase hydropower production, decision makers should not look only at fossil fuels and meeting energy demands; they must also include in the decision process the neighboring ecosystems, effects on water availability and possible effects that may increase food prices (Bird & Dodds, 2014; Smajgl et al., 2016).

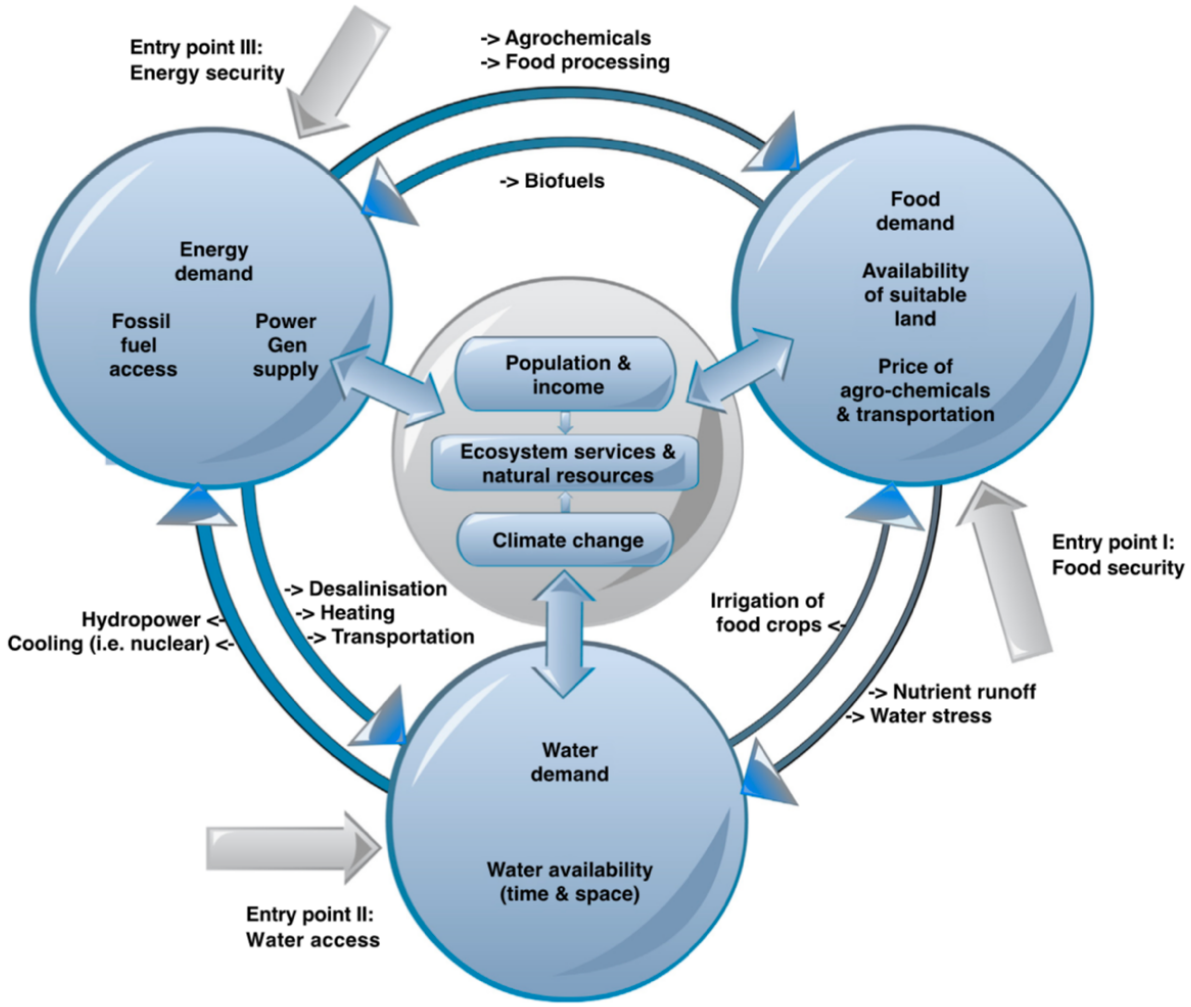

Figure 1.2. Water-energy-food nexus (WEF-nexus) (Smajgl et al., 2016)

Ringler et al., (2013), stated that not only water, energy and food are related. There is also a relationship with land. Therefore, in their research, they stablished the term WELF (Water, Energy, Land and Food) to identify the relationship among the actors. For instance, higher food prices are a signal of the natural resources scarcities; if the oil and food prices change this could affect land prices. It is clear the relationship between: water and energy; water and food; energy and food. However, the land-energy-food relationship is present when people used wood as their primary fuel to cook food.

Besides, Ringler et al., (2013), created a nexus framework (Figure 1.3). This chart includes all possible relationships among the actors as well as direct and indirect drivers of change

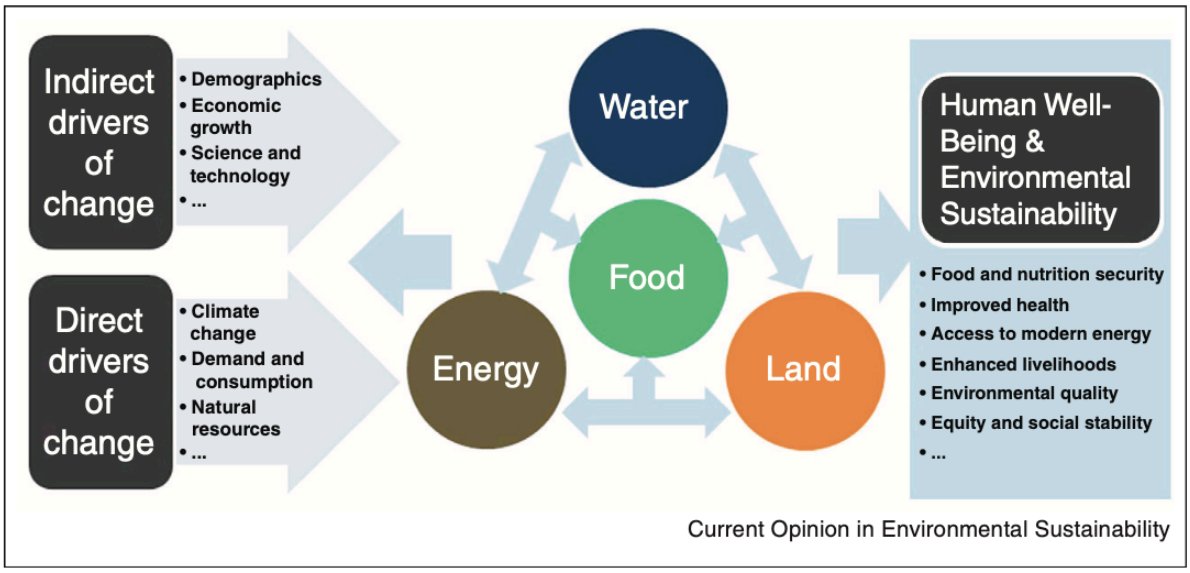

Figure 1.3. Extended water, land, energy and food nexus framework (Ringler et al., 2013)

1.2. Problem Statement and general objectives

Several regions and countries across the globe face a difficult challenge in meeting the growing demands for food, water, and energy (Smajgl et al., 2016). This challenge is additionally complicated due to climate change. Effective adaptation to this change requires the efficient use of land, water, energy and other vital resources, and coordinated efforts to acknowledge trade-offs and maximize synergies. Whereas the concept of a water–energy–food nexus is gaining attention, and adaptation to climate change has become an urgent need, better knowledge is required about the linkages between them (Rasul & Sharma, 2016).

An option to approach the WEF-nexus problem is by establishing a nexus thinking, which encompasses several components where governments and industries determine policies in one sector and thereby take into account the implications for other sectors (Bird & Dodds, 2014). This means e.g. that water, food and energy security must be integrated with climate concerns (Benson et al., 2015). This approach offers opportunities to connect water resource planning with broader development planning including food and energy provision (Entholzner & Reeve, 2016). From the nexus approach it is clear that policy interventions about food, water and energy cannot be made in a sector specific and independent manner. The nexus approach thus aims for cross-sectoral coordination to exploit synergies and avoid negative and unintended side-effects (Smajgl et al., 2016).

The WEF-nexus approach, which holistically considers the dynamic interlinkages between water, energy, and food resources, has become the main concept within scientific and practice communities in this area of knowledge. Supporters of this approach state that sustainable solutions can be revealed through the use of this approach, rather than with conventional approaches that often overlook the interlinkages (Kulat et al., 2019). With the confluence of population growth, climate dynamics, urbanization, and environmental deterioration, various water issues are emerging into the global arena and becoming the central component within the nexus to consider (Bird & Dodds, 2014). Conventional

engineering systems and management decision making processes for water resources tend to primarily consider cost and quantity criteria. However, long term, optimal, sustainable water allocation, and management decisions require a more holistic approach that considers all stakeholders and the associated, interdependent systems, such as energy costs, footprints of water production and distribution, and tradeoffs of water allocation between sectors (agriculture, energy production, and ecosystems) (Kulat et al., 2019).

Obviously, water is not only required for hydropower production and irrigated agriculture, it is also needed for domestic and industrial use and for ecosystem functioning. The availability of water, both surface and ground water, is variable in space and time and this variability often does not match with the spatially and temporally distributed use pattern of consumers. For instance, agriculture requires irrigation water when precipitation is low and power needs to be generated throughout the year, also when river flow is low.

To overcome the temporal discrepancy between water availability and consumption, reservoirs are built. Monitoring the water available in the reservoirs, and predicting the needs of the consumers and the losses throughout the water system is crucial for fair allocation. Gathering and processing these data are tedious issues, not only because of the spatially and temporally distributed nature of them, but also due to the complexity of the measurements and communication devices which are needed (Hanasaki et al., 2006).

Water allocation problems have challenged water managers for decades (Yeomans & Gunalay, 2009). Allocation can become controversial when competition for water increases among sectors and individual users. Increased population shifts and decreasing water supplies magnify this type of competition in many regions across the globe. Moreover, this competition is aggravated if natural conditions become more unpredictable and concerns for water quantity and quality grow. Hence, a poorly-planned system for allocating water can be at the origin of serious societal problems. It is now recognized that the efficiency, equity and environmental soundness of water allocation and management must be improved and integrated into environmental policy preparation and implementation (Ahmad et al., 2014; Yeomans & Gunalay, 2008). All this has called for computational tools as a requirement for optimising water allocation.

There are several considerations to take when making decisions about the construction of reservoirs, not only about the reservoir itself but also about options for water allocation and energy production development and, therefore, about a range of social, environmental and political choices (World Commission on Dams, 2001). One of the biggest challenges is to reconsider the management of fresh water. During the 20th century, large reservoirs proved to be one of the most important tools to help communities to extract, store and manage the water resource. The World Commission on Dams, (2001), states that between 30 and 40% of the irrigated lands rely on reservoirs. Aditionally, this commission estimated that 19% of the electricity around the world is generated by hydropower plants that rely on reservoirs. On the other hand, there is a high variability in large reservoirs in terms of delivering the predicted levels of water and electricity. While some reservoirs are not able to meet the targets, others continue to generate benefits during several decades (World Commission on Dams, 2001).

In Figure 1.1, the construction of reservoirs is on the chronic part of the acute-chronic axis and this process might be affected for several external factors that cannot be identified at first sight (C. Zhang et al., 2018). Regarding the environmental impacts of reservoirs, (Kondolf et al., 2014) state that they are related with transient and long-term impacts. The first class of impacts is related to the building and filling phase of the reservoir while the second class is related to the hydrological and ecological changes they inflict. These ecological changes include the conversion from flowing to still water, which might lead to quality problems resulting from the interaction of nutrients, and changes in sediment load and channel form. Moreover, there are several ecological problems, e.g., fish are not able to migrate and this might result in extinction (Galizia Tundisi, 2018; Kondolf et al., 2014). Both authors state that there is a big difference on managing a single reservoir and a reservoir system in cascade.

Several researchers have worked on planning and managing reservoirs systems (Ahmad et al., 2014; Cheng & Chau, 2004; Galelli et al., 2014). However, there is a lack of scientifically valid tools to support strategic and operational decisions regarding the allocation of water from a "river-with-reservoirs system" to spatially distributed and temporally variable demands.

To address this lack of tools, the main objectives of this research are to develop and test methods to:

(1) Determine the optimal allocation of water available through space and time in a surface water system without or with one or more reservoirs to spatially and temporally variable demands and;
(2) Determine the optimal location of new reservoirs in such surface water system.

Both objectives are addressed from the strategic perspective. For (1) the aim is to come up with methods that are capable of evaluating past allocation practices as a basis for future improvements while the decision to construct new reservoirs at a to-be-selected location is for sure a strategic decision.

1.3. State of the art in modelling water allocation and in optimization of reservoir location

1.3.1. Optimization of surface water allocation

1.3.1.1. Supply Chain Optimization (SCO)

According to Beamon, (1998) and Serdarasan, (2013), a supply chain can be considered as an integration of several actors (producers, suppliers, distributors, retailers and clients) which aim at producing and delivering to consumers a specific product. Lu, (2011) defines a supply chain (SC) as a group of independent components connected together through the products and services that they provide to the different consumers. Bowersox et al., (2002) state that, in order to identify all the components in a supply chain, a generalized supply chain model must be created.

Commonly, this kind of models is network-based, i.e., all actors should be connected in order to identify their interaction. Important issues to consider are transportation and its cost.

Transportation is considered as the key element that joins two or more separate components (Fallis, 2013; Stadtler, 2015; Tseng, 2005). Kilger, (2015b) states that, in order to optimize a process, all components and their relationships must be identified and then used to create a supply chain.

Different techniques for supply chain optimization have been proposed and applied in different areas. Table 1.1 presents a non-exhaustive overview.

Table 1.1. Fields where SCO has been implemented

Field	Authors	Title	Technique
Bio-Engineering	De Meyer et al., (2014)	Methods to optimize the design and management of biomass-for-bioenergy supply chains: A review.	Linear Programming (LP), Integer Programming (IP), Mixed Integer Linear Programming (MILP), Non Linear Programming (NLP), Heuristics, and multicriteria decision analysis.
Mathematical programming models	Mula et al., (2010)	Mathematical programming models for supply chain production and transport planning.	Linear Programming, Non Linear Programming, Multi-objective Programming, Fuzzy Programming, Stochastic Programming, Heuristics, Metaheuristics and Hybrid models.
Bio-Engineering	Srivastava, (2007)	Green supply-chain management: A state-of-the-art literature review.	Linear Programming, Non-Linear Programming, Markov Chains, Mixed Integer Linear Programming.
Chemical-Engineering	Häberle & Kilger, (2015)	Strategic Network Design in the Chemical Industry	Linear Programming
Demands	Wagner & Kilger, (2015)	Demand Planning	Mathematical models and Heuristic models.
Food	Wagner & Meyr, (2015)	Food and Beverages	Linear Programming
Computer Assembly	(Kilger, 2015a)	Computer Assembly	Mathematical models
Oil Industry	Meyr & Roitsch, (2015)	Oil Industry	Mathematical models and Heuristic models.
Logistics	(Lautenschläger, 2015)	Event-Based Planning for Standard Polymer Products	Mixed Integer Linear Programming

Holweg et al., (2005) conducted an extensive literature review in order to identify how different authors have modelled their supply chain (SC) when there are several external components. An analogy was implemented in order to explain how water allocation is related with SCO. Thus, water stored represented an inventory and the flow of water represented products sales. They concluded that the effectiveness of supply chain collaboration relies on two factors: a) the level on how the SC can integrate external and internal operations, and b) the level of effort on how the SC must include the different settings related with geographical dispersions, demand pattern and the product itself.

1.3.2. Water flow discretization

As water flows within a river bed in a continuous manner, it is necessary for a proper algorithm to discretize the water flow (Vaghefi et al., 2018). Thus, Pasumarthy et al., (2012),

states that the process of discretization the behavior of an open channel water flow it is complex due to the fact that water is not constant or steady; it is required to know the geometry of the river and some parameter such as: depth and shape of the river bed, evaporation, infiltration, water flow velocity, etc. In contrast, Shimizu et al., (2019), states the piped water systems are steadier, the cross section of pipes is typically rounded, water velocity is constant and can be regulated with pumps and valves.

Lagacherie et al., (2010) created an approach to discretize the spatial landscape in order to develop a computational tool (Geo-MHYDAS) to model hydrological processes. The main objective is to process geographical objects whose limits are considered as hydrological discontinuities. Those limits can be natural or artificial (man-made). Moreover, several authors such as Dongquan et al., (2009), Kneis et al., (2009) and Rathjens & Oppelt, (2012) have conducted research in order to obtain a spatial discretization.

1.3.3. Hydrological modelling and scenario analysis

The spatio-temporal availability of water in a surface water network is conditioned by the hydrological cycle. Hence a water allocation model needs observed or modelled data of the water inputs in the network. Models that are capable of generating these inputs and describing the propagation of water through the network are rainfall-runoff models and integrated hydrological-hydraulic models.

Devi et al., (2015) stated that the most known and used hydrological/hydraulic modelling tools are MIKE SHE (Système Hydrologique Européen) (Abbott et al., 1986), HBV model (Hydrologiska Byrans Vattenavdelning model) (Bergstrom S., 1995), TOPMODEL (TOPography based hydrological MODEL) (Beven et al., 1984), VIC model (Variable Infiltration Capacity model) (Liang et al., 1994) and SWAT (Soil and Water Assessment Tool) (Neitsch et al., 2009). We elaborate here upon SWAT since we make use of that model in chapters 3 and 5.

The Soil and Water Assessment Tool (SWAT) is a hydrological modelling tool that predicts the impact of land management practices on water quantity and quality in large watersheds over long periods of time. This model integrates information on weather, soil properties and vegetation to simulate physical processes associated with water (e.g., sediment transport) (Arnold & Fohrer, 2005; Neitsch et al., 2005, 2009).

Watersheds might be divided into a number of subbasins when one or several areas are dominated by a specific climate, land use or soil type. An example of subbasin delineation is shown in Figure 1.4. Within each subbasin the input data is grouped into hydrological response units (HRU). These HRUs are lumped land areas within the subbasin that are comprised of unique land cover type, soil type, and management combinations (Arnold & Fohrer, 2005; Neitsch et al., 2005, 2009).

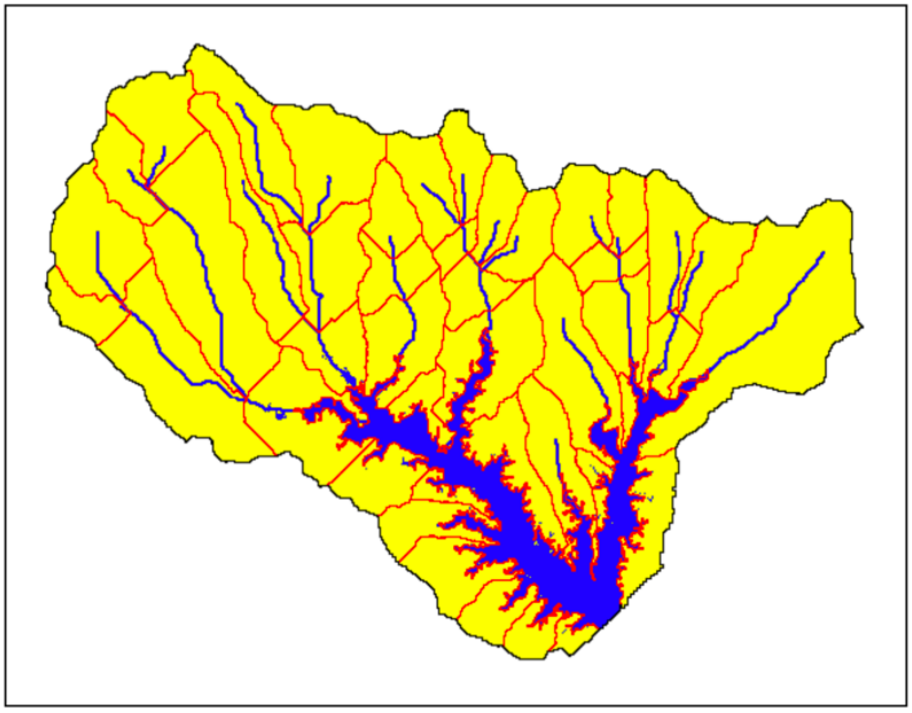

Figure 1.4. Subbasin delineation for a watershed (Neitsch et al., 2009)

The SWAT model simulates the water flow within a watershed. This simulation process consists of two phases: the land phase and the routing phase of the hydrological cycle. The land phase is based on Equation (1.1). In this equation, the final soil water content is represented by SW_t, which corresponds to the summation of the initial soil water content (SW_0) on day *i* and the total amount of the precipitation (R_{day}) on day *i* minus the surface runoff (Q_{surf}) on day *i*, the amount of water lost by evapotranspiration (E_a) on day *i*, water lost through seepage (w_{seep}) on day *i* and the amount of return flow (Q_{gw}) on day *i*.

$$SW_t = SW_0 + \sum_{i=1}^{t} \left(R_{day(i)} - Q_{surf(i)} - E_{a(i)} - w_{seep(i)} - Q_{gw(i)}\right) \qquad (1.1)$$

With the delineation of HRUs within the watershed, the accuracy of the water balance simulations will be increased since the total runoff can be predicted for each HRU in a separate way and different evapotranspiration values can be obtained for various crops and fields (Arnold & Fohrer, 2005; Neitsch et al., 2005, 2009).

To model the land phase, different inputs are required. Weather data such as daily precipitation, minimum and maximum temperature, relative humidity, solar radiation and wind speed are essential. As rain falls, it might be intercepted by vegetation canopy or fall on the surface and water that reaches the surface can either infiltrate into the soil or flow overland as runoff. Figure 1.5, gives a more detailed overview of which pathways are taken into account by SWAT (Arnold & Fohrer, 2005; Neitsch et al., 2005, 2009).

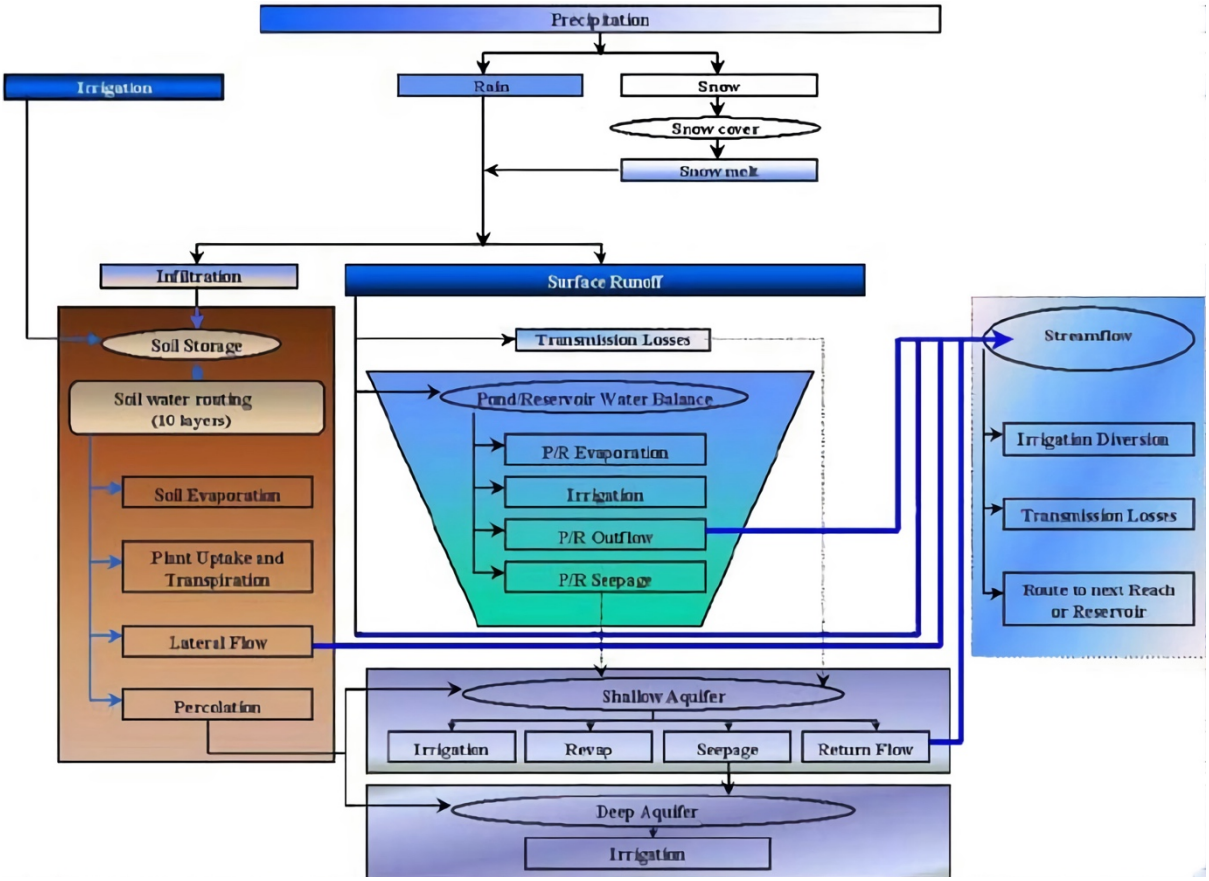

Figure 1.5. Schematic of pathways available for water movements in SWAT (Neitsch et al., 2009)

Evapotranspiration is a key factor in hydrology calculations. The evapotranspiration value corresponds to the total summation of the water evaporated directly from the water surface or from the soil (evaporation) and water lost through vegetation (transpiration). Since the evapotranspiration rate is strongly affected by micro-climatic processes, potential evapotranspiration is calculated in a first stage (Arnold & Fohrer, 2005; Neitsch et al., 2005, 2009).

Potential evapotranspiration can be defined as the rate at which evapotranspiration would occur in an area that is completely and uniformly covered with a short green grass crop and with an unlimited supply of soil water. In SWAT, three methods are incorporated to estimate the potential evapotranspiration, namely the Penman-Monteith (Monteith, 1965) method, the Priestley-Taylor method (Priestley & Taylor, 1972) and the Hargreaves method (Hargreaves et al., 1985). The most frequently used method is Penman-Monteith (Equation **Error! Reference source not found.**)) and requires information about solar radiation, air temperature, relative humidity and wind speed (Arnold & Fohrer, 2005; Neitsch et al., 2005, 2009).

$$\lambda E = \frac{\Delta \cdot (H_{net} - G) + \rho_{air} \cdot c_p \cdot \left(\frac{e_z^0 - e_z}{r_a}\right)}{\Delta + \gamma \cdot \left(1 + \frac{r_c}{r_a}\right)}$$

Where,

λE [MJ m-2 d-1]: latent heat flux density
E [mm d-1]: depth rate evaporation
Δ [kPa °C-1]: slope of the saturation vapor pressure-temperature curve
H_{net} [MJ m-2 d-1]: net radiation
G [MJ m-2 d-1]: soil heat flux
ρ_{air} [kg m-3]: air density
c_p [MJ kg-1 °C-1]: specific heat at constant pressure
e_z^0 [kPa]: saturation vapor pressure of air at height z
e_z [kPa]: water vapour pressure of air at height z
γ [kPa °C-1]: psychometric constant
r_c [s m-1]: plant canopy resistance
r_a [s m-1]: aerodynamic resistance

The final evapotranspiration is calculated immediately after the calculation of the potential evapotranspiration. In a first step, SWAT considers the evaporation of the rain that is intercepted by vegetation. If the potential evapotranspiration is less than the amount of free water that can be held by the canopy, the actual evapotranspiration is equal to the potential evapotranspiration and a certain amount of water may remain in the canopy. On the other hand, if the potential evapotranspiration is greater than the amount of free water held in the canopy, there is no water left on the canopy and additional water needs to be lost by evapotranspiration. In a second step, the maximum amount of transpiration is calculated, based on the potential evapotranspiration and the leaf area index. In a next step, water is evaporated from the soil and snow through sublimation. Water will be first removed from the snow pack and if an evaporation demand still exists afterwards, this demand must be divided between the different soil layers. SWAT assumes that 50% of the evaporative demand is extracted from the first 10 mm of soil and 95% is extracted from the first 100 mm of soil (Arnold & Fohrer, 2005; Neitsch et al., 2005, 2009).

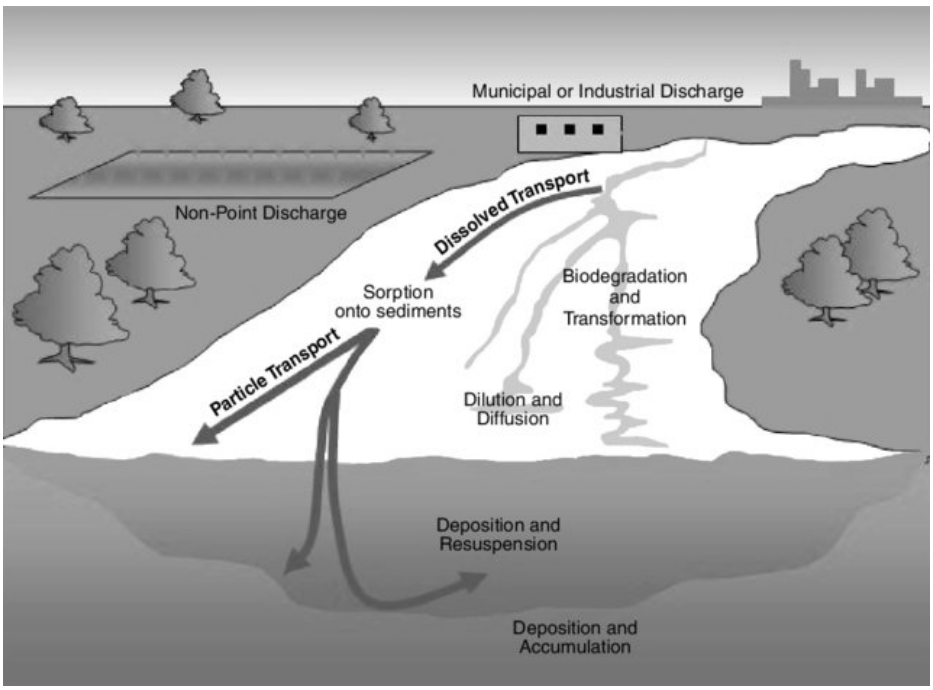

Figure 1.6. Schema of the water routing process from SWAT (Neitsch et al., 2009)

The second phase in SWAT's simulation approach is to model the water routing through the watershed. Water flows directly over the land or through channels. Four flow components can be considered during the process, namely: water, sediment, nutrients and organic chemicals (Figure 1.6).

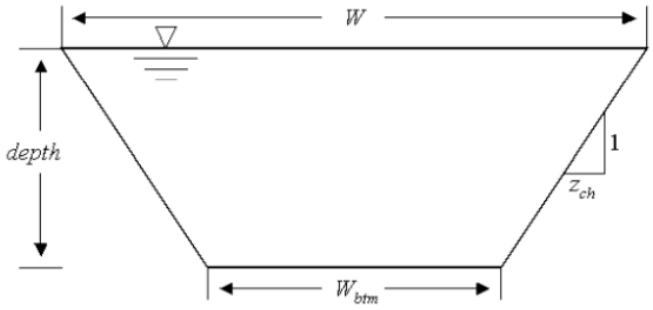

Figure 1.7. Schema of the trapezoidal shape in a channel (Neitsch et al., 2005, 2009)

In order to model water routing, channel characteristics must be determined. An important factor in this regard is the shape of the main channel; SWAT assumes a trapezoidal shape and characteristics such as depth and top width (W) that must be provided by the user as inputs (Figure 1.7). The next step is to calculate the remaining channel characteristics including the cross-sectional area of flow within the channel (A_{ch}), the hydraulic radius for a given depth of flow (R_{cn}) and the slope along the channel length (slp_{ch}). These parameters are needed to calculate the flow rate and the velocity in each segment of the water channel. Equation (1.2) is used to calculate the volumetric flow q_{ch} whereas Equation (1.3) is used to calculate the velocity v_c. Equation (1.2) and (1.3) are known as the Manning equations. The constant n represents the Manning's coefficient for the water channel segment. In the SWAT model, temporary losses such as transmission losses and bank storage are taken into account (Arnold & Fohrer, 2005; Neitsch et al., 2005, 2009).

$$q_{ch} = \frac{A_{ch} * R_{ch}^{2/3} * slp_{ch}^{1/2}}{n} \tag{1.2}$$

$$v_c = \frac{R_{ch}^{2/3} * slp_{ch}^{1/2}}{n} \tag{1.3}$$

Impoundments, e.g., reservoirs, ponds, wetlands and depressions, located within the subbasins play an important role in water supply and flood control. Equation (1.4) allows to calculate the total volume of water stored in a reservoir. The water balance in this case is defined as the sum of the total volume of water volume stored initially (V_{stored}) plus the volume that is entering (V_{flowin}) plus the volume of precipitation that is falling on the reservoir (V_{pep}) minus the volume that is flowing out of the water body ($V_{flowout}$) minus the volume that is removed by evaporation (V_{evap}) minus the volume lost through seepage (V_{seep}) (Arnold & Fohrer, 2005; Neitsch et al., 2005, 2009).

$$V = V_{stored} + V_{flowin} + V_{pep} - V_{flowout} - V_{evap} - V_{seep} \tag{1.4}$$

SWAT cannot account for the hydraulic effects along the river and/or canal network, such as backwater effects, the effect of hydraulic regulation, etc. Hydraulic models as well as full hydrodynamic models have been replaced by simplified, conceptual or grey-box models. Grey-box models usually combines some real-world data with data from machine learning models such as artificial neural networks (Acuña et al., 1999).

1.3.4. Other approaches in water allocation

The aim of getting a balanced allocation of water has been under debate for many years. To this end, several researchers have created models based on different conditions and requirements. This kind of research has been widely applied in countries that are suffering from droughts and floods. This topic becomes even more important in regions where water availability is too low to satisfy the population needs. In the past, many methods have been proposed to tackle this problem. These methods have been traditionally based on differential equations including iterative processes (Arnold & Fohrer, 2005). For instance, MIKE SHE (DHI, 2019). Along this research line, (Tinoco et al., 2016) and (Tinoco et al., 2014) report on studies in the Macul basin, located in northern Ecuador. The objective of those studies was to create a mathematical model to achieve an optimal distribution of water from rivers to the different irrigation projects. This optimization approach consists of a trial-and-error process following these steps: 1) River/reservoir system modelling, in order to simulate and optimize water availability for a period of historical data; 2) Post-statistical analyses of each of the resulting reservoir outflows and reservoir water levels; and, 3) Extreme value analysis of the minimum reservoir water levels.

Table 1.2 shows a non-exhaustive list of the most commonly used approaches to model water allocation processes.

Table 1.2. Approaches for water allocation

Authors	Title	Approach
Yan et al., (2017)	Many-objective robust decision making for water allocation under climate change	Multi-objective evolutionary algorithms
Ghosh et al., (2017)	Water allocation and management along the Santa Cruz border region Sanchari	Mathematical and Linear programming
Jafarzadegan et al., (2014)	A stochastic model for optimal operation of inter-basin water allocation systems: a case study	Stochastic model.
Condon & Maxwell, (2013)	Linear optimization fully integrated with physical hydrology model.	Linear optimization allocation with an integrated physical hydrology model.
Ashraf Vaghefi et al., (2013)	Integration of hydrologic and water allocation models in basin-scale water resources management considering crop pattern and climate change: Karkheh River Basin in Iran	Linking SWAT and MODSIM (Labadie, 2006)
Thevs et al., (2015)	Water allocation and water consumption of irrigated agriculture and natural vegetation in the Aksu-Tarim river basin, Xinjiang, China	Evapotranspiration mapping and water balance calculations

Water allocation problems are typically tackled with computational models, for instance: WEAP (Yates et al., 2005), WaterWare (Environmental Software and Services, 1995), MODSIM (Labadie, 2006), RiverWare (Zagona, 2001), REALM (Perera et al., 2005), MIKE Hydro Basin

(DHI, 2019), MULINO-DSS (Giupponi et al., 2004), etc. These tools must be provided together with a set of constraints, priorities, and water demands. To carry out optimization tasks, several other conditions must be provided, for instance, operating policies, decision steps, etc. Typically, allocation tools require limited inputs and computational resources, allowing users to carry out calibration and tuning procedures in a reasonable time frame (Refsgaard & Storm, 1996).

1.3.5. Water Resource Management (WRM)

The World Bank, (2017), defines WRM as the process related with the process of planning, developing and managing of water resources and ecosystems in quality and quantity across water demands. It also includes institutions, infrastructures and ICT system. The main aim of WRM is to ensure that sufficient water will be delivered to the users (drinking, sanitation, food production, irrigation, energy production, etc.)

The WRM paradigm has been recognized widely as the current feasible way to ensure a sustainable planning and management of water systems (Calizaya et al., 2010). Applying an optimization process to the water resource management problem may help to store water during the wet periods and deliver it during the dry ones. Thus, water resource might be assured (Shahid, 2010).

Nowadays, seasons are becoming more extreme due to global warming (Trenberth et al., 2014) and, therefore, reservoirs are becoming a key point in water resource management, since they allow for storing water during the rainy season and supply it during the dry season (Das et al., 2015). Grigg, (2016) states that WRM is the process on how to distribute water in an efficient and equitable manner among different consumers and users. This process takes into account suppliers and several factors such as: climate, poverty, pollution, infrastructures, geology, etc. that may influence water availability.

Several authors also state that, currently, there are many issues within the water allocation process such as: deficit in irrigation systems (Reca et al., 2001), unfair allocation of water for human consumption (Syme et al., 1999), power generation (Kadigi et al., 2008) and WEF-nexus (Namany et al., 2019; Türkeş et al., 2020).

For instance, Akram & Mendelsohn, (2017) could verify from a use case in Pakistan that the allocation process within an irrigation system is not completely balanced: users at the beginning of the irrigation network received more water compared with the users at the end.

1.3.6. Optimization approaches for managing reservoirs

Several researchers are trying to create and apply different approaches. Labadie, (2004) provides a comprehensive review on the optimization of reservoir system management and operation. That review reports on methods like 1) Implicit stochastic optimization, 2) Linear programming models, 3) Network flow optimization models, 4) Nonlinear programming models, 5) Discrete dynamic programming models, 6) Explicit stochastic optimization, 7) Real-time control with forecasting, and 8) Heuristic programming models.

According to Md. Azamathulla et al., (2008), there is an increasing awareness among irrigation planners and engineers to operate reservoir systems in a more efficient way. In their research, they developed and made a comparison between genetic algorithms (GA) and linear programming (LP) models that were applied to an existing reservoir system in Madhya Pradesh, India. They found that GA was superior in performance compared to LP. Another approach is the one from Chou & Wu, (2014) presented a method to establish the objective function of a network flow programming model for simulating river–reservoir system operations and the associated water allocation. This research also included the development of an optimization model based on a linear programming approach to minimize water surplus assigning priorities to the different water usages.

In this regard, Abdulbaki et al., (2017) report on the development of a model to optimally allocate water resources in reservoir systems by applying an Integer Linear Programming (ILP) approach. The goal of this model is to minimize total water cost considering treatment and distribution costs.

Several researches have been performed in order to optimize water reservoir systems. Mao et al., (2016), state that an optimization process applied to systems of reservoirs might help in flood control, drought mitigation and biodiversity conservation. In their research, they developed an optimization model based on genetic algorithms (GA).

Another way of applying water optimization was addressed by Moridi & Yazdi, (2017). They focused on the minimization of damage caused by flood in downstream sites and the simultaneous minimization of the reduction on hydro-power generation. Their model was based on MILP as the main optimization technique.

In addition to the previously mentioned techniques, Table 1.3 presents a non-exhaustive list of research articles regarding the optimization of water allocation.

Table 1.3 reveals that the applied methods for optimizing water allocation belong to two main categories: exact and heuristic models. Exact models provide an optimal result from a set of feasible solutions. The exact approaches applied in this context are typically based on linear, integer and mixed integer linear programming (Horne et al., 2016). On the other hand, heuristic models provide an acceptable close-to-optimal solution that might not be the best (Winston & Goldberg, 1994).

There some methods which are related with Machine Learning which try to perform optimization. In this matter, Gambella et al., (2021), states that this kind of methods are based on the experience and with this solve complex problems under condition which are varying from past information. Moreover, Sun et al., (2020) , stated that there is an additional category which is related with optimization called “Machine Learning models”; in their research they stated that once a machine learning method is formulated, the problem can be solved as the optimization problems. Besides, one of the most used methods is based in neural networks (deep learning) such as: Convolutional Neural Networks (CNN) and Recurrent Neural Networks (RNN).

Table 1.3. Approaches in water optimization allocation

Authors	Optimization technique	Approach
Ha & Gao, (2017)	Mixed Integer Linear Programming	Water allocation under climate change
T. Wang et al., (2017)	Genetic Algorithms, Support Vector Machines, Artificial Neural Networks and Multiple loop iterations	Multi-Dimensional equilibrium allocation model of water resources.
Li et al., (2017)	Dynamic Programming	Multiple water resources allocation
Jamshid Mousavi et al., (2017)	Mixed Integer Non-linear Programming (MINLP)	Multi-Objective optimization-simulation in water allocation.
Kermani et al., (2017)	Mixed Integer Linear Programming	Optimization of water allocation and energy production.
Singh, (2017)	Linear Programming	Optimal allocation of water and land resources to maximize farm income and to minimize irrigation-induced environmental problems.
(Liu et al., 2017)	Least Squares Support Vector Machines and Artificial Neural Networks	Rank solutions of multi-objective water resources allocation models.
Olofintoye et al., (2016)	Artificial Neural Networks and Pareto multi-objective differential evolution	Real-time optimal water allocation from hydropower generation.
Al-Zahrani et al., (2016)	Goal Programming	Multi-objective optimization for water resources management.
Nguyen et al., (2016)	Ant Colony Optimization	Crop and water allocation optimization.
Hu et al., (2016)	Compromise Programming	Optimal allocation of regional water resources.
Z. Wang et al., (2015)	Linear Programming	Optimal water resources allocation under the land use constraint.
F. Chang et al., (2014)	Genetic Algorithms	Optimal reservoir operation and water allocation.
Horne et al., (2017)	Mixed Integer Programming	Design of an environmental flow regime, in the context of optimization.
Freire-González et al., (2018)	Linear Programming	Water allocation during droughts in the United Kingdom.

1.3.7. Optimization of reservoir location

The optimization of a reservoir location, requires a complete evaluation of the possible combinations of the decision variables such as reservoir properties (minimum and maximum capacities), locations and water production scheduling parameters. The exploration of all possibilities may be impractical due to the computation time (Bittencourt & Horne, 1997). With this regard, this research project is focused on the optimization of the (water) locations with a reservoir or system of reservoirs.

Chhuon et al., (2016), proposed a method to optimize water allocation to the different demand users along the Prek Te River basin in Cambodia. In their research, they used SWAT to simulate the behaviour within the basin with a set of possible locations for new reservoirs. Afterwards, they have used MODSIM for planning and management of the reservoir systems. The output provided a decision support system to optimize the water allocation process based on the water demands.

A different approach was developed by Walsh et al., (2015). They created a tool called “NC-RES”. This application is a web-based geographic information system to help non-scientific and non-specialist users to assess possible locations for reservoirs. Besides, the tool uses terrain data from North California's LiDAR-derived, high-resolution digital terrain model. Among the features of the proposed tool there is the possibility of analyzing possible inundation and drainage areas.

1.4. Specific Objectives and Selected Approaches

A rather original approach emerging from the literature is to address the water allocation problem as an instance of the supply chain approach (chapter 2, section 2.2.1) by considering the allocation as a “Network Flow Optimization Problem (NFO-P)” (Winston & Goldberg, 1994). There are two approaches to address this problem Lalehzari et al., (2016) and Sechi & Zucca, (2015). The first approach is based on trial-and-error mechanisms, establishing an objective function to minimize with the correspondent thresholds and priorities. This process involves several iterations in which the total cost is being reduced. The second approach makes use of mathematical models. In particular linear programming (LP) and mixed integer linear programming models (MILP) have been applied to allocate water to the different demand users and is mainly based on priority setting among the demands to be fulfilled (Heydari et al., 2015). Besides, a penalization in monetary units is associated to the amount of water not delivered. Thus, those models are oriented to the minimization of these costs (Jamshid Mousavi et al., 2017; Moridi & Yazdi, 2017; Morsi et al., 2012; Singh, 2017). Several studies are available about the application of such mathematical models for operational optimization (Galelli et al., 2014; Lalehzari et al., 2016; Mao et al., 2016; Z. Wang et al., 2015). However, there is a lack of research to address the NFO-P taking the distribution in space and the temporal variability of water availability and water demand into account.

For this PhD-project, we selected linear programming (LP) as the approach for optimizing the allocation of water supplied by a system of multiple rivers with one or more reservoirs, towards multiple downstream uses such as irrigation, hydropower generation, human consumption, ecosystem functioning, industrial use, etc. with a view to satisfy the needs as good as possible from a WEF-nexus perspective. In order to tackle this problem, the flow of water in a river with a reservoir system is considered from a discrete point of view. Conceptually, batches of water are transported between or stored in nodes, just like this would happen in a freight transportation network, considering losses and transport capacity constraints.

For the reservoir location problem we opted for extending the LP-model towards a MILP-model in which binary variables express whether a reservoir at one or more candidate location leads to an optimised allocation.

To formulate and test the LP and MILP models, an artificial surface water system is used. Next the models are used in real world case studies, i.c. the Machángara River Basin in southern Ecuador, the Omo River Basin in Ethiopia, Kenya and Southern Congo.

As a consequence of these choices we reformulated our general research objectives into two more specific research questions:

- RQ1: What are the strengths and weaknesses of LP and MILP-approaches for the ex-post evaluation of the performance of a given water supply network (WSN) given historic supply and demand?
- RQ2: What are the strengths and weaknesses of LP and MILP-approaches to optimize the WSN in terms of the location of new reservoirs of a predefined capacity?

Figure 1.8, shows the work flow to tackle the research questions (objectives). This figure, considers the scenario where there are no long-term time-series of observed data available. In this case, data simulated with the SWAT model were used as input data for the LP and MILP models. Finally, the model is considered as a DSS (Decision Support System) to determine the allocation of water to the different users.

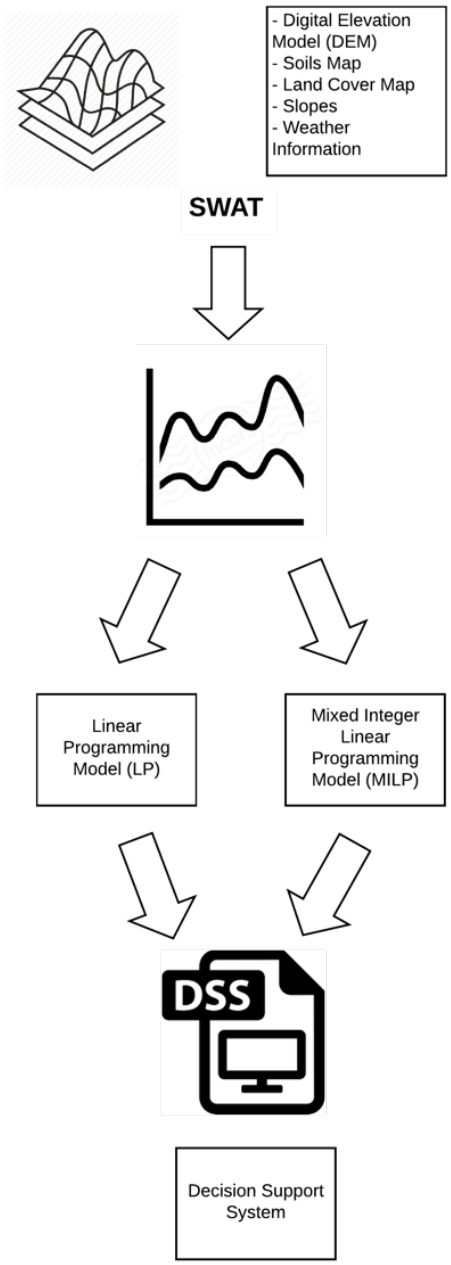

Figure 1.8. General work flow of the research project

1.5. Outline of this dissertation

The outline of this manuscript is shown in Figure 1.9. In the present chapter 1 the problem is stated together with the general objectives and research questions. Besides, chapter 1 includes a review of the scientific literature of the modelling of water allocation and the optimization of reservoir location.

In chapter 2, a Network Flow Optimization - linear programming model (NFO-LP) for the allocation of surface water to spatially distributed and temporally variable demands is proposed.

In chapter 3, the NFO-LP model is calibrated, validated and applied to real world data (the Machángara River Basin in southern Ecuador). In order to obtain the required input data, ARCSWAT (Texas A&M University, 2009) was used. As a result, we managed to obtain georeferenced time series of water availability in the river network.

In chapter 4, an extension of the NFO-LP model is presented. With this extension, the model can simultaneously allocate water and recommend the potential location of new reservoirs. To achieve these goals, the NFO-LP model was upgraded to a Mixed Integer Linear Programming model (NFO-MILP). This involved adding several binary variables associated to each possible reservoir plus the inclusion of a building and management cost. Dummy input data is used to illustrate the model.

In chapter 5 a different region was studied: the Omo River Basin. As a result of the application of the extended NFO-MILP model, a recommendation for the potential location of new reservoirs was obtained as well as an optimal allocation scheme of water resources. New reservoirs were selected from a set of “possible reservoirs”.

chapter 6 summarizes all findings, discusses them and presents the conclusions of the complete research project and proposes future work.

Finally, a complete list of the cited references is given.

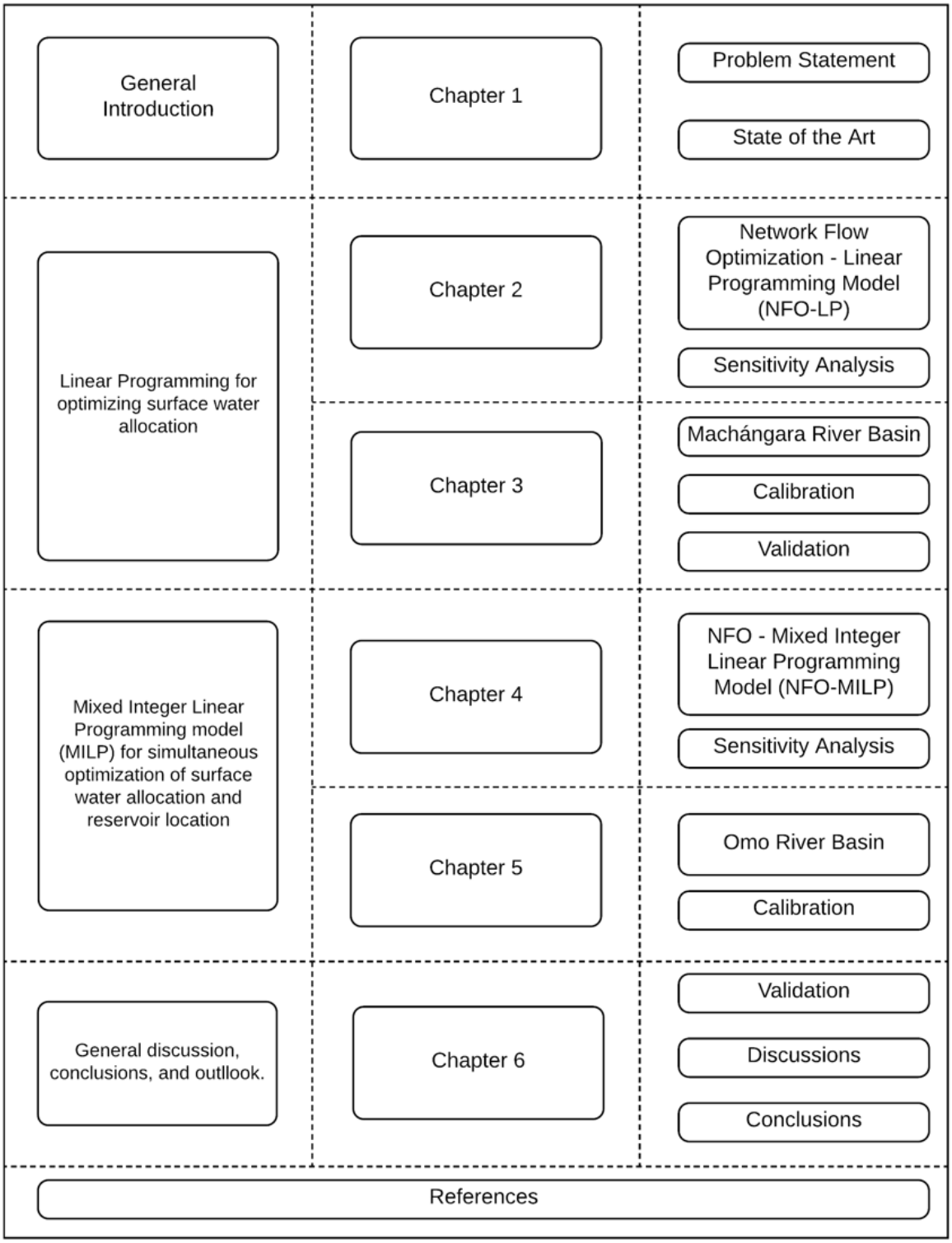

Figure 1.9. Outline of this dissertation.

Chapter 2
Network Flow Optimization - Linear Programming model (NFO-LP) for optimizing water allocation

The core of this chapter has been published as:

Veintimilla-Reyes, J.; Cattrysse, D.; De Meyer, A. Van Orshoven, J. Mixed Integer Linear Programming (MILP) approach to deal with spatio-temporal water allocation. Procedia Eng. 2016, 162, 221–229.

Veintimilla-Reyes, J., De Meyer, A., Cattrysse, D., Van Orshoven, J., 2018. A linear programming approach to optimize the management of water in dammed river systems for meeting demands and preventing floods. Water Sci. Technol. Water Supply 18, 713–722. https://doi.org/10.2166/ws.2017.144.

2.1. Introduction

Exacerbated by climate change, access to sufficient quantity of water of sufficient quality is becoming one of the biggest problems around the world (Turral et al., 2011). This problem is more evident in countries with pronounced and long dry seasons (Bangash et al., 2012). To support the allocation of water as a scarce resource, water allocation models have been developed using heuristics, trial-and-error and mathematical approaches (Labadie, 2004, 2006; Tinoco et al., 2016; Yeomans & Gunalay, 2009).

The present chapter proposes a new linear programming (LP) model for optimizing the allocation of the water available in a river-with-reservoirs-system to different downstream uses. To address the spatial heterogeneity and temporal variability of the water availability, the proposed model departs from a spatially explicit Water Supply Network (WSN) (Qiao et al., 2007; Sarkis, 2012) which allows to tackle the water allocation problem as a Network Flow Optimization Problem (NFO-P). The WSN-approach allows for the comprehensive representation of all components of the surface water system so that a generic optimization model can be created that is applicable to different river basins. Whereas for the design of the model and its testing in a case study fictitious data were used, in follow-on chapters, the model is calibrated for and applied to real world cases.

2.2. Materials and methods

2.2.1. Approach

The WSN and the water allocation problem to be modelled have the following characteristics: (1) the quantity of water available in river segments and reservoirs is variable in time; (2) multiple water users are distributed in space but connected to the river-with-reservoirs-system and have water demands which vary in time; (3) unmet demands must be minimized, floods of river segments and reservoirs must be avoided to the extent possible and presence at all times of a minimal amount of water in river segments and reservoirs must be guaranteed for ecological reasons.

A conceptual representation of the problem was presented in chapter 1 section 3. This abstraction encompasses three main components: 1) inputs (water availability generated by the SWAT-model from geographical and climate information of the study area); 2) optimization model (NFO-LP) and 3) outputs (water allocated to the different demands in the study area).

The WSN (Coulthard & Van De Wiel, 2012; Merkuryeva et al., 2015; Qiao et al., 2007; Sarkis, 2012; Shafroth et al., 2010) is a general abstraction of all components of the river-with-reservoirs-system needed to model and optimize the water allocation. The WSN has a topological arc-node data structure in which nodes are characterized by time series of water availability or flow at a sufficient temporal resolution. The time series may be acquired by sensors (real time and/or historical archives) or derived from forecasted time series (e.g., using machine learning methods). The ecological role of the river is taken into account by integrating in the WSN a downstream demand node and by continuity constraints so that at each time step, a minimum amount of water remains present in the river segments.Since the

goal of the optimization is to manage the water levels in the reservoirs and river segments and to allocate the available water resources so that spatially and temporally distributed demands are optimally met with no floods, the Network Flow Optimization problem is considered to be an instance of the Minimum Cost Flow Problem (MCFP) (Chou & Wu, 2014), which can be solved with an LP model (Chou & Wu, 2014; Frizzone et al., 1997; Kolb et al., 2012; Labadie, 2004; Winston & Goldberg, 1994). In this kind of problems, the aim is to determine the most efficient way to send a specific amount of flow through a network.

The described MCF-problem was modelled using the optimization solver Gurobi (Gurobi, 2015). This solver was preferred above other solver software packages (CPLEX from IBM (IBM, 2020), LINGO from LINDO (Lingo, 2006), etc.) due to its support for the Python programming language and because of the adequate availability of documentation.

2.2.2. Generic model

First the generic WSN was conceived, as shown in Figure 2.1. A distinction is made between three types of nodes: R (reservoir), T (transfer node) and D (demand node). River segments (X) have a start node and an end node which can be of any of the three types. For instance: river segment $X_{n,d}$, starts at transfer node ($n \in T$) and ends in demand node ($d \in D$) whereas $X_{n,r}$, is a segment between a transfer node ($n \in T$) and a reservoir node ($r \in R$). Apart from river segments that have a start and an end node, also input segments (I) are considered. Input segments have no defined start node but are used to model the inflow of water running off from the land in the river-with-reservoirs-system. A node may be the end node of several input segments and at the same time receive water from regular river segments (Figure 2.1).

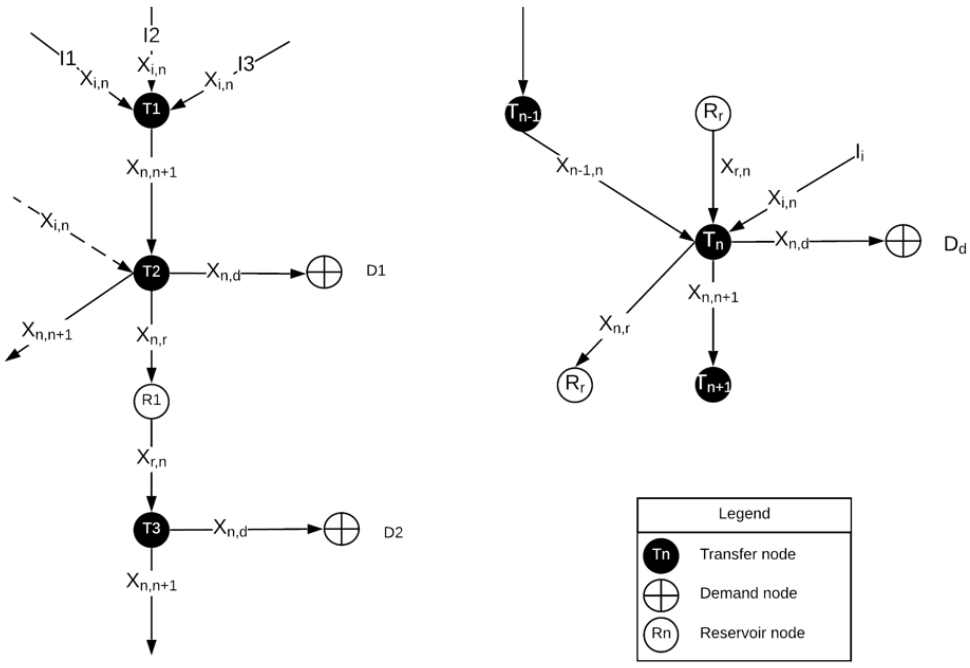

Figure 2.1. Graphical representation of the generic WSN: water flows through segments which are connected by transfer nodes, reservoir nodes and demand nodes (left); Flow generalization in one transfer node (right)

In line with the characteristics of the problem (Section 2.1) and the generic representation of the WSN (Figure 2.1), the objective function of the LP-model is formulated in Equation (2.1). It expresses the objective as optimally meeting water demands while simultaneously avoiding floods, respecting the maximum and minimum capacities in rivers, demand segments and reservoirs. It is complemented by the available water and by a set of penalties related to not meeting the mentioned demands or to not reaching or exceeding the set limitations. The logic of the penalty values is that they are established in a way that the largest values are assigned to the demands with the highest priority. If it turns out to be impossible to meet all demands the model minimizes the sum of the penalties.

$$\begin{aligned}\text{Minimize } \sum_{n}\sum_{d}\sum_{t}\left(P_d * S_{n,d}^{t-}\right)+\sum_{n}\sum_{d}\sum_{t}\left(E_d * S_{n,d}^{t+}\right)+\sum_{r}\sum_{t}(U_r * SH_r^{t-})+\sum_{r}\sum_{t}(A_r * OF_r^{t+})+\sum_{n}\sum_{t}(W_n * T_{n,n+1}^{t+})+\sum_{n}\sum_{t}(B_n * Q_{n,n+1}^{t-})+\sum_{n}\sum_{d}\sum_{t}(F_d * \text{MinXD}_{n,d}^{t-})+\\ \sum_{n}\sum_{d}\sum_{t}\left(G_d * \text{MaxXD}_{n,d}^{t+}\right)\end{aligned} \tag{2.1}$$

Equation (2.1) is composed of eight terms:

- The first term refers to the unmet demands ($S_{n,d}^{t-}$) and their corresponding penalties (P_n);
- The second term ($S_{n,d}^{t+}$) is related to the penalties when more water than required is allocated to a demand node;
- The third (SH_r^{t-}) and the fourth (OF_r^{t+}) terms are related to a penalization for not reaching the minimum volume in and for exceeding the maximum capacity of the reservoirs respectively;
- The fifth term ($T_{n,n+1}^{t+}$) is related to the penalty for a flood of a river segment;
- The sixth term ($Q_{n,n+1}^{t-}$) refers to the penalty associated to the case when there is not enough water in a river segment;
- The seventh ($\text{MinXD}_{n,d}^{t-}$) and the eighth ($\text{MaxXD}_{n,d}^{t+}$) terms are related to penalization of not reaching the minimum volume and exceeding the capacity of a demand segment respectively.

The driver for water flow in the conceived WSN is the demand. In the absence of any demand, water would not be displaced from one node to the next. Hence to model the continuous nature of water flow in the WSN and regulate the flow, constraints are introduced. These constraints can be grouped according to six different types: (a) Constraints preserving the mass balance of the water flowing from one node to the next; (b) Constraints considering the physical and regulatory limitations such as capacity restrictions of reservoirs and river segments; (c) Constraints to model the continuity of water flow; (d) Constraints for modelling temporal delays in the water transportation process, due e.g. to return flow of flooded water; (e) Constraints related to water loss; and (f) Constraints to model water excess (floods).

The temporal dimension of the modelling process is discretized in time steps that correspond to the assumed time required for the water to flow from one node to another.

a) Mass balance constraints

1. Transport (n)

$$X_{n-1,n}^{t} + \sum_i X_{i,n}^{t} + \sum_r X_{r,n}^{t} + V_n^{t-1} + TD_{n-2,n-1}^{t-2} + TDFW_{n-2,n-1}^{t-2} + RW_{n-1,n}^{t} + OF_r^{t+} + \sum_d RD_{\mathrm{d}-2,d-1}^{t-2} = V_n^{t} + LP_n^{t} + X_{n,n+1}^{t} + \sum_r X_{n,r}^{t} + \sum_d X_{n,d}^{t} + TD_{n,n+1}^{t} + L_{n-1,n}^{t} + L_{r,n}^{t} + L_{n,d}^{t} \quad n \in N,\ n > 1,\ \forall_t \in T,\ \forall_i \in I \quad (2.2)$$

2. Reservoir (r)

$$\sum_n X_{n,r}^{t} + \sum_i X_{i,r}^{t} + V_r^{t-1} = \sum_n X_{r,n}^{t} + V_r^{t} + \sum_n X_{r,\mathrm{d}}^{t} \quad \forall_r \in R,\ \forall_n \in N \quad (2.3)$$

b) Network limitations and capacity constraints

1. Network limitations

Inputs (i)

$$\sum_i X_{i,n}^{t} = X_{n,n+1}^{t} \quad n \in N,\ n > 1,\ \forall_i \in I \quad (2.4)$$

Sources (i)

$$\sum_n X_{i,n}^{t} = I_i^{t} \quad n \in N,\ \forall_i \in I \quad (2.5)$$

Demands (d)

$$\sum_n X_{n,d}^{t} + S_d^{t-} - S_d^{t+} = D_d^{t} \quad n \in N,\ n > 1,\ \forall_d \in D \quad (2.6)$$

2. Capacity constraints

River Segment (n)

$$X_{n,n+1}^{t} + T_{n,n+1}^{t-} - T_{n,n+1}^{t+} = Cmax_{n,n+1}^{t} \quad n \in N,\ n > 1,\ \forall_t \in T \quad (2.7)$$

$$X_{n,n+1}^{t} + Q_{n,n+1}^{t-} - Q_{n,n+1}^{t+} = Cmin_{n,n+1}^{t} \quad n \in N,\ n > 1 \quad (2.8)$$

Reservoir (r)

$$V_r^{t} - LP_r^{t} - OF_r^{t+} + OF_r^{t-} = Rmax_r^{t} \quad \forall_r \in R \quad (2.9)$$

$$V_r^{t} - LP_r^{t} + SH_r^{t-} - SH_r^{t+} = Rmin_r^{t} \quad \forall_r \in R \quad (2.10)$$

Demand segment (d)

$$X_{n,d}^{t} + MinXD_{n,d}^{t-} - MinXD_{n,d}^{t+} = Cmin_{n,d}^{t} \quad n \in N,\ n > 1,\ \forall_d \in D \quad (2.11)$$

$$X_{n,d}^{t} + MaxXD_{n,d}^{t-} - MaxXD_{n,d}^{t+} = Cmax_{n,d}^{t} \qquad \begin{matrix} n \in N \\ n > 1 \\ \forall_d \in D \end{matrix} \qquad (2.12)$$

c) Continuity constraints

$$V_n^t \leq \beta_n^t * \left(\sum_i X_{i,n}^{t-1} + \sum_r X_{r,n}^{t-1} + V_n^{t-1} + X_{n-1,n}^{t} + RW_{n-1,n}^{t} + TDFW_{n-2,n-1}^{t-2}\right) \qquad \begin{matrix} n \in N \\ n > 1 \\ \forall_i \in I \\ \forall_r \in R \end{matrix} \qquad (2.13)$$

$$V_n^t \geq \gamma_n^t * \left(\sum_i X_{i,n}^{t-1} + \sum_r X_{r,n}^{t-1} + V_n^{t-1} + X_{n-1,n}^{t} + RW_{n-1,n}^{t} + TDFW_{n-2,n-1}^{t-2}\right) \qquad \begin{matrix} n \in N \\ n > 1 \\ \forall_i \in I \\ \forall_r \in R \end{matrix} \qquad (2.14)$$

d) Time delay constraints

Transfer nodes

$$TD_n^t = \delta_n^t * \left(X_{n,n+1}^{t}\right) \qquad \begin{matrix} n \in N \\ n > 1 \end{matrix} \qquad (2.15)$$

Flooded Water (n)

$$TDFW_{n,n+1}^{t} = \mu_n^t * \left(T_{n,n+1}^{t+}\right) \qquad \begin{matrix} \forall_n \in N \\ n > 1 \end{matrix} \qquad (2.16)$$

e) Losses

In river segment (n)

$$L_{n-1,n}^{t} = \propto_{n-1,n}^{t} * \left(X_{n-1,n}^{t}\right) \qquad \begin{matrix} n \in N \\ n > 1 \end{matrix} \qquad (2.17)$$

In segment between reservoir and transfer node (r)

$$L_{r,n}^{t} = \propto_{r,n}^{t} * \left(X_{r,n}^{t}\right) \qquad \begin{matrix} n \in N \\ n > 1 \\ \forall_r \in R \end{matrix} \qquad (2.18)$$

In segment between transfer and demand node (d)

$$L_{n,d}^{t} = \propto_{n,d}^{t} * \left(X_{n,d}^{t}\right) \qquad \begin{matrix} n \in N \\ n > 1 \\ \forall_d \in D \end{matrix} \qquad (2.19)$$

In Reservoir (r)

$$LP_r^t = \theta_r^t * (V_r^t) \qquad \forall_r \in R \qquad (2.20)$$

Of flooded water (n)

$$LFW_{n,n+1}^{t} = \Delta_{n,n+1}^{t} * \left(T_{n,n+1}^{t+}\right) \qquad \begin{matrix} n \in N \\ n > 1 \end{matrix} \qquad (2.21)$$

f) Floods

Flood water returning to river segment (n)

$$RW_{n,n+1}^{t} = T_{n,n+1}^{t+} - LFW_{n,n+1}^{t} - TDFW_{n,n+1}^{t} \qquad n \in N,\ n > 1 \qquad (2.22)$$

Water returning from a demand node to a reservoir node

$$RD_{r,d}^{t} = (1 - \propto_{r,d}^{t}) * \left(X_{r,d}^{t}\right) \qquad \forall_d \in D,\ \forall_r \in R \qquad (2.23)$$

The indices, parameters, variables and slack variables used in the LP model are given in Table 2.1.

Table 2.1. Notation and units of model indices, parameters and variables

Type	*Notation*	*Description*	*Unit*
Indices	i	input node ∈ I	-
	r	reservoir node ∈ R	-
	d	demand node ∈ D	-
	n	transfer node ∈ N	-
	t	time step ∈ T	-
Parameters	P_d	Penalty for not meeting the demand with one unit	Monetary units (mu)/volume (uv)
	E_d	Penalty for exceeding the demand with one unit	mu/uv
	F_d	Penalty for not meeting the minimum capacity in a demand segment with one unit	mu/uv
	G_d	Penalty for exceeding the maximum capacity in a demand segment with one unit	mu/uv
	W_n	Penalty for having a one unit flood in segment (n, n+1)	mu/uv
	B_n	Penalty for not meeting the minimum capacity in segment (n, n+1) with one unit	mu/uv
	U_n	Penalty for not meeting the minimum capacity of a reservoir with one unit	mu/uv
	A_n	Penalty for exceeding the maximum capacity of a reservoir with one unit	mu/uv
	$\propto_{n,n+1}^{t}$	Loss factor associated with the river segment (n, n+1) at time step (t), to be calibrated	-
	$\propto_{r,d}^{t}$	Loss factor associated with the reservoir node and a demand node (r, d) at time step (t), to be calibrated	-
	$\propto_{n,d}^{t}$	Loss factor associated with the transfer node and a demand node (n, d) at time step (t), to be calibrated	-
	$\theta_{\mathrm{r}}^{\mathrm{t}}$:	Loss factor associated to a reservoir at time step (t), to be calibrated	-
	$\mu_{n,n+1}^{t}$	Time delay factor associated with the water excess in a river segment (n, n+1) at time step (t), to be calibrated	-
	$\Delta_{n,n+1}^{t}$:	Loss factor associated with the water excess in a river segment (n, n+1) at time step (t), to be calibrated	-
	β_n^t:	Percentage of water that must flow from the nth node to the next one at step time (t), to be calibrated	-
	$\gamma_{n,}^{t}$:	Percentage of water that must remain in the nth node until the next time step (t), to be calibrated	-
	$\delta_{n,n+1}^{t}$:	Percentage of water that flows to the next node with a time delay in time step (t), to be calibrated	-
	$Cmin_{n,n+1}^{t}$	Minimum capacity of the river segment (n, n+1) at time step (t)	uv

	$Cmax_{n,n+1}^{t}$	Maximum capacity of the river segment (n, n+1) at time step step (t).	uv
	$Cmin_{n,d}^{t}$	Minimum capacity of a demand segment (n,d) at time step (t)	uv
	$Cmax_{n,d}^{t}$	Maximum capacity of a demand segment (n,d) at time step (t)	uv
	I_{i}^{t}	Amount of water arriving at the input node (i) at time step (t)	uv
	$Rmax_{r}^{t}$	Maximum capacity of a reservoir at time step (t)	uv
	$Rmin_{r}^{t}$	Minimum capacity of a reservoir at time step (t)	uv
Variables	V_{n}^{t}	Amount of water in a node (n) at time step (t)	uv
	$\mathrm{D}_{\mathrm{d}}^{\mathrm{t}}$	Amount of water needed to meet demand (d) at time step (t)	uv
	V_{r}^{t}	Amount of water in the reservoir (r) at time step (t)	uv
	$X_{n,n+1}^{t}$	Flow between the nodes (n) and (n+1) at time step (t).	uv / time step
	$X_{r,n}^{t}$	Flow between a reservoir node (r) and a transfer node (n) at time step (t)	uv / time step
	$X_{n,r}^{t}$	Flow between a transfer node (n) and a reservoir node (r) at time step (t)	uv / time step
	$X_{i,n}^{t}$	Flow between an input node (i) and a transfer node (n) at time step (t)	uv / time step
	$X_{i,r}^{t}$	Flow between an input node (i) and a reservoir node (r) at time step (t).	uv / time step
	$X_{n,d}^{t}$	Flow between a transfer node (n) and a demand node (d) at time step (t)	uv / time step
	$X_{r,\mathrm{d}}^{t}$	Flow between a reservoir node (r) and a demand node (d) at time step (t)	uv / time step
	TD_{n}^{t}	Delayed flow from upstream nodes and coming into node (n) at time step (t)	uv / time step
	$L_{n,n+1}^{t}$	Amount of water lost during the flow from transfer node (n) to transfer node (n+1) in time step t	uv
	$L_{r,n}^{t}$	Amount of water lost during the flow from reservoir node (r) to a transfer node (n) in time step t	uv
	$L_{n,\mathrm{d}}^{t}$	Amount of water lost during the flow from transfer node (n) to demand node (d) in time step t	uv
	LP_{r}^{t}	Amount of water lost in a reservoir node (r) during time step t	uv
	$LFW_{n,n+1}^{t}$	Amount of water lost from the water flooded while flowing from node (n) to node (n+1) in time step t	uv
	$RW_{n,n+1}^{t}$	Amount of flooded water flowing back to a node (n+1) from node (n) during time step t	uv
	$RD_{r,d}^{t}$	Amount of water flowing back to a reservoir node (r) from a demand node (d) in time step t	uv
	$TDFW_{n,n+1}^{t}$	Amount of water flowing from node (n) to node (n+1) with a delay due to flooding in time step t	uv
Slack Variables	$S_{n,d}^{t-}$	Amount of water that cannot be allocated to demand (d) at time step (t)	uv
	$S_{n,d}^{t+}$	Amount of water that exceeds the demand (d) at time step (t)	uv
	$\mathrm{T}_{\mathrm{n,n+1}}^{\mathrm{t+}}$	Amount of water above the maximum capacity of segment (n, n+1) at time step (t)	uv
	$\mathrm{T}_{\mathrm{n,n+1}}^{\mathrm{t-}}$	Amount of water under the maximum capacity of segment (n, n+1) at time step (t)	uv
	$Q_{n,n+1}^{\mathrm{t-}}$	Amount of water under the minimum capacity of segment (n, n+1) at time (t)	uv
	$Q_{n,n+1}^{t+}$	Amount of water above the minimum capacity of segment (n, n+1) at time step (t)	uv
	OF_{r}^{t+}	Amount of water above the maximum capacity of reservoir (r) at time step (t)	uv
	OF_{r}^{t-}	Amount of water under the maximum capacity of reservoir (r) at time step (t)	uv
	SH_{r}^{t-}	Amount of water under the minimum capacity of reservoir (r) at time step (t)	uv
	SH_{r}^{t+}	Amount of water above the minimum capacity of reservoir (r) at time step (t)	uv
	$MinXD_{n,d}^{t-}$	Amount of water under the minimum capacity of demand segment (n, d) at time step (t)	uv

$MinXD_{n,d}^{t+}$	Amount of water above the minimum capacity of demand segment (n, d) at time step (t)	uv
$MaxXD_{n,d}^{t-}$	Amount of water under the maximum capacity of demand segment (n, d) at time step (t)	uv
$MaxXD_{n,d}^{t+}$	Amount of water above the maximum capacity of demand segment (n, d) at time step (t)	uv

Equation (2.2) represents the mass balance constraint, i.e., the amount of water that comes into a node minus the leaving amount of water; this represents the change in water content of that node. This equation applies to all nodes except reservoir nodes for which Equation (2.3) applies.

Equations (2.4), (2.5) and (2.6) represent the limitations and capacity of the nodes/segments. Equation (2.4) considers inputs from different sources and the delivery to the corresponding node in the network. Equation (2.5) considers water coming directly from a river or any other water source (I_i^t) to a specific node. Equation (2.6) is related to the amount of water required by a specific demand node (D_d^t). This equation also represents the amount of water that cannot be allocated (S_d^{t-}) to a demand node. Thus, this value is used to penalize this mismatch. Besides, the term S_d^{t+}represents the amount of water exceeding the demand. This water is flowing back to the next river segment

Equations (2.7) and (2.8) define the capacity of and the required minimum amount of water in a river segment. In each of these equations, two slack variables $T_{n,n+1}^{t-}$ and $T_{n,n+1}^{t+}$ respectively. $Q_{n,n+1}^{t-}$ and $Q_{n,n+1}^{t+}$ are introduced. $T_{n,n+1}^{t+}$ takes a positive value when the capacity of the river segment is exceeded, i.e. when a flood occurs. This situation incurs a penalization. Equation (2.8) is related to the minimum amount of water required for the river segment and works in the opposite way as Equation (2.7). If the slack variable $Q_{n,n+1}^{t-}$ takes a positive value, a penalization is applied.

Equation (2.9) and (2.10) define the capacity and the minimum required amount of water in a reservoir (r) at a certain time (t). Both equations, in the same way as for a river segment, Equations (2.7) and (2.8) introduce slack variables to store the amount above (OF_r^{t+}, SH_r^{t+}) the capacity or below (OF_r^{t-}, SH_r^{t-}) the minimum requirement. In this case, the excess is penalized. A similar approach is taken through Equations (2.11) and (2.12) in which slack variables are introduced to avoid floods ($MaxXD_{n,d}^{t+}$) and shortages ($MinXD_{n,d}^{t-}$) in the demand segments.

The purpose of Equations (2.13) and (2.14) is to guarantee continuous water flow, also in the absence of any demand. In order to keep the water move, the fraction of the water that can remain in a node must be at least γ_n^t percent and less than β_n^t percent. Therefore, the remaining 1-β_n^t percent will flow through the segment to the next node.

Equations (2.15) and (2.16) express the time delays for a part of the water flowing between nodes. Equation (2.15) refers to water delayed from one transfer node to the next. Equation (2.16) determines the amount of water flowing over land to the next node after a flood. Parameters $\mu_{n,n+1}^t$ and $\delta_{n,n+1}^t$ represent the delay percentage in equations (2.15) and (2.16) respectively. These parameters are associated to the geographical characteristics of the nodes.

Equations (2.17) to (2.21) are introduced to model the water loss that occurs during the water transportation process. Equations (2.17), (2.18) and (2.19) are each related to one type of node (transfer, reservoir and demand): A percentage of the flow is lost. Equation (2.20) models the loss of water that is stored in a reservoir during time step t, typically through evaporation or seepage. Furthermore, equation (2.21) models the amount of water leaving the river system during a flood.

Excess water allocated to different uses might return to the main river (segment). Therefore, Equation (2.22) models the amount of water returning to a segment resulting from a flood upstream in the river network. It considers the amount of flooded water, a loss percentage as well as a delay in the return to the river system. Finally, Equation (2.23) models the amount of excess water returning from a demand node after reduction with a loss percentage. For instance, when a flood occurs in a river segment, part of water infiltrates to the ground and later returns to the river.

2.3. Case-study

2.3.1. Description

The network configuration used to test the allocation model is shown in Figure 2.2. In this network, the three types of nodes are present: two reservoir nodes (R1, R11), ten transfer nodes (T2, T3, T4, T5, T6, T8, T9, T12, T14, T15 and T17) and six demand nodes: D1(4), D2(7), D3(10), D4(13), D5(16), D6(18). The latter demand node D6(18) represents the downstream ecosystem that requires a permanent availability of a minimum amount of water.

The reservoirs are alimented with water coming from several rivers or overland flow (inputs I1, I2, I3, I10 and I11). Both reservoirs have a maximum capacity and must remain filled with a minimum volume of water. The latter is set to facilitate the appropriate functioning of the aquatic ecosystem of the reservoir.

The demand nodes obtain water either directly from a reservoir or via a transfer node downstream of the reservoir.

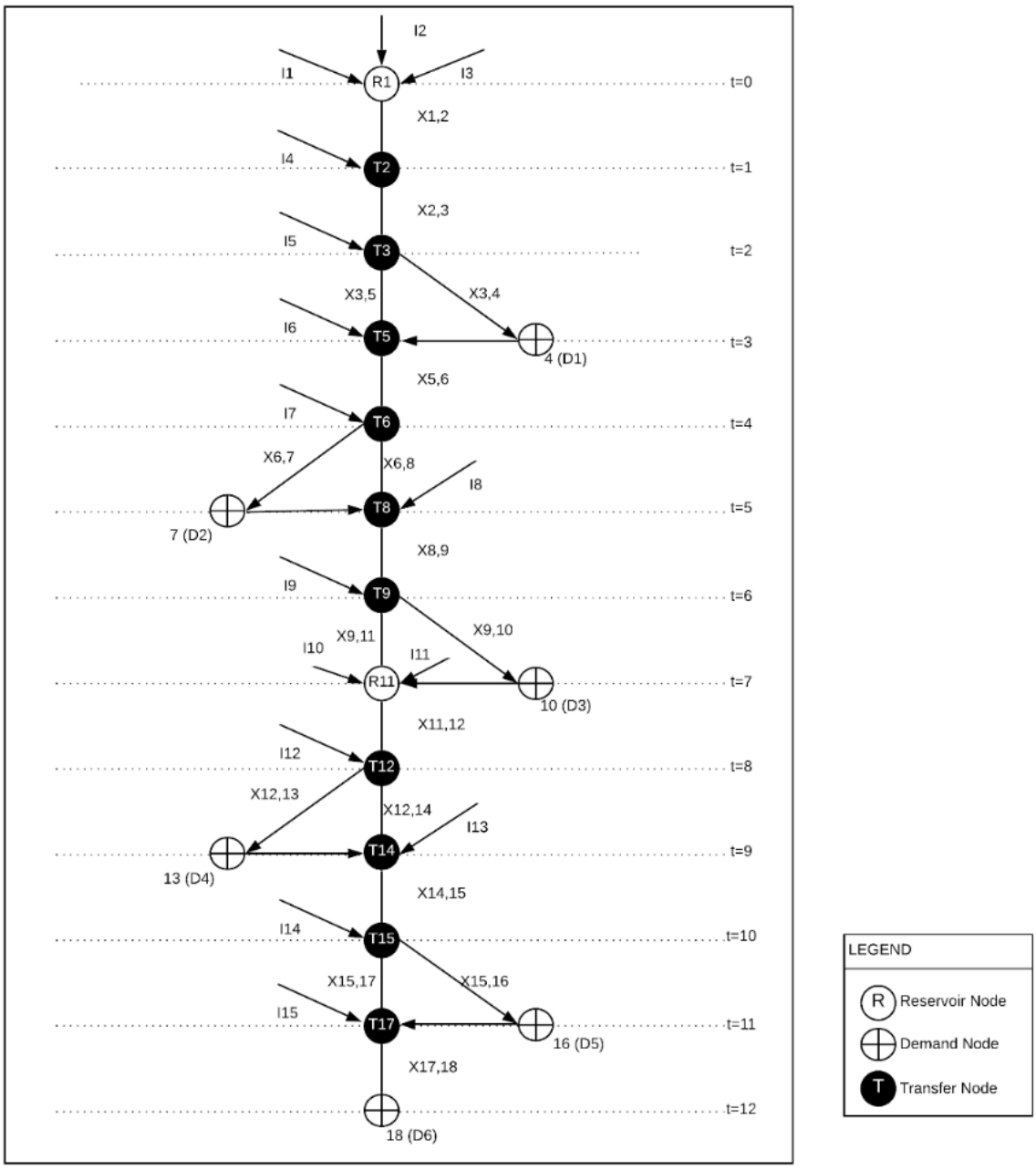

Figure 2.2. River-with reservoir-network configuration for case study

A river segment is defined by two nodes. As such segment X23 is represented as a connection between node T2 and node T3. Each river segment (X_{ij}^{t+1}) has a maximum discharge capacity. Floods occur in case this capacity is exceeded. Moreover, a minimum required volume of water is set for each river segment.

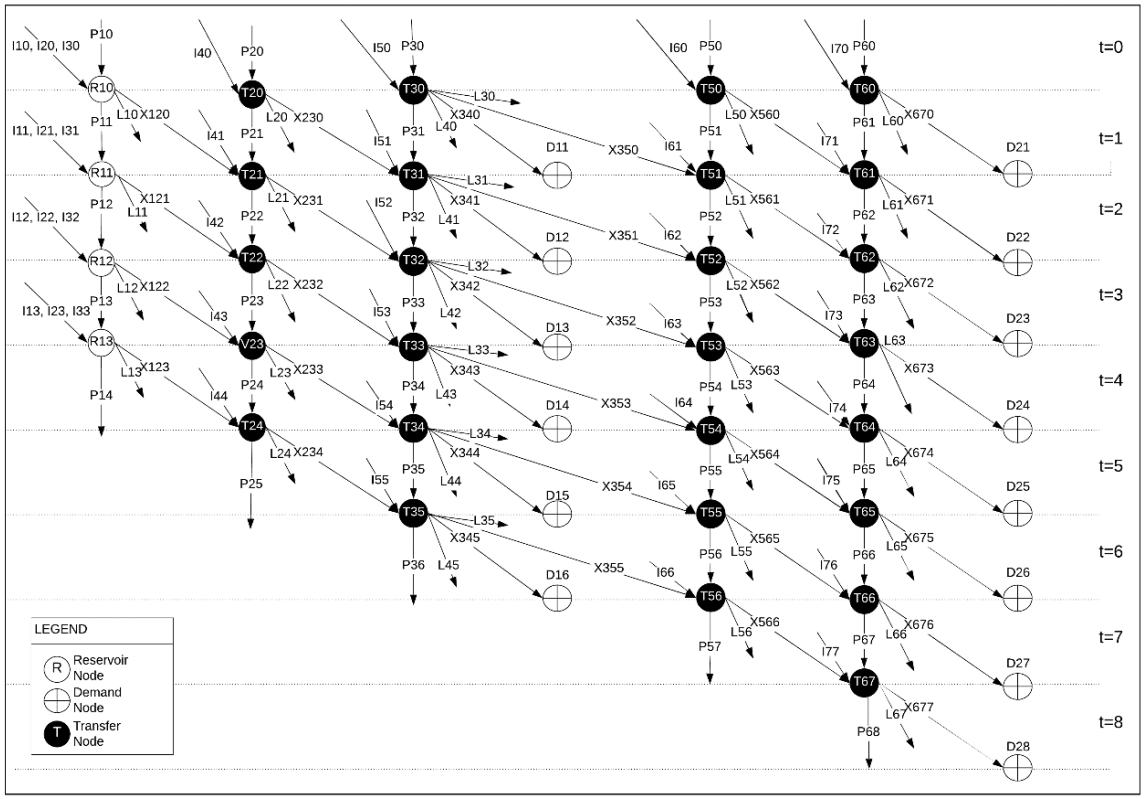

Figure 2.3. Scheme of how water flows through the network (from left to right) through time (from top to bottom; the second digit of the node-code refers to the time step)

Each node, segment and reservoir losses water through evaporation and seepage. To take these losses into account, loss factors have been included. The case study is limited to 15-time steps of which Figure 2.3 only shows the first 8 ones. The number of time steps depends on the network configuration. It is assumed that the network is configured such that water needs one time step to move to the next node, except when the return flow of flooded water to the river system is at stake. To make clear that water flows from node 1 (R1 - reservoir node) to node 2 (T2 - transfer node) the link between node R1 and T2 is tagged $X_{12}^{t=0}$. Water stored previously in a transfer node, is represented as an additional input (P). For instace, water remaining in node 2 (T2) at t=1 is denoted by P21. Hence, each node keeps a specific amount of water already stored in the node from the previous time step. On the other hand, two links start in node 3 (T3) at t=2: one is connected to node 4 (D1) (demand node) and the other to node 5 (transfer node). In this specific case, the total amount of water leaving node 3 (T3) is divided in two parts: one is allocated to node 4 (D1) and the other part flows directly through segment X35 to node 5 (T5) from which it is further distributed to the other nodes downstream.

Figure 2.3 shows how the water flows over the different time steps from the initial node (reservoir) to the final node (the ecosystem demand node in this use case). For the sake of simplification, only the first 8 of 15 time steps are considered. Each node has at least two inputs: water remaining in the node after the previous time step (V_i^{t-1}) and water coming directly from the upstream river segment (X_{ij}^{t-1}). In case the current node is a reservoir, extra inputs can be present. All nodes in this configuration have at least two outputs. The first

output is the water flowing to the next node in time (V_i^{t+1}) and the second output corresponds to the water lost ($\propto_{n,n+1}^{t}$)L. Furthermore, a third output can be present when a demand node is directly connected to a specific transfer node.

For this case study, the water demands are set constant (100 units of water) through time as: 100 (D1), 100 (D2), 100 (D3), 100 (D4), 100 (D5) and 100 (D6). The initial value in reservoirs 1 and 11 are 10000 units at time step t = 0. Extra inputs (units of water) are limited to t=0: 40 (I1), 10 (I2), 20 (I3), 40 (I5), 50 (I6), 60 (I8), 30 (I9), 40 (I11), 20 (I12), 30 (I14), 40 (I15) and 50 (I17). Inputs are no constant in time (arbitrary values are assigned). The loss factors ($\propto_{n,n+1}^{t}$, $\propto_{r,d}^{t}$, $\propto_{r,n}^{t}$ and θ_{r}^{t}) are set to 10%. This implies that the demanded amount plus this loss must be supplied considering a limitation in the capacity of 2000 units of water in each river segment. In order to avoid floods, a penalty value of 2 monetary units per unit excess water is considered. Moreover, a penalty (2 monetary units) is applied if a unit demand is not met. The initial value/ water content of river segments (X) is 0.01 units of water.

2.3.2. Results and discussion

The results of the model execution (penalties generated along the complete 15 time step period) are summarized in Figure 2.4 It is evident that, in the initialization stage (i.e. the first time step), only in node D6 (X1718) the demand was partially met; water received as an input is used directly to meet the first demand. Figure 2.4 also shows that from time step 5 onwards, penalties are decreasing due to a direct contribution from the first reservoir (node 1). In addition, we can see that from time step 11 onwards, all demands are met.

The orange line in Figure 2.4 indicates that the penalties amount to 1072 monetary units in time step 1, while in later time steps the penalties are reduced drastically. This behavior is explained by the optimal use of the water available in the reservoirs.

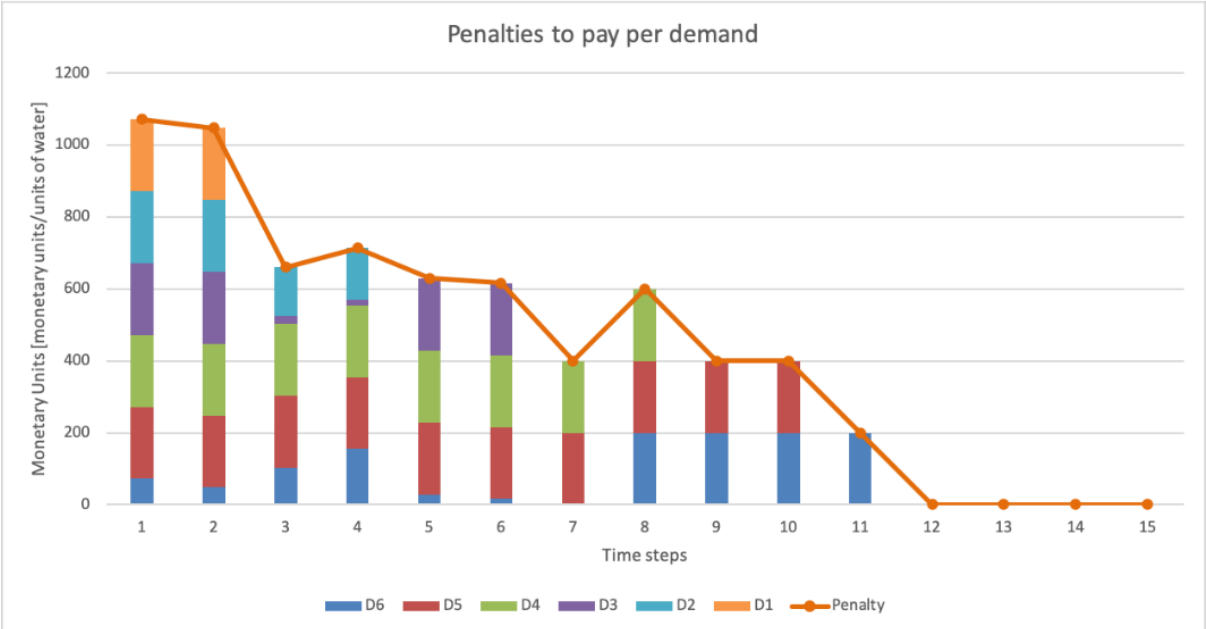

Figure 2.4. Evolution of the penalties incurred over the time steps

Figure 2.4 illustrates how water is flowing through the river segments. This value is the cumulative amount of water that entered the reservoir in the previous time period directly from the rivers (inputs). Each of the nodes along the network is receiving an additional amount of water in the initialization process. In time step 1, the amount of water flowing directly from node 1 (T1) to node 2 (T2) through segment 1 (X12_0) is 600 uv (Figure 2.5); this means that 9400 uv of water will remain in the reservoir for the next time step. In the same way, water passing from node 2 (T2) to node 3 (T3) at t = 1 is 600 uv; water flowing from node 3 (T3) to node 5 (T5) at t = 2 is 500; eventually node 18 (D6) is reached at time step t= 12 with 100 uv to meet demand node 18 (D6).

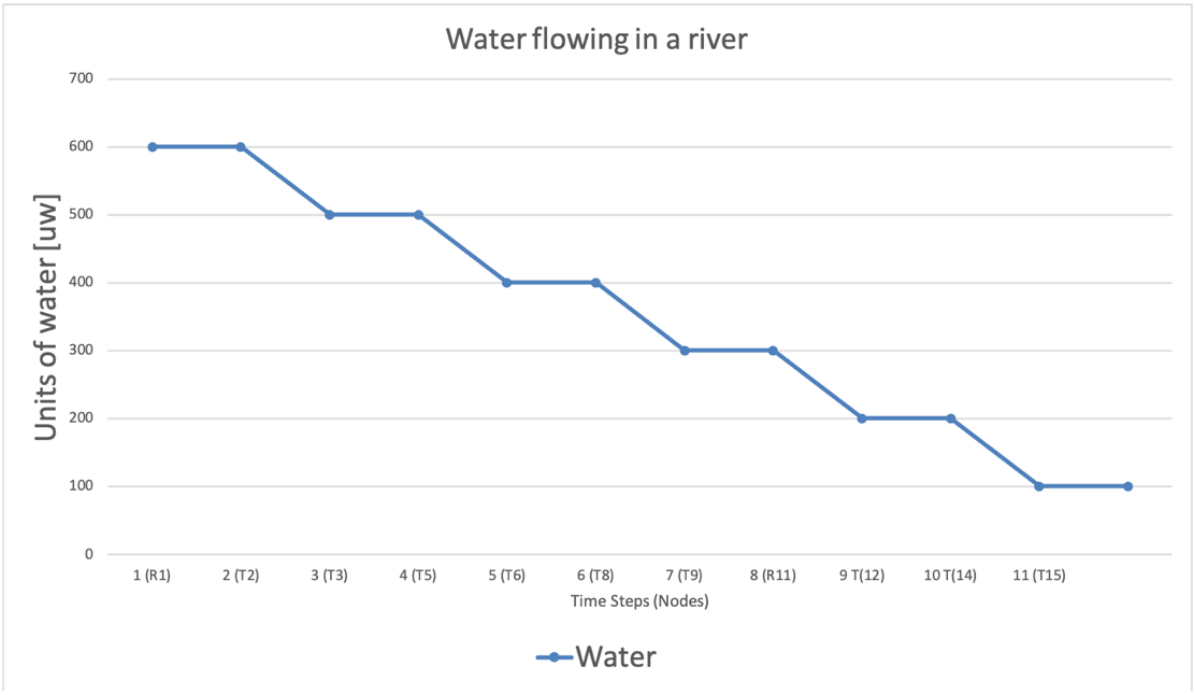

Figure 2.5. First 12 times steps for water flowing from node 1 (reservoir) to node 18 (ecosystem demand)

Figure 2.5 also shows that the amount of water flowing through the complete system is decreased when there is a demand node associated. For instance, there is a demand (D1) node (X34_3) which requires exactly 100 wu per time step. This pattern becomes constant until the end of the river segment at node 18 (D6). In this node, there is also a demand of 100 wu per time step.

Figure 2.6 shows the water available at each time step in the first reservoir (node 1 – R1). In this specific use case, maximum and minimum capacity constraints were set, i.e., reservoir levels started in 10000 units and stayed above 500 units. Additionally, no extreme rainfalls/inputs were considered during this period. Therefore, floods did not occur and the corresponding penalties were avoided.

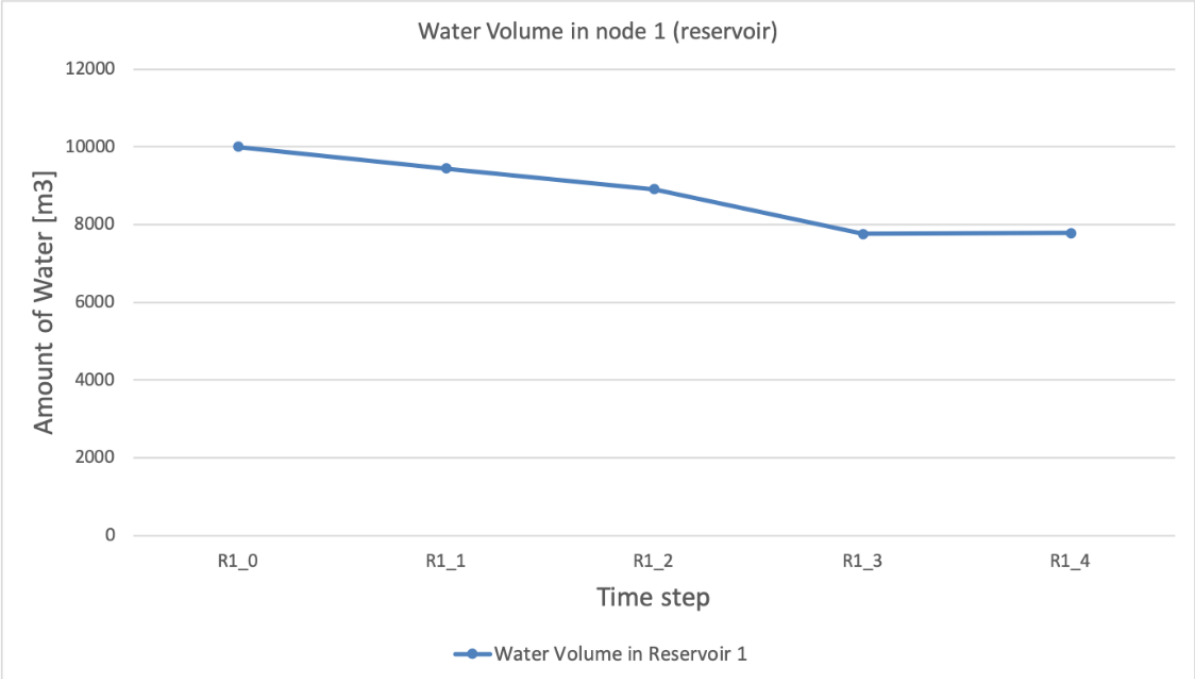

Figure 2.6. Evolution of the amount of water present in the first reservoir

2.4. Conclusions

In this chapter, we approached the spatio-temporal allocation of water available in a river-with-reservoirs system to multiple users as a network flow optimization problem. A generic linear programming model was formulated considering spatially and temporally distributed inputs to and demands for water from the system and specifying reservoir and transportation capacity constraints. The model was tested by means of a hypothetical use case and revealed a satisfactory behavior since water can be allocated to the different demands while constraints are being satisfied. Encouraged by these results, we plan to introduce more complexity into the model in order to make it applicable to real world cases (chapter 3 and 5). Thus, constraints related with: a) water availability which is variable with time and space; b) water demands which are variable with time and space; c) capacities of reservoirs reduces due to the sedimentation process; d) building and management cost when a new reservoir is required.

Chapter 3
Application of the NFO-LP model for optimizing surface water allocation in the Machángara River Basin, Ecuador

The core of this chapter was published as:

Veintimilla-Reyes, J., De Meyer, A., Cattrysse, D., Tacuri, E., Vanegas, P., Cisneros, Felipe, & Van Orshoven, J. (2019). MILP for Optimizing Water Allocation and Reservoir Location: A Case Study for the Machángara River Basin, Ecuador. Water, 11(5), 1011. https://doi.org/10.3390/w11051011

3.1. Introduction

In this chapter, the Network Flow Optimization Linear Programming model (NFO-LP) proposed in chapter 2 (Veintimilla-Reyes et al., 2017) is applied to the Machángara river-with-reservoir basin in Ecuador.

Whereas in chapter 2, the NFO-LP-model parameters requiring calibration were identified, a default value was assigned to them so that the model principles could be demonstrated for a hypothetical river-with-reservoir system. Apart from applying and evaluating the model for a real-world system, a main objective of this chapter is to come up with and illustrate a procedure for calibration of these model parameters.

The data used for setting up and evaluating this model was provided by the (PROMAS, 2019). This data encompassed a digital elevation model, geodatasets of soil and land cover/land use types and of river segments, locations and characteristics of reservoirs, locations and time series of water demand and georeferenced time series of daily meteorological data. By means of the ArcSWAT-extension of the ArcGIS-software (Texas A&M University, 2009) the geometry of the WSN was generated and time series of water inputs in the various nodes of the WSN computed. The period for which data were available was split in three sub-periods, one for calibration of the parameters of the NFO-LP-model, one for validation and one for application.

In a first step, default values were assigned to all model parameters. The calibration phase was then executed in order to tune the model parameters according to reality. This was done in an iterative trial-and-error process. The validation phase was then carried out to verify the correctness of the parameter values obtained during the previous phase. During the validation, parameters were allowed to be adjusted again. Finally, during the application phase, the model was executed to allocate water among the different demands so that penalties were minimized.

3.2. Materials and Methods

3.2.1. Study Area

3.2.1.1. The Machángara River Basin

The Machángara River Basin is an Andean basin located in the Azuay and Cañar provinces in the south of the republic of Ecuador (Figure 3.1). The total area of the basin is 323.55 km^2. The Machángara river is an affluent of the Cuenca River which in turn belongs to the hydrographic demarcation of the Santiago River, which is one of the tributaries of the Amazon River (Jerves-Cobo et al., 2017).

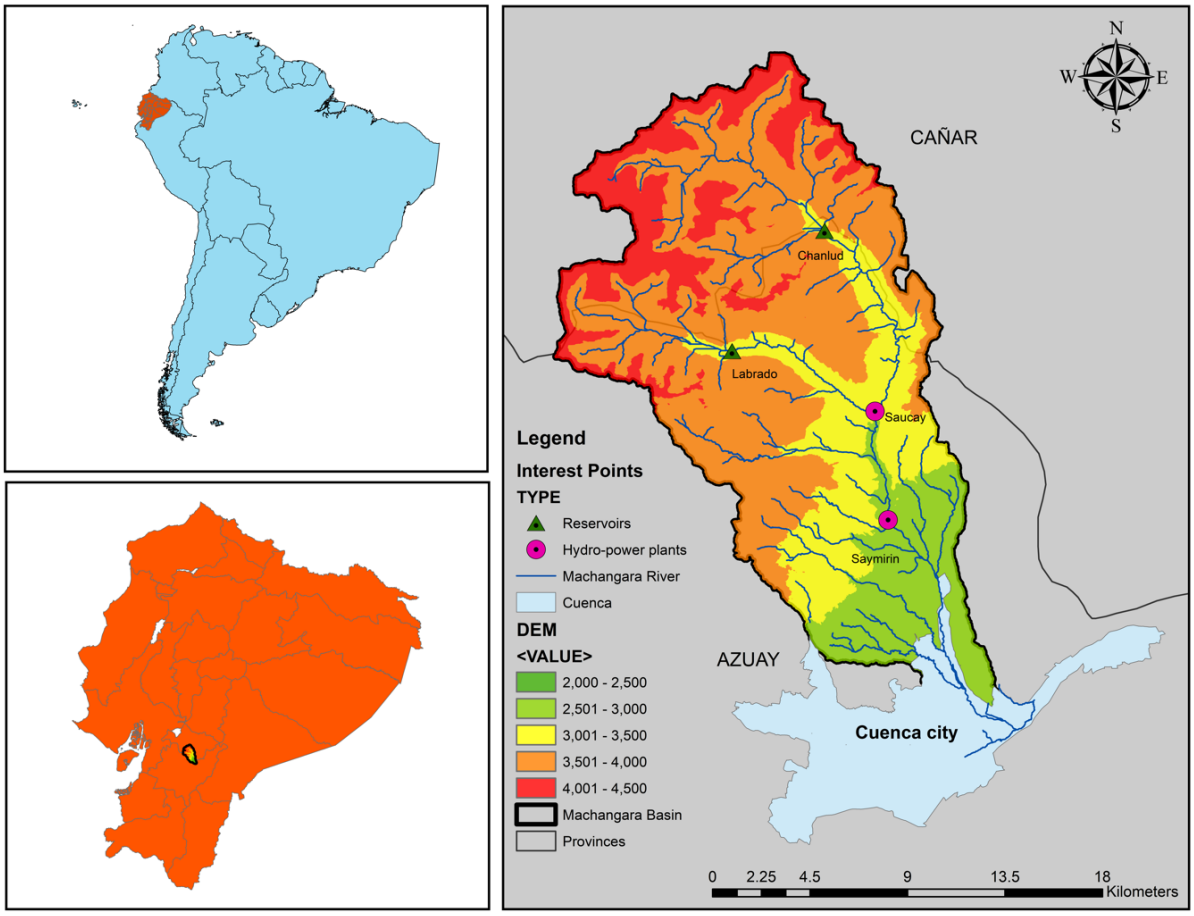

Figure 3.1. Machángara River Basin in the south of Ecuador (based on data provided by Programa para el Manejo del Agua y el Suelo, Universidad de Cuenca, Ecuador (PROMAS, 2019))

The length of the main branch of the Machángara river is about 37 km. It crosses the capital of the Azuay province, Cuenca (INEC, 2010). The altitude in the basin ranges between 2424 masl and 4436 masl with an average of 3420 masl. According to PROMAS, (2019a), land use types in the basin are spatially distributed as follows: 6.4% is populated area, 11.3% cropland, 0.5% infrastructures, 59.1% paramo (a treeless vegetation type occurring at higher altitudes), 9.3% pasture, 1.2% native forest, 4.2% forest plantation, 6% shrub vegetation, 1% other herbaceous vegetation, and 1% water bodies (Figure 3.2). Land cover map was generated based on RapidEye classification (2010).

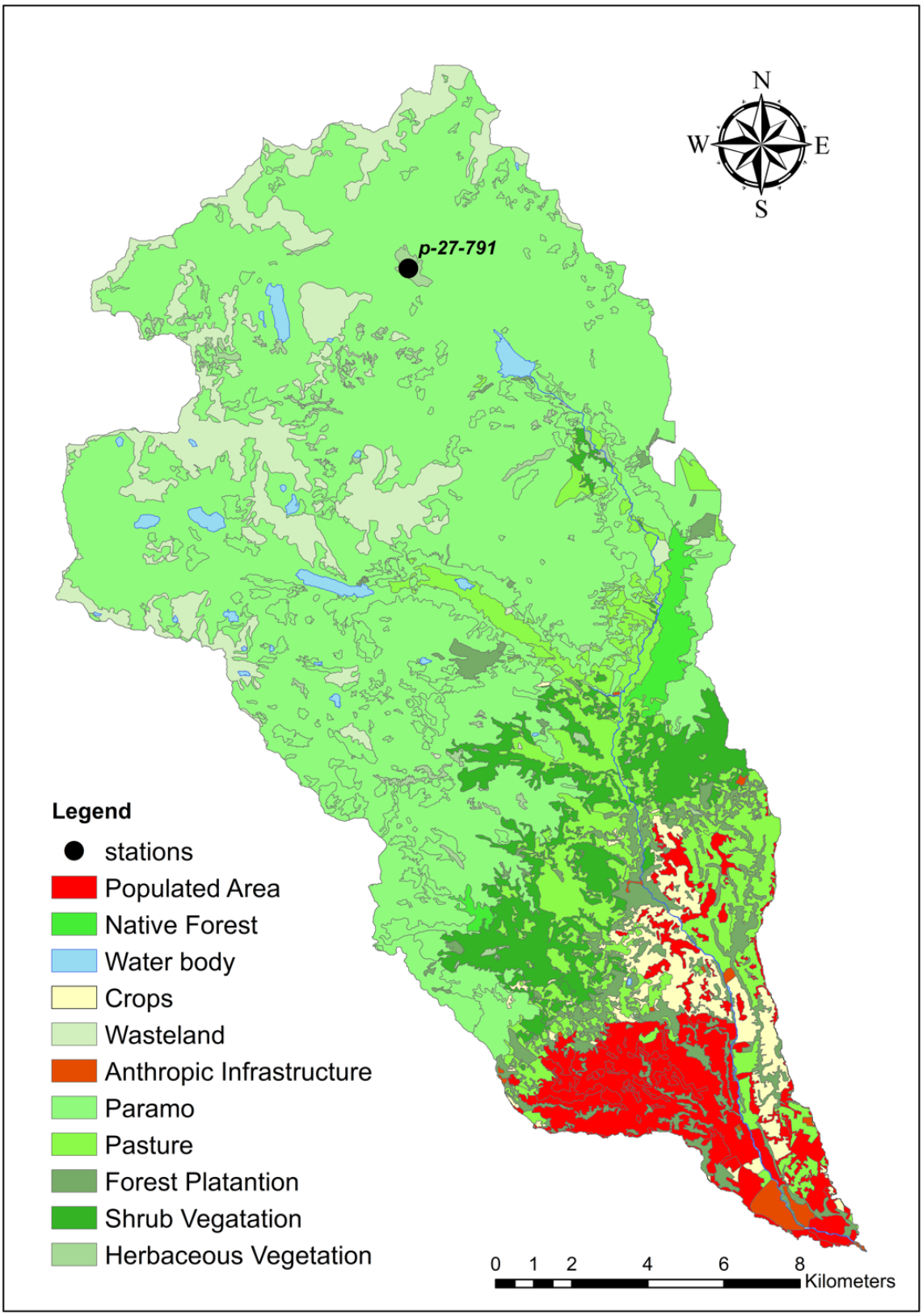

Figure 3.2. Land use distribution in the Machángara basin (based on data provided by Programa para el Manejo del Agua y el Suelo, Universidad de Cuenca, Ecuador (PROMAS, 2019)

The average annual rainfall depth is 3090 mm of which 2900 mm pertains to the wet season (October–May) and 190 mm to the dry season (June-September). In the 2006-2013 period, rainfall events surpassing 60 mm were not exceptional during the wet season (Figure 3). In the years 2011, 2012 and 2013, total annual rainfall was significantly lower than the average while extreme rainfall events were less frequent or even absent (2013) (Jacobsen & Encalada, 2016). Information data was extracted from the Climate Forecast System Reanalysis (CFSR) global weather dataset of the National Centers for Environmental Prediction (NCEP) (Texas A&M University, 2018). This dataset contains only one weather station, called "P-27-791" located in the Machángara basin. This station can be considered as a "virtual station" since the weather data was the result of a modelling by the Global Weather Data for SWAT project (Texas A&M University, 2018).

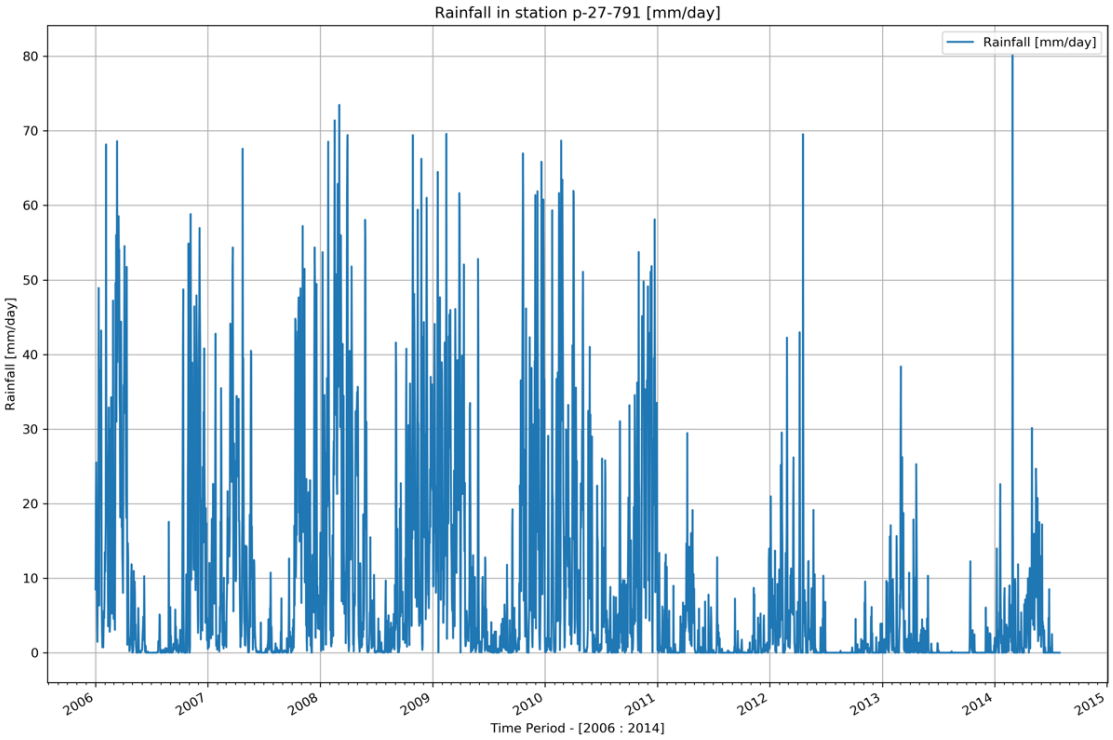

Figure 3.3. Modelled daily rainfall for the period 2006–2014 in station P-27-791 (rainfall) located in the Machángara Basin. Source: Climate Forecast System Reanalysis (CFSR) (Texas A&M University, 2018).

Figure 3.4 (left panel) shows a temperature chart and in the right panel a climatogram for the city of Cuenca (Ecuador). Cuenca is located near the outlet of the Machángara river at an altitude of 2550 masl. The average monthly temperature ranges throughout the year from 12 °C to 14 °C. The warmest month is November, with an average of 13.5 °C and the lowest temperatures are observed in July, with an average of 10.9 °C. The climatogram in the right panel of Figure 4 indicates that the driest month is August with an average of 63 mm of rainfall and the wettest month is March, with an average of 190 mm. annual rainfall is around 1612 mm.

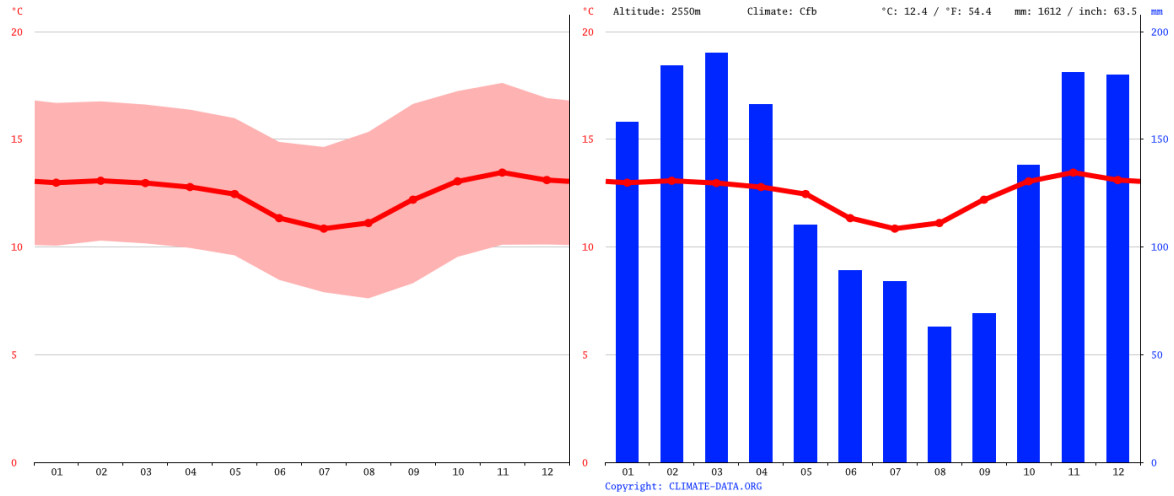

Figure 3.4. Temperature chart (left) and a climatogram (right) of the city of Cuenca, Ecuador for the period 2006 – 2014 (Climate-Data.org, 2019)

3.2.1.2. Reservoirs, hydropower production and other water uses

The water of the Machángara river is used mainly for domestic and industrial purposes, irrigated agriculture, and hydropower generation. Two reservoirs (Chanlud and Labrado) and two hydropower plants with reservoirs (Saucay and Saymirin) are located along the Machángara river.

The Labrado reservoir is located 40 km north of the city of Cuenca at 3500 masl. Its storage capacity is 6.15 hm^3 (1hm^3 = 1E+06 m^3)(Elecaustro, 2011, 2014; Matute, 2014). The regulated discharge is 2.4 m^3/s (Elecaustro, 2014; Herrera & Carrera, 2017; Matute, 2014).

The Chanlud reservoir is located 45 km to the north-east of Cuenca. Its storage capacity is 17 hm^3; the maximum discharge is 4.18 m^3/s. The outflow of this reservoir enters the two reservoirs of two hydropower plants (Saucay and Saymirin) as well as the Tixán drinking water treatment plant. The Chanlud reservoir also provides water to several irrigation systems and integrates flood control mechanisms (Matute, 2014).

The Saymirin reservoir is located 15 km to the north of Cuenca. The maximum discharge is 4.10 m3/s It serves several hydropower units with a cumulated installed capacity of 7.5 MW (Elecaustro, 2014; Matute, 2014).

The Saucay reservoir is located 24 km to the north of Cuenca. Its associated hydropower plant has an installed capacity of 24 MW. Its turbines require a maximum discharge of 7.2 m^3/s (Elecaustro, 2011, 2014; Matute, 2014).

The hydroelectricity generated by the Saucay and Saymirin plants is used to cover the requirements of the provinces of Azuay, Cañar and Morona Santiago, which amounted to a total population of 1,313,334 inhabitants in 2018 (Elecaustro, 2014; SENPLADES, 2019).

In the Machángara basin, there is approximately 1300 hectares of irrigated cropland and 133 industrial estates are registered as water users. The Tixán drinking water plant processes 0.6 m^3/s to supply water to 140,000 inhabitants of Cuenca city (Matute, 2014).

3.2.2. Linear Programming model for optimizing water allocation

3.2.2.1. Introduction

The NFO-LP model introduced in chapter 2 is meant for an optimal spatio-temporal allocation of the water available in a river system to several spatially distributed and temporally variable demands. The model requires a network schematization of the river system in which reservoir nodes and transfer nodes are connected by river segments while demand nodes are connected to a reservoir or a transfer node by a demand segment. Reservoir and transfer nodes are characterized by a time series of incoming water while demand nodes are characterized by a time series of water demand. Moreover, reservoirs and segments have minimum and maximum capacities. Exceeding the maximum capacity leads to flooding and a delayed return flow of part of the flooded water to the river. Not reaching the minimum capacity leads to flow discontinuity and pressure on biodiversity. The objective function of the model (Equation (2.1) in chapter 2) is formulated as to allocate water from the reservoirs to the demand nodes in order to meet the demands optimally, minimize floods of reservoirs and segments, and minimize the non-fulfilment of the minimum capacities.

3.2.2.2. Preliminary River Network Configuration and Water Availability

The configuration of the Machángara river network used in this chapter, was derived from a Digital Elevation Model (DEM) with a resolution of 3 meters using the ArcSWAT-extension of the ArcGIS-software (2012.10.21, University A&M Texas, College Station, TX, USA) (Texas A&M University, 2009). ArcSWAT makes use of the hydrology toolbox of the ArcGIS-software. It extracts the boundaries of a basin and its sub-basins and the flow paths using the flow accumulation algorithm. Transfer nodes are created at the outlet of each sub-basin while reservoir nodes must be added by the user. To obtain a time series of water inflow in the network through the transfer nodes, in the absence of discharge measurements, a rainfall-runoff simulation was performed, using the same ArcGIS-extension. To this end, each sub-basin is discretized into so-called Hydrological Response Units (HRUs), which are assumed to be homogeneous in terms of slope class, soil type and land cover type. For each HRU the rainfall-runoff relationship is modeled by assessing the soil water balance in which the runoff is estimated using the curve number method (Texas A&M University, 2009). All water running off from an HRU is assumed to end up in the river system after a time delay. Finally, the inflowing water is propagated through the river segments to eventually reach the outlet. ArcSWAT can quantify major hydrological processes by using water balance equations (chapter 2, section 2.2). The ArcSWAT model generates hydrographs at all nodes. The core of ArcSWAT is the Soil and Water Assessment Tool (SWAT) (Texas A&M University, 2009). SWAT is a semi-distributed model of the land and river phase of the hydrological cycle that has been developed to quantify the impact of land management practices on water, sediment, and agricultural chemical yields. SWAT also models physical processes related to water movement, sediment movement, crop growth, etc. Figure 3.5 displays the DEM-derived slope map and the soil map, the scale if soil map is 1:200000 and this map is the result of the

research project fund by PRONAREG (Dirección de Regionalización Agraria, Ecuador) – ORSTOM (Office de la Recherche Scientifique et Technique d'Outre-Mer, France) from January 1984. Regarding the DEM, the resolution is 20 m and the scale is: 1:2500, this map was produced by Hidropaute (2000). Land cover map was generated based on RapidEye classification (2010).

Daily weather data (rainfall, solar radiation, temperature, relative humidity, and wind direction) were retrieved through the Global Weather Data tool which is accessible from the SWAT-website (Texas A&M University, 2018) (section 3.2.1). For this study area, only one weather station (Figure 3.2) was available, with modelled data for the period 1979–2014. In this study, only data for 2006 –2013 were effectively used.

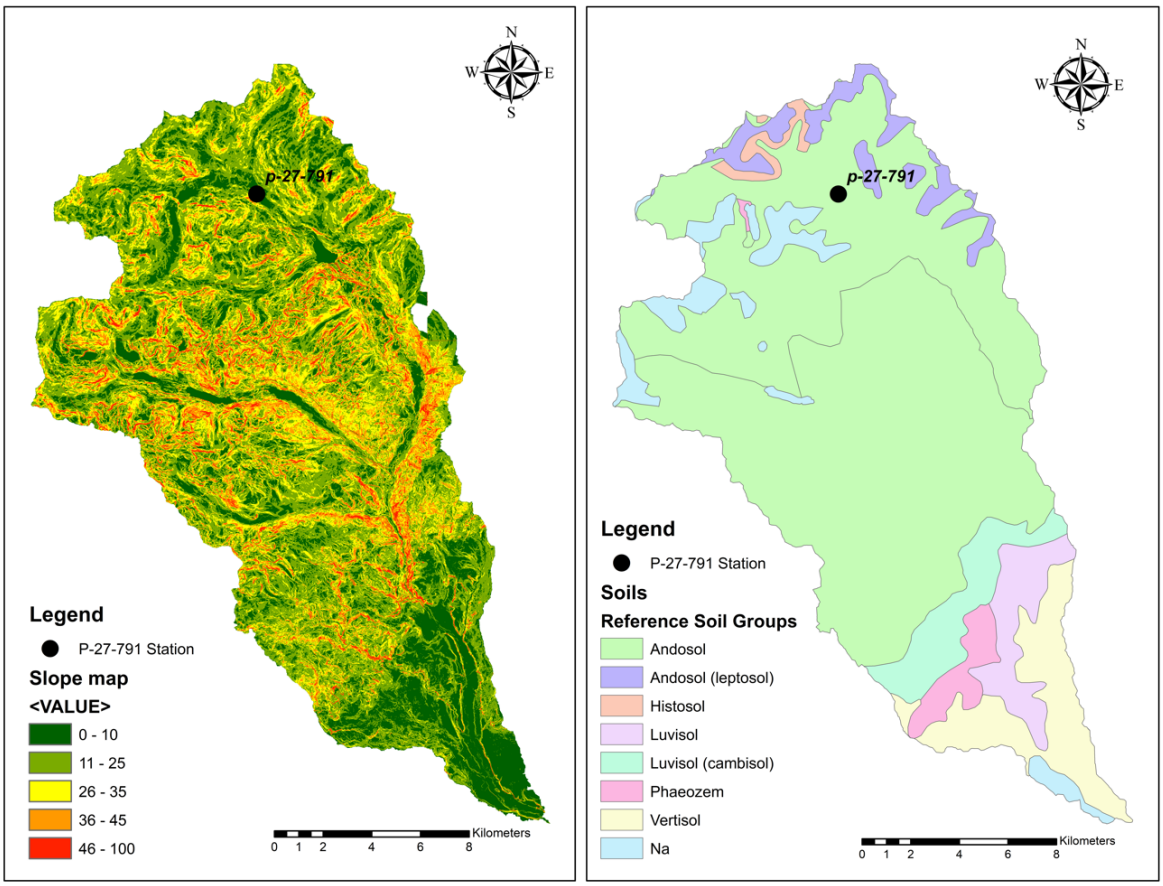

Figure 3.5. Digital slope model (degrees) and soil map of the Machángara basin (PROMAS, 2019).

Figure 3.6 shows the basin subdivision and network configuration generated by ArcSWAT encompassing a) the outlets or transfer nodes (red or blue points), b) the river segments (blue lines), and c) the reservoirs (pink points). A transfer node is a location through which water flows from a previous segment to the connected segment. Similarly, a river segment is the portion of the river that connects two nodes. A reservoir node represents a location where a reservoir is present. Additionally, demand nodes represent locations where water is abstracted for various uses.

In Figure 3.6, each transfer node is identified by a code "Tx", while the code "Rx" is used for reservoir nodes: R1 is Chanlud, R2 is Labrado, R3 is Saucay and R4 is Saymirin. The map in

Figure 3.6 also includes the location of the virtual weather station “p-27-791” (Texas A&M University, 2018).

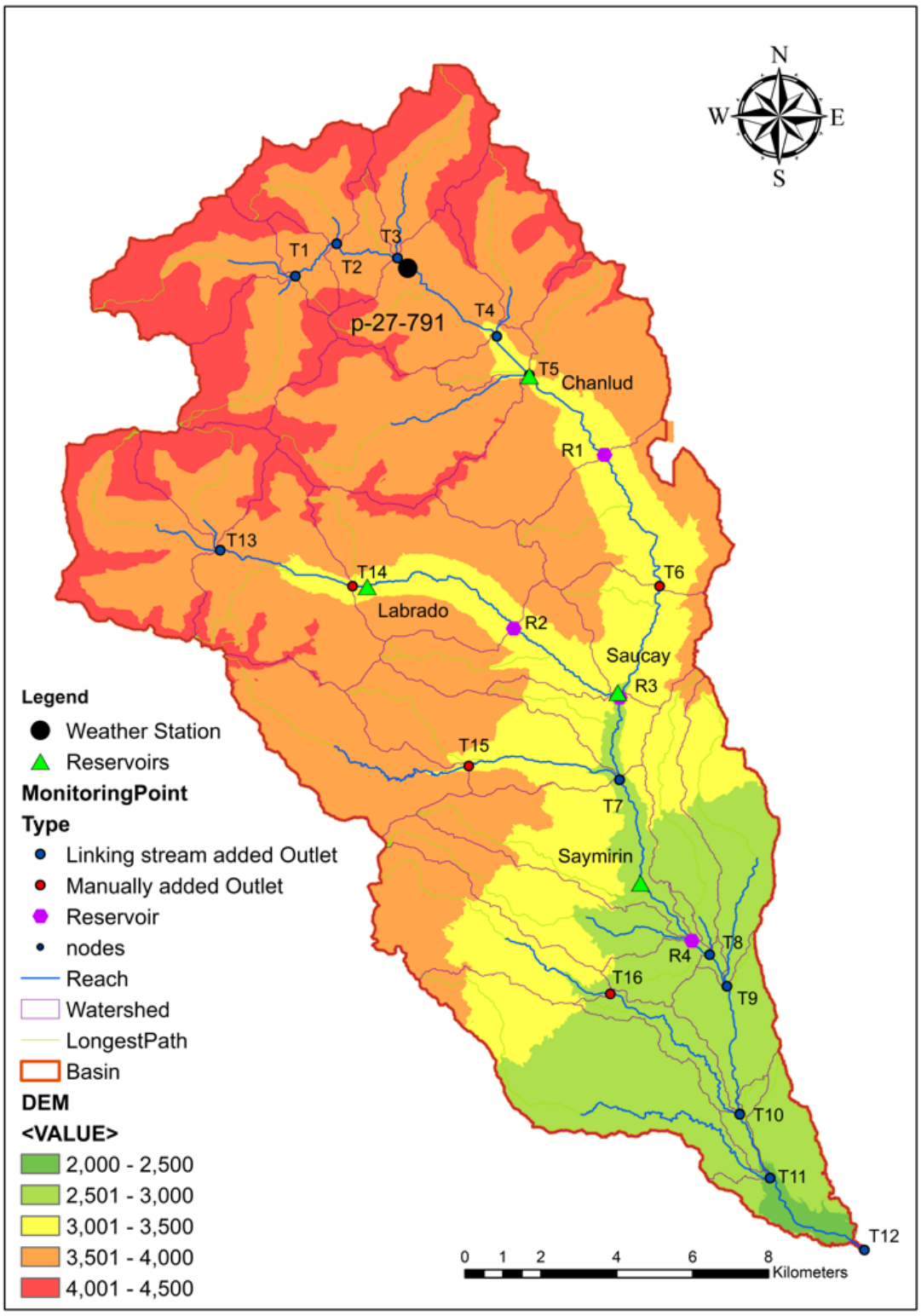

Figure 3.6. River network configuration for the Machángara basin.

Figure 3.7 shows the inflow (m^3/s), simulated using ArcSWAT, for transfer node T1 over the period 2006–2013. The rainfall pattern from Figure 3.3 is clearly reflected: intensive rains in the beginning of the year and a drastic reduction starting in the middle of the year.

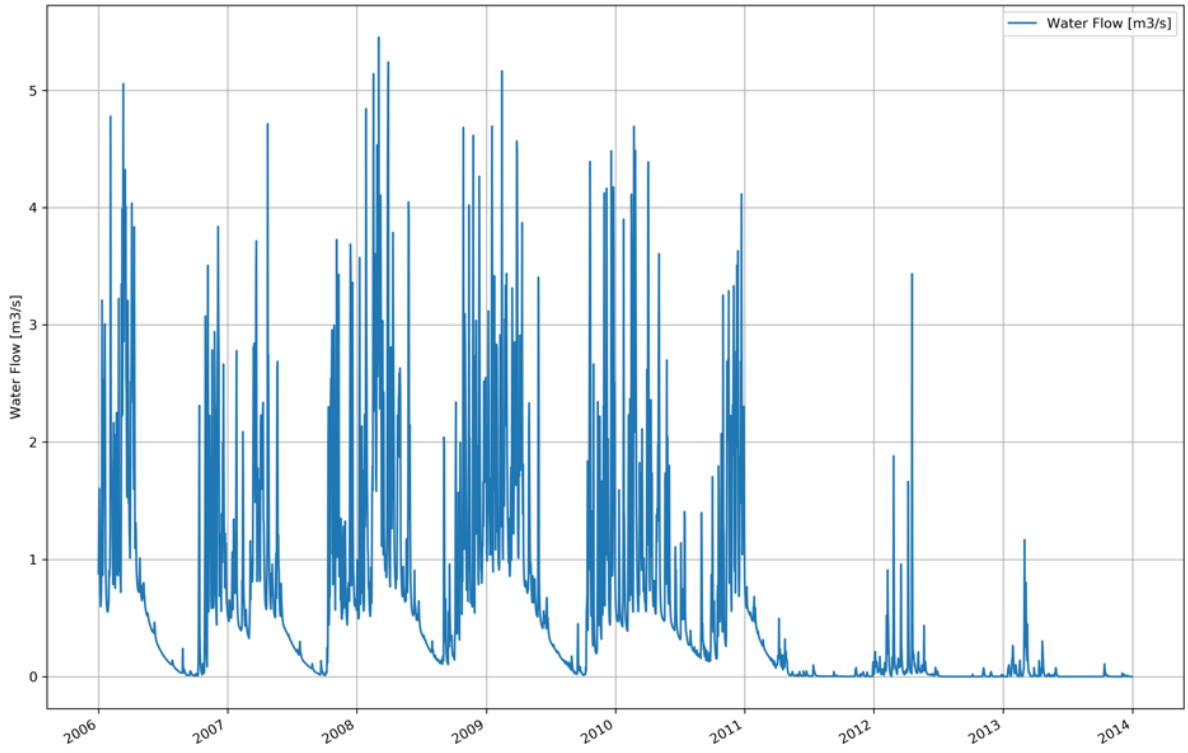

Figure 3.7. Simulated water inflow in the Machángara river system at transfer node T1 (the total sum of the outputs of all subbasins).

3.2.2.3. Water Demand and Final River Network Configuration

The network configuration resulting from the preprocessing consists of 16 transfer nodes (T), 4 reservoir (R) nodes and 19 river segments. The length and width of each segment were derived from Google Earth, assuming a depth of 3m to compute the cross section (FAO, 2017; Google, 2007).

This preliminary network is yet to be extended with demand nodes (D) and related demand segments so that it can be used as a basis for the NFO-LP linear programming model (Figure 3.8).

In order to incorporate the water abstraction in the configuration, 6 demand nodes were added. The first demand node (D1) is associated with reservoir node R3 and corresponds to the amount of water required daily by R3 (Saucay) to generate hydroelectricity. Water used to generate electricity is assumed to flow back to the river through the next node with a delay of one-time step. The second demand node (D2) is associated with the irrigation system Machángara. The third demand node (D3) is associated with reservoir R4 (Saymirín) and represents the amount of water required by this hydropower plant. The fourth demand node (D4) is associated with the drinking water treatment plant Tixán and is connected directly with transfer node T7. The fifth demand node (D5) encompasses the amount of water needed by the irrigation system Ricaurte and it is connected to node T10. The last demand node (D6) represents the minimum amount of water that needs to flow out of the system in order to preserve its ecological functioning. For the present exercise, the water demands of all six nodes are assumed to be constant through time, this assumption is not realistic water

requirements may change throught time and space. Although the model is able to work in this way, data is not completely available in the area. These demand values were calculated based as a daily average of the water requirements from the operation of the power plants as well as the irrigation requirements in the area. The corresponding amounts are listed in Table 3.1.

Table 3.1. Daily water required by the demand nodes (PROMAS, 2019).

Node	Use	Value (hm^3/day)
D1	Saucay powerplant	0.6208
D2	Machángara irrigation system	0.0432
D3	Saymirín powerplant	0.6912
D4	Tixán drinking water system	0.12096
D5	Ricaurte irrigation system	0.02592
D6	Ecosystem function	0.01728
Note: 1 hm^3 = 1E+06 m^3		

Figure 3.8 shows the final network configuration with the main river (Machángara) and the three tributaries (Chulco, Chachayacu and Patamarca). The Chulco river is connected to the Machángara river through reservoirs R2 and R3. The Chachayacu river provides input to transfer node T15 and the corresponding segment is connected to the Machángara river through transfer node T7. Finally, the Patamarca river provides input to node T16 and is connected through node T10 with the Machángara river. It is assumed that water needs one-time step (one-time step corresponds to one day in this case study) to flow from one node to the next.

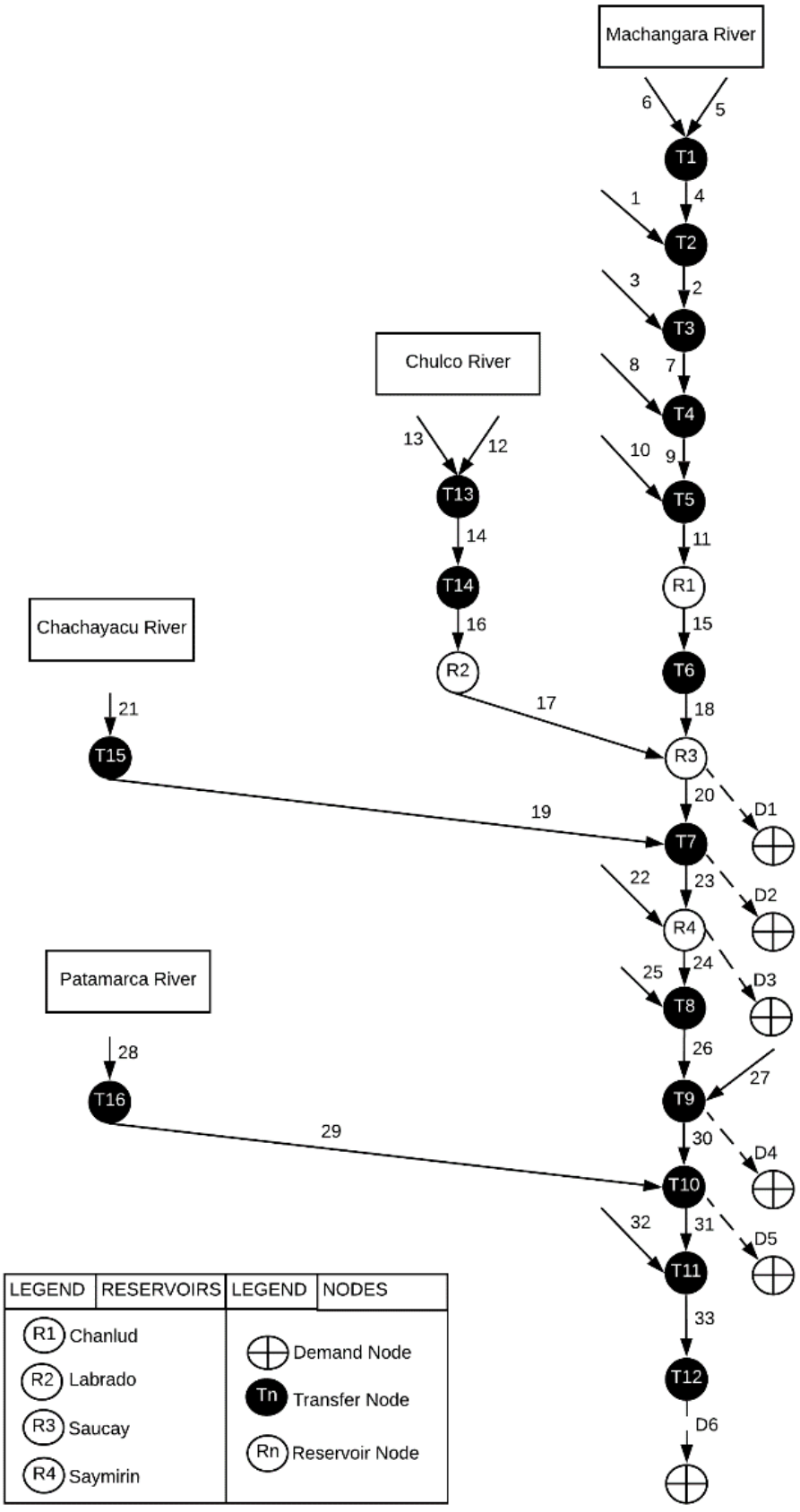

Figure 3.8. The final network configuration of the Machángara river system.

3.2.2.4. Objective Function and Constraints

The objective function of the linear programming model is the one presented in Equation (2.1) of chapter 2 (Veintimilla-Reyes et al., 2016a, 2016b; Veintimilla-Reyes, De Meyer, et al., 2018; Veintimilla-Reyes, Meyer, et al., 2018) , while the applicable constraints are expressed in Equations (2.1)–(2.23) in chapter 2. Furthermore, indices, parameters, variables and slack variables appearing in the objective function and in the constraint, equations are explained as well in chapter 2.

The objective function of the LP model minimizes the total penalty resulting from water allocation through time to the spatially distributed demand nodes in the network. The total penalty is the result of penalization of the water excess in river segments (floods, T), shortage in river segments (Q), shortages in allocation to demand nodes (S^{t-}), excess allocation to demand nodes or water flooding (S^{t+}), shortage in reservoirs (SH), overflow of reservoirs (OF), shortage in demand segments (MinXD), and overflow of demand segments (MaxXD).

Whereas the list and meaning of the indices, parameters, variables and slack variables used in the LP-model are given in Table 2.1 of chapter 2, in Table 3.2 only the penalty parameters and their value are given and also the parameters to be calibrated, with their initial value.

Table 3.2. Penalties and parameters with their assigned value for this case study. The parameter values will be further calibrated.

Type	Notation	Description	Unit	Value Use Case
Penalties	P_d	Penalty for not meeting the demand with one unit	euro/hm³	1.0
	E_d	Penalty for exceeding the demand with one unit	euro/hm³	20.0
	F_n	Penalty for not meeting the minimum river segment capacity with one unit	euro/hm³	5.0
	G_n	Penalty for exceeding the maximum capacity in a demand segment with one unit	euro/hm³	20.0
	W_n	Penalty for having a one unit flood in segment (*n, n+1*)	euro/hm³	4.0
	B_n	Penalty not meeting the minimum capacity in a demand segment (*n, n+1*) with one unit	euro/hm³	2.0
	U_n	Penalty for not meeting the minimum capacity of a reservoir with one unit	euro/hm³	8.0
	A_n	Penalty for exceeding the maximum capacity of a reservoir with one unit	euro/hm³	7.0
Parameters	$\propto^t_{n,n+1}$:	Loss factor associated with the river segment (*n, n+1*) at time (*t*)—to be calibrated	-	0.1%
	$\mu^t_{n,n+1}$:	Time delay factor associated with the water excess in a river segment (*n, n+1*) at time (*t*) to be calibrated	-	0.1%
	$\Delta^t_{n,n+1}$:	Loss factor associated with the water excess in a river segment (*n ,n+1*) at time (*t*) to be calibrated	-	20%
	β^t_n:	Percentage of water that must flow from the nth node to the next one at time (*t*), to be calibrated	-	10%
	$\gamma^t_{n,}$:	Percentage of water that must remain in the nth node until the next time step (*t*), to be calibrated	-	1%
	$\delta^t_{n,n+1}$:	Percentage of water that comes to the next node with a time delay in time step (*t*) to be calibrated	-	0.1%
	θ^t_r:	Loss factor associated to a reservoir to be calibrated	-	0.1%
Note: Penalty values are assigned in order to establish priorities over constraints				

Reservoirs

In Table 3.3, the characteristics of the four reservoirs present in the study region are given: the initial volume of stored water and the maximum and minimum volume of water allowed.

Table 3.3. Reservoir characteristics considered in the LP-model.

Node	Reservoir	Initial Value (hm^3)	Maximum Capacity (hm^3)	Minimum Capacity (hm^3)
17	R1	5	6.15	1.23
18	R2	15	16.3	3.26
19	R3	0.7	1	0.2
20	R4	0.7	1	0.2

To run this use case, parameters and configurations from ArcSWAT were set to the default values except the information related to the reservoirs. Reservoirs used the information included in Table 3.3. Regarding water in river segments, it was assumed that flow is reaching the minimum capacity in order to keep the ecosystem functioning. The initial value in the segment was an arbitrary value.

3.3. Results

3.3.1. Calibration and Evaluation of the LP-Model

Seven parameters of the LP-model listed in Table 3.2 need to be calibrated. Since observed data on water availability and flow in the river system were not available, the water flow in the nodes of the river configuration computed by the ArcSWAT-tool was taken as the reference. The first four years (2006–2009) of data of the studied period (2006–2013) were used for calibration. For an appropriate calibration, the LP-model was used in simulation rather than in optimization mode just like was done for generating the reference flows by means of ArcSWAT. This was configured by setting the water demands to zero.

3.3.1.1. Calibration

The seven parameters in the LP model that require calibration are $\propto_{n,n+1}^{t}$; $\Delta_{n,n+1}^{t}$; θ_{r}^{t}; $\delta_{n,n+1}^{t}$; $\mu_{n,n+1}^{t}$; β_{n}^{t} and $\gamma_{n,}^{t}$ (Table 3.2). All these parameters represent fractions ranging from 0 to 1.

For this process, all water demands were set to 0 in order to determine the influence of the parameters in the water flow. In a first step, a sensitivity analysis was carried out. Each parameter was iteratively adjusted by a 0.05 step, covering the range from 0 to 1. For each combination of parameter values, the model was executed, and the component penalties and total penalty computed. Charts A to F in Figure 3.9 display the results of this univariate sensitivity analysis. For two parameters, i.e., the minimum and maximum fractions of the amount of water that must remain in the node (β) (γ), there is only one chart (F) since beta (β) must always be smaller than gamma (γ) to avoid that the model becomes infeasible. Thus, as more water stays in a node the node is acting like a reservoir. Figure 3.9 shows that parameter θ (loss factor in reservoirs – chart C) is the most sensitive one.

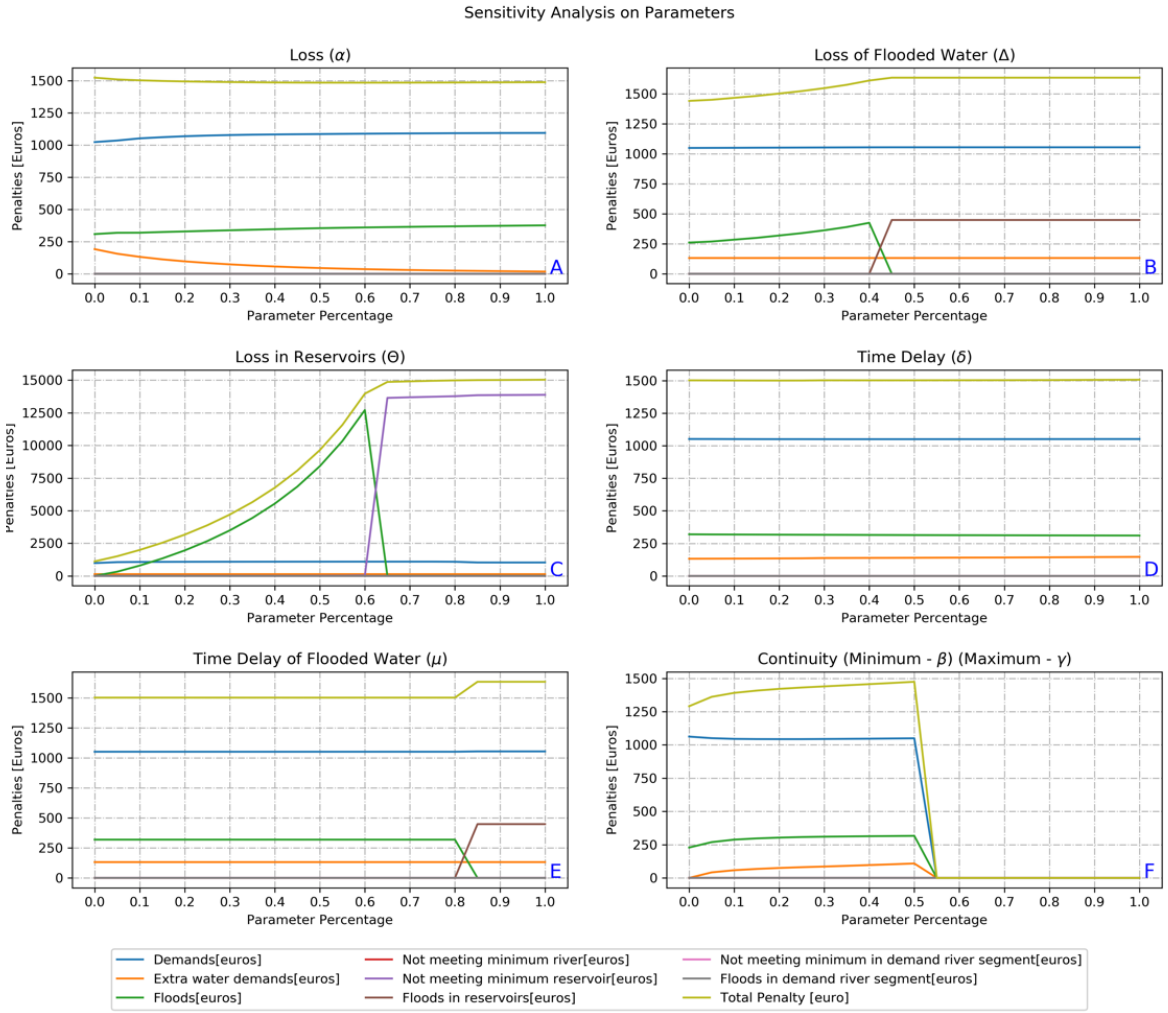

Figure 3.9. Results of the sensitivity analysis performed on the LP-model parameters.

Based on this sensitivity analysis, the calibration consisted of an iterative trial-and-error procedure in which the most sensitive parameters were adjusted in order to minimize the difference between the total penalty value obtained from the LP model and the reference value generated by the ArcSWAT model. The adjustment was not performed for each of the 19 segments but rather for each of five branches of the river system as depicted in Figure 3.10. These branches were identified by taking into account the connectivity of their segments.

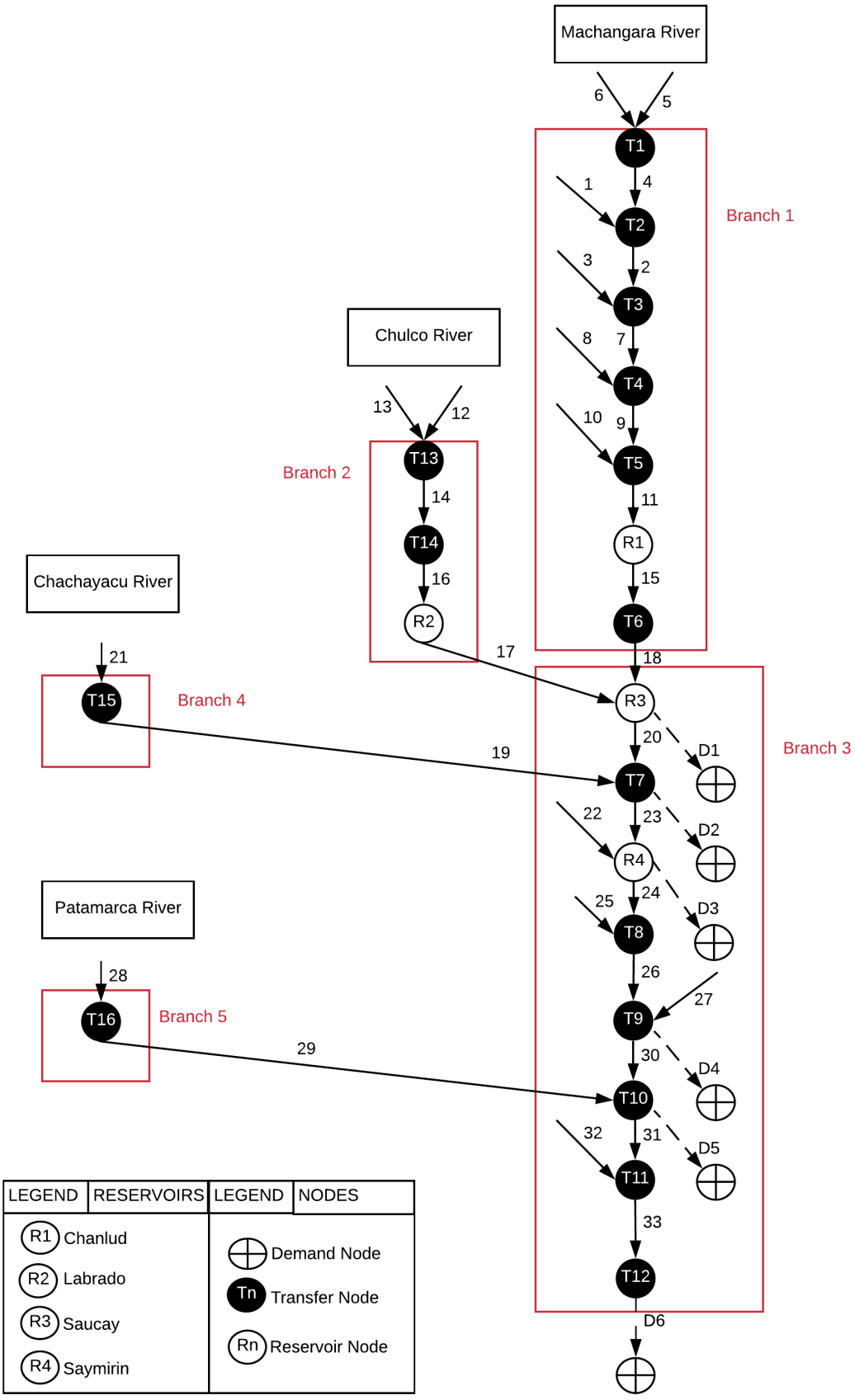

Figure 3.10. River network branches used for the calibration of the LP-model parameters.

Table 3.4 shows the default values assigned to each branch before the calibration process. The first iteration uses values between 0 and 1 (Table 3.4). Once this iteration is finalized, the total penalty is calculated and this value is compared with the values from the previous iterations. Later, based on the sensitivity analysis, most influent parameters are adapted and the model is executed again to obtain new penalty values.

Table 3.4. Default parameter values assigned to the five branches

Parameter	Loss (∝)
Loss (∝)	0.001
Loss Flooded Water (Δ)	0.01
Time Delays (δ)	$1x10^{-5}$
Time Delay Flooded Water (μ)	0.001
Minimum Water to Stay (β)	0.01
Maximum to Stay (γ)	0.1
Loss in Reservoirs (θ)	0.001

Table 3.5. Initial and calibrated value for the parameters of the LP model.

Use cases	Adapted parameter	Branch	Original value	New value	Sum of RMSD [hm³]
Use case 1	-	-	-	-	62.81
Use case 2	Minimum water to stay (β)	1,2,3,4,5	0.01	0.0001	62.22
	Maximum water to stay (γ)		0.1	0.0002	
Use case 3	Loss (∝)	1,2,3	0.001	$1x10^{-5}$	62.54
Use case 4	Time delays (δ)	1,2,3	0.001	$1x10^{-5}$	62.49
Use case 5	Loss in reservoirs (θ)	1,2,3	0.001	$1x10^{-5}$	62.56
Use case 6	Loss in reservoirs (θ)	1,2,3	$1x10^{-5}$	0.01	62.55
Use case 7	Time Delay Flooded Water (Δ)	1,2,3	0.01	0.001	62.49
Use case 8	**Time delays (δ)**	1,2,3	**$1x10^{-5}$**	**0.01**	**61.90**
Use case 9	Minimum water to stay (β)	1,2,3	0.0001	0.001	62.30
	Maximum water to stay (γ)	1,2,3	0.0002	0.002	

$$RMSD = \sqrt{\frac{\sum_{i=1}^{n}(P_i - O_i)^2}{n}} \tag{3.1}$$

The Root Mean Square Deviation (RMSD) was used to evaluate the performance of the LP-model. This indicator is calculated based on equation (3.1). Where, P_i is the value calculated by the model; O_i is the value obtained from the reference model (ArcSWAT). Thus, this indicator determines the deviation of the output of the LP-model (values of water in each node) from the reference model (ArcSWAT). From Table 3.4 and Figure 3.11, it is notorious that the most suitable parameters are met during the use case 8 with a value of 61.90 hm^3.

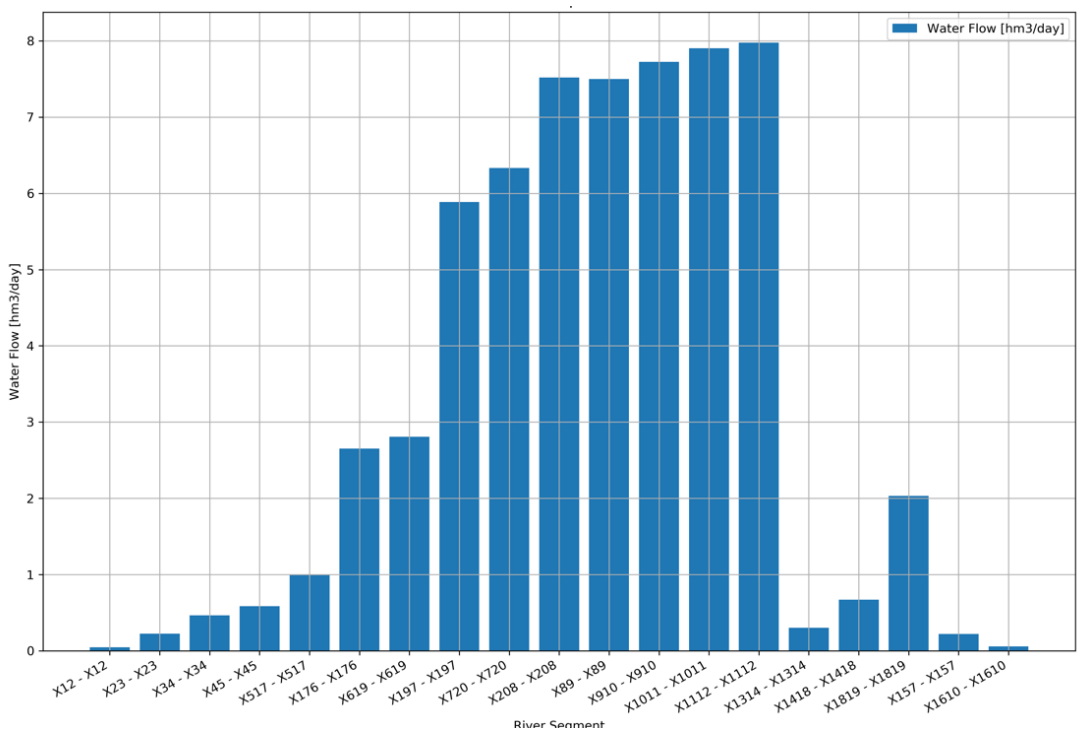

Figure 3.11. Root Mean Square Deviation [hm³/day] between the simulated water flow in ArcSWAT (reference) and the simulated water flow by the LP model using the parameters of use case 8 for the 2006-2009 time period.

3.3.1.2. Validation

The evaluation of the parameterized LP-model was performed again with no water demand values and by comparing its outputs with the resulting ArcSWAT time series for the period 2010–2011 (Figure 3.12). The parameter values used are the ones obtained from the calibration process (dataset 2006–2009).

The purpose of the evaluation process was to verify whether the parameter values obtained from the evaluation process are appropriate when the model is applied for different conditions. In this execution the total sum of RSME was 45.13 hm^3 which is 25% lower than at calibration. Hence the NFO-LP-model was judged to be fit for application for cases with non-zero demands.

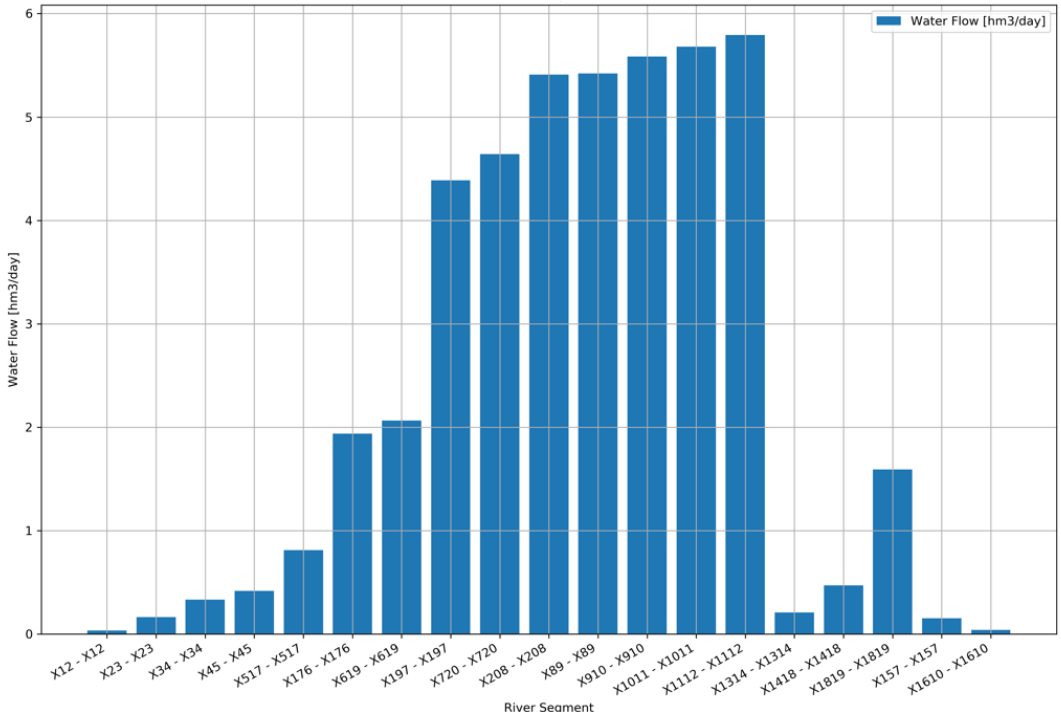

Figure 3.12. Root Mean Square Deviation [hm³/day] between the simulated water flow in ArcSWAT (reference) and the simulated water flow by the LP model for the period 2010 - 2011.

3.3.2. Application of the Calibrated and Validated LP-model

The calibrated and evaluated LP-model was applied to the period 2012–2013 (using the outputs for the period 2010–2011 to initialize the model) with the purpose of optimally allocating the available water to the demand nodes (Figure 3.8) considering their daily demands for water (Table 3.1) and the unit penalty values of not meeting or exceeding these demands and the penalties related to the river segments ($\propto$, Δ, δ, μ, β, and γ), the reservoirs (θ), and the demand segments ($\propto$, Δ, δ, and μ) (Table 3.2).

Figure 3.13 shows the total volume of water stored in each of the four reservoirs during the considered 2012-2013 period whereby the maximum value corresponds to the maximum reservoir capacity shown in Table 3.3. In reservoir R1 (Node 17), the seasonal rainfall pattern and water levels are always between the maximum and minimum capacities. This reservoir is located upstream on the main river "Machángara." Reservoir R2 (node 18) is also located upstream, but in the "Chulco" subbasin. Despite optimal water allocation, this reservoir is gradually exhausted. Reservoirs R3 (node 19) and R4 (node 20) are located downstream in the river system and receive water directly from tributaries apart from regulated water inputs through the upstream reservoirs. This regulation is clearly visible in the fact that the seasonal rainfall pattern is no longer present. Besides, from Figure 3.13, it is noticeable that reservoir R3 has a non-stable behavior in the first part of the data from 2011, this could be the result that reservoirs in the upper part of the study area are full and water is flowing directly to this reservoir.

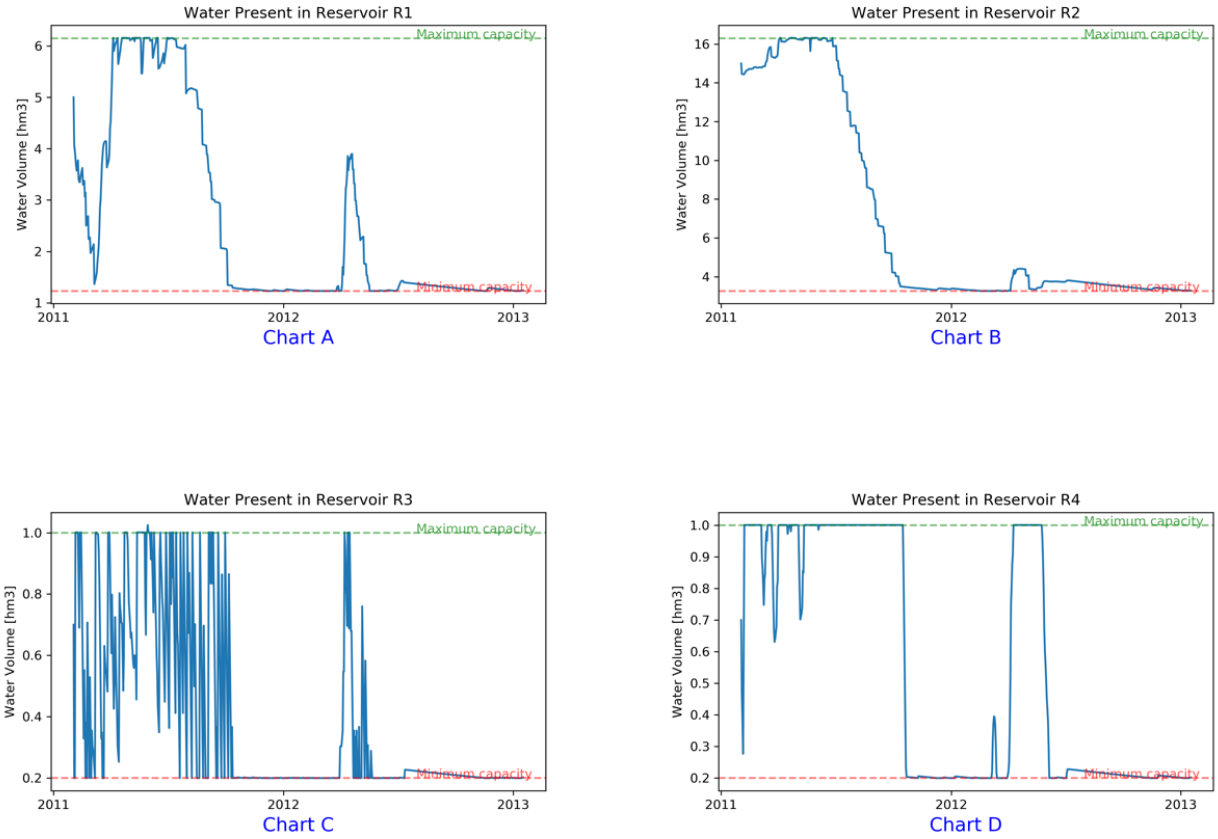

Figure 3.13. Volume of water stored in reservoirs

3.3.2.1. Penalties

From Table 3.6 and Figure 3.14 it is clear that the major terms in the total penalty are the shortages in the amount of water delivered to the demand nodes (chart A), starting in the second half of the 2-year period, and the delivery of an excessive amount of water in the first six months of the period. This behavior corresponds to the seasonal pattern of rainfall distribution. This means extreme rain during the first half of the years 2011 and 2012 and dry periods during the second half the same years. However, for this particular case, the second half of 2012 and the first half of 2013 is unusually dry.

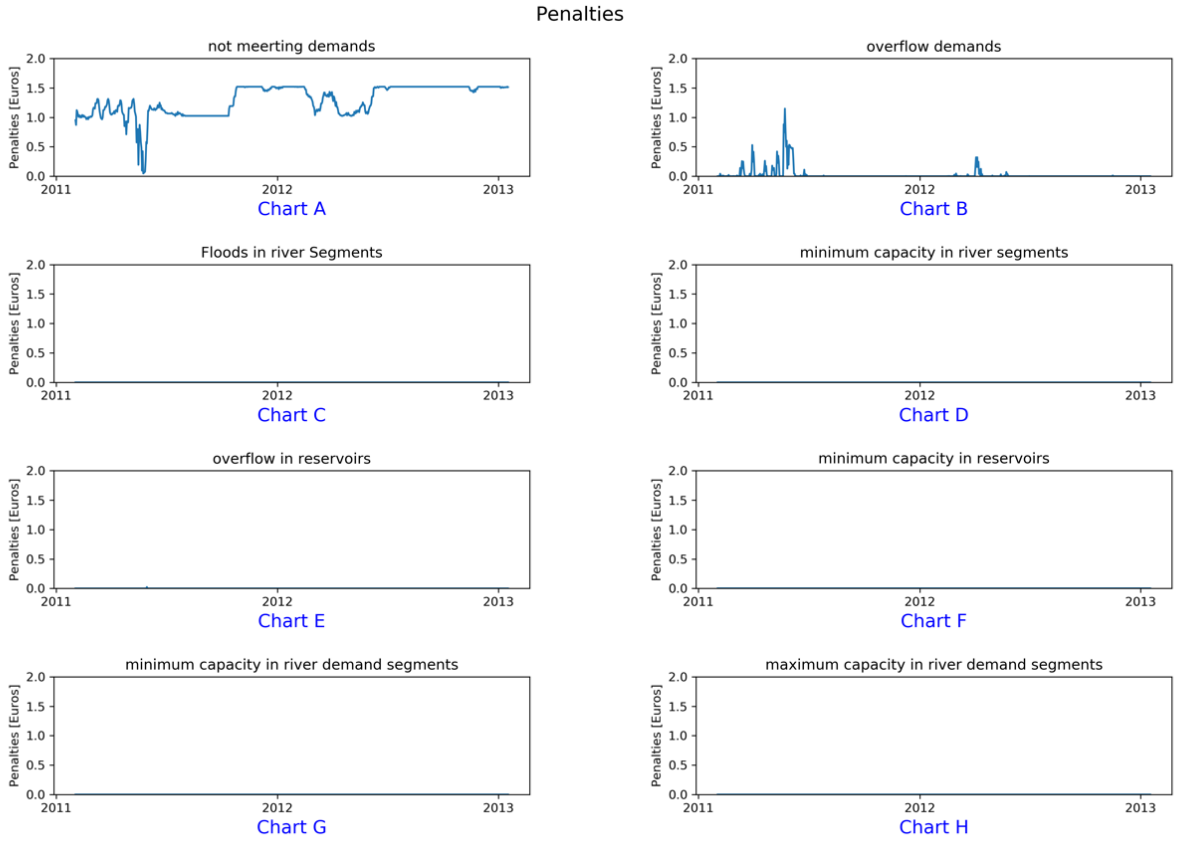

Figure 3.14. Penalties during the 2-year period; charts C - H have not penalties.

Table 3.6. Deviation of the aimed volume of water from the volume achieved after optimization (hm^3) and associated penalties (€).

Penalty cause	Volume [hm^3]	Values [euros]
(A) Penalty for not meeting the demands	920.81	920.81
(B) Penalty for floods the demands	17.17	343.48
(C) Penalty for floods in river segments	0.00	0.00
(D) Penalty for not meeting the minimum capacity in the river segments	0.00	0.00
(E) Penalty for floods in reservoirs	0.03	0.18
(F) Penalty for not meeting the minimum capacity in reservoirs	0.00	0.00
(G) Penalty for not meeting the minimum capacity in demand segments	0.00	0.00
(H) Penalty for flooding in demand segments	0.00	0.00
Total (A) + (B) + (C) + (D) + (E) + (F) + (G) + (H)	938.01	1,264.47

3.4. Discussion and conclusions

Although no real-world data are available about how appropriately the demands for water in the Machángara River Basin were met in the period 2012–2013, this study shows that the optimal allocation scheme (resulting from our LP-model) of the available water to the spatially distributed nodes with constant temporal demands is not capable of meeting all demands at all times. This means that a nexus between the availability of water and the demands for hydropower production, irrigated agriculture, and domestic and industrial use exists, and it will remain present because these demands are expected to increase with the growth of the population. Building one or more reservoirs will probably mitigate this nexus but remains to be further investigated. In this context, would it be recommendable to perform a deep

analysis to determine whether reservoirs in the upstream and downstream parts are enough or a new reservoir could improve the water allocation process.

Through a trial-and-error calibration procedure, water flow dynamics in the river system were modeled with an acceptable accuracy with respect to simulated reference values, although peak discharges were underestimated.

As for any model, the quality of the input data and the quantification of the initial situation is crucial for our LP-model. In this study, water inputs to the system simulated by the well-established SWAT-model were used. To obtain these inputs, in the ArcSWAT, the default parameter values from the time series of meteorological data provided by NECP Climate Forecast System Version 2 were used. These input and reference output data allowed us to formulate and assess our LP modeling approach. However, for a more realistic application of our model, those datasets should be replaced by observed meteorological time series and observed river discharge measurements. This means that, for the calibration and validation phase, data about effective water abstraction and the possible return of water to the river systems must be taken into account.

From a simulation perspective, the LP-model proposed in this chapter is relatively simple compared to physically based models (Ashraf Vaghefi et al., 2013; Labadie, 2006; Shourian et al., 2008) that are routinely used to study the impacts of changing meteorological, hydrological, infrastructural, and demand conditions on the availability of water in a given river system in space and time. This LP-model uses only a few parameters to model the temporal dynamics and loss of water coming into the river system, assuming that the time needed for water released in one node to flow to the next is always one-time step.

The effectivity of the LP-model does not depend on how sophisticated the simulation of water retention and flow is, but on its capability to optimize the allocation of the available water to spatially distributed demand nodes, in addition to considering temporal variability of the demand (which was not taken into account in this study). Few other models have been reported in the literature that were developed for this purpose. (Hu et al., 2016; Labadie, 2004) state that optimization of the water allocation process is possible. There are several hydrological models based on differential equations that model the behavior of a river basin (Devia et al., 2015) and even produce a water allocation scheme (Ashraf Vaghefi et al., 2013; Labadie, 2006; Shourian et al., 2008). However, those models are not capable of optimizing water allocation. Therefore, optimization of water allocation is a fundamental functionality provided by the LP-model described in this chapter. Furthermore, Water Supply Networks (WSN), such as the one used in this study, and the associated generic LP-model can be easily extended to include additional components (more nodes, water demand users, etc.) to create a network that represents reality closer.

Chapter 4
Mixed Integer Linear Programming Model

The core of this chapter was published as:

Veintimilla-Reyes, J., Meyer, A. De, Cattrysse, D., & Van Orshoven, J. (2018). From Linear Programming Model to Mixed Integer Linear Programming Model for the Simultaneous Optimisation of Water Allocation and Reservoir Location in River Systems. Proceedings, 2(11), 594. https://doi.org/10.3390/proceedings2110594

Veintimilla-Reyes, J., De Meyer, A., Cattrysse, D., Tacuri, E., Vanegas, P., Cisneros, F., & Van Orshoven, J. (2019). MILP for Optimizing Water Allocation and Reservoir Location: A Case Study for the Machángara River Basin, Ecuador. Water, 11(5), 1011. https://doi.org/10.3390/w11051011

4.1. Introduction

The availability of surface water is the foundation of socio-economic development in river basins worldwide. Often the current water requirements of the different stakeholders (for hydropower, agriculture, livestock, fisheries, mining, industrial and domestic use and for nature conservation) cannot be satisfied at all locations nor at all times (Bertoni et al., 2017; Nyabe et al., 2017). It is expected that water shortages will increase in the coming decades due to increased demand related to socio-economic and demographic growth and to changing weather patterns. In regions like those mentioned above, there is an urgent need for tools that support the optimal allocation of the limited water resources through space and time in a transparent, fair and cost-efficient way. Whereas process-based combined hydrological and hydraulic modelling is the established approach to study this extended Water-Energy-Food nexus and assess the impact of human interventions and changing boundary conditions, such approach does not fulfil the requirement of producing optimal allocation schemes.

A river system can be modeled as a topological network of nodes and segments. Based on this, the management of the water flowing through this system can be formulated as a Network Flow Optimization Problem (NFOP). In chapter 2, a generic Linear Programming model (LP) for optimizing the allocation of water available in the reservoir nodes and in the network reaches (segments) was introduced. This model allocates water to a set of spatially distributed users whose water requirements can change through time. The objective function in the model consists of eight cost terms that penalize the following undesired situations: not meeting / exceeding the demands in a node, not enough flow / excess flow (hence floods) in the network segments, not reaching the minimal allowed volume / overflows in reservoirs, and exceeding / not reaching maximum and minimum capacities, in demand nodes. One question not addressed in this model is where one or more new reservoirs should be located to further minimize the objective function. To deal with reservoir location optimization, Z. Zhang et al., (2014) created a model based on particle swarm optimization of which the main objective was to determine reservoir location to optimize the power generation. The model was verified by applying it to two different use cases: 1) Three Gorges Project (TGP) in China and 2) XiLuoDu Project also in China. Researchers considered the results obtained to be valid. Roozbahani et al., (2021) developed a model based on a stochastic modelling approach which includes several constraints related with water demand in the basin (Sefidrud Basin, Iran); this model is able to determine the location of the new reservoirs.

Roozbahani et al., (2017), constructed a mixed-integer linear programming model to determine the location of new dams based on the water requirements of a basin as first step. The second step includes a sensitivity analysis which determines the correct number of dams; this model was developed by using data from the Sefidrud Basin in Iran.

We decided to extend the LP-model from chapter 3 into a Mixed Integer Linear Programming Model (MILP) that is capable of selecting the nodes in the network where the construction of additional reservoirs of a predefined capacity would further improve the allocation of water. The aim of this extension is to determine whether the current performance of the WSN can be improved by including a new reservoir on one or more of candidate locations.

4.2. Materials and methods

4.2.1. From river system to network configuration

As a first step in the LP-approach proposed in chapter 2, the river system under study must be modeled as a network configuration. The specific network configuration studied in this chapter corresponds to the Machángara River Basin, which was also used in chapter 3. This network contains 4 reservoir nodes, 16 transfer nodes and 6 demand nodes. Nodes are connected by segments that allow water transfer among them. The left panel in Figure 4.1 represents the network configuration used with the LP model (chapter 3), while the right panel shows the configuration to which the MILP model will be applied. Within the MILP network configuration, all of the existing reservoir nodes and the transfer nodes are considered as "candidate reservoir locations".

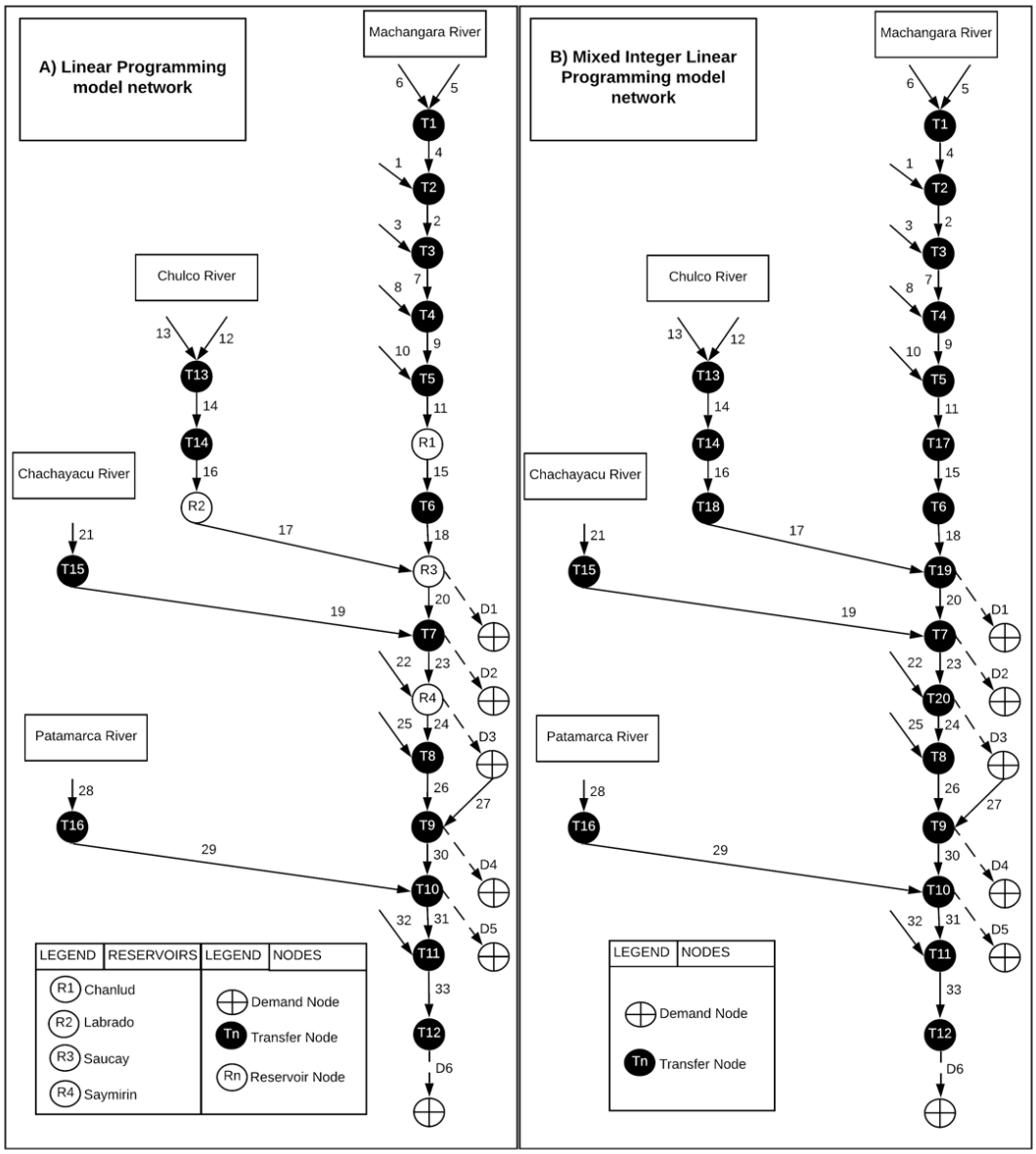

Figure 4.1. Graphical representation of the studied network configuration. (Left) LP network configuration also used in chapter 3. (Right) MILP network configuration (all nodes as transfer of candidate nodes).

The parameters, variables and slack variables for the network configurations in Figure 4.1A (LP) and Figure 4.1B (MILP) are the same as those used in chapter 3 section 2.2.2. This also applies to the rainfall data.

4.2.2. Generic optimization model

4.2.2.1. Linear programming model

The generic LP model explained in chapter 2 addresses a river system as a network configuration for optimizing the allocation of the water available in the reservoir nodes and river segments to a set of spatially distributed water users of which the demand for water can vary in time.

The objective function of the LP-model consists of eight terms as represented in equation (2.1 and explained in chapter 2 section 2.2.2.

4.2.2.2. Mixed Integer Linear Programming model

In the MILP-model, transfer nodes in the network configuration (Figure 4.1B) are considered as "candidate reservoirs", that is, potential locations for building reservoirs with a predefined capacity. The model is formulated with the purpose to determine the locations for reservoirs of predefined capacity that minimize the sum of penalties associated to water allocation. As explained above, these penalties are related to not meeting and exceeding demands, to water shortage in and overflow of the reservoirs, not meeting the minimum flow in and flooding of a river segment, not meeting the minimum flow or exceeding the maximum capacity in demand river segments and, in addition, the building and management costs of reservoirs. Therefore, the objective function of the LP model, explained in chapter 2 section 2.2.2 is extended to include an approximation of the building and management cost term ($\mathrm{BC_n}$) for every possible reservoir ($\mathrm{Y_n}$) (Equation (4.1). $\mathrm{Y_n}$ is a binary variable indicating whether location n is or is not selected to build a reservoir. With the incorporation of the binary variable $\mathrm{Y_n}$, the LP-model becomes a MILP-model.

Objective function

$$\begin{aligned} \text{minimize} \sum_n \sum_t (W_n * T_{n,n+1}^{t+}) + \sum_n \sum_d \sum_t \left(P_n * S_{n,d}^{t-}\right) + \\ \sum_r \sum_t (U_r * SH_r^{t-}) + \sum_r \sum_t (A_r * OF_r^{t+}) + \sum_n \sum_t (B_n * Q_{n,n+1}^{t-}) + \\ \sum_n \sum_d \sum_t \left(E_n * S_{n,d}^{t+}\right) + \sum_n \sum_d \sum_t (F_n * \mathrm{MinXD}_{n,d}^{t-}) + \\ \sum_n \sum_d \sum_t \left(G_n * \mathrm{MaxXD}_{n,d}^{t+}\right) + \sum_{\boldsymbol{n}} (\boldsymbol{BC_n} * \boldsymbol{Y_n}) \end{aligned} \tag{4.1}$$

Two major characteristics of candidate reservoirs must be taken into account, i.c. the storage capacity and the minimum volume of water which needs to be maintained at alle times to guarantee ecological functioning. To consider these characteristics, the reservoir capacity constraints in the LP-model, expressed in Equations (2.9) and (2.10) are adjusted as in equations (4.2), (4.3) and (4.4). Equation (4.5) is added to specify the minimum number of reservoirs requested. This constraint allows to stablish a fixed number of reservoirs from a situation where there are no reservoirs to the situation where all nodes are becoming

reservoirs. No changes are required of the flow balance, capacity, limitation, continuation or time delay constraints that were already included in the LP-model of chapter 2.

Capacity constraints

Reservoir(s)

$$V_r^t - OF_r^{t+} - R_{r\,max}^t <= M_r * (1 - Y_r) \qquad \forall_t \in T,\ \forall_r \in R \quad (4.2)$$

$$-V_r^t \leq -R_{r\,min}^t + \left(M_r * (1 - Y_r)\right) \qquad \forall_t \in T,\ \forall_r \in R \quad (4.3)$$

$$OF_r^{t+} \leq M_r * (1 - Y_r) \qquad \forall_t \in T,\ \forall_r \in R \quad (4.4)$$

Number of reservoirs

$$\sum_i Y_i \geq 0 \qquad Y_i = 0\ or\ 1 \quad (4.5)$$

In Equations (4.2), (4.3) and (4.4), the parameter M is a number with a value sufficiently large as to ensure that these equations are satisfied for all values within the constraints. Thus, this M-parameter allows to implement either-or-constraints. Then the model is able to choose which of the nodes might be transformed into a new "candidate reservoir" (Winston & Goldberg, 1994). For all other variables see Table 2.1 in chapter 2 section 2.2.2.

Water input, reservoir characteristics and water demand

The time series of water inflow simulated by means of ArcSWAT (chapter 3) for four years (2006-2009) (Figure 3.3) were used for calibration; two years (2010-2011) for validation and the two subsequent years (2012-2013) for application. To cope with the limited information about the river network segments, capacities (maximum and minimum) of the river segments were estimated by means of length, width and depth of each segment derived from (FAO, 2017; Google, 2007).

Table 4.1. Characteristics of the existing and potential new reservoirs included in the LP model

Node	Reservoir	Initial Value [hm^3]	Maximum capacity [hm^3]	Minimum capacity [hm3]	Building + management cost [euros per two years]
1, 2, 3	Candidates	2.6	13	1.3	195,000
4 … 16	Candidates	2.6	13	2	195,000
17	R1	5	6.15	1.23	150,000
18	R2	15	16.3	3.26	215,000
19	R3	0.7	1	0.2	100,000
20	R4	0.7	1	0.2	100,000

In Table 4.1, the characteristics of the “candidate reservoirs” and the four existing reservoirs present in the river system are given: the volume of water initially present, the maximum capacity and minimum volume of water that must be maintained and a bi-annual cost associated with the building and management of the reservoir. Therefore, a maximum (R_{max}) and a minimum capacity (R_{min}) had to be established. In this case, data is not available and it must be estimated. The estimation procedure started with a standard capacity and it was

multiplied by a factor. This factor is based on the steepness of a valley. It is assumed that the capacity in a narrow valley is lower than in a plain. Factors were adapted in order to obtain similar values as the ones for the existing reservoirs. Likewise, a building and management cost had to be estimated. Then, a standard cost was selected and it was multiplied by a geo-factor. The base cost was estimated by taking the mean of the building costs of the existing reservoirs. The calculation of this geo-factor is based on two components: a) the shape of the valley (derived from the DEM) and b) the distance to the nearest road. It is assumed that the construction of a reservoir is more expensive in a plain valley than in a narrow valley. In the same way, the costs are assumed to be higher when a reservoir is located far from a road. It should be noted that in the model it is assumed that the only the fraction of the total building cost that is paid off over the two considered years are taken into account for simplification reasons (a lifespan of a reservoir could be more than 30 years).

Table 4.2 shows the water requirements of the 6 demand nodes as well as the penalty values for not meeting these requirements. For this test case demands are constant through time and all demand nodes have the same penalty value (1 euro per day). The constraints try to keep water within minimum and maximum capacities in reservoirs, river and demand segments and to avoid floods (Table 2.1 in chapter 2 section 2.2.2)

Table 4.2. Water requirement and penalty for not meeting demand per node, in the LP and MILP models (Extension of table Table 2.1)

Label	Demand node	Value [hm^3 per day]	Penalty [euros x hm^3 per day]
D1	Sucay powerplant	0.62208	1.0
D2	Machángara irrigation project	0.0432	1.0
D3	Saymirín powerplant	0.6912	1.0
D4	Tixán	0.12096	1.0
D5	“Sociedad de Riego Ricaurte” - irrigation	0.02592	1.0
D6	Ecosystem	0.01728	1.0

4.3. Results

4.3.1. Linear Programming model

Results from the execution of the LP-model in the Machángara River Basin are included in chapter 3 section 3.3.

4.3.2. Mixed Integer Linear Programming model

In this MILP-exercise, the main objective is to determine which of the node(s) (reservoir/transfer) must be turned into a reservoir given their predefined characteristics (i.e. location, initial water level, minimum volume and maximum capacity) in order to minimize the sum of penalties for not meeting demands, for occurrence of floods, for not reaching the minimum required water volume in the reservoirs and the building and management costs for the considered period.

The output of the LP model encompassing the 4 existing reservoirs (nodes 17, 18, 19 and 20 in Table 3.6) are considered as the reference results. It shows a total penalty of 1,264.47 euros for the application period. The MILP model was executed iterating over the number of the candidate reservoirs included in the solution. For this execution all nodes are considered "candidates" except the existing reservoirs (nodes 17 to 20). In Table 4.3, red numbers point to the node-ID's which are selected for reservoir construction in the iteration and the green ones represent the existing reservoirs. Table 4.3 also shows that, as more reservoirs are included, the total water not allocated to meet demands is reduced. Moreover, from the execution of iteration 6, the total water not allocated is reduced by using 5 reservoirs: nodes 10, 12, 17, 19 and 20. Furthermore, as more reservoirs are included in the solution, the amount of water that is not allocated to the demand nodes becomes smaller. It is also clear that, from the existing reservoirs in the original river system, only in use case 21, reservoir 18 is included in the solution.

Table 4.3. Nodes selected by the MILP-model for reservoir and corresponding volume of water not allocated and costs

Use Case	Number of Reservoirs	Reservoirs included in the solution	Water Not Allocated [hm^3]	Penalties [euros]	Building + management [euros]	Total
1	0		894,77	1091,39	0	1091,39
2	1	19	895,78	1092,40	100000	101092,40
3	2	19,20	896,96	1095,49	200000	201095,49
4	3	17,19,20	903,71	1175,51	350000	351175,51
5	4	12,17,19,20	896,32	963,20	545000	545963,20
6	5	10,12,17,19,20	889,88	889,88	740000	740889,88
7	6	12,15,16,17,19,20	890,38	890,38	935000	935890,38
8	7	8,9,10,12,17,19,20	881,19	881,19	1130000	1130881,19
9	8	12,13,14,15,16,17,19,20	889,81	889,81	1325000	1325889,81
10	9	11,12,13,14,15,16,17,19,20	888,99	888,99	1520000	1520888,99
11	10	10,11,12,13,14,15,16,17,19,20	885,65	885,65	1715000	1715885,65
12	11	9,10,11,12,13,14,15,16,17,19,20	881,49	881,49	1910000	1910881,4
13	12	8,9,10,11,12,13,14,15,16,17,19,20	879,17	879,17	2105000	2105879,17
14	13	7,8,9,10,11,12,13,14,15,16,17,19,20	878,47	878,47	2300000	2300878,47
15	14	6,7,8,9,10,11,12,13,14,15,16,17,19,20	878,05	878,05	2495000	2495878,05
16	15	5,6,7,8,9,10,11,12,13,14,15,16,17,19,20	877,64	877,64	2690000	2690877,64
17	16	4,5,6,7,8,9,10,11,12,13,14,15,16,17,19,20	877,26	877,26	2885000	2885877,26
18	17	3,4,5,6,7,8,9,10,11,12,13,14,15,16,17,19,20	876,86	876,86	3080000	3080876,86
19	18	2,3,4,5,6,7,8,9,10,11,12,13,14,15,16,17,19,20	876,49	876,49	3275000	3275876,49
20	19	1,2,3,4,5,6,7,8,9,10,11,12,13,14,15,16,17,19,20	876,11	876,11	3470000	3470876,11
21	20	1,2,3,4,5,6,7,8,9,10,11,12,13,14,15,16,17,18,19,20	880,66	880,66	3685000	3685880,66

4.4. Discussion and Conclusions

In this chapter, an extension of the conceptual LP-approach introduced in chapters 2 and 3 is presented. This elaborated version of the model considers (a subset of) transfer nodes in the river network as candidate locations for building a reservoir with predefined storage characteristics. This extension was implemented by adding a term with a binary variable in

the objective function of the original LP-model, generating a MILP-model that is able to select the most appropriate locations for new reservoirs with a view to optimize water allocation while taking investment and management costs into account.

The selection of a new "candidate" reservoir is made taking into account the water demand requirements in the closest nodes, penalties associated to the minimum and maximum capacities in river segments, reservoirs and demand nodes. Variable geographical conditions are also considered mainly during the creation of the WSN. Therefore, the order whereby candidate nodes are selected is not known in advance.

From the results summarized in Table 4.3, it is clear that only one existing reservoir is necessary to reduce the total penalty. Besides, only the four existing reservoirs are included in the solution at the last iteration. This situation might introduce the criterion that the current configuration of the basin is not the optimal. Special attention must be given to the fact that in the first iteration, the total penalty is less than the total value obtained with the four existing reservoirs. For this particular case, it is assumed that more water is flowing withing the river network since only one reservoir is being used. This, the minimum capacity constraint is only keeping water in one reservoir. Another situation to consider is that the capacities and the building and management costs of the new reservoirs have been estimated. Thus, results of the execution of the MILP-model with real values might be totally different.

Moreover, from Table 4.3 it is also noticeable that with the inclusion of a new reservoir, the allocated water to water demands node is not drastically reduced; only a reduction of 2% (894.77 to 880.66). Besides, for this exercise, all new reservoirs are established with a predefined initial water level for simplification reasons. Therefore, the process of building a new reservoir includes a filling phase which may reduce de water flowing within the river network resulting in the increment of the total penalty values.

In Table 4.3 it is clear to see that the most influent parameter is the building and management cost. This value in real world depends on several conditions such as: location of the new reservoir, access roads to transport building materials, weather conditions, geographical conditions of the area, etc. Therefore, it is recommendable to perform a complete analysis of this cost. In this way, in chapter 5, apart of the execution of the LP and MILP models in a new study area (Omo River Basin in Africa), four scenarios will be tested in order to clarify the process of selecting a new reservoir as solution in the MILP model.

One of the benefits of using the MILP model is mainly the capacity to obtain a basic idea of the location of the new reservoirs and its influence in the water availability within the river network.

Chapter 5
Application of the NFO-MILP-model to the Omo River Basin

5.1.Introduction

One of the most important benefits of a balanced distribution of surface water is the increase in the availability of energy, considering that global energy consumption has doubled levels observed in 1990 and 2019 and is becoming higher in less developed countries (Ritchie & Roser, 2019). In 2009, less than 20% of the population from Ethiopia and Kenya had access to electricity. This percentage had increased to 42.9% and 56.0%, respectively, in 2016 (Tesfa, 2013; World Bank, 2016). It is a fact that energy access is closely related to well-being and prosperity; according to (Chen & Swain, 2014), this fact is also applicable to the social and economic development of those regions. On the other hand, having access to enough amounts of water makes it possible to use this resource in large scale irrigation; to reach this purpose, reservoirs are built (Hanasaki et al., 2006). As a result, agricultural production might be boosted, and therefore, economy will grow and availability of workplaces will increase (Kamski, 2016; Sugar Corporation, 2019). Eventually, if the availability of water is ensured, well-being is also ensured.

Tesfa, (2013) states that building reservoirs is a very appealing solution to mitigate extreme hydrological events, improve water conservation and produce electricity by means of hydropower generation plants. However, there are some associated disadvantages related to the environmental impacts of building a reservoir (McEntee, 2019). In the past, there were no proper methods to assess the social and environmental impact of building a reservoir. For instance, the effect of the construction of the GIBE III reservoir were not carefully considered on the Kenyan part of the ORB, resulting in the wrong assumption the reservoir would contribute to a positive water balance for Lake Turkana. An appropriate assessment was carried out only after three years the construction works had started (Avery, 2017).

In chapter 2, a Linear Programming model (LP) was introduced meant to optimally allocate water available in a river-with-reservoir system. Both, water availability and demand are spatially distributed and variable in time. In chapter 4, the LP-model in chapter 2 was extended towards a Mixed Integer Linear Programming model (MILP) to determine locations of new reservoirs from a set of candidate locations, still with the aim to optimally allocate the available water in order to satisfy demands. The MILP-modelling approach was illustrated by an application to the Machángara River Basin.

This chapter, describes the application of both, the LP and MILP models to the Omo River Basin (ORB) and discusses their strengths and weaknesses.

5.2. Materials and methods

5.2.1. Study Area

5.2.1.1. The Omo River Basin

The Omo River Basin is located in central-east Africa between 8.97 - 4.60 degrees latitude north and 35.40 - 38.50 degrees longitude east. This basin comprises part of the territories of

three countries: Ethiopia (90.7% of the basin area), Kenya (2.4%) and South Sudan (7.0%) (Figure 5.1). The area of the full basin is about 71,000 km² (Dondeyne et al., 2021).

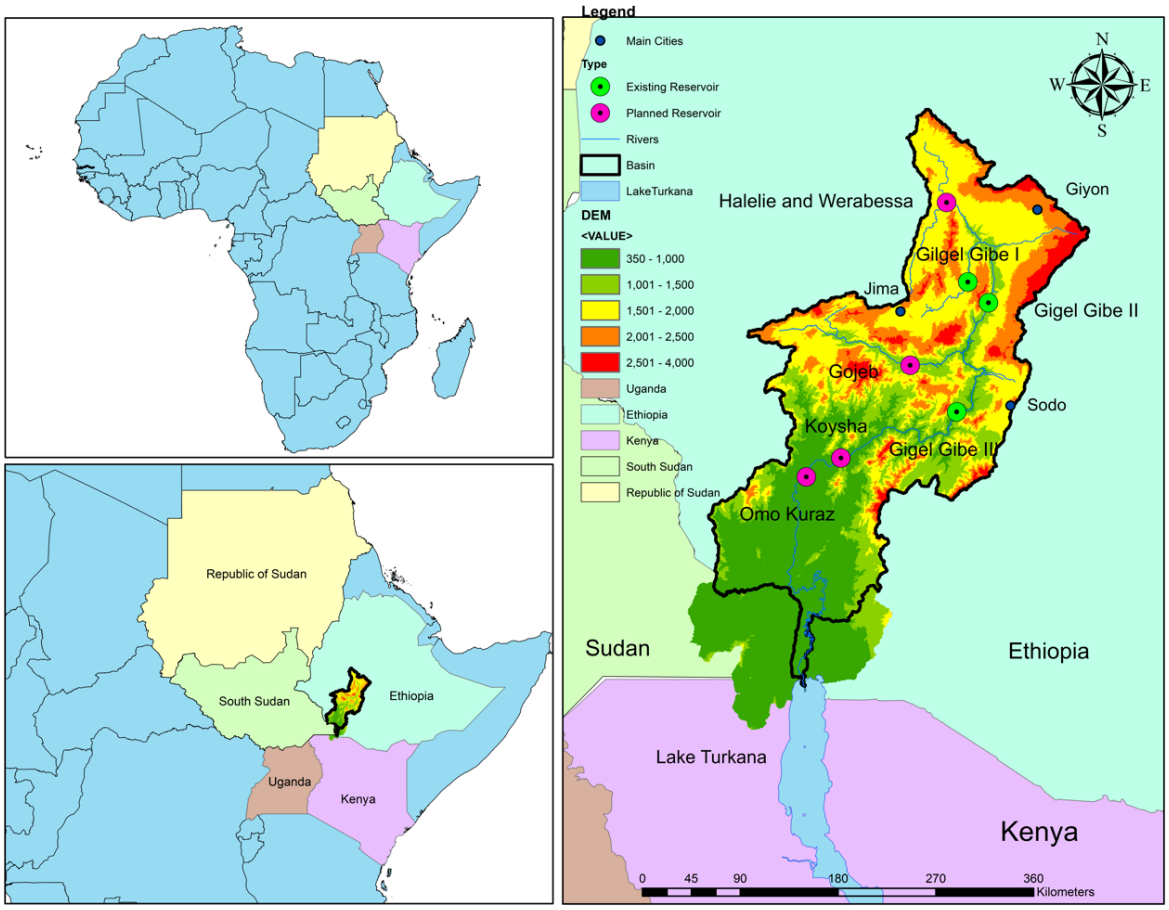

Figure 5.1. The Omo River Basin in central east Africa (Dondeyne et al., 2018)

The climate in the ORB is characterized by a strong spatial and within-year variability mainly determined by the basin's topographic heterogeneity and equatorial position. The variability in rainfall, which is mainly driven by the migration of the Intertropical Convergence Zone (ITCZ) and upper-tropospheric easterlies, is represented in Figure 5.2 by climatograms from four different locations in the basin (Berhanu et al., 2014). Figure 5.3 shows the location of the corresponding climate stations (dataset collected between 1999 and 2019) as well as the Digital Elevation Model (DEM) of the ORB.

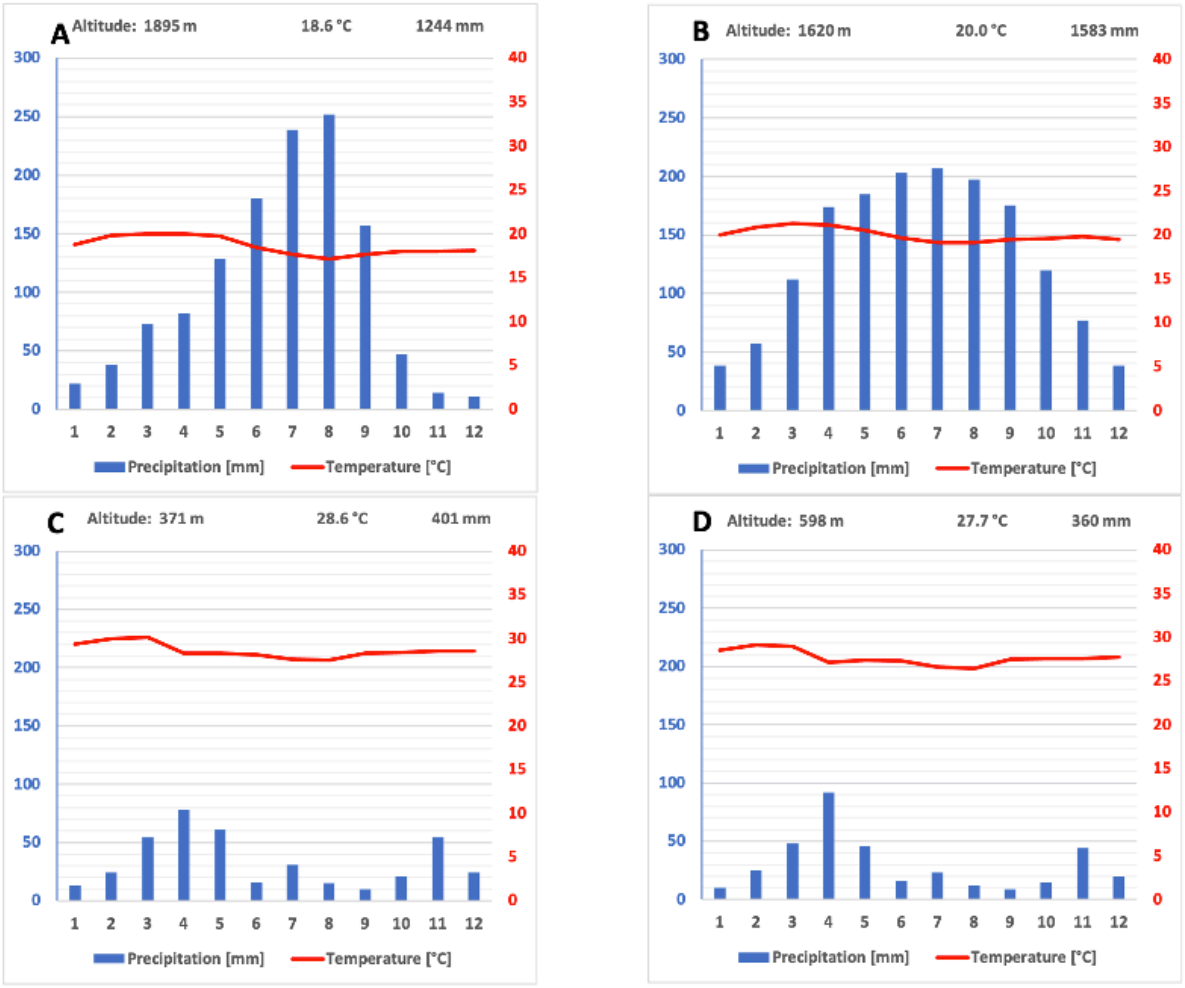

Figure 5.2. Climatograms of four locations in the ORB: A) Welkite (latitude: 8.2833°N, longitude: 37.7833°E; B) Chida (latitude: 7.167642°N, longitude: 36.79108°E); C) Omorate (latitude: 4.803135°N, longitude: 36.054172°E) and D) Kaaling (latitude: 4.372622°N, longitude: 35.550738°E); (Climate-Data.org, 2019)

The Ethiopian part in the north of the basin (charts A and B of Figure 5.2) has two climatological seasons. The wet season is called "Keremt" or summer season. This season goes from June until September. During this period, the Inter Tropical Convergence Zone (ITCZ) (Royal Meteorological Societ, 2019) is at the northernmost position. The light rain season occurs from October to May. During this season the amount of precipitation is limited. In the south of the Ethiopian part of ORB (chart C of Figure 5.2) and in the north and middle of the Kenyan part (chart D of Figure 5.2) there are two separate wet seasons, caused by the passage of the ITCZ (Berhanu et al., 2014). The rainy season in spring is called "long rains" while in autumn it is called "short rains" (Hastenrath et al., 2011).

Figure 5.2 shows that the Ethiopian Highlands (northern ORB), is the most humid part of the basin. For instance, in Welkite and Chida the mean annual rainfall is 1244 mm and 1583 mm, respectively. Moreover, the average daily temperature is almost constant around 20 ºC all year round. Around Lake Turkana and in the lower part of the Omo valley, precipitation rates are much lower (e.g. 360 mm in Kaaling) and average daily air temperatures range between 27 and 29°C.

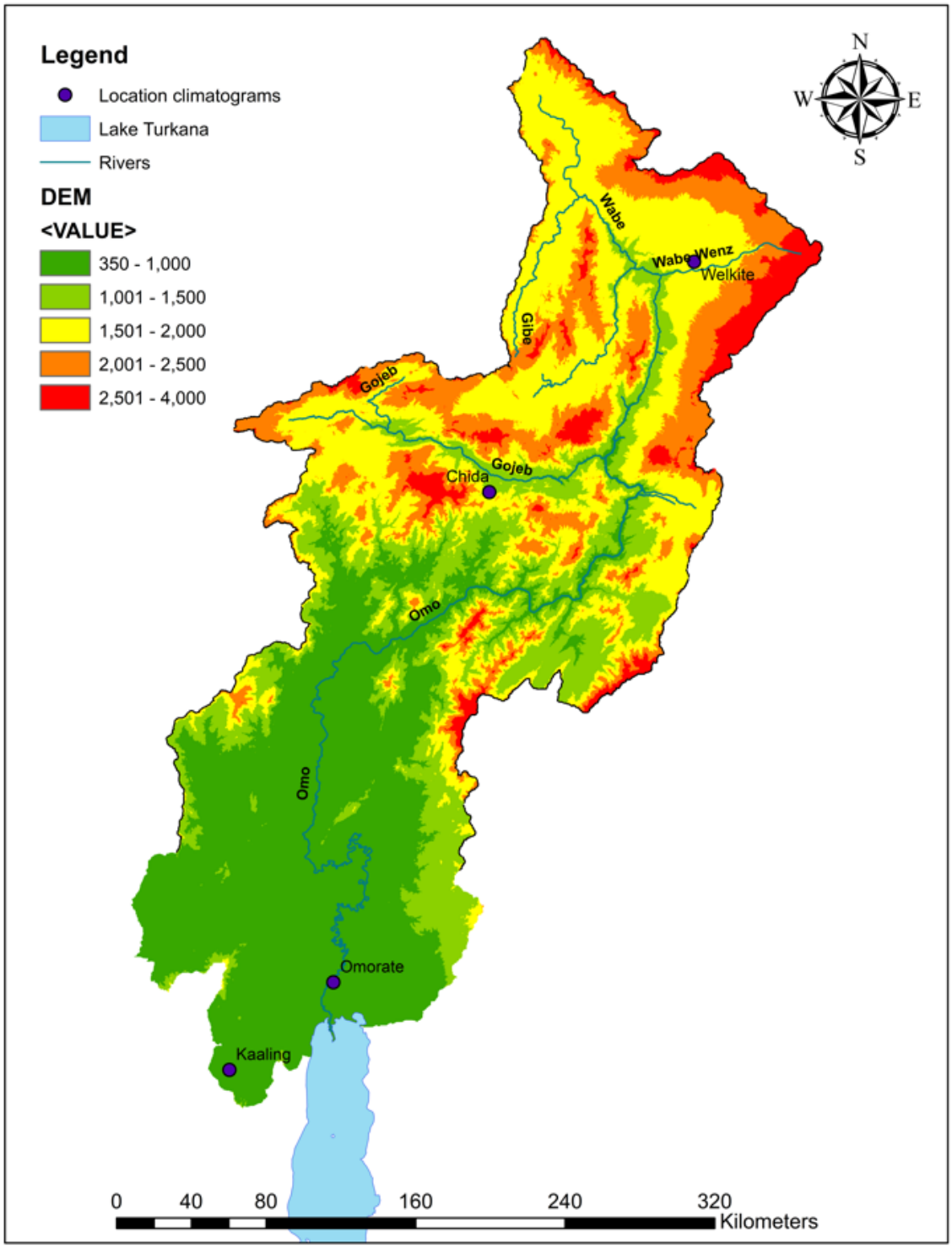

Figure 5.3. Location of climatograms listed in Figure 5.2 (DAFNE, 2018)

The ORB is an endoreic basin, which means that runoff water does not reach a sea or ocean. Indeed, water flows end up in Lake Turkana, which is the world largest desert lake. The Turkana Lake stores approximately 200 km^3 of water. Apart from the Omo river, four rivers are feeding the lake from Ethiopia: Shebe, Abelti, Gojeb and Wolkite. The Omo is the most important river in the basin since its contribution corresponds to about 90% of the incoming water to the Turkana Lake. This river is highly suitable for hydropower generation due to the difference in altitude between its highest and lowest point (1800 m) (Merrick, 2018;

Yewhalaw et al., 2009). There are several tributaries to the Omo river, such as Gilgel Gibe. The Gilgel Gibe River, located in the south-western part of Ethiopia, is the largest tributary of the Omo river (Merrick, 2018; Yewhalaw et al., 2009). The Turkwel and Kerio rivers, located in the Kenyan part of the basin, contribute a small part to the incoming volume to the lake. The contribution of these rivers depends largely on the season (Avery, 2010, 2012; Dondeyne et al., 2018, 2021).

The construction of several dams (Figure 5.1) caused the interruption of the natural course of the Omo river and its tributaries.

Figure 5.4. Location of runoff gauges in the Omo basin (Dondeyne et al., 2018)

In Figure 5.4, the location of the runoff gauges is provided. These gauges are important since they provide the input data for the modelling of water inputs in the WSN of ORB and hence in the LP- and MILP-models, by means of the ArcSWAT model.

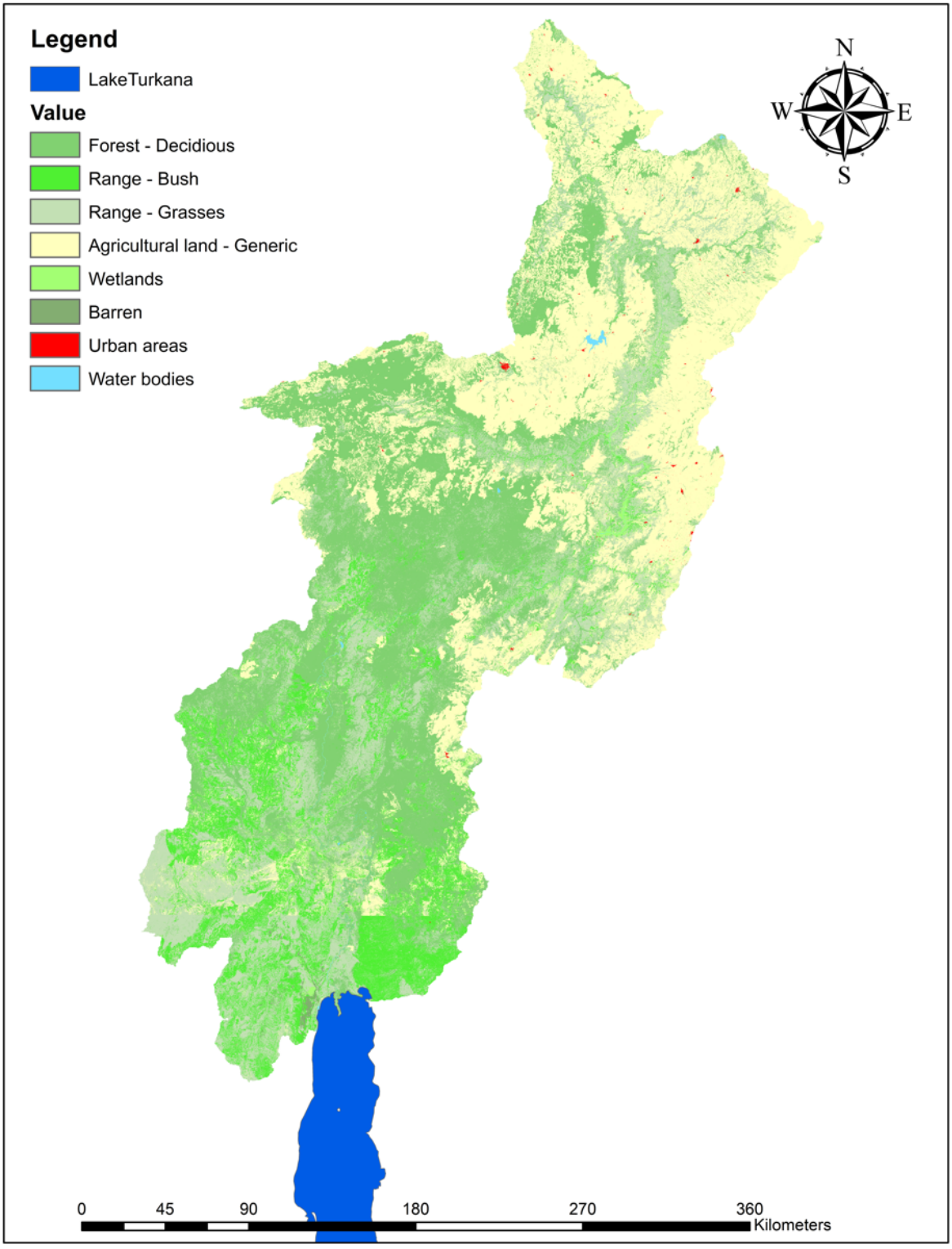

Figure 5.5. Land use distribution in the ORB (DAFNE, 2018; ESA, 2015)

Figure 5.5 shows the spatial distribution of the different land cover types found in the ORB (DAFNE, 2018; ESA, 2015) according to the European Space Agency (ESA) land cover dataset with a resolution of 20 m and with 9 legend units (forest deciduous, range brush, range grasses, agricultural land, wetlands, barren, urban areas and water bodies). The northern humid part of the basin is mainly covered by cropland. Overall, the study area is covered by

a) 32.0% of Forest – deciduous; b) 12.0% of Rangeland – Grasses; c) 21.9% of Rangeland – Brush; d) 33.0% of Agricultural land – generic; e) 0.2% of Barren land; f) 0.1% of Urban areas; g) 0.2% of wetlands and h) 0.5% of water bodies. The Turkana Lake, which comprises almost the totality of water bodies with 0.5% of the basin area (outlet of the basin) (Figure 5.5), is a source of drinking water and a resource for fishing for several hundreds of thousands of people (Michigan State University, 2019).

There are two national parks located in the ORB. The Mago National Park, located in the lower part of the ORB, and the Omo National Park, located in the west part. Tribal communities reside within these national parks and also a wide range of plant species and wildlife can be found (Vreugdenhil, 2018).

Thus, based on the land cover present in the study area, water requirements are estimated. Therefore, in the ORB several water demands have been identified such as: agriculture, private households, hydropower plants, wetlands and, in a small scale, industry (DAFNE, 2018; ESA, 2015).

5.2.1.2. Reservoirs, Hydropower Production and Other Water Uses

Currently, three reservoirs are present along of the Omo river: Gilgel Gibe I, II and III. The construction of four other reservoirs is envisaged, all in Ethiopia: a) Koysha, b) Gojeb, c) Halelie & Werabessa, and d) Omo Kuraz. The characteristics of these reservoirs are summarized in Table 5.1 and Figure 5.6.

Table 5.1. Characteristics of the reservoirs in the ORB (already built and planned) (Bertoni et al., 2017; DAFNE, 2018)

Reservoir	River	Reservoir capacity [hm³]	Maximum height [m]	Installed capacity [MW]	Operational since	Built / Planned
Gilgel Gibe I	Gilgel Gibe	920	40	180	2004	Built
Gilgel Gibe II	Omo	920	50	420	2010	Built
Gilgel Gibe III	Omo	14700	243	1870	2015	Built
Gojeb	Omo	1000	Unknown	Unknown	Not Available	Planned
Halelie & Werabessa	Omo	5700	Unknown	Unknown	Not Available	Planned
Koysha	Omo	6000	179	2200	Not Available	Planned
Omo Kuraz	Omo	4410	Unknown	Unknown	Not Available	Planned

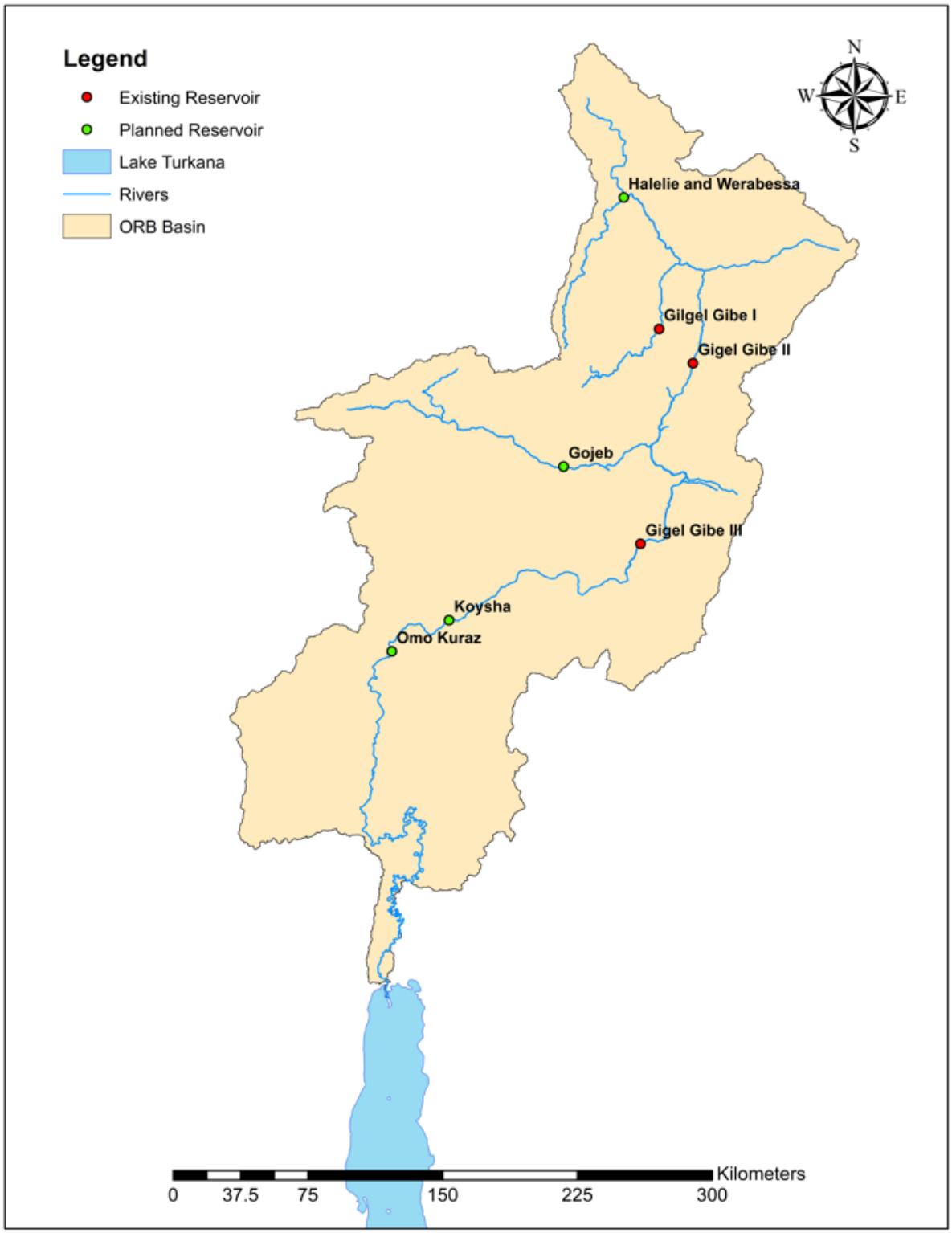

Figure 5.6. Location of existing (red) and planned (green) reservoirs on the river network of the Omo-Turkana basin.

5.2.2. Linear Programming model for optimizing water allocation

5.2.2.1. General

The Linear Programming model, introduced in chapter 2, Section 2.2, and applied in chapter 3 to the Machángara River Basin, has been used in this chapter as a basis for further evaluation on a different study area.

5.2.2.2. Preliminary River Network Configuration and Water Availability

The configuration of the ORB river network was obtained from a DEM with a resolution of 200 m (Figure 5.1 and Figure 5.3). As for the Machangára case study (chapter 3), the river network configuration was generated by using the ArcSWAT-extension of the ArcGIS software (2012.10.21, University A&M Texas, College Station, TX, USA) (Texas A&M University, 2009).

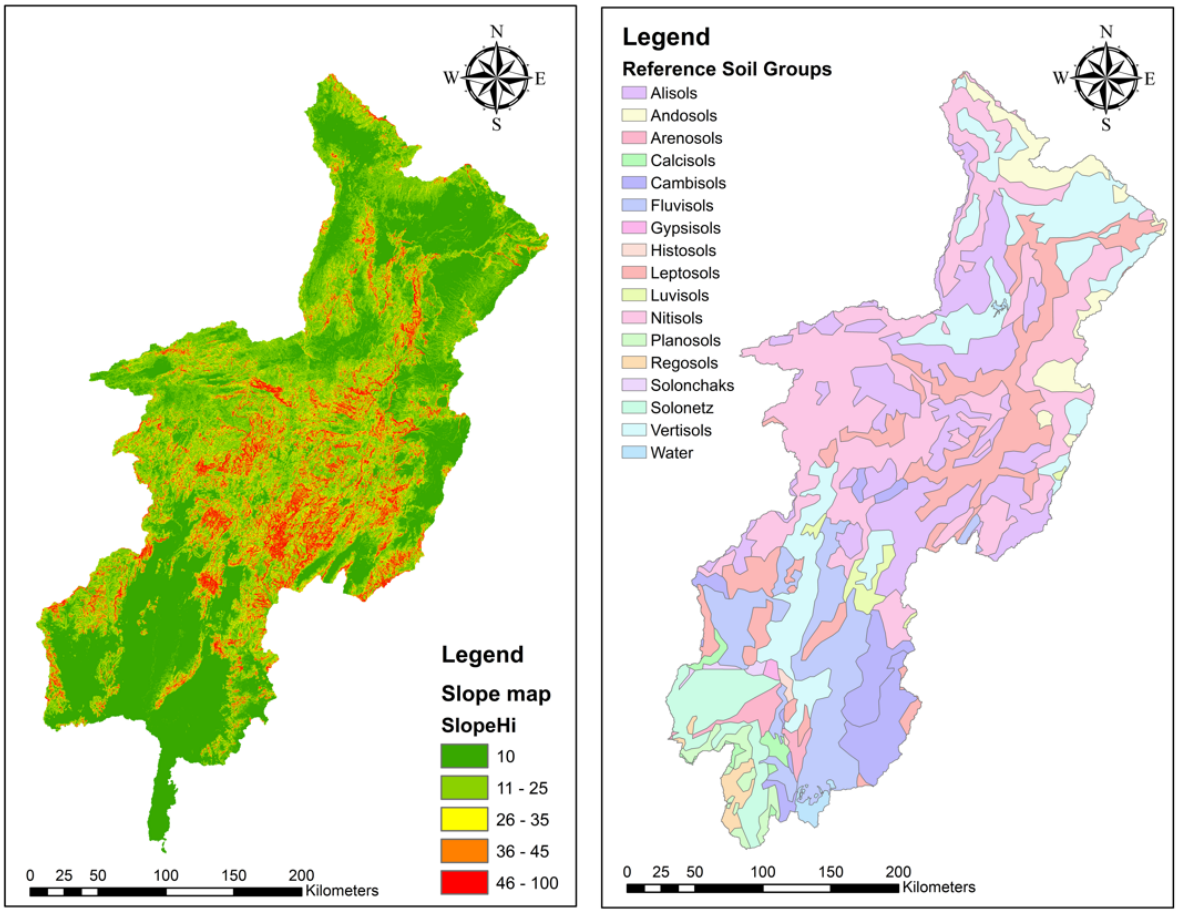

Figure 5.7. Slope [%] (left) and soil maps (right) of the ORB.

The procedure to generate the river network comprised the following steps:

i) Using the DEM (Figure 5.1 and Figure 5.3), the basin was delineated and subdivided into sub-basins for which outlet nodes were created. Additional outlet

nodes were added manually to represent reservoirs and other important points and to reduce the length of a river segment;

ii) A soil map (Figure 5.7, left) and a land cover map (Figure 5.5) were uploaded;

iii) Slope ranges were derived from the DEM (90 m resolution).

iv) The geo-datasets with reference soil groups, land cover types and slope classes were overlaid to generate Hydrologic Response Units (HRUs, groups of pixels belonging to the same soil type, land cover type and slope class);

v) Finally, weather information was entered from the Global Weather Data for SWAT database (Texas A&M University, 2018). This weather data was extracted for 72 grid points (Figure 5.8) from the Climate Forecast System Reanalysis (CFSR) global weather dataset of the National Centers for Environmental Prediction (NCEP). At the time of this research (2020) the CFSR-weather time series available through the ArcSWAT website contains data from 1979 to 2014, that is, 35 years of forecasted information.

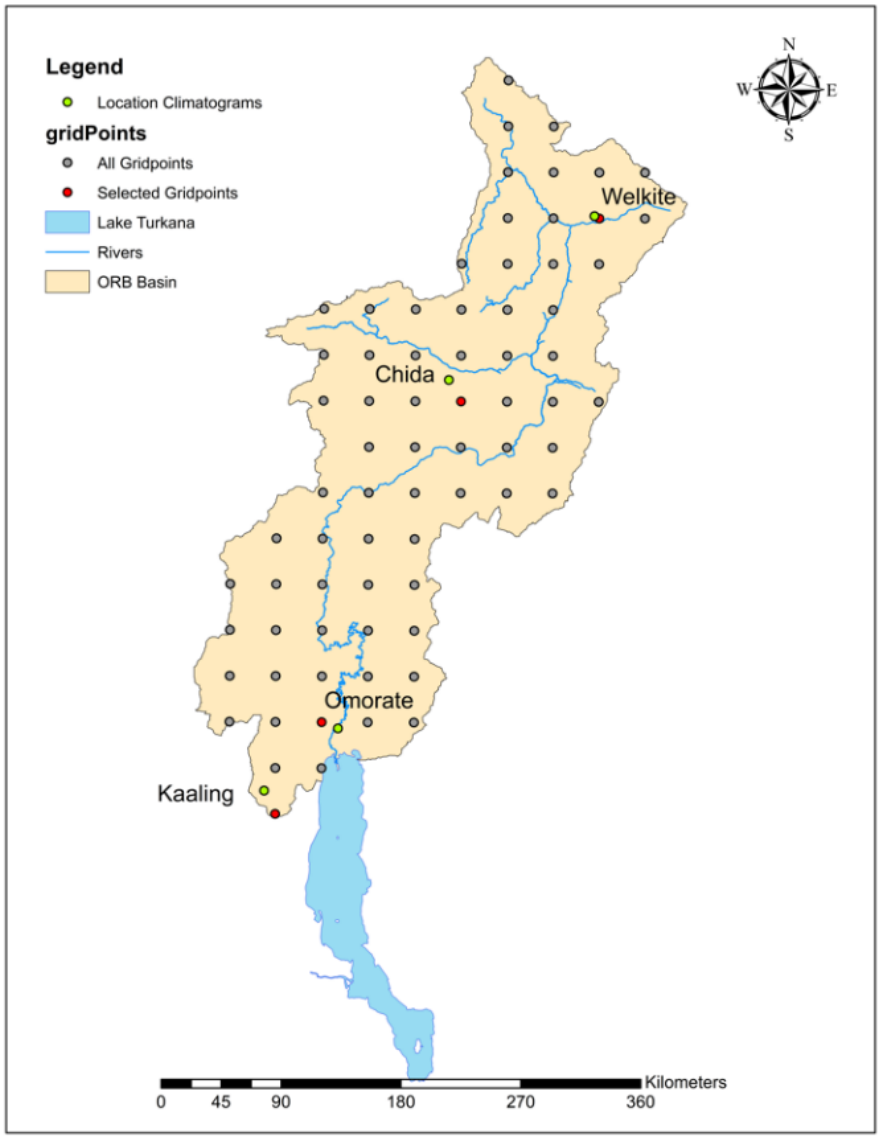

Figure 5.8. The 72 grid points (grey) extracted from the Global Weather Data for SWAT database (Texas A&M University, 2018). The location of the four grid points of which data is used to create the climatograms of Figure 5.9 are indicated in red and the location of the climatograms of Figure 5.2 are indicated in green.

In order to evaluate the quality of the rainfall and temperature data, the climatograms of different locations of the study area, described in section 5.2.1.1, are compared with data from the corresponding grid points in the CFSR dataset. The four grid points closest to the locations of the climatograms were selected. From these grid points, new climatograms were created by making use of eight years time series (2006-2013) (Figure 5.9). Figure 5.8 shows the selected grid points (red) together with the location of the climatograms described in section 5.2.1.1. (green) and all grid points with data used in ArcSWAT (grey).

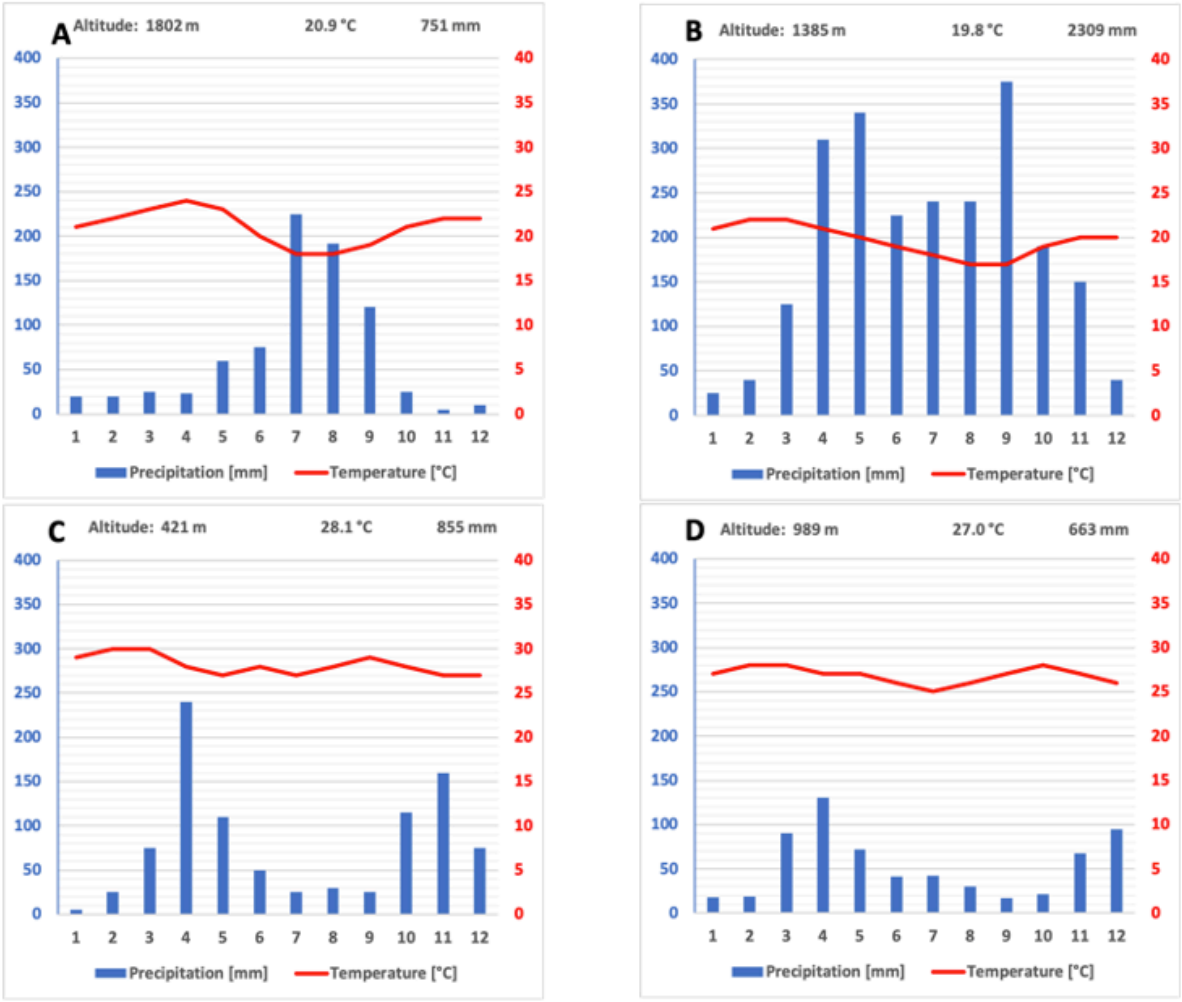

Figure 5.9. Climatograms constructed for four grid points selected from the CFSR dataset. Data from 2006 to 2013 were used. The location of the selected grid points are indicated in Figure 5.8 and they are the nearest grid points with respect to the four climatograms of Figure 5.2. A) Welkite, B) Chida, C) Omorate and D) Kaaling, (Texas A&M University, 2018)

From Figure 5.2 (reference climatograms from the study area) and Figure 5.9 (climatograms from the CFSR dataset) a similar distribution is observable. Regarding temperature, the existing climatograms and the ones from the CFSR dataset are almost identical. There is only a difference of 2.3 °C (18.6 °C in Figure 5.2 and 20.9 °C in Figure 5.9) in the average temperature per year in Figure 5.9 A (Welkite). Notorious differences can be observed in precipitation data. For instance, in Welkite the annual precipitation average is 1244 mm (Figure 5.2) and the one from CFSR dataset is 751 mm (Figure 5.9); almost two times the original one. However, the distribution is closely similar. For Chida, both charts are different.

In the original a big peak of precipitation is noticeable whereas in the second one, two small peaks are present. Regarding the annual precipitation, in this chart, there is a variation from 1583 mm (existing) mm to 2309 mm (CFSR dataset). In contrast, in Omorate the annual precipitation is closely similar in both charts. However, the total amount of rain is doubled in the CFSR datasets. For example: in Kaaling, the existing climatogram indicates a total of 360 mm of precipitation whereas the one from CFSR indicates a value of 663 mm. In Kainuk, charts (existing and from CFSR) are also different. The annual precipitation in the existing one is 534 mm and in the CFSR dataset is 734 mm. However, several authors stated that in mountainous regions, temperature, precipitation and other meteorological parameters might be variable. Moreover, data from the CFSR dataset is the result of an interpolation from a specific number of measuring stations. Thus, one pro of using this data is that covers the entire study area.

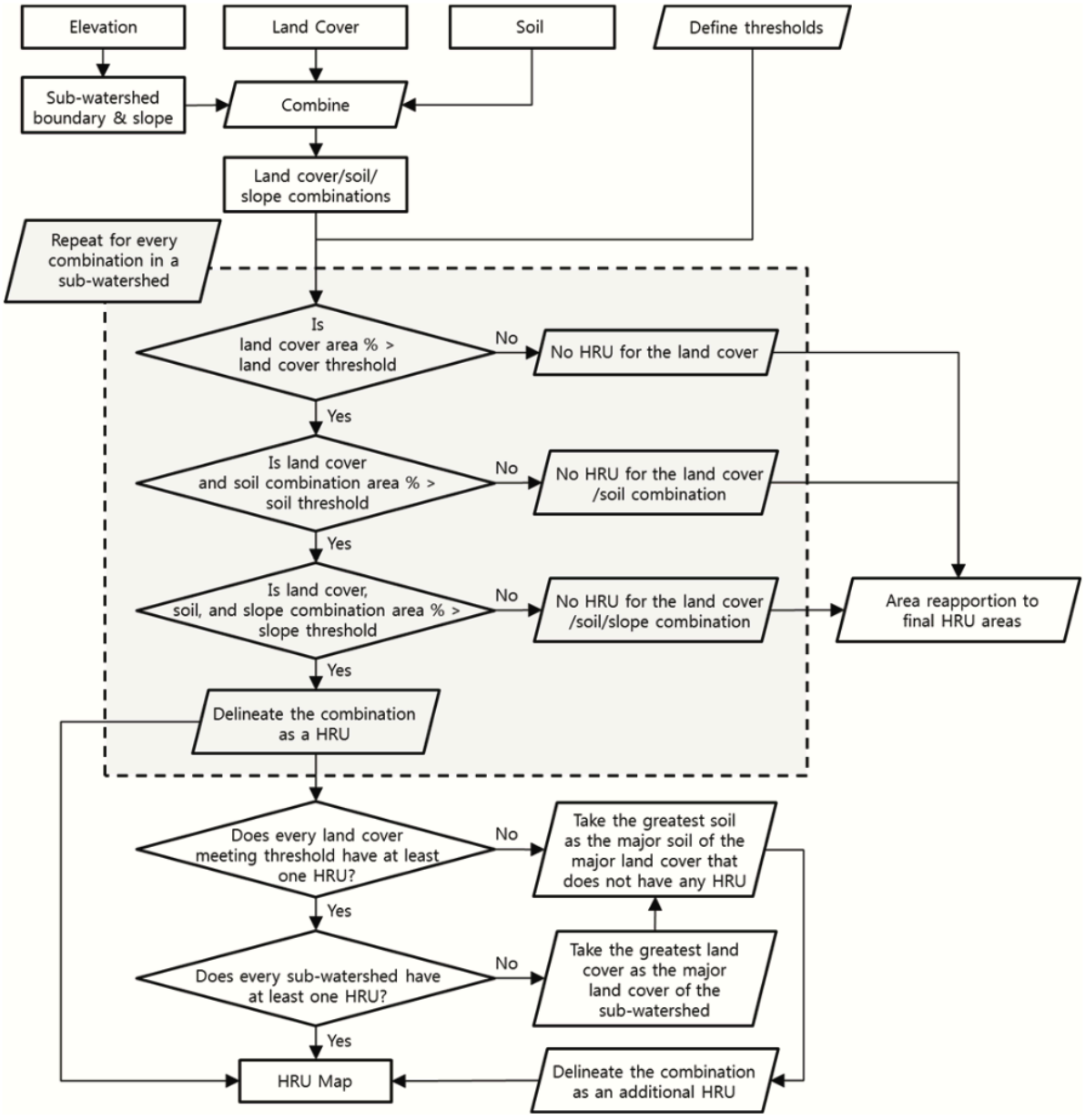

Figure 5.10. Flowchart of a HRUs definition by ArcSWAT (Her et al., 2015)

As a result of this process HRUs (Hydrological Response Units) are identified. HRUs are physically homogenous and non-contiguous areas that can respond in a similar way to the inputs. In ArcSWAT, HRUs are defined by a combination of land cover, soil, slope classes and elevation (DEM) information and a single HRU might be found in different location within the entire watershed (Figure 5.10) (Her et al., 2015).

Applying ArcSWAT tools and making use of the time series of water flow at inlets and outlets of the river network, a model is defined to establish the rainfall-runoff relationship for each HRUs. In order to define the river network, each outlet is considered as a node of the WSN with inputs (inflow) and outputs (outflow).

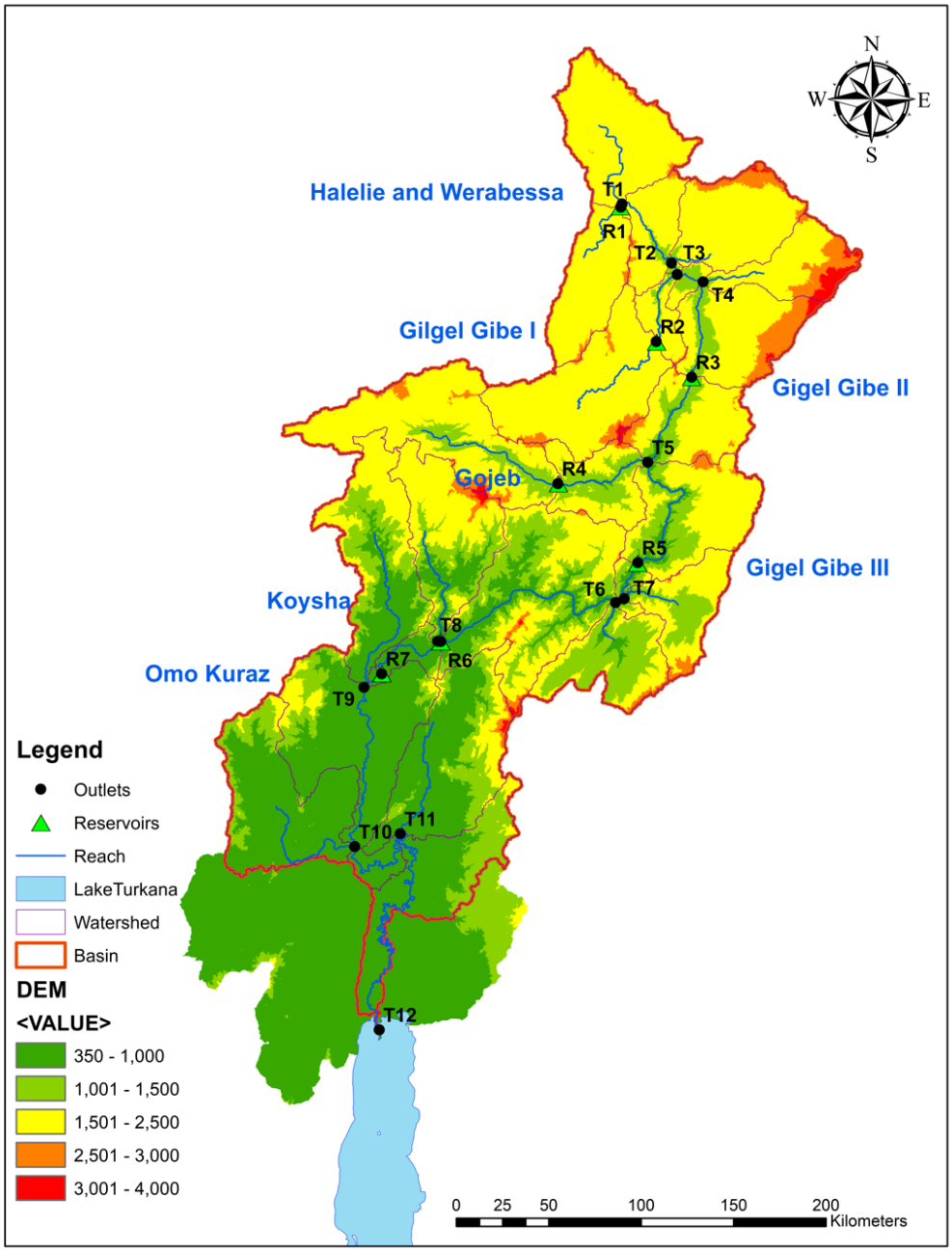

Figure 5.11. Spatial river network configuration of the ORB as derived from the DEM by means of the ArcSWAT-tools. The displayed nodes are either transfer (T) or reservoir nodes (R).

The configuration of the river network for ORB obtained with ArcSWAT is shown in Figure 5.11. There are 16 nodes (T1, T2, …, T16) in total. Each one corresponds to the outlet of a sub-basin and T1 is the inlet of the all ORB. Figure 5.11 also shows the seven reservoirs in this basin, all of them included within the river network: R1 (Halelie and Werabessa), R2 (Gigel Gibe I), R3 (Gigel Gibe II), R4 (Gojeb), R5 (Gigel Gibe III), R6 (Koysha) and R7 (Omo Kuraz). Lake Turkana (the basin outlet – T12) might be considered as a special type of reservoir, however for this research no specific information about the volume was available. The final step to define the river network scheme configuration is to specify the features of each reservoir (maximum capacity, minimum volume, height, etc.).

Whereas weather data are available from 01/01/1979 to 31/07/2014, only data from 01/01/2003 to 31/12/2013 was used. The first 3 years (2003-2005) were considered as a model warm up period which simulation results are not further analyzed. This first period is applied to initialize water availability in the river network, starting from a dry situation on 01/01/2003. Subsequent 4 years (2006-2009) were used for calibration, data from 2010 to 2011 for validation and finally data from 2012 to 2013 for application of both models (LP and MILP).

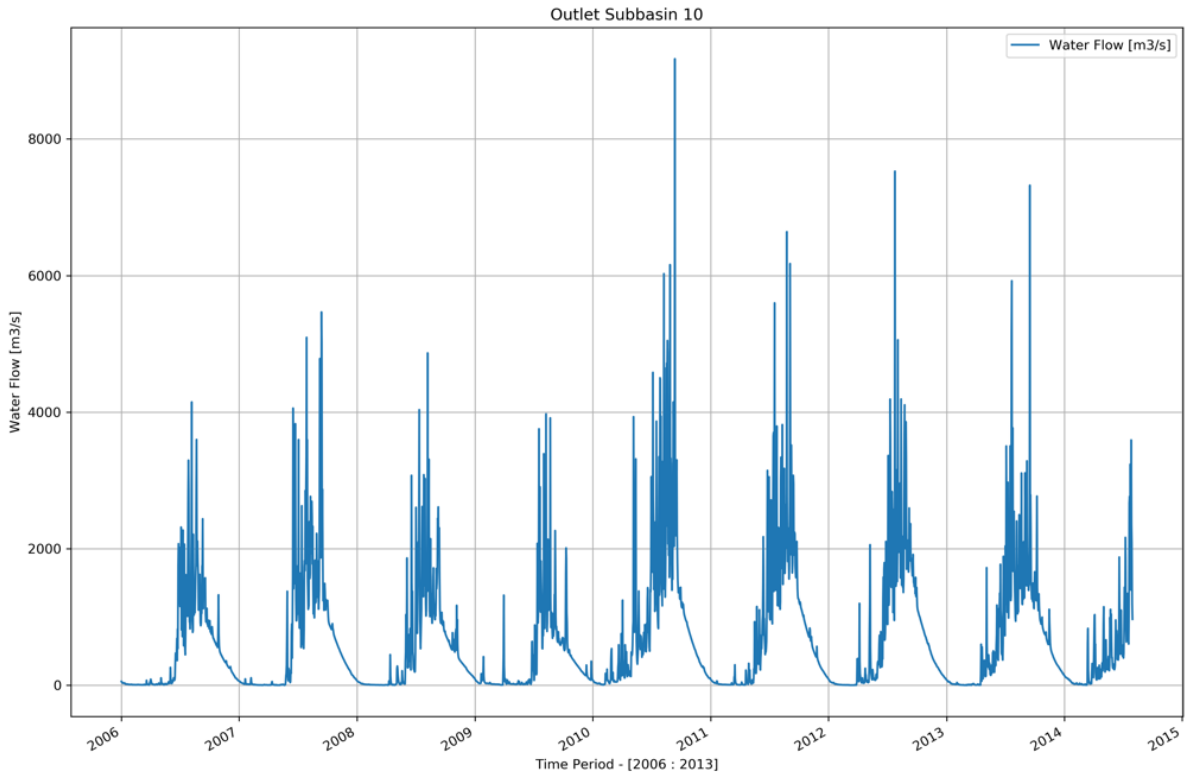

Figure 5.12. Simulated water inflow from sub-basin 10 through node T4

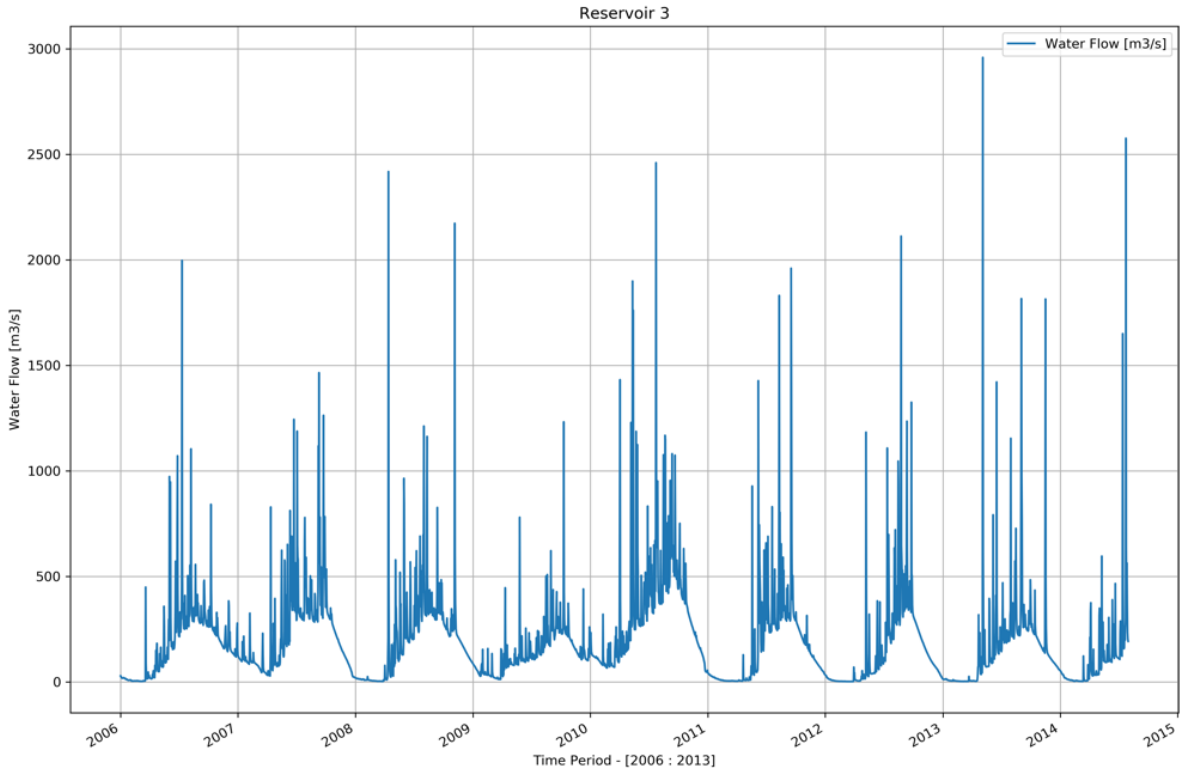

Figure 5.13. Simulated water inflow into Gilgel Gibe II (reservoir node R3).

ArcSWAT simulations generate time series of water discharge into each transfer or reservoir node. The example given in Figure 5.12 shows water discharging out of sub-basin 1 and accumulating in the Gilgel Gibe II (node R3). In the northern part of the basin there is only one rainy season, so that it is reasonable to observe a single discharge peak each year. Figure 5.13 shows the time series of simulated water inflow into Gilgel Gibe II (reservoir 3).

5.2.2.3. Water Demands and Final River Network Configuration

Five types of water use were identified: a) industrial, b) hydropower production, c) wetlands conservation, d) households use, and e) irrigated agriculture. The procedure applied to calculate water demands is explained below:

a) Water demand for industrial use: only water required for the Kuraz sugar industry (Sugar Corporation, 2019) was taken into account (2 factories). As a reference, a factory that processes 140000 kg of sugarcane per day requires, approximately, a daily volume of 2000 m^3 of water (Cortes et al., 2011);

b) The volume of water required by the hydropower plants was calculated with the equation from (Renewables First, 2018) which takes into account the installed capacity and the height of the reservoir. The four hydropower plants, each one with a reservoir, located in the basin are Gilgel Gibe I, II, and II (ACSA, 2017; Bertoni et al., 2017). Hydropower is, in contrast with the other demands, a delaying demand, which means that water is not consumed but flows back into the system;

c) Water demand for wetlands and Lake Turkana: according to (Kuo & Shih, 2015), the annual water depth required to conserve wetlands ranges from 15 to 60 mm. This demand was calculated by multiplying the total wetland area by the required mean water depth and the number of months of water shortage. Just like with the reservoirs, evapotranspiration losses must be compensated. Based on calculations for the Awash basin, an Ethiopian basin northeast of the Omo basin, an annual average evapotranspiration loss of 1 m was selected for all wetlands (Karimi et al., 2015). In Lake Turkana annually up to 2.2 to 2.4 m of water is lost due to evaporation (Pearce, 2014b; UNEP, 2013);

d) Water needed by households (human consumption, hygiene, laundry, etc.) corresponds to 100 to 200 of liters per person per day (WHO, 2015);

e) Water demand for irrigation: according to Van Orshoven et al., (2018), maize is the main crop within the ORB. In order to calculate this demand, an assumption was made stating that irrigation schemes (Figure 5.14) produce maize. Water demand was estimated by subtracting the annual rainfall from the annual crop water need. It was assumed that maize has a growing period of 153 days and needs 650 mm during this period, which results in an average crop water demand of 4.25 mm per day. Then, this value (net irrigation demand), was converted into gross irrigation demand by taking into account an irrigation efficiency of 70%, which resulted in an average crop water demand of 6.07 mm per day in the growing period (Van Orshoven et al., 2018).

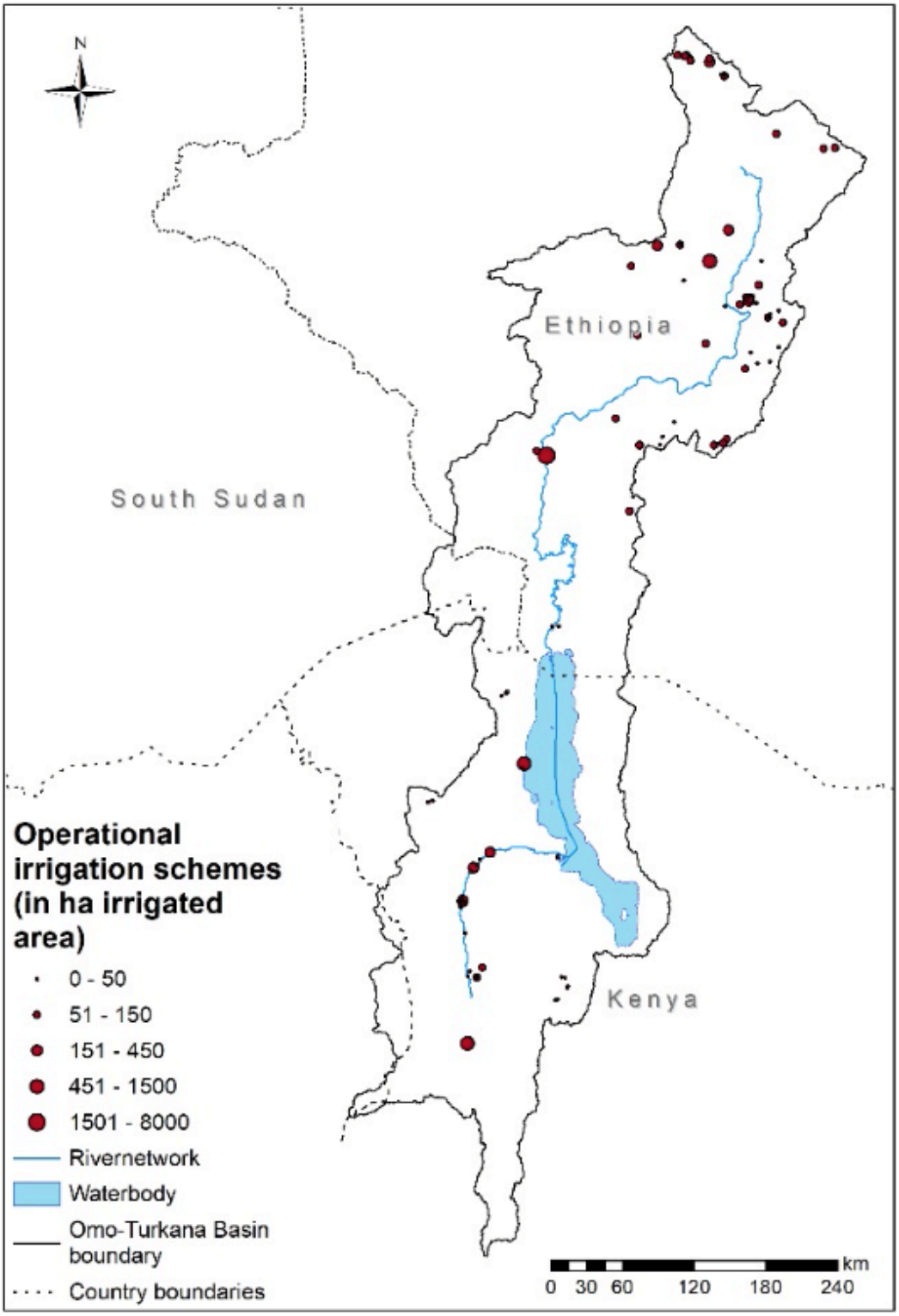

Figure 5.14. Operational irrigation schemes in the Omo-Turkana River Basin (Van Orshoven et al., 2018).

Table 5.2 lists a summary of the water demands in the ORB as compiled by DAFNE (2018). Each demand node is associated to a node (T or R) in Figure 5.11. There are five types of demands spread over 19 demand nodes each with an assumed constant daily water requirement.

Table 5.2. Daily water demands in the ORB (DAFNE, 2018)

Node	Demand for Industrial use [hm³/day]	Demand for Hydropower [hm³/day]	Demand for household consumption [hm³/day]	Demand for wetland conservation [hm³/day]	Demand for irrigated agriculture [hm³/day]	Sum of all demands [hm³/day]
D1	-	-	1.16E-02	-	1.28E-04	1.17E-02
D2	-	-	1.61E-02	8.97E-04	-	1.70E-02
D3	-	-	7.18E-03	-	7.93E-05	7.26E-03
D4	3.68E-05	6.30E-03	3.39E-02	-	5.17E-03	4.54E-02
D5	-	-	3.57E-03	-	2.29E-06	3.58E-03
D6	-	4.91E-03	2.17E-02	-	6.67E-04	2.73E-02
D7	-	-	2.15E-02	-	-	2.15E-02
D8	-	6.60E-03	2.92E-02	-	8.98E-04	3.67E-02
D9	-	-	3.35E-02	3.83E-04	1.43E-03	3.53E-02
D10	-	1.05E-02	4.45E-02	-	1.44E-02	6.94E-02
D11	-	3.10E-04	1.15E-03	-	1.94E-04	1.65E-03
D12	-	2.90E-03	1.07E-02	-	1.81E-03	1.54E-02
D13	-	6.99E-03	2.59E-02	-	4.36E-03	3.72E-02
D14	-	-	9.26E-03	-	-	9.26E-03
D15	1.99E-03	-	1.88E-04	-	-	2.18E-03
D16	-	-	6.47E-03	-	-	6.47E-03
D17	-	-	2.79E-03	1.03E-02	6.94E-02	8.25E-02
D18	-	-	1.52E-03	5.60E-03	3.78E-02	4.49E-02
D19	-	-	9.96E-04	1.34E-01	1.65E-01	2.95E-02

Figure 5.11 nodes labeled R (reservoir) and T (transfer node). Besides, in this figure associated to each node there is a demand node (D). Reservoir nodes are characterized by a maximum capacity and a minimum volume to be kept. At transfer nodes, water flows from an upstream segment draining the corresponding sub-basin, into the connected downstream segment which might be a regular river segment or a segment leading to a demand node. Thus, transfer nodes which correspond to the outlet of a sub-basin receive runoff water from the HRUs present in the sub-basin as modelled by ArcSWAT and also water from the upstream segment. Demand nodes are associated to the time series of water volumes required for a specific purpose. A regular “river segment” is bounded by two T-nodes or one T- and one R-node. Segments that end up in a D-node are termed “demand segments”.

The geographic configuration shown in Figure 5.11 can be transformed into the schematic network displayed in Figure 5.15. It encompasses 3097 HRUs, 18 river segments, 12 transfer nodes, 7 reservoir nodes and 19 demand nodes (hydro-power generation, irrigation or human consumption). Through the ArcSWAT-approach five rivers are maintained in the network: Gibe, Wave, Gilgel Gibe, Omo and Gojeb. In order to clarify the configuration, transfer nodes T6, T7 and T12 would have associated demand nodes D11, D12 and D19 which represent the water demand for Lake Turkana.

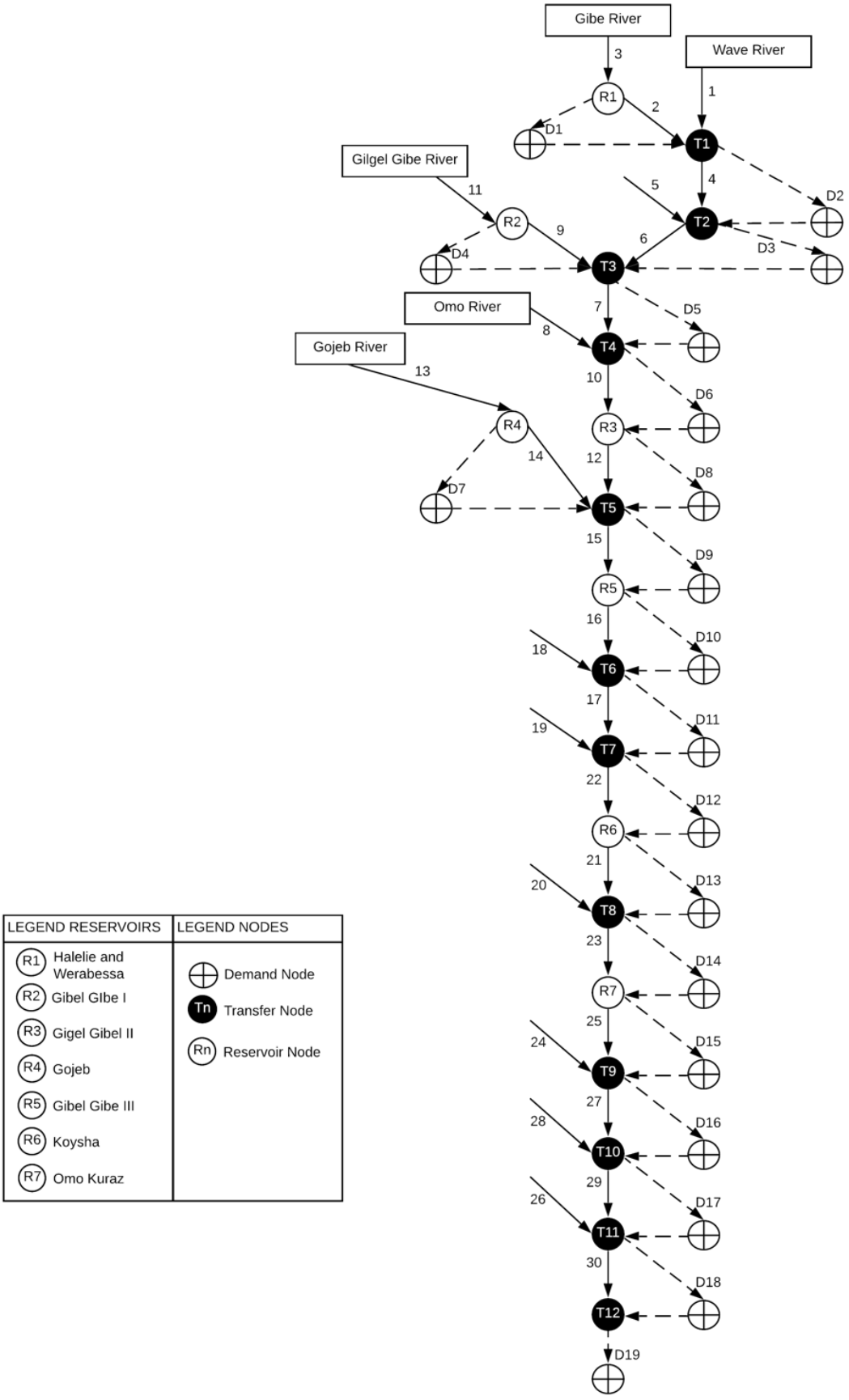

Figure 5.15. Final network configuration used in the ORB.

5.2.2.4. Objective Function and Constraints for the NFO-LP- and NFO-MILP-models

The Linear Programming model for network flow optimization, introduced in chapter 2, and its extension towards the Mixed Integer Linear Programming model, presented in chapter 4 are applied to the ORB. Hence the objective function is the one of equation 1 in section 4.2.2.2 of chapter 4. The penalty values associated to the components of the objective function are listed in Table 5.3 and the constraints are the ones listed in section 2.2.2 of chapter 2. They encompass flow balance constraints, network limitations and capacity constraints, continuity constraints, time delay constraints, constraints related to losses and floods. The default values for the parameters in the constraint equations are given in Table 5.4.

Table 5.3. Penalties associated to the boundaries of the LP model.

Parameter	Penalty	Unit	Value
P_d	Penalty for not meeting the demand with one unit	euro/hm³	1
E_d	Penalty for exceeding the demand with one unit	euro/hm³	20
W_n	Penalty for having a one unit flood in segment (n, n+1)	euro/hm³	4
B_n	Penalty not meeting the minimum capacity in segment (n, n+1) with one unit	euro/hm³	5
A_r	Penalty for exceeding the maximum capacity of a reservoir with one unit	euro/hm³	7
U_r	Penalty for not meeting the minimum capacity of a reservoir with one unit	euro/hm³	8
F_n	Penalty for not meeting the minimum demand segment capacity with one unit	euro/hm³	2
G_n	Penalty for exceeding the maximum capacity in a demand segment with one unit	euro/hm³	20
	Note: Penalty values are assigned in order to establish priorities over constraints		

Table 5.4 displays and the default values that to be calibrated.

Table 5.4. Parameters associated to the LP and MILP models.

Parameter	Description	Initial Value
$\propto_{n,n+1}^{t}$:	Loss factor associated with the river segment (n, n+1) at time (t)	10%
$\mu_{n,n+1}^{t}$:	Time delay factor associated with the water excess in a river segment (n, n+1) at time (t)	10%
$\Delta_{n,n+1}^{t}$:	Loss factor associated with the water excess in a river segment (n, n+1) at time (t)	10%
β_{n}^{t}:	Percentage of water that must flow from the nth node to the next one at time (t)	5%
γ_{n}^{t}:	Percentage of water that must remain in the nth node until the next time step (t)	20%
$\delta_{n,n+1}^{t}$:	Percentage of water that comes to the next node with a delay in time step (t)	10%
θ_{r}^{t}:	Loss factor associated to a reservoir	10%

5.2.2.5. Reservoirs

Table 5.5 lists the characteristics of the existing and envisaged reservoirs (Table 5.1) which are used to parameterize them in the (MI)LP-model constraints.

The initial values of the reservoir were calculated based on the simulation during the warm up period (2003 - 2005); this simulation process started with empty reservoirs and river segments. Regarding water demand requirements, the model included current values.

Table 5.5. Reservoir characteristics used in the LP model.

No.	Reservoir	Initial Value [hm^3]	Maximum capacity [hm^3]	Minimum volume [hm^3]	Building + management cost [euro]
1	R1 - Halelie & Werabessa	1520	5700	1140	1.28E+09
2	R2 - Gilgel Gibe I	239	920	186	1.66E+09
3	R3 - Gilgel Gibe II	239	920	186	1.53E+09
4	R4 - Gojeb	267	1000	200	1.66E+09
5	R5 - Gilgel Gibe III	3917	14700	2950	1.91E+09
6	R6 - Koysha	1747	6000	760	2.23E+09
7	R7 - Omo Kuraz	1176	4410	882	2.68E+09
	Note: 1 hm^3 = 1E+06 m^3				

5.2.2.6. Calibration and validation of the LP-model

The seven parameters of the LP-model listed in Table 5.4 need to be calibrated. Since observed data on water availability and flow in the river system were not available, water flow in the nodes of the river configuration computed by the ArcSWAT-tool was taken as a proxy for reality. Years from 2003 – 2005 were used as a warm up dataset to obtain initial values in reservoirs as well as in nodes. Likewise, data from 2006 to 2009 was used to calibrate the models. In order to perform the validation process, data from 2010-2011 were used. During calibration, the LP-model was executed in simulation rather than optimization mode. Simulation mode is configured by setting the water demands to zero in order to obtain a model which is able to transport water. Water demands will be incorporated in further phases.

The calibration process tries to adapt model parameters in such a way that the modelled data fit as close as possible with the simulated output from ArcSWAT without considering demands. The parameters which are tested are: 1) loss in river segment ($\propto$), 2) loss of flooded water (Δ), 3) loss in reservoirs (θ), 4) time delay (δ), 5) time delay of the return of flooded water (μ) and 6) continuity, which contains the minimum (γ) and maximum (β) amount of water to stay in a node. The main objective of this process is to identify which of the parameters have a big impact on the model. Therefore, a sensitivity analysis is performed. Thus, in the sensitivity analysis, increasing value parameter in steps of 5% until 100%. For instance, first iteration starts in 0%; second starts in 5%; third in 10% and so on to reach 100%.

For each river segment, the modelled flow is compared to the simulated flow in ArcSWAT and the root-mean-square deviation (RMSD) is computed. Despite the RMSD being calculated for all segments individually, only the sum of the RMSD over all segments per use case is considered since the model considers only one value per parameter. Later, the WSN will be split in branches with similar characteristics in order to make the calibration and validation procedure easier.

5.2.2.7. Application of the LP-model

Whereas model's calibration and validation are executed without considering demands, the latter are used to run the model with the application dataset. Quantification of demands per node are presented in Table 5.2. Furthermore, penalties for unsatisfied constraints are shown in Table 5.3.

Once the LP-model was calibrated and validated, it was executed applying the dataset corresponding to the 2012–2013 period (using the outputs of the 2010–2011 simulation period to initialize the model) to optimally allocate the available water to demand nodes (Figure 5.15) according to their daily water requirements (Table 5.2).

5.2.2.8. Application of the MILP-model

A description of the Mixed Integer Linear Programming model (MILP) can be found in chapter 4 and in Veintimilla-Reyes, Meyer, et al., (2018). In this section the MILP model is applied to ORB data for the years 2012 and 2013.

The MILP model considers each transfer node as a "candidate reservoir". Maximum and minimum capacities, building and management costs were calculated as we already explained in chapter 4, section 3.

5.3. Results

5.3.1. Calibration of the LP-model

In Chart A of Figure 5.16, it is clear that, initially, the total penalty decreases when the loss factor ($\propto$) is increased. However, for values higher than 70%, total penalty remains almost constant. In Chart B - loss on flooded water (Δ)-, a slight increment in the total penalty is observed for values higher than 40%. Chart C – loss in reservoirs (θ) - shows that penalties when the minimum flow in rivers is not kept and the maximum capacity is exceeded in demand segments do not depend on this parameter; on the other hand, an increment is observed in the total penalty in the other components when this parameter value is increased. Charts D – time delay (δ) and E – time delay on flooded water (μ) show that values below 80% for the parameters time delay and time delay of flooded water do not affect the total penalty values whereas a slight increase in the total penalty value is observed for parameter values higher than 80%. Finally, Chart F – Continuity minimum (γ) and maximum (β) percentage of water to stay in a node as soon as the amount of water becomes higher, the total penalty is algo becoming higher. The approach of the calibration of γ and of β is to start in the minimum (0 %) until the maximum value (100 %). Thus, in the first iteration 5% is added to the minimum and 5% is removed from the maximum. Therefore, an increment in the total penalty is observed between 0% and 10%. After, the total penalty is remaining stable and only after the 50% both parameters are overlapping. From 60% the model is unfeasible due to the situation where the value of the minimum constraint is overlapping the maximum.

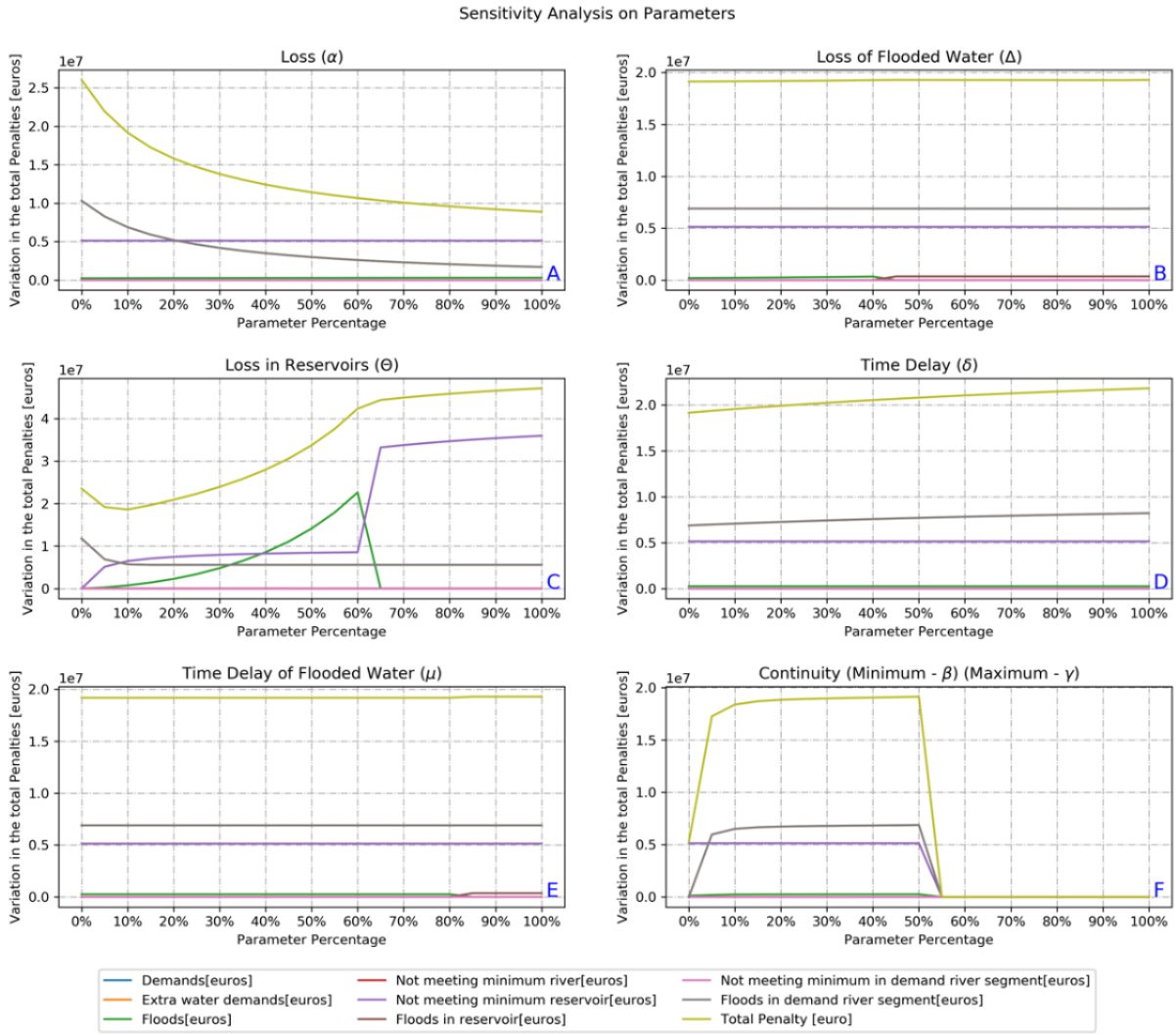

Figure 5.16. Sensitivity analysis of penalty values for 6 parameters of the LP model. Penalties [euro] related to A) Loss, B) Loss in flooded water, C) Loss in reservoirs, D) Time delay: E) Time delay in flooded water; F) Continuity

As conclusion, the most sensitive parameters are losses in reservoirs (θ) and the continuity parameters (minimum (γ) and maximum (β) amount of water that can stay in a node). This will be the starting point for the calibration stage.

The objective of the calibration phase is to adapt all parameter values with the aim of getting results that are as close as possible to a reference. In the absence of observed data (i.e. in the absence of demands), simulated water flow time series at specific nodes obtained with the ArcSWAT-model operated in simulation mode, is applied. In other words, the goal of the calibration procedure is to adjust the parameter values with the objective to reduce the gap between water flow simulated by the LP model and the corresponding values obtained from ArcSWAT.

As stated before, information from 01/01/2006 to 31/12/2009 was applied as input to calibrate the model. The reference dataset includes time series of flow in river segments and flow coming into the reservoirs. Data resulting from the execution of ArcSWAT are assumed to be a fair approximation to reality.

The calibration is based on a trial-and-error approach in which parameter values are iteratively adjusted. In order to reduce the complexity, this procedure was not applied to each of the 22 segments of the river network, but only to each of the five branches depicted in Figure 5.17. The purpose was to assign the same parameter values to all segments and nodes in the same branch.

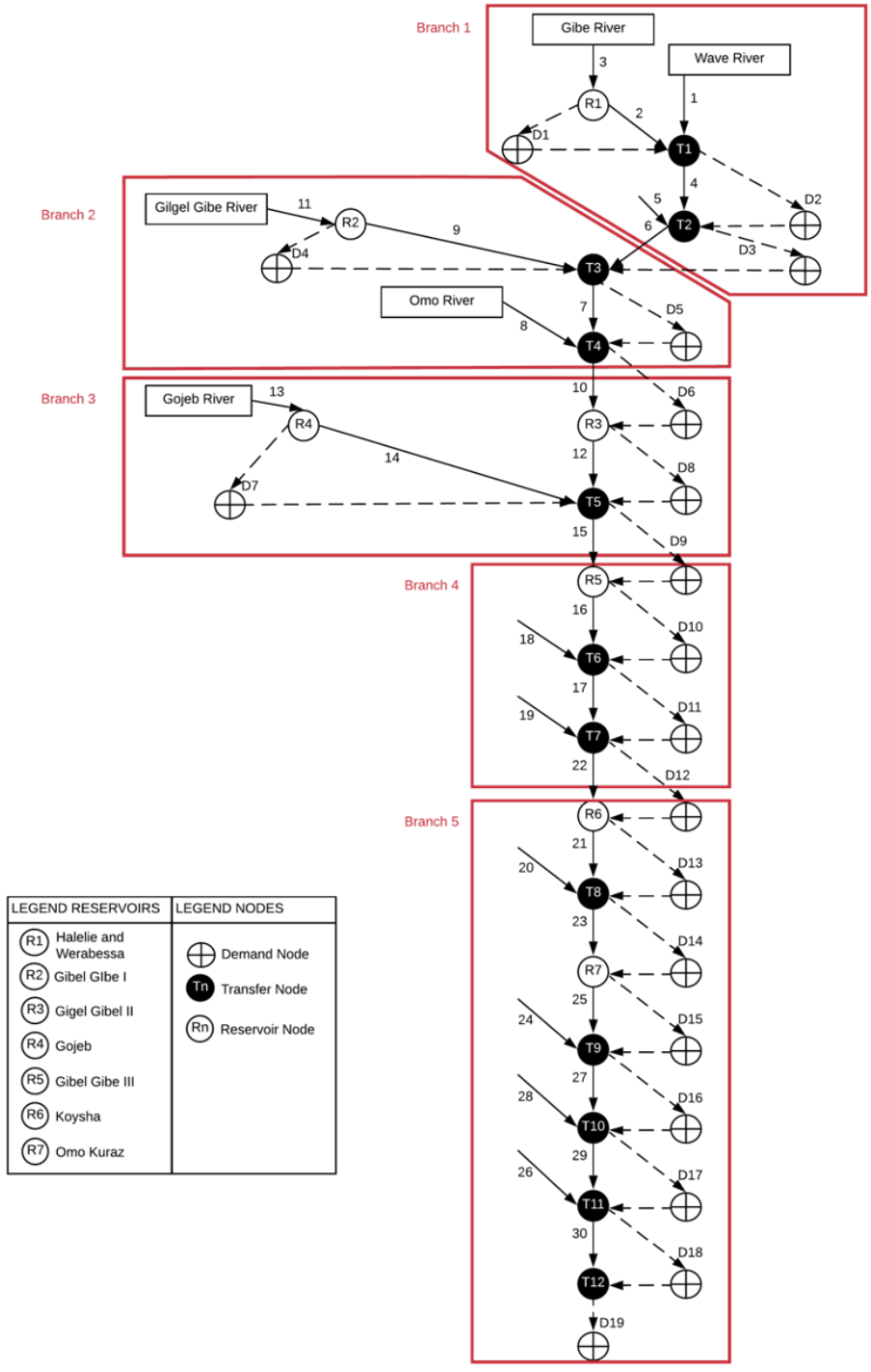

Figure 5.17. Branches of the river network used for calibration of the LP-model parameters.

Table 5.6. Default parameter values assigned to the segments and nodes in the five branches

Parameter	Loss ($\propto$)
Loss ($\propto$)	0.001
Loss Flooded Water (Δ)	0.2
Time Delays (δ)	$1x10^{-5}$
Time Delay Flooded Water (μ)	0.001
Minimum Water to Stay (γ)	0.01
Maximum to Stay (β)	0.1
Loss in Reservoirs (θ)	$1x10^{-5}$

Ten use cases were executed in order to perform the calibration process, whereby in the first use case all parameters were set to the default values in Table 5.6. A few parameters were adapted during the execution of use cases (uc) 2 to 6 in all branches: Loss in reservoirs (uc 2); continuity (maximum and minimum water to stay in a node) in uc 3; Losses in uc 4; Time delay in uc 5; Time delay flooded water in uc 6. In use case 7 only some parameters in some branches were adapted exclusively those experiencing a reduction of the total RMSD calculated in the previous use case. Thus, the adapted parameters were: "loss in reservoirs" parameter for branches 1, 3 and 5, "time delay" parameter in branches 1, 2, and 5 and "continuity" parameter in branches 1, 2 and 3. In use case 7, the selected parameters were: continuity, and losses in reservoirs. In use case 8, the selected parameters were: the ones from uc 7 plus losses in river segments. Besides, uc 9, modified parameters from uc8 plus time delay. Finally, uc 10 includes all adaptations from uc 9 plus time delay in flooded water which reduces the total value of the RMSD. Computation results for the ten use cases are included in Table 5.7.

Table 5.7. Tested parameters during the calibration of the LP model.

Use cases	Adapted parameter	Original value	New value	Sum of RMSE [hm³]
Use case 1	-	-	-	
Use case 2	Loss in reservoirs	$1x10^{-5}$	0.001	11410
Use case 3	Minimum water to stay	0.01	0.001	10658
	Maximum water to stay	0.1	0.001	
Use case 4	Loss	0.001	$1x10^{-5}$	11553
Use case 5	Time delay	$1x10^{-5}$	0.001	11573
Use case 6	Time delay flooded water	0.001	$1x10^{-5}$	11523
Use case 7	Minimum water to stay	0.01	0.001	10580
	Maximum water to stay	0.1	0.001	
	Loss in reservoirs	$1x10^{-5}$	0.001	
Use case 8	Loss	0.001	$1x10^{-5}$	10537
	Minimum water to stay	0.01	0.001	
	Maximum water to stay	0.1	0.001	
	Loss in reservoirs	$1x10^{-5}$	0.001	
Use case 9	Time delay	$1x10^{-5}$	0.001	10499
	Loss	0.001	$1x10^{-5}$	
	Minimum water to stay	0.01	0.001	
	Maximum water to stay	0.1	0.001	
	Loss in reservoirs	$1x10^{-5}$	0.001	
Use case 10	Time delay flooded water	0.001	$1x10^{-5}$	10586
	Time delay	$1x10^{-5}$	0.001	
	Loss	0.001	$1x10^{-5}$	
	Minimum water to stay	0.01	0.001	
	Maximum water to stay	0.1	0.001	
	Loss in reservoirs	$1x10^{-5}$	0.001	

According to Table 5.7 the lowest value for the sum of RMSD can be found for use case 9. Figure 5.18, shows a graphical representation of the RMSD for each river segment and for the 2006-2009 period, using the parameters of use case 9. From this figure, it is clear that the highest errors are obtained from river segments which are in the Omo river (right side of the

graph) since most water flows through these segments. Besides, it is noticeable that water flowing out from a reservoir does not have a regulation; sometimes a big amount of water and sometimes a small amount of water is flowing to the next connected river segment causing that the error becomes higher downstream the river network.

Figure 5.18 includes all river segments in river network. the nodes labeled as 13, 14, 15, 16, 17, 18 and 19 are not present in Figure 5.15. This is due to the database notation; those numbers correspond to reservoirs R1, R2, R3, R4, R5, R6 and R7 respectively. Thus, river segment "X188" represents the segment connecting node 18 (R6) with node 8 (T8).

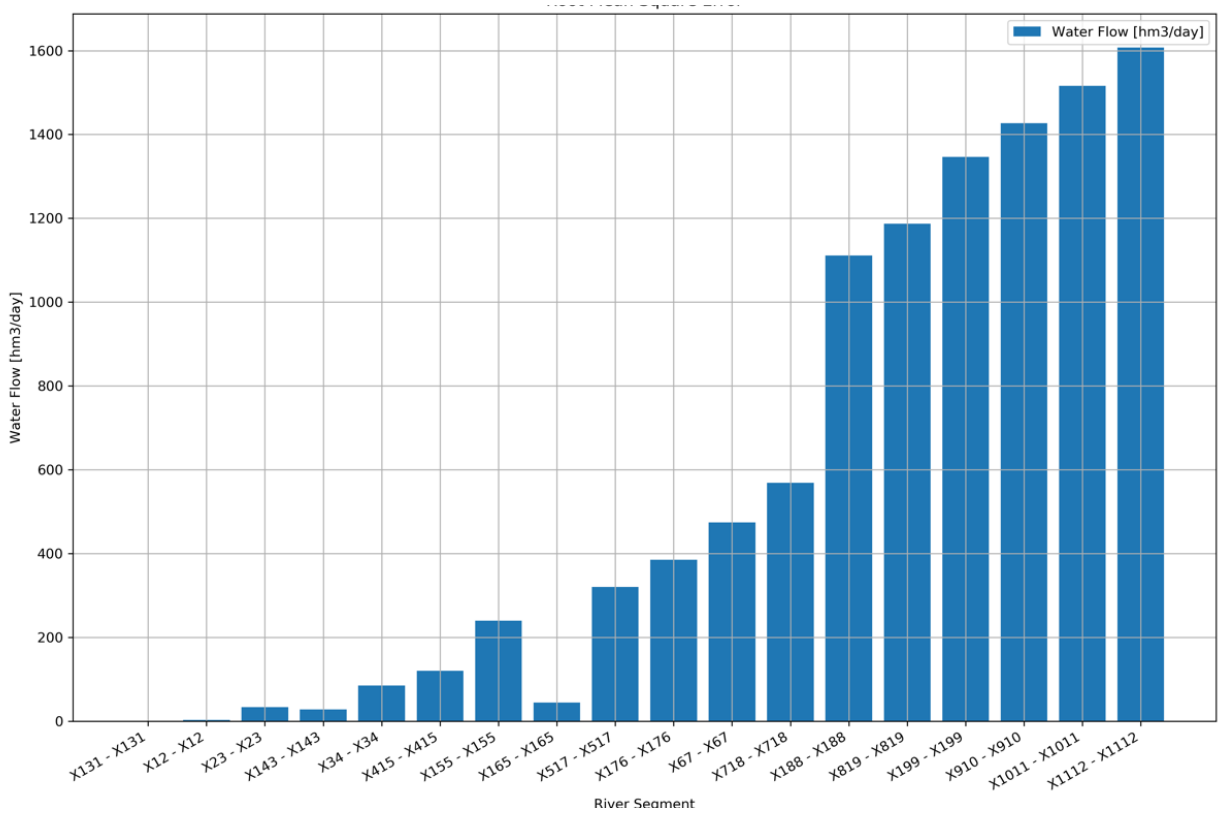

Figure 5.18. Root Mean Square Deviation[hm³/day] between the simulated water flow in ArcSWAT (reference) and the simulated water flow by the LP model using the parameters of use case 9 for the 2006-2009 time period.

5.3.2. Validation of the LP-model

This section describes the observed LP performance, when executed for the 2010-2011 dataset, after setting its parameters with values determined as result of the calibration procedure, and initializing the model with outputs achieved from the 2006-2009 dataset.

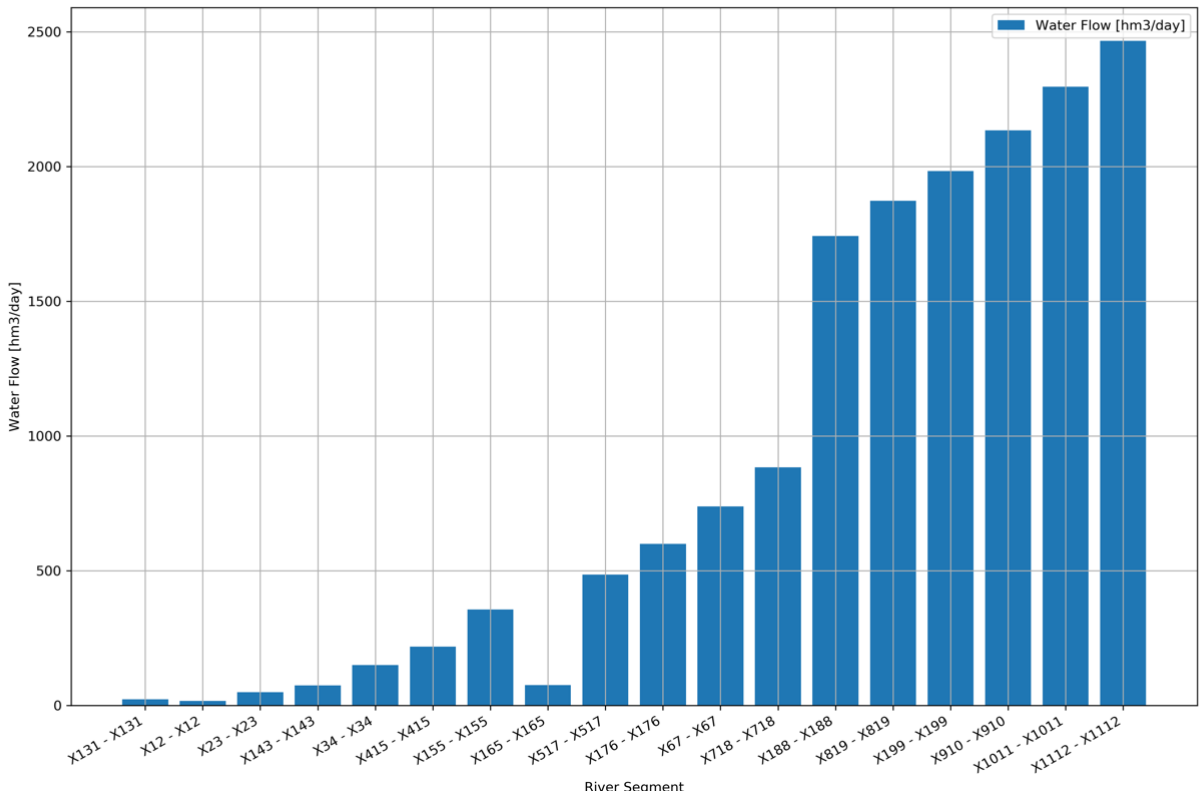

Figure 5.19. Root Mean Square Deviation [hm³/day] between the simulated water flow in ArcSWAT (reference) and the simulated water flow by the LP model for the period 2010 - 2011.

The sum of total RMSD for the period 2010 – 2011 is 16168.09 hm³/day. Figure 5.19 is similar in shape to the one from the calibration section; the main difference between both charts is the amount of water flowing in each segment. Then, for this dataset the total amount of water in the WSN is 54% higher than the best from calibration period (use case 9). Thus, the results shown in Figure 5.19 allow to assume that parameter values obtained during the calibration phase lead to a relatively good performance of the LP model, with positive perspectives to apply to different datasets.

5.3.3. Application of the Calibrated and Evaluated LP-model

5.3.3.1. Water in Reservoirs

Figure 5.20 shows water stored in the reservoirs (hm³) of the basin, throughout the 2012 - 2013 application period. Charts for some of the reservoirs (R1, R3, R4, R5 and R7), show a filling process during the wet period, immediately followed by a decreasing process. This phenomenon, evidently matches with the seasonal rainfall behavior. By contrast, in reservoirs R2 and R6 the filling process is relatively constant through time. This pattern is also present for reservoirs R5, R6 and R7. It is evident that R5, R6 and R7 are geographically close reservoirs. All this makes that the water availability follows similar patterns in those three reservoirs. However, reservoir R2, is located upstream in the basin and it only requires 4.538E-02 hm³ per day (D4). It is clear that for all reservoirs water volume is always within the minimum volume and the maximum capacity so no penalties are incurred.

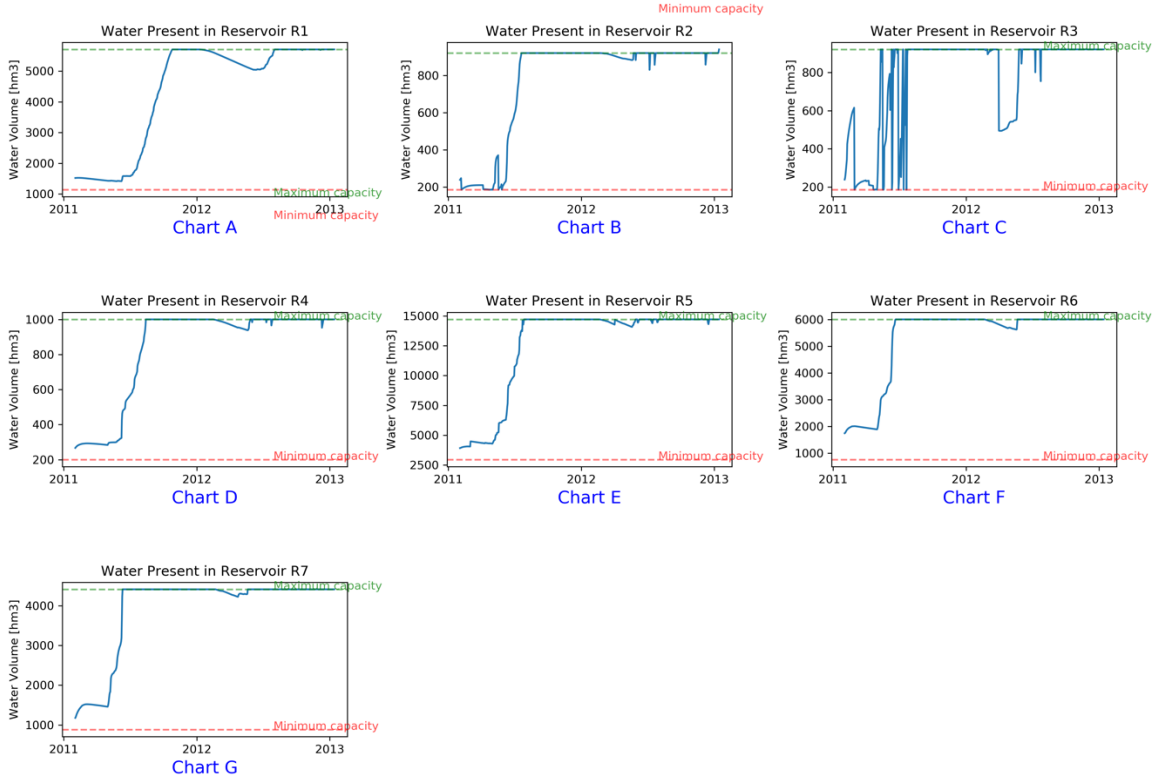

Figure 5.20. Water stored in the reservoirs

5.3.3.2. Penalties

The main objective of the LP-model is to determine whether water demands can be fulfilled with optimized allocation of the available water. Table 5.8 includes the summary of the penalties for not meeting demands as well as penalties for not fulfilling constraints. This table shows that the current demands for water in the ORB cannot be completely met after optimization, given the availability of surface water through space and time and given the available reservoirs infrastructure. However, penalties for not meeting demands are extremely low in comparison to other penalty types.

Table 5.8. Deviation of the aimed volume of water from the volume achieved after optimization (hm^3) and associated penalties (€).

Penalty cause	Volume [hm^3]	Values [euros]
(A) Penalty for not meeting the demands	6.08	6.08
(B) Penalty for floods the demands	0.00	0.00
(C) Penalty for floods in river segments	17.78	71.13
(D) Penalty for not meeting the minimum capacity in the river segments	0.00	0.00
(E) Penalty for floods in reservoirs	32.95	230.63
(F) Penalty for not meeting the minimum capacity in reservoirs	0.00	0.00
(G) Penalty for not meeting the minimum capacity in demand segments	0.00	0.00
(H) Penalty for flooding in demand segments	0.00	0.00
Total (A) + (B) + (C) + (D) + (E) + (F) + (G) + (H)	56.81	307.84

In Figure 5.21 and Table 5.8 it is clear that despite optimization of water allocation penalties remain, namely for not meeting demands, flood in river segments and overflows in reservoirs. There is a small penalty for floods of reservoirs Gilgel Gibe II (R3), Gilgel Gibe III (R5), Koysha (R6) and Omo Kuraz (R7). The monetary value of these penalties is relatively small since exceeding the maximum capacity of a reservoir results in sending extra water through the segments to connected transfer or demand nodes, which in turn causes floods in the vicinity of the reservoirs. Later, a percentage of this water is lost and the remaining is flowing back to the river segment with a delay.

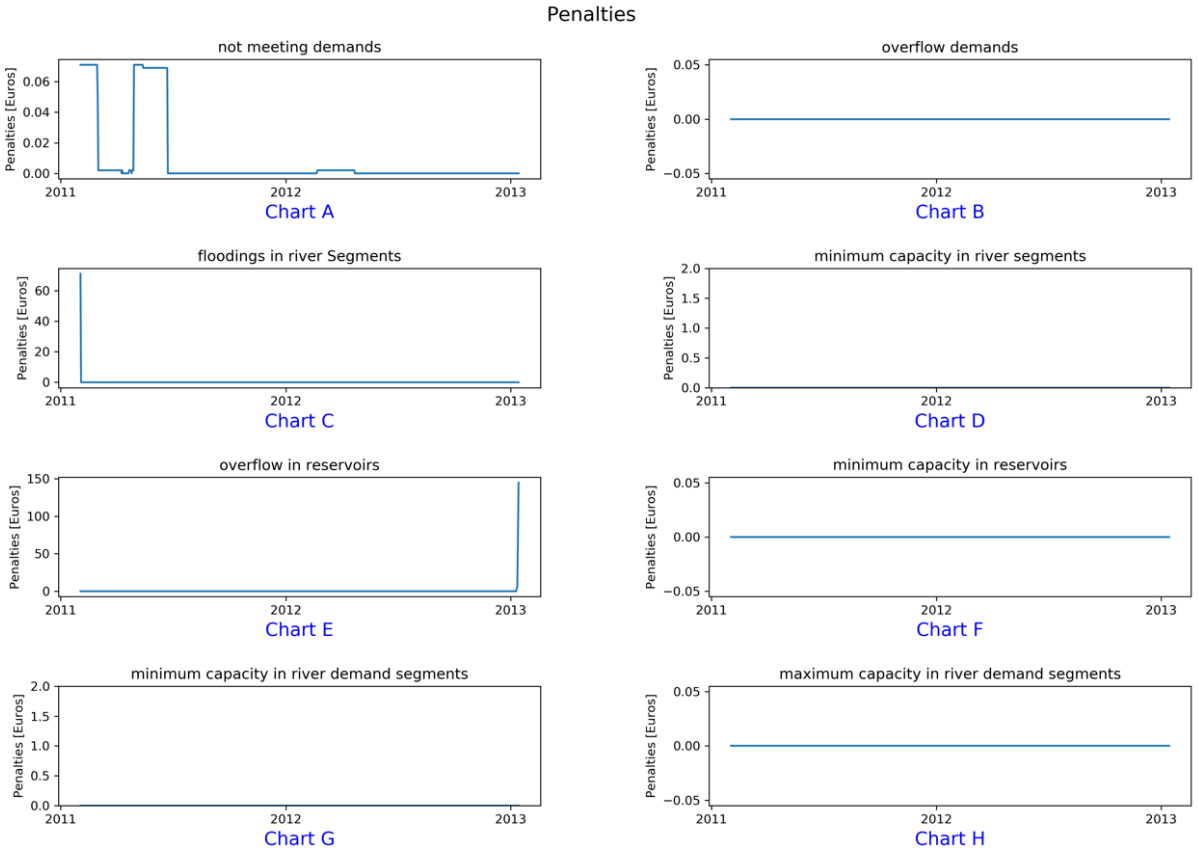

Figure 5.21. Daily penalty values (euros) observed during the full study period (scale of y-axis is variable).

The largest penalties are assigned to both no meeting demands (Figure 5.21 – Chart A - overflow demands) and exceeding the maximum capacity of a reservoir (Figure 5.21 – Chart E – overflow in reservoir).

5.3.4. Application of the MILP-Model

The dataset applied to execute the MILP-model corresponds to the period from 2012 to 2013. Moreover, to set the initial values for the water network configuration, the resultant water values from the validation process (31-december-2011) were used. The complete process to execute the MILP model application was explained in section 5.2.2.8.

5.3.4.1. Network Configuration

The network configuration used in the LP model (left) and the MILP model (right) is displayed in Figure 5.22. In the LP model, 19 nodes were considered, 12 of them were transfer nodes and 7 reservoir nodes. For the MILP model, each of the 19 nodes, is assumed as a “candidate reservoir”, i.e. treated as transfer nodes.

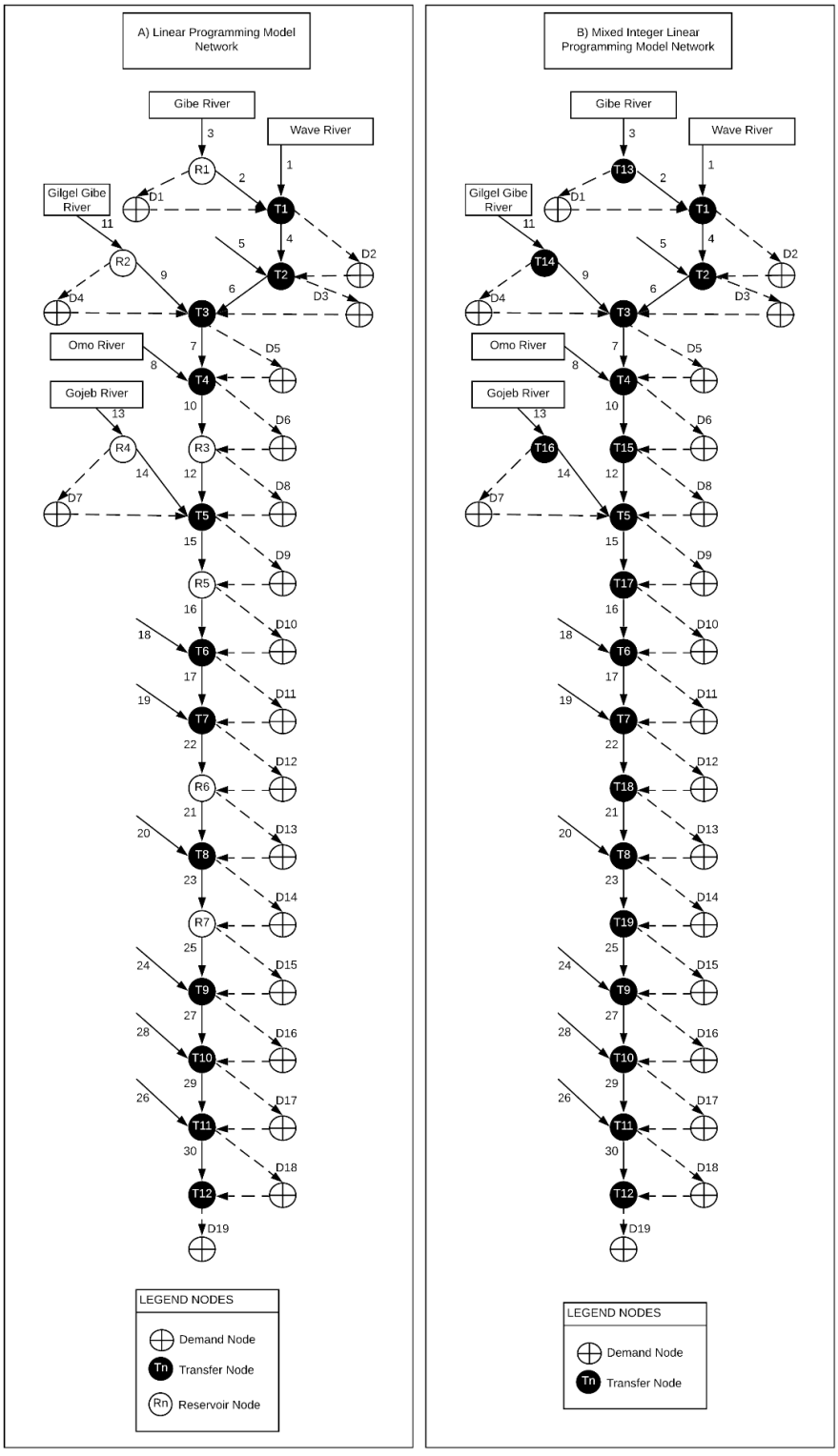

Figure 5.22. Network configuration of the MILP model

5.3.4.2. Candidate Reservoirs

Characteristics of the 7 reservoirs already considered in the LP-model are those listed in Table 5.5. Characteristics of the other candidate reservoirs are listed in Table 5.9 (including characteristics from Table 5.5). These characteristics are explained in detail in section 2.2.8.

Table 5.9. Characteristics of the "candidate reservoirs".

Node	Initial volume [hm^3]	Maximum capacity [hm^3]	Minimum capacity [hm^3]	Total Building + management cost [euro]
1	785	1125	78	1.59E+09
2	785	1125	78	1.72E+09
3	785	1125	78	2.23E+09
4	785	1730	120	2.68E+09
5	785	1730	120	1.91E+09
6	785	1730	120	2.04E+09
7	785	1730	120	2.17E+09
8	785	1730	120	2.30E+09
9	785	1730	120	2.55E+09
10	785	1730	120	2.68E+09
11	785	1730	120	1.91E+09
12	785	1730	120	2.04E+09
13	1520	5700	1140	1.28E+09
14	239	920	186	1.66E+09
15	239	920	186	1.53E+09
16	267	1000	200	1.66E+09
17	3917	14700	2950	1.91E+09
18	1747	6000	760	2.23E+09
19	1176	4410	882	2.68E+09

5.3.4.3. Model scenarios

Four scenarios were settled up to execute the MILP model. Two of the scenarios, include existing and planned reservoirs. Each time a new candidate reservoir is included as part of the model, its penalties are computed. Therefore, it is feasible to determine whether adding a given reservoir contributes to reduce penalties. The other two scenarios proceed in a similar manner, but start without reservoirs. By executing these scenarios, it is feasible to determine whether locations of already existing and planned reservoirs are good quality approximations to optimal locations.

Whereas scenarios 2 and 4 initialize reservoirs water volume from zero, condition close to reality, scenarios 1 and 3 started with a pre-defined water volume. On the other hand, in scenarios 3 and 4, building and management costs are set to zero, in order to focus the study on the impact of reservoirs penalty values, regardless of building and construction costs. One extra situation is that scenario 1 and scenario 2 are working with 7 existing reservoirs.

5.3.4.4. Results of the MILP model

Scenario 1: Adding new reservoirs to the network with existing reservoirs. New reservoirs have an initial water volume.

Table 5.10. Results generated by the MILP model when new reservoirs are added to the seven existing ones (Scenario 1). The newly added reservoir in each iteration is indicated in red and in green the existing reservoirs

Iteration	Model	Number of reservoirs	Reservoirs (nodes)	Penalties for not meeting demands [euro]	Total Penalties [euro]	Building + management [euro]	Total [euro]
1	LP	7	13,14,15,16,17,18,19	6.08	307.84	-	307.84
2	MILP	8	1,13,14,15,16,17,18,19	6.08	77.248	1.45E+10	1.45E+10
3	MILP	9	1,2,13,14,15,16,17,18,19	6.14	77.317	1.63E+10	1.63E+10
4	MILP	10	1,2,5,13,14,15,16,17,18,19	6.28	2733.88	1.82E+10	1.82E+10
5	MILP	11	1,2,5,11,13,14,15,16,17,18,19	6.29	2733.89	2.01E+10	2.01E+10
6	MILP	12	1,2,5,6,11,13,14,15,16,17,18,19	5.12	2732.71	2.21E+10	2.21E+10
7	MILP	13	1,2,5,6,11,12,13,14,15,16,17,18,19	5.12	2732.71	2.42E+10	2.42E+10
8	MILP	14	1,2,5,6,7,11,12,13,14,15,16,17,18,19	5.34	2732.94	2.63E+10	2.63E+10
9	MILP	15	1,2,3,5,6,7,11,12,13,14,15,16,17,18,19	5.34	5557.51	2.86E+10	2.86E+10
10	MILP	16	1,2,3,5,6,7,8,11,12,13,14,15,16,17,18,19	1.03	5553.20	3.09E+10	3.09E+10
11	MILP	17	1,2,3,5,6,7,8,9,11,12,13,14,15,16,17,18,19	0.83	5553.00	3.34E+10	3.34E+10
12	MILP	18	1,2,3,5,6,7,8,9,10,11,12,13,14,15,16,17,18,19	0.83	5553.00	3.61E+10	3.61E+10
13	MILP	19	1,2,3,4,5,6,7,8,9,10,11,12,13,14,15,16,17,18,19	0.83	5553.00	3.88E+10	3.88E+10

Scenario 1 illustrates what will happen if subsequently the best candidate reservoir is added to the previous solution. In this particular case, after adding five reservoirs (total = 12), the optimal solution is that 5.12 hm^3 (5.12 euros) cannot be allocated to fulfill demands during the two considered years. Comparing the results of the first two iterations and the results of iterations 6 and 7 in table 5.10, penalties for not meeting demands are lower for the latter. Table 5.10, also shows, as more reservoirs are added, the total penalty for not meeting demands becomes stable. However, the biggest penalty value is associated to flood in river segments. Besides, in this execution, the building and management cost is a highly influential variable which is notorious in Figure 5.23 chart A.

Scenario 2: Adding new reservoirs to the network with the existing ones. New reservoirs are initially empty

From Table 5.11 and Figure 5.23, it is clear that 8 reservoirs are sufficient to minimize penalties. The distinguishing feature of this scenario is that all reservoirs included in the solution must go through a filling process since the initial volume is set to zero. Therefore, the best solution contains 17 reservoirs and produces a volume of 0.13 hm^3 of water that cannot allocated. One extra feature is that in scenario 1 and scenario 2, the model selects almost the same candidate reservoirs in each iteration.

Table 5.11. Results generated by the MILP model when new reservoirs are added to the eight existing ones and the initial water volume of the added reservoirs is set to zero (Scenario 2). The newly added reservoir in each iteration is indicated in red and in green the existing reservoirs.

Iteration	Model	Number of reservoirs	Reservoirs (nodes)	Penalties for not meeting demands [euro]	Total Penalties [euro]	Building + management [euro]	Total [euro]
1	LP	7	13,14,15,16,17,18,19	6.08	307.84	-	307.84
2	MILP	8	1,13,14,15,16,17,18,19	6.15	77.32	1.45E+10	1.45E+10
3	MILP	9	1,2,13,14,15,16,17,18,19	6.29	77.46	1.63E+10	1.63E+10
4	MILP	10	1,2,5,13,14,15,16,17,18,19	6.43	32.92	1.82E+10	1.82E+10
5	MILP	11	1,2,5,11,13,14,15,16,17,18,19	6.44	32.93	2.01E+10	2.01E+10
6	MILP	12	1,2,5,6,11,13,14,15,16,17,18,19	5.27	31.77	2.21E+10	2.21E+10
7	MILP	13	1,2,5,6,11,12,13,14,15,16,17,18,19	5.27	31.77	2.42E+10	2.42E+10
8	MILP	14	1,2,5,6,7,11,12,13,14,15,16,17,18,19	5.61	32.10	2.63E+10	2.63E+10
9	MILP	15	1,2,3,5,6,7,11,12,13,14,15,16,17,18,19	5.61	5.65	2.86E+10	2.86E+10
10	MILP	16	1,2,3,5,6,7,8,11,12,13,14,15,16,17,18,19	0.36	0.40	3.09E+10	3.09E+10
11	MILP	17	1,2,3,5,6,7,8,9,11,12,13,14,15,16,17,18,19	0.13	0.17	3.34E+10	3.34E+10
12	MILP	18	1,2,3,5,6,7,8,9,10,11,12,13,14,15,16,17,18,19	0.13	0.17	3.61E+10	3.61E+10
13	MILP	19	1,2,3,4,5,6,7,8,9,10,11,12,13,14,15,16,17,18,19	0.19	0.23	3.88E+10	3.88E+10

From Table 5.11 and Figure 5.23, it is clear that 8 reservoirs are sufficient to minimize penalties. The distinguishing feature of this scenario is that all reservoirs included in the solution must go through a filling process since the initial volume is set to zero. Therefore, the best solution contains 17 reservoirs and produces a volume of 0.13 hm^3 of water that cannot allocated. One extra feature is that in scenario 1 and scenario 2, the model selects almost the same candidate reservoirs in each iteration.

Scenario 3: Starting with zero reservoirs until including all reservoirs without considering building cost but with considering initial water volume in the reservoirs

In scenario 3, the best solution minimizing penalties for not meeting the demands consists of ten reservoirs: 7,8,9,10,11,12,13, 17, 18 and 19. Among them only four reservoirs are planned or existing: nodes 13 (planned), node 17 (existing), node 18 (planned) and node 19 (planned). The volume of water that this solution is not able to allocate over 2012 and 2013 is 0.12 hm^3. Similarly, to the previous use cases, as more reservoirs are added to the solution, the total penalty for not meeting demands becomes stable; this is mainly due to the maximum and minimum capacity restrictions in reservoirs, Thus, the excess water is flowing to the next connected river segment and later to the WSN. It is remarkable that when the model establishes the number of 5 reservoirs, almost all existing and planned reservoirs are selected except node 14 (R2 – Gigel Gibe I), 15 (R3 – Gigel Gibe II) and 16 (R4 – Gojeb); the selected new reservoir in this case is node 12. In this scenario, the total penalty is becoming higher as reservoirs are added (Figure 5.23 chart C); this is the result of not fulfilling the minimum capacity constraint in a reservoir due to the filling process in the new added reservoirs.

Table 5.12. Results generated by the MILP model when all nodes are considered candidate reservoirs and the building costs are set to zero (Scenario 3). The newly added reservoir in each use case is indicated in red and in green the existing reservoirs.

Iteration	Model	Number of reservoirs	Reservoirs (nodes)	Penalties for not meeting demands [euro]	Penalties [euro]	Building + management [euro]	Total [euro]
1	LP	7	13,14,15,16,17,18,19	6.08	307.84	-	307.84
2	MILP	0	-	0.58	71.71	0	71.71
2	MILP	1	17	10.71	82.11	0.00	82.11
3	MILP	2	17,18	6.42	77.55	0.00	77.55
4	MILP	3	13,17,18	7.53	78.70	0.00	78.70
5	MILP	4	13,17,18,19	1.40	72.57	0.00	72.57
6	MILP	5	12,13,17,18,19	1.41	72.58	0.00	72.58
7	MILP	6	11,12,13,17,18,19	1.41	72.58	0.00	72.58
8	MILP	7	10,11,12,13,17,18,19	1.41	72.58	0.00	72.58
9	MILP	8	9,10,11,12,13,17,18,19	1.22	72.39	0.00	72.39
10	MILP	9	8,9,10,11,12,13,17,18,19	1.23	72.40	0.00	72.40
11	MILP	10	7,8,9,10,11,12,13,17,18,19	0.12	71.29	0.00	71.29
12	MILP	11	6,7,8,9,10,11,12,13,17,18,19	0.83	72.00	0.00	72.00
13	MILP	12	5,6,7,8,9,10,11,12,13,17,18,19	0.83	2728.42	0.00	2728.42
14	MILP	13	4,5,6,7,8,9,10,11,12,13,17,18,19	0.83	2728.42	0.00	2728.42
15	MILP	14	4,5,6,7,8,9,10,11,12,13,16,17,18,19	0.83	2728.43	0.00	2728.43
16	MILP	15	4,5,6,7,8,9,10,11,12,13,15,16,17,18,19	0.83	2728.43	0.00	2728.43
17	MILP	16	4,5,6,7,8,9,10,11,12,13,14,15,16,17,18,19	0.83	2728.43	0.00	2728.43
18	MILP	17	3,4,5,6,7,8,9,10,11,12,13,14,15,16,17,18,19	0.83	5553.00	0.00	5553.00
19	MILP	18	2,3,4,5,6,7,8,9,10,11,12,13,14,15,16,17,18,19	0.83	5553.00	0.00	5553.00
20	MILP	19	1,2,3,4,5,6,7,8,9,10,11,12,13,14,15,16,17,18,19	0.83	5553.00	0.00	5553.00

Scenario 4: Starting with zero reservoirs until including all reservoirs with an initial volume of zero and without considering building cost

In scenario 4 (Table 5.13) the initial amount of water in the reservoirs and building and management costs are assumed to be 0. This assumption results in the necessity of a filling process for each included reservoir. When meeting demands is the objective, no reservoirs are required to reduce the penalty (use case 2 – penalty 0.58 hm^3). This behavior is also present in scenario 3. Thus, from Figure 5.23 chart D, it is clear that the total penalty is growing since the minimum capacity in a reservoir is not being satisfied due to the filling process. Moreover, the reduction of penalty related with not meeting demand occurs when nine reservoirs are added; among them only three reservoirs are planned or existing: 17 (existing), 18 (planned) and 19 (existing), the rest are new reservoirs (6, 8, 9, 10, 11 and 12).

Table 5.13. Results generated by the MILP model when all nodes are considered candidate reservoirs and the building costs as well as the initial volumes are set to zero (Scenario 4). The newly added reservoir in each use case is indicated in red and in green the existing reservoirs.

Iteration	Model	Number of reservoirs	Reservoirs (nodes)	Penalties demands [euro]	Penalties [euro]	Building + management [euro]	Total [euro]
1	LP	7	13,14,15,16,17,18,19	6.08	307.84	-	307.84
2	MILP	0	-	0.58	71.71	0.00	71.71
3	MILP	1	17	10.95	77221.64	0.00	77221.64
4	MILP	2	17,18	7.62	94341.68	0.00	94341.68
5	MILP	3	17,18,19	4.54	114584.81	0.00	114584.81
6	MILP	4	12,17,18,19	4.55	114584.82	0.00	114584.82
7	MILP	5	11,12,17,18,19	4.55	114584.82	0.00	114584.82
8	MILP	6	10,11,12,17,18,19	4.37	114584.55	0.00	114584.55
9	MILP	7	9,10,11,12,17,18,19	4.39	114618.65	0.00	114618.65
10	MILP	8	8,9,10,11,12,17,18,19	1.04	113461.68	0.00	113461.68
11	MILP	9	6,8,9,10,11,12,17,18,19	0.97	113256.80	0.00	113256.80
12	MILP	10	6,7,8,9,10,11,12,17,18,19	0.99	113166.04	0.00	113166.04
13	MILP	11	5,6,7,8,9,10,11,12,17,18,19	0.99	113120.12	0.00	113120.12
14	MILP	12	4,5,6,7,8,9,10,11,12,17,18,19	0.99	110346.75	0.00	110346.75
15	MILP	13	3,4,5,6,7,8,9,10,11,12,17,18,19	0.99	108394.01	0.00	108394.01
16	MILP	14	2,3,4,5,6,7,8,9,10,11,12,17,18,19	0.99	108113.53	0.00	108113.53
17	MILP	15	1,2,3,4,5,6,7,8,9,10,11,12,17,18,19	0.99	108113.53	0.00	108113.53
18	MILP	16	1,2,3,4,5,6,7,8,9,10,11,12,15,17,18,19	1.09	110506.70	0.00	110506.70
19	MILP	17	1,2,3,4,5,6,7,8,9,10,11,12,14,15,17,18,19	5.27	216908.17	0.00	216908.17
20	MILP	18	1,2,3,4,5,6,7,8,9,10,11,12,14,15,16,17,18,19	8.01	372345.45	0.00	372345.45
21	MILP	19	1,2,3,4,5,6,7,8,9,10,11,12,13,14,15,16,17,18,19	10.23	1795383.54	0.00	1795383.54

After solving the scenarios using the MILP model, adding new reservoirs does not avoid penalties for not meeting water demand. However, penalties can be reduced by building extra reservoirs. For all scenarios, level of penalties is inversely proportional to the number of reservoirs in the solution. In scenarios 3 and 4, reservoirs: Gigel Gibe I (node 14), Gigel Gibe II (node 15) and Gojeb (node 16) are appearing later as part of the solution. In Figure 5.23, four charts of total penalties and penalties for not meeting water demands are included; it is notorious the influence of the building and management cost in charts A and B, while the penalty for not meeting demands is decreasing, the total penalty is increasing. Charts C and D, show that without building and management costs at some point penalties start increasing again.

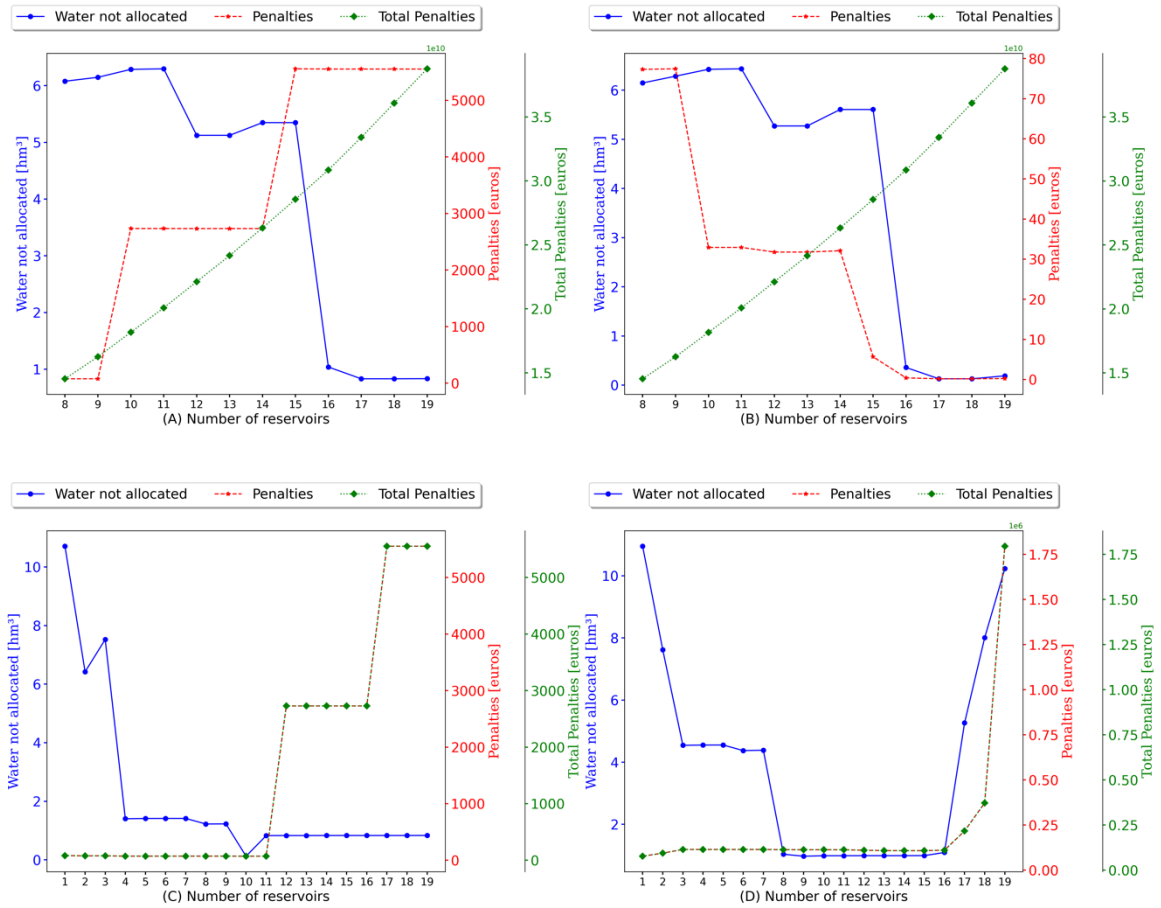

Figure 5.23. Total amount of costs corresponding to the number of selected reservoirs in scenarios.

5.1. Discussion

5.1.1. Strengths of the NFO-(MI)LP-models

From the model's execution, it is noticeable that MILP, as an extension of the LP model allows to perform a quick evaluation of the location of existing and planned reservoirs. In the same way, those models provide a rapid assessment of a reservoir and determine if a shortage or a flood could be expected.

LP and MILP models are scalable; a new restriction or constraint might be added without introducing a high complexity or without incurring several changes. In the same way and in order to test the model under different conditions, several use cases might be addressed and the results verified. For instance, climate change scenarios could be analyzed. In this case, a reduction of the precipitation could result in a drier basin and therefore more shortages can be coped with more reservoirs.

5.1.2. Weakness of the NFO-(MI)LP-models

Based on the results of model's execution, it is feasible to conclude that the most determining parameter in the selection of a new reservoir is the one associated with the building and management cost. In this chapter, there was no information available and a geo-factor was

applied to estimate the building and management costs. However, this cost might be determined by some other factors which are not considered now; besides, the total cost should be distributed over the decades or during the life time and not only for the simulation period. Therefore, it is necessary to emphasize the need for better data on the reservoir's construction and annual management costs in the region.

As a weakness, a big amount of data is required to run these models. Most of the process to obtain this data is not automated yet; e.g. adding or shifting a node within the configuration network implies that the river network and datasets need to be completely recreated. Therefore, automatizing data preparation is a key issue to run models scenarios.

5.2. Conclusions

Whereas the LP model allows to allocate water to fulfill several demands as good as possible, the MILP model determines whether the current river network configuration can satisfy all water demands, or whether there are too many reservoirs, or whether the construction of new reservoirs is necessary. Therefore, using the results provided by the MILP model, the river network configuration might be improved in order to reduce penalties.

Both the LP and MILP models use of data simulated by ArcSWAT. Although ArcSWAT is a physically based model taking inputs as land use maps, soil maps, DEMs, the time series resulting from its execution are not error free. It is, therefore, recommended to use data observed directly by sensors.

For this chapter, Gibe II was assumed to be a reservoir since the LP-model requires that a hydropower plant must have a reservoir associated. As future work, this dependence will be removed in order to treat hydropower plants in a proper manner.

From results described in this chapter, it can be concluded that, as more reservoirs are included as part of the solution, total penalty decreases. However, building and management costs will raise total expenses and will also determine which reservoirs would be in the final solution. In this particular case, it is recommendable to find a balance point between costs and penalties. Besides, in each river segment connect to a reservoir it is noticeable that a procedure to regulate the outflow of is required.

For the calibration process, it became evident that a constraint associated to the reservoir outflow should be included in order to regulate flow and produce a constant output. This is also evident for river segments following a reservoir. Additionally, the model could be extended in order to consider sedimentation within reservoirs, since this is a relevant factor that influences maximum capacities and minimum volumes.

Reservoir planning and construction must be carried out in a sustainable way, in order to minimize negative social and environmental impacts and maximize the benefits (Chen & Swain, 2014). Therefore, decisions in this regard cannot be made only based on water availability and demand but require an extensive analysis of the WEF nexus together with considering climate change, population growth and industrial development.

Chapter 6
General discussion and conclusions

6.1. Discussion

Reservoirs play an important role within the water management process due to, among other factors, climate change. The link among water, food and energy (water-food-energy nexus) is becoming more notorious (Galizia Tundisi, 2018). The optimization of water allocation is one of the options to face these challenges (Aljanabi et al., 2018; Dai et al., 2018).

Several authors Hu et al., (2016); Labadie, (2004) state that the optimization of the water allocation process is possible. As we have shown throughout this manuscript, mathematical optimization models can be applied to regions with heterogeneous characteristics.

A Linear Programming (LP) model was formulated using artificial data in chapter 2. In chapter 3, the same model was applied to the Machángara basin, located in the southern part of Ecuador, to verify the applicability of this model to real-world study regions. Chapter 4 focused on determining the optimality of the network configuration provided. To this aim, a Mixed Integer Linear Programming (MILP) model was formulated. Chapter 5 described a verification of the performance of this model by applying it to a different study area: the Omo-river basin located in Ethiopia in the central-eastern part of Africa.

The summary above shows that both the LP and the MILP models have been tested under several conditions, namely: a) two different study areas, one in Africa and one in South America; b) the size of the study areas: big (Omo), and small (Machángara); and, c) starting from basic models that were gradually elaborated by including several extensions.

A general abstraction of this research project is shown in Figure 1.8 in chapter 1. In this approach discharge time series are required as inputs, which are entered to the LP and MILP models. After these models are executed, policy makers and stakeholders can base their strategic decisions on the results produced by the models. In this sense, the models proposed in this research work can be considered part of a Decision Support System (DSS).

Since in our case studies no discharge time series are available a hydrological model like SWAT (Texas A&M University, 2018) based on geographical information can be executed to generate the missing information. In order to be executed, SWAT must be provided with several input datasets, such as a Digital Elevation Model (DEM), a soil map, a land cover map and weather information. This model is able to generate discharge time series, rainfall time series, etc. for the locations of interest in the study region.

6.1.1. WEF-nexus and reservoirs

From the literature review river basins like the Omo are suffering problems due to an unequal water distribution. A solution for this problem might be the use of reservoirs/dams.

Environmental impacts are increased as the number of reservoirs in a complex grows. Regulated water flow and transformation of national parks into sugar cane plantations are destroying local biodiversities. For instance, filling the reservoirs results in a reduction of the water level of Lake Turkana. When filling the Gibe III reservoir in 2016, the lake level dropped by 2 m and it is predicted that this level will decrease by another 0.9 m when the Koysha reservoir is filled (Avery, 2017).

Reservoirs have impact on water management and flood control. Tesfa, (2013) states that building new reservoirs is a very useful tool to mitigate extreme hydrological events as well as promote the water conservation in the lower Omo area.

Nevertheless, associated to advantages, there are also disadvantages of building reservoirs. Thus, the process of damming rivers may cause large environmental damage (McEntee, 2019). Moreover, previous reservoirs built in the Omo River Basin (Gibe III) did not use a process to assess the social and environmental impact (Avery, 2017). Then, the impact of building new reservoirs will affect the environment and the biodiversity in the area.

Reservoir planning and construction must be carried out in a sustainable way in order to minimize negative impacts (both social and environmental) and maximize benefits (Chen & Swain, 2014). Therefore, in this process, it is necessary to consider a variety of criteria, such as climate change, population growth, industrial development, the WEF-nexus, etc., and not only water availability and demand.

6.1.2. ArcSWAT and datasets

There are a variety of models that can be used to simulate hydrological processes, for instance SWAT, Mike SHE, HBV, TOPMODEL, etc. (Devia et al., 2015). Due to the fact that no ground truth data were available for the study area, we decided to apply the ArcSWAT model to obtain the required discharge time series. ArcSWAT requires several input datasets and involves a wide number of parameters that can be adjusted in order to improve its performance; however, for this project, the default parameter values were used. It is reasonable to assume that the calibration of these parameters may improve the results. Additionally, for the use cases considered in this research project, the DEMs, soil maps and land cover maps should have a high resolution in order to generate a realistic river network and meaningful Hydrological Response Units (HRUs). The weather information used in this research project was obtained from the Global Weather Database for SWAT (Texas A&M University, 2018). This weather information was interpolated based on a few weather stations located in the area. Although accurate ground measured precipitation data is the most important input for modelling river discharges, it is often not available in remote areas (Roth & Lemann, 2016). (Roth & Lemann, 2016) compared the GWD4S dataset with conventional weather data for discharge modelling with SWAT in small catchments located in the Ethiopian Highlands. They concluded that the GWD4S weather data contain unsatisfactory discharge outputs, while for conventional weather data, the quality of the results was high. (Roth & Lemann, 2016) also observed that the seasonal pattern is well represented in the dataset. However, there is a mismatch with the amount of real rainfall. This statement is clearly represented on the results we obtained for the two studied basins (Omo and Machángara).

As it is shown in chapters 3 and 5, the river network resulting from the ArcSWAT model provides a realistic representation. By providing the location of the basin outlet, its sub-basins can be delineated and their corresponding outlets located. After the river network was generated, reservoirs and additional outlet nodes could be indicated. A limitation of the tools used in this research was the lack of an efficient way to transfer the output of ArcSWAT to the LP and MILP models. Specifically, every time ArcSWAT was executed, its results had to be copied as inputs for the LP and MILP models. In case observed discharge time series for this

basin would have been available, this process could have been avoided, allowing for more efficient tests of different river network configurations.

The two following sections analyze the validity of the weather datasets retrieved from the GWD4S used in this project: the Machángara river basin dataset (chapter 3) and the Omo River Basin dataset (chapter 5).

6.1.2.1. Machángara River Basin (Chapter 3)

As stated in chapter 3, the Machángara river basin is located in the southern provinces of Azuay and Cañar, in Ecuador. The data generated for the virtual station p-27-791 of the GWD4S were used as the input for SWAT to obtain the required discharge time series in each of the nodes (outlets) of the WSN. To validate the dataset, we used the information from a physical weather station labeled as El Labrado. The monitoring data are dispersed in several databases ruled by different institutions: Instituto Nacional de Meteorología e Hidrología (INAMHI), Instituto Ecuatoriano de Recursos Hídricos (INERHI), and Instituto Ecuatoriano de Electrificación (INECEL). In 1987, the "Plan Nacional de Riego" project INERHI ORSTOM developed a complete assessment of the existing data bases, including the revision on the quality of the data and merged the different databases in one database called BIDRIE (Le Goulven et al., 1987).

El Labrado stations has 30 years of data (1960 – 1990) and is located: latitude: -2.732°S; longitude: -79.073°O. GWD4S includes 35 years of data (1979 – 2014).

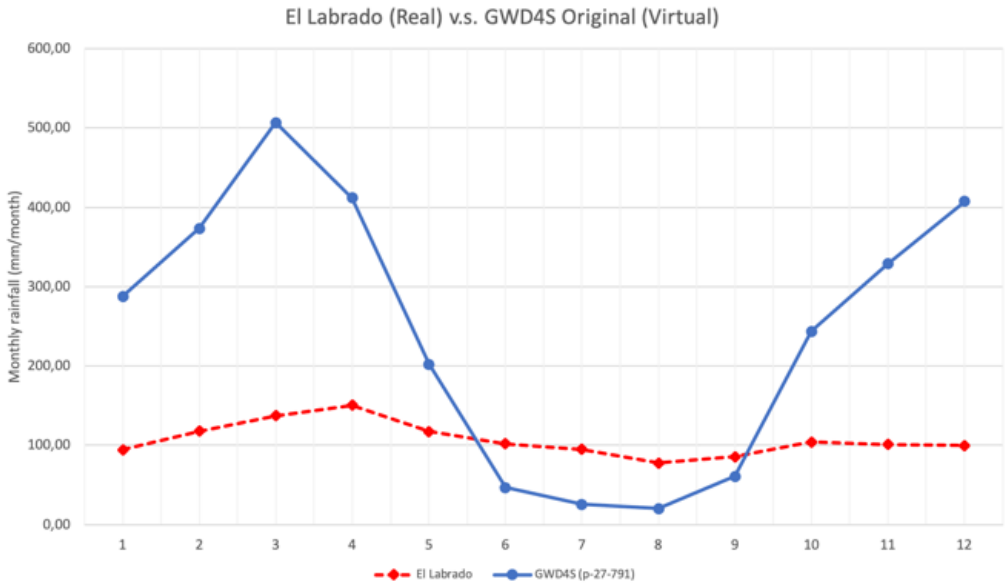

Figure 6.1. Comparison of average monthly precipitation values from GWD4S and El Labrado stations

Figure 6.1, monthly average values are compared, this figure also shows that the precipitation values from the two stations are inconsistent. In the dataset from GWD4S the magnitude is three or four times higher than El Labrado during the rainy periods (January – May and October - December) and lower during the dry period (June - September). These differences resulted in a RMSD value of 202.56 mm/month.

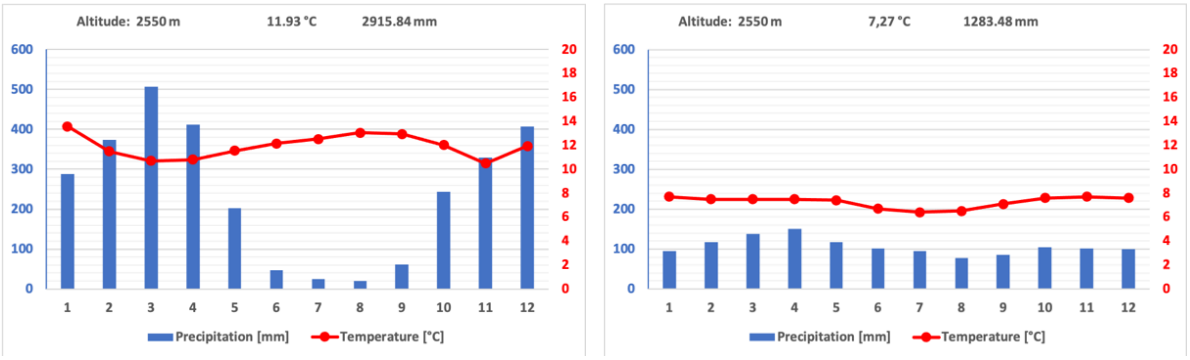

Figure 6.2. Climatograms from GWD4S (left) and WorldClim dataset (CRU-TS 4.03) (right)

In Figure 6.2, the climatogram at the left corresponds to the GWD4S dataset. It shows a mean temperature of 11.93 °C and 2915.84 mm of rainfall. The climatogram at the right corresponds to the WorldClim dataset (Harris et al., 2014). It presents a mean temperature of 7.27 °C and a rainfall of 1283.48 mm, which is consistent with the information in Mora et al., (2014). Furthermore, there are some values in the GWD4S dataset that are not plausible for the Machángara basin. For instance, in the period between 2011 – 2014, the maximum temperature reaches 30 °C, which is not reasonable, considering that the study area is located close to the Andean highlands.

As a conclusion and based on the value of the RMSD and Figure 6.2, the GWD4S dataset clearly overestimates the precipitation and temperature values.

Global Weather Data for SWAT Scaled

In order to use GWD4S, the temperature and precipitation values must be rescaled. This process should include observed data to determine the proportion of change in each measure. Several mesuarement in the period of 2011 – 2014 have extreme values of temperature between 28 and 30 degrees which is not possible in the area. Therefore, in order to keep “normal” data from temperature and rainfall, a subset (2011 – 2014) was removed from the GWD4S. Thus, the available period goes from 1979 – 2010 (31 years). The rescaled process for rainfall was done by Prof. Guido Wyseure and the rescaled process for temperature was done by Prof. Diego Mora. The resulting values of precipitation are plotted in Figure 6.3. The RMSD for El Labrado and Scaled GWD4S is 9.30 mm/month, which is lower compared with the RSMD from the datasets in Figure 6.1.

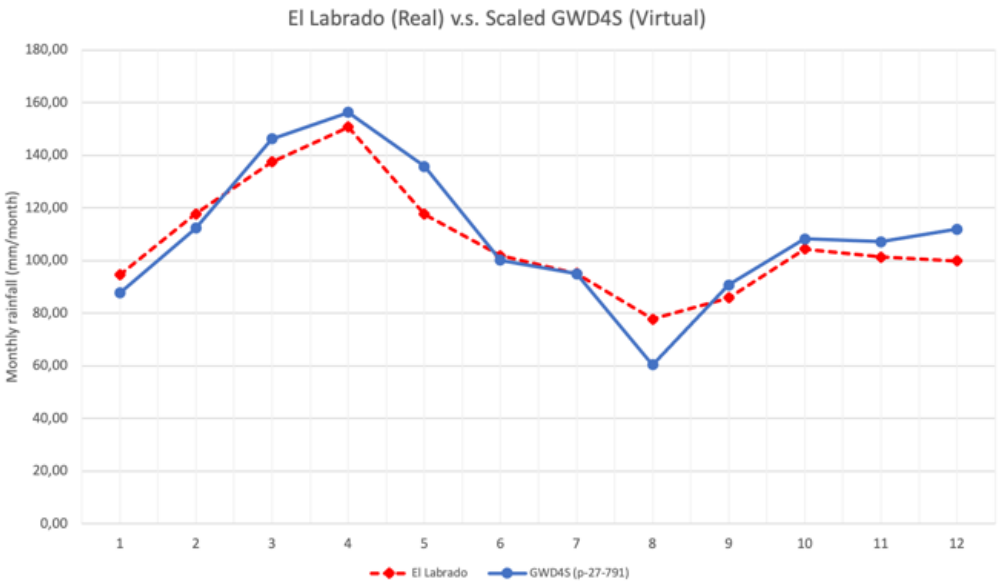

Figure 6.3. Comparison of average monthly precipitation values from Scaled GWD4S and El Labrado stations

The values of precipitation (1310.95 mm) and temperature (8.64 °C) shown in Figure 6.4 are closest to the ones stated in Mora et al., (2014).

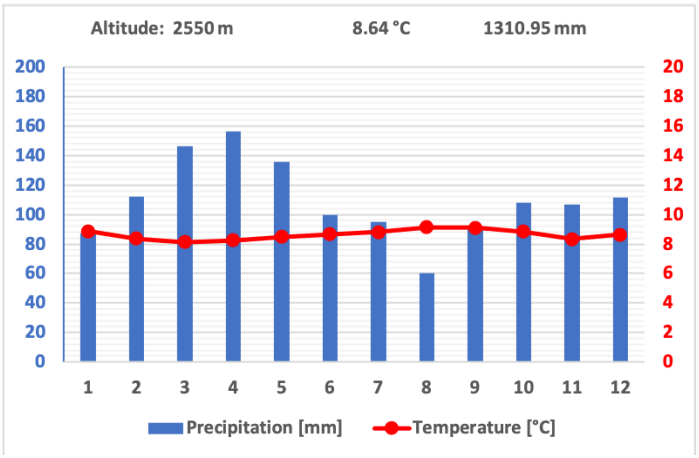

Figure 6.4. Climatogram from GWD4S scaled.

Linear Programming model (LP) applied to the scaled GWD4S dataset

Using the rescaled GWD4S-rainfall time series we redid the calibration, validation and application of the LP-model.

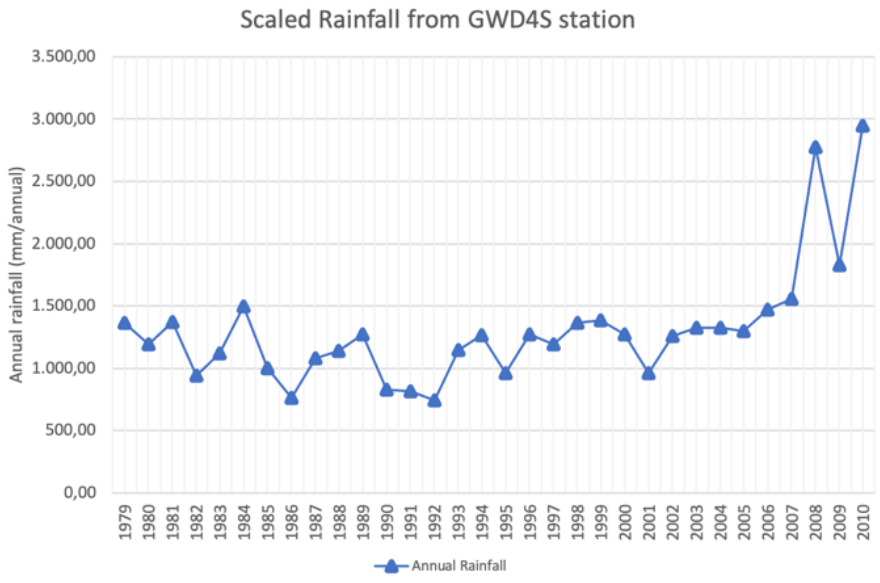

Figure 6.5. Annual rainfall in the rescaled GWD4S

In Figure 6.5, the annual rainfall in the scaled GWD4S is shown for 1979 to 2010. It can be observed that from 1979 to 2007 the value of annual rainfall is between 1000 and 1500 mm, as stated in Mora et al., (2014). However, in 2008, 2009, and 2010 the rainfall values are significantly higher than the previous years. Therefore, this period was excluded from the dataset, assuming that those values are outliers. Thus, the period used to run the LP model goes from 01/01/1998 until 31/12/2005. The period 1998 – 2001 was used for calibration, 2002 – 2003 for validation, and 2004 – 2005 for application.

Calibration

Table 6.1. Initial and calibrated value for the parameters of the LP model.

Use cases	Adapted parameter	Branch	Original value	New value	Sum of RMSD [hm³]
Use case 1	-	-	-	-	48.34
Use case 2	Minimum water to stay (β)	1,2,3,4,5	0.01	0.0001	47.33
	Maximum water to stay (γ)		0.1	0.0002	
Use case 3	Loss ($\propto$)	1,2,3	0.001	$1x10^{-5}$	47.73
Use case 4	Time delays (δ)	1,2,3	0.001	$1x10^{-5}$	47.32
Use case 5	Loss in reservoirs (θ)	1,2,3	0.001	$1x10^{-5}$	46.34
Use case 6	Loss in reservoirs (θ)	1,2,3	$1x10^{-5}$	0.01	45.88
Use case 7	Time Delay Flooded Water (Δ)	1,2,3	0.01	0.001	45.78
Use case 8	**Time delays (δ)**	1,2,3	**$1x10^{-5}$**	**0.01**	**45.77**
Use case 9	Minimum water to stay (β)	1,2,3	0.0001	0.001	46.59
	Maximum water to stay (γ)	1,2,3	0.0002	0.002	

Similarly to chapter 3, the calibration process included two phases: sensitivity analysis and the selection of the most suitable parameter values per branch (Table 6.1). For the sensitivity analysis, the results show that parameter θ (loss factor in reservoirs) is the most sensitive, which is in agreement with chapter 3, section 3.3.1.1.

To determine the values of the parameters, the WSN was split into five branches as in chapter 3 and nine use cases were executed. The original and the new values, as well as the RMSD are summarized in Table 6.1. The lowest RMSD occurred for use case 8 with a value of 45.77 hm^3. Therefore, values obtained in use case 8 were used for the next phases.

Validation

The dataset including years 2002 – 2003 was used for validation. The parameters were assigned the same values as for the calibration process. The resulting RMSD was 54.04 hm^3.

Application

For the application phase, the scaled weather dataset from 2004 – 2005 was used. Figure 6.6 shows the behaviour of the reservoirs. In R1 (chart A) and R2 (chart B) the filling and the emptying processes are evident. These two reservoirs are bigger than reservoirs R3 (chart C) and R4 (chart D). Reservoirs R3 (Saucay) and R4 (Saymirin) have a maximum capacity of 1 hm^3 and, due to this, the filling and the emptying are very prominent. Besides, both reservoirs are associated to a hydropower plant.

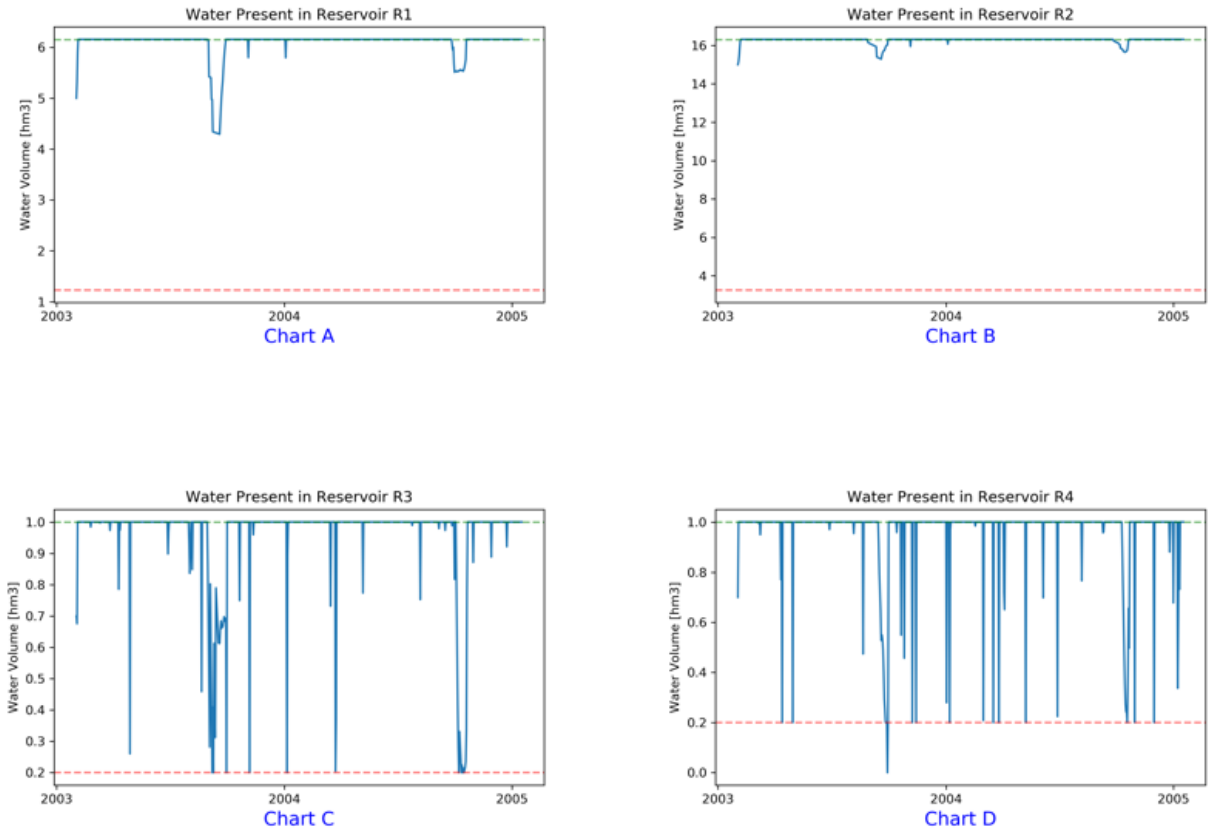

Figure 6.6. Volume of water stored in reservoirs

Penalties

The LP-model mainly produced penalties related to not meeting demands and not meeting the minimum capacity in reservoir R3 (0.20 hm^3). The results are visualized in Figure 6.7 and in Table 6.2.

Table 6.2. Deviation of the aimed volume of water from the volume achieved after optimization (hm^3) and associated penalties (€).

Penalty cause	Volume [hm^3]	Values [euros]
(A) Penalty for not meeting the demands	50.96	50.96
(B) Penalty for floods the demands	0.00	0.00
(C) Penalty for floods in river segments	0.00	0.00
(D) Penalty for not meeting the minimum capacity in the river segments	0.00	0.00
(E) Penalty for floods in reservoirs	0.00	0.00
(F) Penalty for not meeting the minimum capacity in reservoirs	0.20	1.60
(G) Penalty for not meeting the minimum capacity in demand segments	0.00	0.00
(H) Penalty for flooding in demand segments	0.00	0.00
Total (A) + (B) + (C) + (D) + (E) + (F) + (G) + (H)	51.16	52.56

Based on the rescaled dataset, there is more water available to allocate than in the original GWD4S (chapter 3). Results from the original dataset are in Chapter 3, section 3.3.2.1. Besides, in the original GWD4S there was a mismatch between the annual average reported by Mora et al., (2014) (1392 mm) and the average for the period 2011 – 2013 (782 mm).

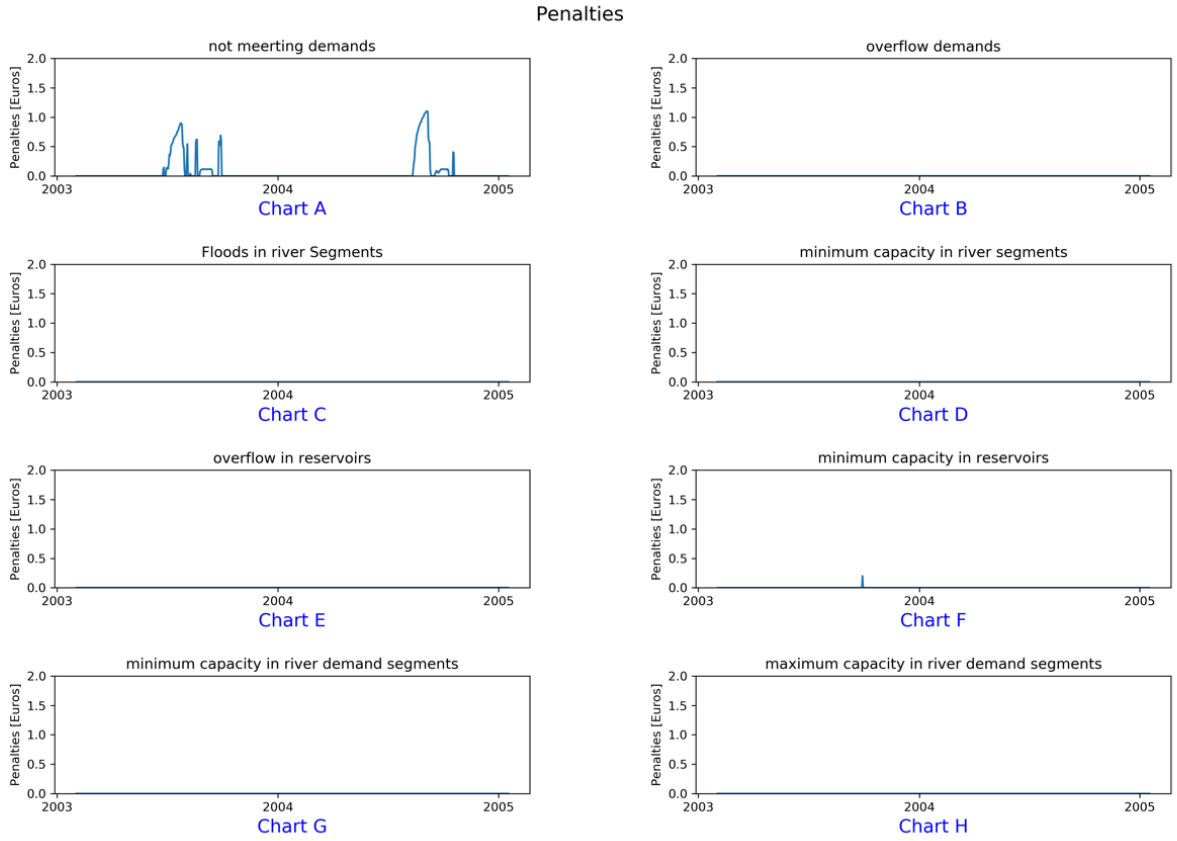

Figure 6.7. Penalties during the 2-year period (2004 - 2005).

6.1.2.2. The Omo River Basin (Chapter 5)

In the same way as for the Machángara river basin, an analysis of the GWD4S was performed for each virtual station (grid point) from Figure 5.8. data from the WorldClim dataset (WC) (Fick & Hijmans, 2017; Harris et al., 2014) were used as a reference.

Welkite

This station is located in the northern area of the Omo River Basin. In Figure 6.8 it is apparent that the GWD4S overestimates the precipitation, with an average annual value of 1524.49 mm (chart B) over the period 1979 – 2014, in contrast to the WC dataset that indicates 1225.50 mm (chart C) over the period 1979 - 2000. Moreover, chart A makes clear that the difference is situated mainly in the rainy period (June - September). In July and August there is an excess of about 150 mm. This behavior was also observed for the Machangara river basin, but for that basin the differences are higher. The RMSD between the two time series is 80.64 mm/month.

Regarding temperature, the average value in the GWD4S is 18.77 °C, whereas for the WC dataset is 19.19 °C.

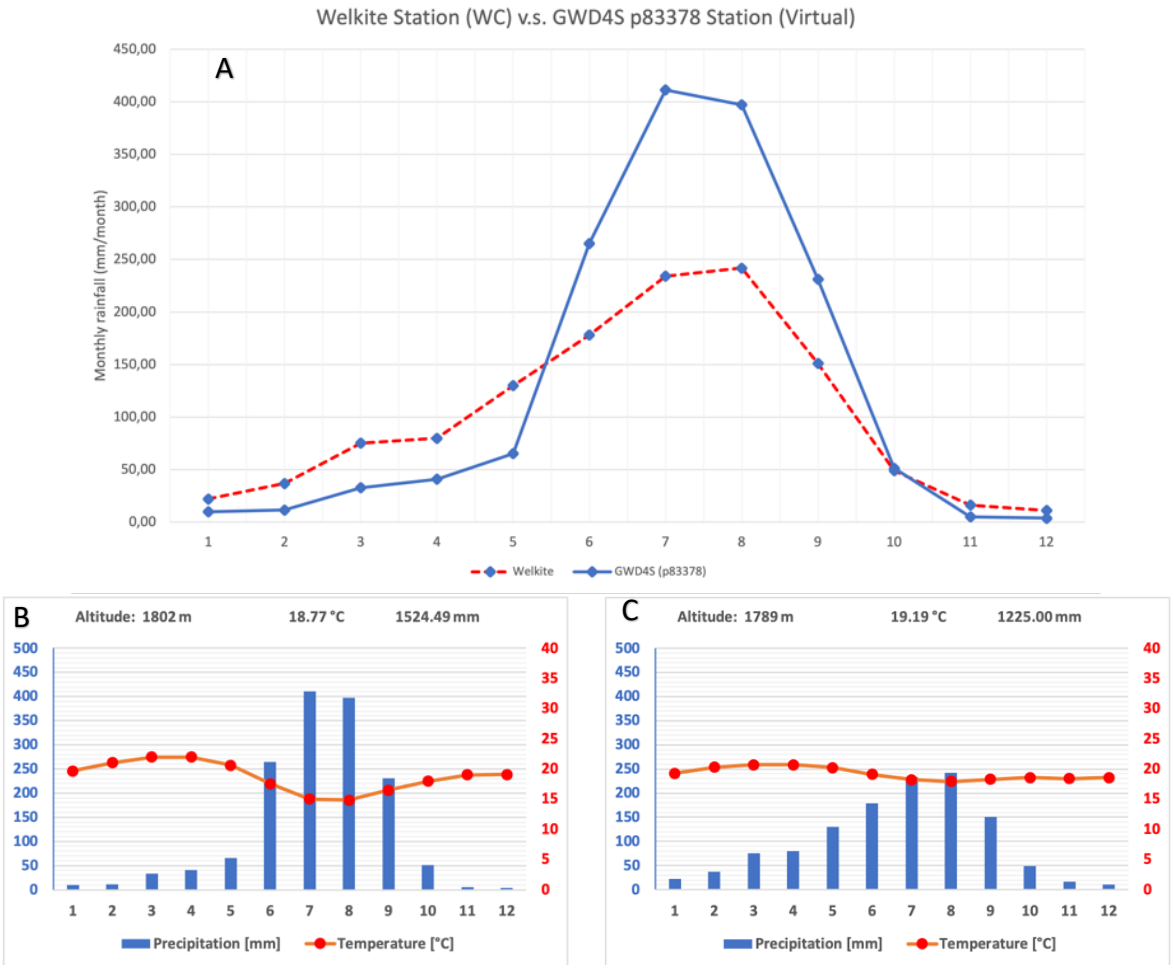

Figure 6.8. (A) rainfall comparison between GWD4S and Welkite (WC); (B) climatogram from GWD4S and (C) climatogram from WC

Chida

This station is located in the central area of the Omo River Basin. Figure 6.9 shows a comparison between the GWD4S and WC datasets. For this location, the GWD4S have lower rainfall values than the WC dataset (chart A). Similarly, to Welkite, the differences for Chita are more notorious during the rainy period (June - September), with a general RMSD of 50.66 mm/month. The annual rainfall is 1038.67 mm for the GWD4S (chart B) and 1560.00 mm for the WC dataset (chart C).

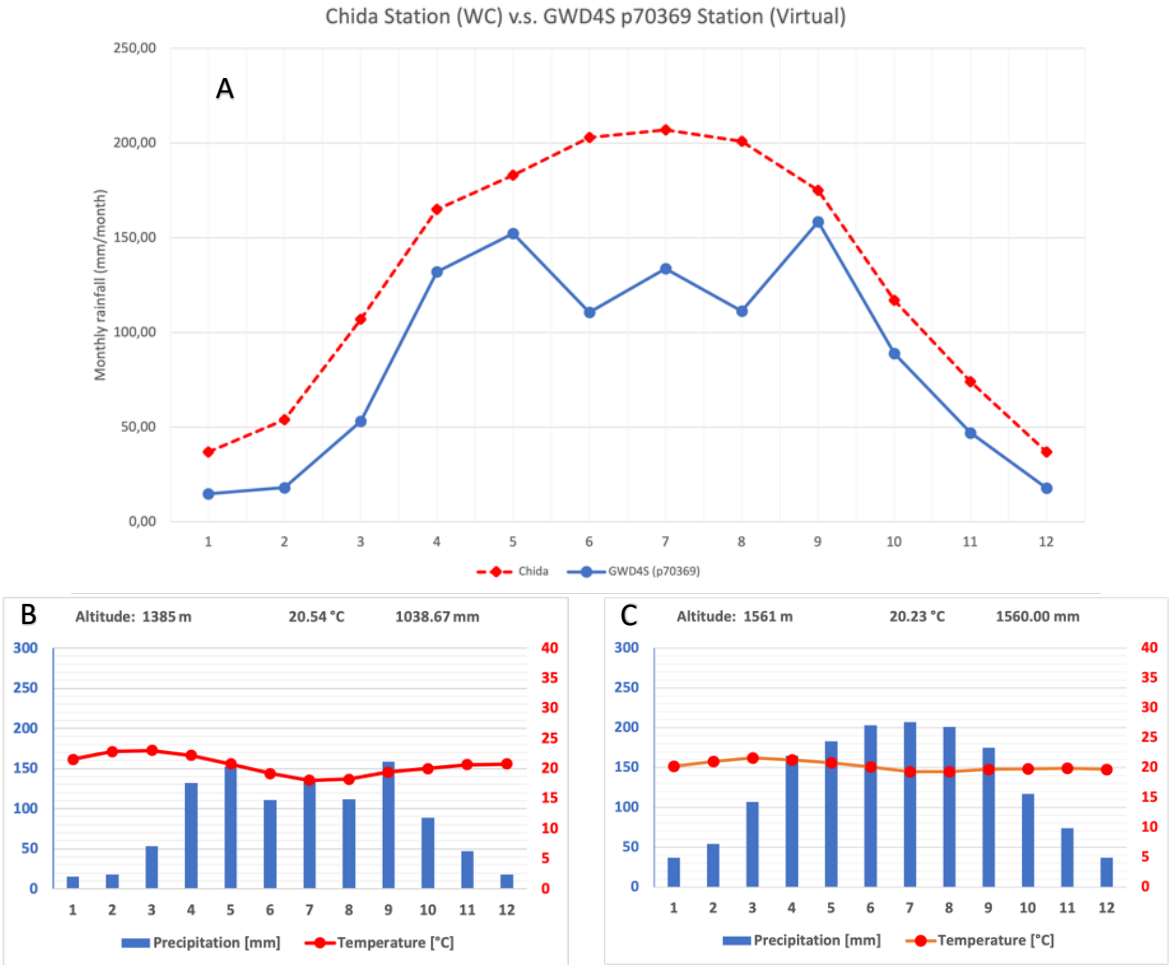

Figure 6.9. (A) rainfall comparison between GWD4S and Chida (WC); (B) climatograms from GWD4S and (C) climatogram from WC.

The average daily temperature is similar for both datasets: 20.54 °C (chart B) and 20.23 °C (chart C).

Omorate

This station is located in the southern area of the Omo River Basin. For this location the GWD4S and WC datasets show almost the same pattern. The amount of rainfall is clearly lower than in the locations analyzed before. The RMSD is 22.07 mm/month. Figure 6.10 shows that the annual rainfall in the WC dataset (386.00 mm) is higher than in the GWD4S (152.54 mm). Charts B and C in Figure 6.10 also present the average temperature: 27.99 °C for GWD4S and 28.67 °C for the WC dataset.

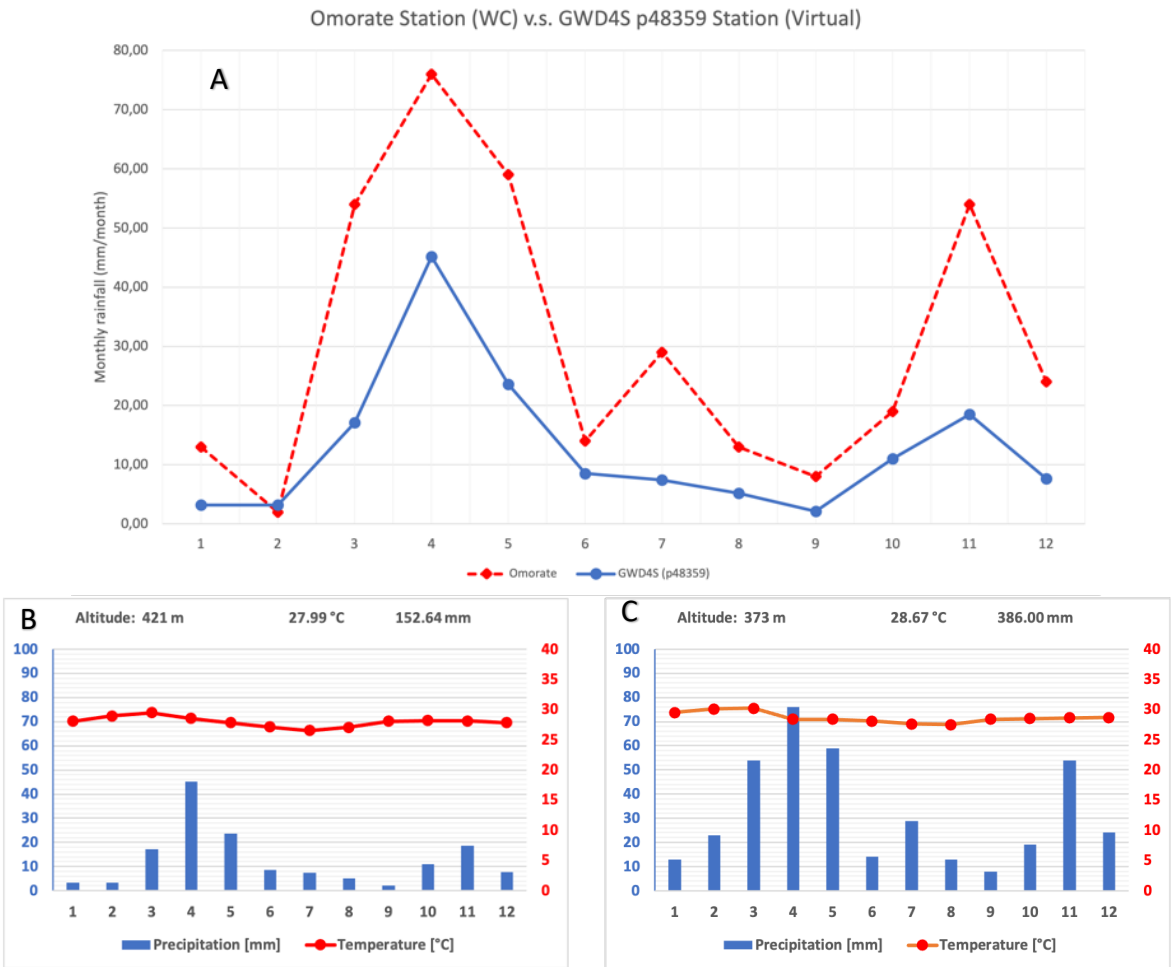

Figure 6.10. (A) rainfall comparison between GWD4S and Omorate (WC); (B) climatogram from GWD4S and (C) climatogram from WC

Kaaling

The Kaaling station is located in the southern part of the Omo River Basin. This region presents a small amount of rainfall compared to Welkite and Chida. Chart A of Figure 6.11 indicates that both datasets show the same pattern with a significant difference in April where the WC dataset indicates a rainfall 40 mm/month higher than GWD4S. The RMSD between the two time series is 22.20 mm/month, with an annual rainfall of 281.37 mm in the GWD4S and 369.90 mm in the WC dataset. Additionally, charts B and C of Figure 11 show that the temperature in the GWD4S is 27.65 °C and in the WC dataset is 27.74 °C.

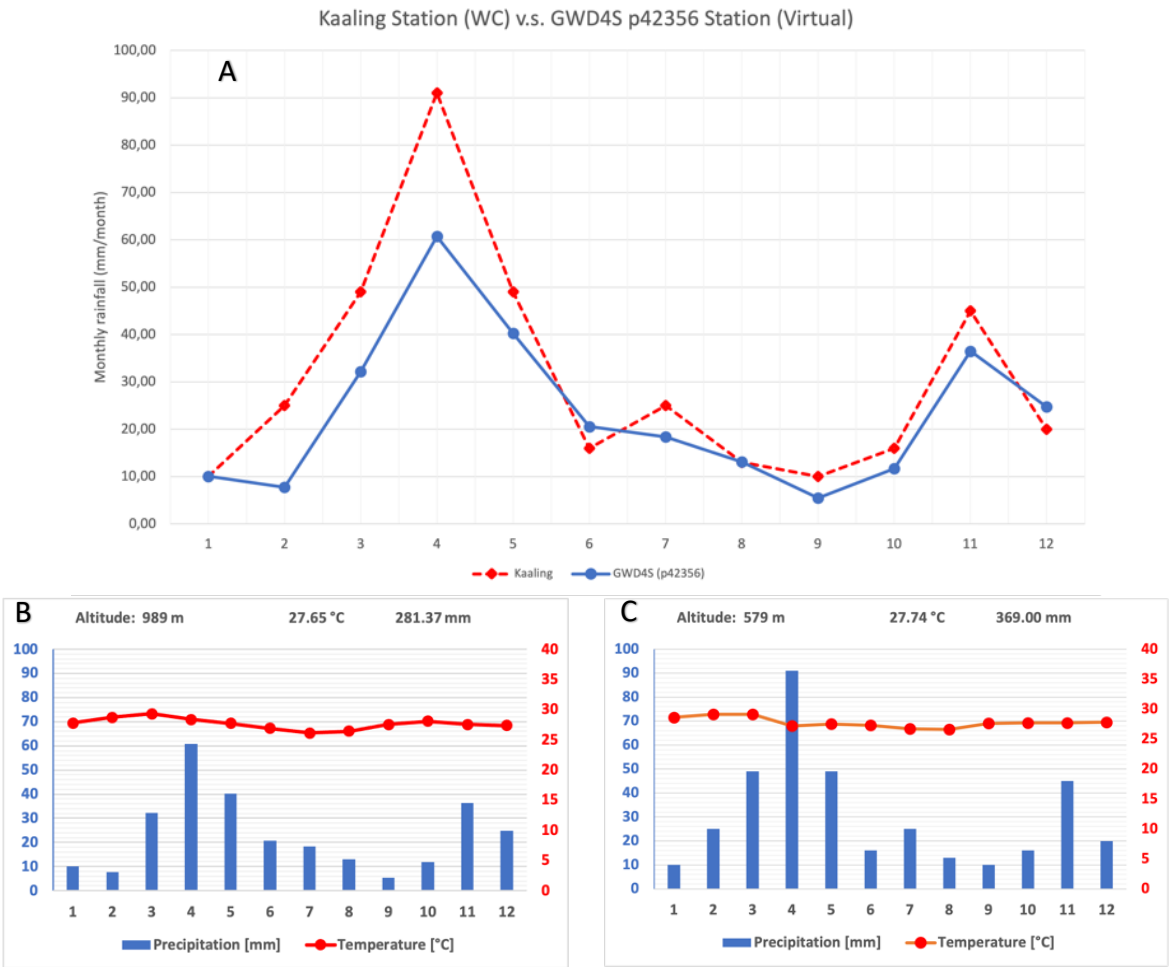

Figure 6.11. (A) rainfall comparison between GWD4S and Kaaling (WC); (B) climatogram from GWD4S and (C) climatogram from WC

6.1.2.3. Conclusions

6.1.2.3.1. Machángara River Basin

After analyzing the GWD4S, it was clear that the values for precipitation and temperature do not correspond with reality, especially for the period 2011 - 2014. Therefore, the original dataset was scaled using real data from El Labrado station. The LP model was executed using the rescaled weather data. From the results it is clear that by using the scaled GWD4S, better results were achieved with the original dataset the total penalty was 1264.47 euros and with the scaled one 52.56 euros. RMSD was also improved passing from 61.90 hm^3 to 45.77 hm^3.

6.1.2.3.2. Omo River Basin

Four stations located within the Omo River Basin were analyzed: Welkite, Chida, Omorate and Kaaling. The WC data were considered as the reference dataset in order to make a comparison with the GWD4S. It was clear that both datasets have differences but in Omo River Basin there are far less extreme than for the Machángara river basin. As a result, we did not re-run the LP and MILP models but consider the chapter 5 results sufficiently reliable where it regards the weather data inputs.

6.1.3. Water demands

In this research, we grouped several different demand types in categories. These demand categories are considered the most important water uses within the study areas, also taking into account the availability of data. This implies that not all real demands were considered in full detail. Demands were also assumed to be constant through time, which is not in agreement to reality. For instance, the amount of water required for irrigation is not constant, while the amount of water needed for human consumption per capita may be more constant. Additionally, water demands also depend on the season, e.g., households requirements will be higher during the dry period (Shahid, 2011).

Several demand types were considered. The most common types are consumptive demands, such as irrigation. There are also delaying demands, for which water returns to the river network after passing through the demand node. An example of the latter is water that is used to produce energy through hydropower plants. These delayed and return flow elements are taken into account in the proposed models.

6.1.4. Linear Programming model

Several models based on differential equations to simulate the hydrological behavior of a river basin (Devia et al., 2015; Martin et al., 2012) and even to allocate water (Ashraf Vaghefi et al., 2013; Labadie, 2006; Shourian et al., 2008) are described in the literature. However, these models are not capable to optimize water allocation through time. This lack of optimization capabilities can be fulfilled using a mathematical programming approach (linear and mixed integer linear programming).

Water networks can consist of a large number of system elements. Specific structures, such as reservoirs, make it even harder to describe these systems in a mathematical way. In order to make them computable and tractable, these systems must be simplified and assumptions have to be made (Martin et al., 2012). Moreover, river network discretization used in this research project assumed that water takes exactly one time step to flow from one node to the next one.

With the aim of including most of the geographical particularities in the study area, several parameters were added to the LP model, such as: losses in river segments, reservoirs and loss of flooded water, time delays, time delays in flooded water, and continuity (minimum and maximum amount of water to stay in a node). The LP-model must go through a calibration/validation process, during which the values for each parameter are selected by means of a trial-and-error procedure.

Reservoirs are fundamental elements in the water allocation process. In this work, reservoir outflow is not assumed to be regulated. Future research works may include this factor as a constraint in both proposed models. Furthermore, exceptional events might be considered within the model. For instance, the Ethiopian government announced that they will release a 1000 m^3/s during ten days in September to produce an ecological flood and prevent Lake Turkana from drying out (Pearce, 2014a).

The definition of the model's boundaries can be improved, e.g., in penalties associated to maximum and minimum capacities in reservoirs, river segments and demand river segments. Therefore, a sensitivity analysis should be performed to obtain more realistic values of the fractional parameters as well as a stakeholder consultation to find out which of them must have the largest weight. Furthermore, The LP and MILP models allocate water based on penalties/priorities. However, not all demand nodes have the same priority (all assumed to be 1 in this research). Finding penalty values that are more realistic for the study area will certainly improve the water allocation schemes produced by the models.

In section 6.1.2 a complete analysis of the time series from GWD4S, INAHMI and WorldClim were performed in order to verify whether they are reflecting the behaviour of the studied areas. Some corrections were made to the GWD4S in order to remove extreme values and to keep rainfall and temperature between the maximum and minimum boundaries. These corrections allow us to obtain a new scaled dataset which was used to run the LP model in the Machángara River Basin. Dataset used in chapter 3 had several issues mainly in the period from 2011 to 2014 where the amount of rainfall was underestimated. Then, results obtained in the new execution indicated that the total penalty were reduced from 1264.47 euros to 52.56 euros. Therefore, the robustness of the LP model was validated. Thus, the LP model can accept data from any source. Even if a pre-process of the data is required.

Regarding computational requirements of the LP model, the execution of the LP Model for Machángara River Basin was made in macbook pro with 2.6 GHz processor with 8 cores and 16 GB of memory. Total time and the number of iterations are:

- Calibration (2006 – 2009): Solved in 106093 iterations and 5.71 seconds
- Validation (2010 – 2011): Solved in 115894 iterations and 6.62 seconds
- Application (2012 - 2013): Solved in 18455 iterations and 4.60 seconds

6.1.5. Mixed Integer Linear Programming model

In this research project, a MILP model was formulated to select locations for building reservoirs from a set of candidate locations considering the water flow in a river network configuration. Values used in this model as building and management costs are estimates and might be more realistic. In particular, a geo-factor was used to estimate the building and management cost, while it would be more convenient to use a geo-factor that takes into account the real shape of the river as well as the distance to the nearest roads. It was assumed that the costs of building a reservoir in a V-shaped valley are lower than building them in a plain. It was also assumed that costs are higher when workers and construction materials have to travel long distances.

One of the advantages of the MILP model is that the building and management cost can be removed from the objective function. In this way, several scenarios can be executed taking into account only the water allocation component. Thus, decision makers are provided with several solutions to analyze.

Regarding robustness, MILP models can accept different sources of data as we stated in section 6.1.4. Furthermore, to have an idea of the computational requirement of the MILP model, results from the execution of the MILP Model (2012 - 2013) for Machángara River Basin is in Table 6.3, which shows the computation time and the number of iterations to obtain the best optimal solution when a number of reservoirs is required. For instance, when 1 reservoir is required, total computation time is 14.25 seconds and 50171 iterations are needed, but when 5 reservoirs are required the computation time is 101.07 seconds and 135936 iterations are required; it represents three times the values obtained in the first execution.

Table 6.3. Results of the execution of the MILP-model for Machángara River Basin

Use Case	Number Of Reservoirs	Computation Time [s]	Iterations
1	0	7,98	37360
2	1	14,25	50171
3	2	8,51	50575
4	3	7,33	49633
5	4	58,34	100955
6	5	101,07	135936
7	6	96,99	147235
8	7	115,13	162985
9	8	140,03	182418
10	9	144,27	183674
11	10	145,13	176685
12	11	164,74	209357
13	12	181,56	209779
14	13	147,85	164677
15	14	98,36	142455
16	15	109,64	145392
17	16	142,78	137284
18	17	112,81	164627
19	18	4,91	22146
20	19	5,11	21466
21	20	4,41	62195

6.1.6. Applicability, limitations and further research

The models proposed in this research project allow for an assessment of when and where water shortages may occur. To do so, decision makers can easily interpret the outputs of both models. However, one of the disadvantages is that both models require a large amount of input information, which in some cases, may not be available. This fact is further complicated when the river network needs to be modified, since, in that case, the whole input datasets must be completely re-generated. As it may be obvious, decisions about building reservoirs cannot be made only based on the results of these models. An extensive analysis of the WEF-nexus must be performed, in order to consider all parameters to obtain costs which will represents real situations.

Regarding limitations, a complete analysis must be performed in order to determine the most suitable values for penalties. For now, arbitrary vales were assigned in order to prioritize water allocation and avoid floods.

The main objective of this research project was to formulate models to optimize water allocation in order to meet all kinds of demands in a river basin. However, during this process, we found that there are several other scenarios or variables that can and should be integrated to make the models approximate the reality of the basin. For instance, climate change factors should be considered in the LP-model. As an example, the decrease in precipitation may be taken into account, since several regions will become drier in the near future. Furthermore, continued population growth and industrial development in the basin are other factors that should be included. The increase in population and industrial activities affect the required amount of water, energy and food. Water demands should also be tuned to get a more realistic representation of the WEF nexus.

6.2. Strengths and Weaknesses of the NFO-LP-model

6.2.1. Strengths of the NFO-LP-model:

Several authors have conducted research using linear programming principals to tackle water allocation problem. Besides, there are several computer tools (solvers) which include modules to solve this type of mathematical models. Moreover, mathematical models are scalable which allows to add more constraints without including extra complexity.

Regarding the schematization of the Water Supply Network (WSN), this research project introduces a relatively simple manner. Thus, nodes and segments are considered as the basis; nodes can represent input, transfer, reservoir or demands and segments can represent rivers. In the same way, segments, reservoirs and demand nodes have fixed capacities which allows to establish boundaries in the water allocation process. Additionally, input and demand nodes must be characterized by time series of water availability and water demand.

The LP (chapter 2, section 2.2) and MILP (chapter 4, section 4.2) models consider several penalties which are used to prioritize a demand during the water allocation process. The objective function in both models is the sum of those penalty terms to be minimized. Therefore, the objective function can be considered relatively simple. Additionally, the complete system includes constraints which express the continuity of water flow, network limitations, capacities, losses and delays due to floods or any other situation. The LP-model have parameters, and those parameters should be calibrated in order to represent real world situations. MILP uses the same parameter values as the LP model. In LP and MILP models, the number of parameters to be calibrated is limited and straightforward to interpret.

Another consideration is that by feeding the model with past time-series as water inputs in the network and setting the penalties in line with the past or current water management practices and priorities conducted by the basin's stakeholders, the potential performance of past management can be assessed and compared with effective performance (not done in this manuscript). In the same way, by feeding the model with expected or hypothetic water

inputs and setting the penalties in line with desired water management practices and priorities, assessments can be made of how the available water can be most optimally used.

The configuration of the WSN depends directly on data availability. Thus, if data about effective performance of the WSN is available a performance gap analysis between potential and effective performance can be conducted. Likewise, if time series of water inputs are available in near real time, e.g., via web-based sensor networks, it is possible to turn the strategic model into an operational one.

Several degrees of freedom are available to decision makers. For instance, can control the water allocation by setting / differentiating penalty values, change the minimum and maximum amounts of water to be kept in reservoirs and river segments, change the minimum and maximum amounts of water that can be present in a node, change the percentage of losses, change the percentage of the water which comes to a node with a delay.

6.2.2. Weaknesses

The LP and MILP models require several types of datasets. Measured time series of water inputs at specific location in the network must be available or such time series must be simulated by other models. In this research project, ArcSWAT has been used to fulfil this requirement.

Regarding the river network, it must be spatially segmented in such a way that can be assumed that water flows from one node to the next in just one-time step. It is not obvious to make this segmentation dynamic to take into account the variable discharge/speed of water.

LP and MILP models are including several assumptions and those assumptions try to stablish a simplification of reality. A list of assumptions is included below:

- Water demands are constant throught time.
- Water flows from one node to next in one time step (1 day for both cases).
- A percentage of water is lost in nodes (transfer and deamands), reservoirs and river segments.
- A percentage of water can stay in node.
- Capacities (maximum and minimum) of nodes and river segments
- A percentage of water flows with a time delay.
- Objective function and constraints are linear.

Besides, as future work it is necessary to determine how these assumptions are going to be addressed in order improve the results of the optimization models. An option is the inclusion of real time or forecasted information in order to reduce the dependence of simulated data.

As the network configuration is derived from available data, introducing a change in the network configuration (e.g. new demand node, new reservoir) can be quite a complex task since the complete process must be re-done from the beginning. Another issue with this matter, is that the data preparation (inputs and outputs) requires several manual handlings or editing.

Although there are a limited number of parameters, the calibration process associated to the different parameters used in the model to represent the river as it is, can take up quite some time to converge. For instance, the sensitivity analysis for the 7 parameters in the Machángara River Basin took: 1178.03 seconds and 4075099 iterations.

6.3. Strengths and weaknesses of the NFO-(MI)LP-modelling approach for optimizing the location of new reservoirs in a given WSN

6.3.1. Strengths of the NFO-MILP-model

As we stated in previous chapters and sections, the NFO-MILP-model is a relatively a simple extension of the NFO-LP-model. Then, all strengths of the LP-model also apply to the MILP-model. However, we have to consider that add new integer variables will increase the running time in the MILP-model.

The NFO-MILP model allows to perform a quick evaluation of a given water supply network (WSN). This evaluation is focused on reservoirs and its capacity to meet all the associated water demands. Moreover, this model is able to recommend the location of new possible reservoirs as well as assess the location of the existing and planned reservoirs.

6.3.2. Weaknesses of the NFO-MILP-model

Given that the NFO-MILP-model is a relatively simple extension of the NFO-LP-model all weaknesses of the LP-model also apply to the MILP-model.

The NFO-MILP-model recommends the location of a candidate reservoir. However, the model only accommodates candidate reservoirs with a predefined capacity (maximum and minimum). However, it is planned to adapt both models to be able to recommend a capacity. Due the inclusion of binary variables (0 or 1 values), time required to obtain a solution might grow based on the number of reservoirs available.

This model requires to associate a building and management cost to a reservoir. Currently this value is determined by using a geo-factor. However, this factor might not represent the reality of the area or any other factors might be included.

6.4. Outlook

Several issues have been identified after the execution of both models (NFO-LP and NFO-MILP). Addressing those issues will allow to improve strengths of the models. For instance: comparison of the potential performance (after optimization, as generated by NFO-LP) with data about real performance (real data).

From the execution of the models in chapters 3 and 5; it was notorious that river segments directly connected to reservoirs are receiving water in a non-regular way (sometimes nothing and sometimes producing floods). Therefore, it is recommendable to add a new constraint to the model. This constraint is oriented to regulate the outflow from reservoirs and with this

reach the minimum water level in the segment to ensure the ecological water requirements within the study areas.

Regarding the NFO-MILP models, it would be recommendable to implement a mechanism of determining the building and management cost of a candidate reservoirs based on the study area. Similarly, both models have several assumptions would it be recommendable to avoid this kind of assumptions by analyzing real data to determine correctly these values.

The water supply network as conceived in this manuscript, assumes that water flows from one node to another in one time step (typically 24 hours). However, a process to discretize water flow should be included; this process should also consider the water velocity as well as the geographical location.

6.5. General conclusions

Mathematical models and, more specifically Linear Programming models proved to be a valid option to solve water allocation problems. However, these types of models require large amounts of input data when the problem conditions vary in time and space. Thus, this research project had to generate several time series from the three study areas by using a hydrological model (ArcSWAT).

One of the requirements found during this research project was a complete description of the Water Supply Network. These components had to be expressed as constraints, variables, parameters and objective functions in mathematical models. The parameters included in the optimization model required to go through calibration and validation procedures to be set to suitable values in order to approximate the model's behavior to the real world. Furthermore, a prior sensitivity analysis proved useful to determine the order in which parameters should be adjusted during the calibration.

Linear Programming models applied to problems that are variable in time and space typically have high demands of computational time and resources. The inclusion of integer or, more specifically, binary variables to obtain a Mixed Integer Linear Programming model, might require long execution times to generate a solution. Execution times can become even longer when a more fine-grained temporal scale is considered in the model.

On the other hand, heuristics, optimization model which provides a feasible solution for a problem could be an approach to tackle this allocation problem. The main difference with mathematical models is that this kind of models provides one feasible solution and the other kind provides the optimal solution. The first types of models require less data and one initial solution. In this context, several authors who applied these kinds of models (Banihabib et al., 2020; Y. Chang & Zhu, 2019; HassanzadehFard & Jalilian, 2016) state that this is applicable.

References

Abbott, M. B., Bathurst, J. C., Cunge, J. A., O'Connell, P. E., & Rasmussen, J. (1986). An introduction to the European Hydrological System - Systeme Hydrologique Europeen, "SHE", 1: History and philosophy of a physically-based, distributed modelling system. *Journal of Hydrology*, *87*(1–2), 45–59. https://doi.org/10.1016/0022-1694(86)90114-9

Abdulbaki, D., Al-Hindi, M., Yassine, A., & Abou Najm, M. (2017). An optimization model for the allocation of water resources. *Journal of Cleaner Production*, *164*, 994–1006. https://doi.org/10.1016/j.jclepro.2017.07.024

ACSA. (2017). *ACSA Integrated Report 2017*. 126.

Acuña, G., Cubillos, F., Thibaule, J., & Latrille, E. (1999). Comparison of methods for training grey-box neural network models. *Computers and Chemical Engineering*, *23*(SUPPL. 1). https://doi.org/10.1016/S0098-1354(99)80138-0

Ahmad, A., El-Shafie, A., Mohd Razali, S. F., & Mohamad, Z. S. (2014). Reservoir optimization in water resources: A review. *Water Resources Management*, *28*(11), 3391–3405. https://doi.org/10.1007/s11269-014-0700-5

Akram, A. A., & Mendelsohn, R. (2017). Agricultural water allocation efficiency in a developing country canal irrigation system. *Environment and Development Economics*, *22*(05), 571–593. https://doi.org/10.1017/S1355770X17000171

Aljanabi, A. A., Mays, L. W., & Fox, P. (2018). A Reclaimed Wastewater Allocation Optimization Model for Agricultural Irrigation. *Environment and Natural Resources Research*, *8*(2), 55. https://doi.org/10.5539/enrr.v8n2p55

Al-Zahrani, M., Musa, A., & Chowdhury, S. (2016). Multi-objective optimization model for water resource management: a case study for Riyadh, Saudi Arabia. *Environment, Development and Sustainability*, *18*(3), 777–798. https://doi.org/10.1007/s10668-015-9677-3

Arnold, J. G., & Fohrer, N. (2005). SWAT2000: current capabilities and research opportunities in applied watershed modelling. *Hydrological Processes*, *19*(3), 563–572. https://doi.org/10.1002/hyp.5611

Ashraf Vaghefi, S., Mousavi, S. J., Abbaspour, K. C., Srinivasan, R., & Arnold, J. R. (2013). Integration of hydrologic and water allocation models in basin-scale water resources management considering crop pattern and climate change: Karkheh River Basin in Iran. *Regional Environmental Change*, *15*(3), 475–484. https://doi.org/10.1007/s10113-013-0573-9

Avery, S. (2010). *Hydrological impacts of ethiopia' s Omo basin on Kenya's lake Turkana water levels & fisheries*.

Avery, S. (2012). *Lake Turkana & the Lower Omo: Hydrological Impacts of Major Dam & Irrigation Development*.

Avery, S. (2017). *Fears over Ethiopian dam's costly impact on environment, people*. https://theconversation.com/fears-over-ethiopian-dams-costly-impact-on-environment-people-80757

Bangash, R. F., Passuello, A., Hammond, M., & Schuhmacher, M. (2012). Water allocation assessment in low flow river under data scarce conditions: A study of hydrological simulation in Mediterranean basin. *Science of the Total Environment*, *440*, 60–71. https://doi.org/10.1016/j.scitotenv.2012.08.031

Banihabib, M. E., Mohammad Rezapour Tabari, M., & Mohammad Rezapour Tabari, M. (2020). Correction to: Development of a Fuzzy Multi-Objective Heuristic Model for Optimum Water Allocation (Water Resources Management, (2019), 33, 11, (3673-3689), 10.1007/s11269-019-02323-7). *Water Resources Management*, *34*(1), 445. https://doi.org/10.1007/s11269-019-02441-2

Beamon, B. M. (1998). Supply Chain Design and Analysis: Models and Methods. *International Journal of Production Economics*, *55*(1), 1–22. https://doi.org/10.1016/S0925-5273(98)00079-6

Benson, D., Gain, A. K., & Rouillard, J. J. (2015). Water governance in a comparative perspective: From IWRM to a "nexus" approach? *Water Alternatives*, *8*(1), 756–773.

Bergstrom S. (1995). The HBV model. *Computer Models of Watershed Hydrology*.

Berhanu, B., Seleshi, Y., & Melesse, A. M. (2014). Surface Water and Groundwater Resources of Ethiopia: Potentials and Challenges of Water Resources Development. In A. M. Melesse, W. Abtew, & S. G. Setegn (Eds.), *Nile River Basin: Ecohydrological Challenges, Climate Change and Hydropolitics* (pp. 97–117). Springer International Publishing. https://doi.org/10.1007/978-3-319-02720-3_6

Bertoni, F., Zamiolo, M., Giulani, M., Castelletti, A., & Soncini-Sessa, K. (2017). *Energy demand and hydropower production*.

Beven, K. J., Kirkby, M. J., Schofield, N., & Tagg, A. F. (1984). TESTING A PHYSICALLY-BASED FLOOD FORECASTING MODEL (TOPMODEL) FOR THREE U . K . CATCHMENTS For many years , attempts at modelling the complex processes by which a basin converts rainfall to runoff were largely concerned with using lumped analogues . Mor. *Hournal of Hydrology*, *69*, 119–143. https://doi.org/10.1016/0022-1694(84)90159-8

Bird, J., & Dodds, F. (2014). Water-Food-Energy Nexus. *Water for Food Faculty Publications*.

Bittencourt, A. C., & Horne, R. N. (1997). Reservoir Development and Design Optimization. In *SPE Annual Technical Conference and Exhibition* (p. 14). Society of Petroleum Engineers. https://doi.org/10.2118/38895-MS

Bowersox, D. J., Closs, D. J., & Cooper, M. B. (2002). Supply chain logistics management. In *McGraw-Hill*. McGraw-Hill.

Brouwer, F., Avgerinopoulos, G., Fazekas, D., Laspidou, C., Mercure, J. F., Pollitt, H., Ramos, E. P., & Howells, M. (2018). Energy modelling and the Nexus concept. *Energy Strategy Reviews*, *19*, 1–6. https://doi.org/10.1016/j.esr.2017.10.005

Calizaya, A., Meixner, O., Bengtsson, L., & Berndtsson, R. (2010). Multi-criteria decision analysis (MCDA) for integrated water resources management (IWRM) in the Lake Poopo basin, Bolivia. *Water Resources Management*, *24*(10), 2267–2289. https://doi.org/10.1007/s11269-009-9551-x

Cambridge Dictionary. (2019). *NEXUS | meaning in the Cambridge English Dictionary*. Cambridge Dictionary. https://dictionary.cambridge.org/dictionary/english/nexus

Chang, F.-J., Tsai, W.-P., Wang, Y.-C., Chen, P.-A., Chang, L.-C., Coynel, A., & Vachaud, G. (2014). Optimal reservoir operation strategy for balancing ecosystem and human needs. *IAHS-AISH Proceedings and Reports*, *363*(October), 2014.

Chang, Y., & Zhu, X. (2019). A novel two-stage heuristic for solving storage space allocation problems in rail-water intermodal container terminals. *Symmetry*, *11*(10). https://doi.org/10.3390/sym11101229

Chen, H., & Swain, A. (2014). The Grand Ethiopian Renaissance Dam : Evaluating Its Sustainability Standard and Geopolitical Significance. *Energy Development Frontier*, *3*(1), 11–19.

Cheng, C.-T., & Chau, K. W. (2004). Flood control management system for reservoirs. *Environmental Modelling & Software*, *19*, 1141–1150. https://doi.org/10.1016/j.envsoft.2003.12.004

Chhuon, K., Herrera, E., & Nadaoka, K. (2016). Application of Integrated Hydrologic and River Basin Management Modeling for the Optimal Development of a Multi-Purpose Reservoir Project. *Water Resources Management*, *30*(9), 3143–3157. https://doi.org/10.1007/s11269-016-1336-4

Chou, F. N.-F., & Wu, C.-W. (2014). Determination of cost coefficients of a priority-based water allocation linear programming model – a network flow approach. *Hydrology and Earth System Sciences*, *18*(5), 1857–1872. https://doi.org/10.5194/hess-18-1857-2014

Climate-Data.org. (2019). *Climate data for cities worldwide - Climate-Data.org*. Climate-Data.Org. https://en.climate-data.org/

Condon, L. E., & Maxwell, R. M. (2013). Implementation of a linear optimization water allocation algorithm into a fully integrated physical hydrology model. *Advances in Water Resources*, *60*, 135–147. https://doi.org/10.1016/j.advwatres.2013.07.012

Cortes, M. G., Verelst, H., Espinosa, R., & Suarez, E. G. (2011). *Water and Wastewater Managment in Sugar Process Production*.

Coulthard, T. J., & Van De Wiel, M. J. (2012). Modelling river history and evolution. *Philosophical Transactions of the Royal Society A: Mathematical, Physical and Engineering Sciences*, *370*(1966), 2123–2142. https://doi.org/10.1098/rsta.2011.0597

DAFNE. (2018). *DAFNE project*. https://dafne.ethz.ch/

Dai, C., Qin, X. S., Chen, Y., & Guo, H. C. (2018). Dealing with equality and benefit for water allocation in a lake watershed: A Gini-coefficient based stochastic optimization approach. *Journal of Hydrology*, *561*(March), 322–334. https://doi.org/10.1016/j.jhydrol.2018.04.012

Das, B., Singh, A., Panda, S. N., & Yasuda, H. (2015). Optimal land and water resources allocation policies for sustainable irrigated agriculture. *Land Use Policy*, *42*, 527–537. https://doi.org/10.1016/j.landusepol.2014.09.012

De Meyer, A., Cattrysse, D., Rasinmäki, J., & Van Orshoven, J. (2014). Methods to optimise the design and management of biomass-for-bioenergy supply chains : A review. *Renewable and Sustainable Energy Reviews*, *31*, 657–670.

Devi, G. K., Ganasri, B. P., & Dwarakish, G. S. (2015). A Review on Hydrological Models. *Aquatic Procedia*, *4*(Icwrcoe), 1001–1007. https://doi.org/10.1016/j.aqpro.2015.02.126

Devia, G. K., Ganasri, B. P., & Dwarakish, G. S. (2015). A Review on Hydrological Models. *Aquatic Procedia*, *4*(Icwrcoe), 1001–1007. https://doi.org/10.1016/j.aqpro.2015.02.126

DHI. (2019). *MIKE HYDRO Basin*. https://www.mikepoweredbydhi.com/products/mike-hydro-basin

Dondeyne, S., Akinsete, E., Sinclair, S., Burlando, P., & Van Orshoven, J. (2018). *Characterisation of Water and Land Rescources in the Omo-Turkana and Zambezi River Basins*.

Dondeyne, S., Kangi, G., Rosier, I., Kassa, H., & van Orshoven, J. (2021). Climate, water and land resources: diversity, uses and changes, in: Lautze, J., McCartney, M., Gibson, J. (Eds.). In *The Omo-Turkana Basin: Cooperation for Sustainable Water Management, Earthscan Series on Major River Basins of the World* (1st ed., pp. 11–36). Routledge.

Dongquan, Z., Jining, C., Haozheng, W., Qingyuan, T., Shangbing, C., & Zheng, S. (2009). GIS-based urban rainfall-runoff modeling using an automatic catchment-discretization

approach: A case study in Macau. *Environmental Earth Sciences*, *59*(2), 465–472. https://doi.org/10.1007/s12665-009-0045-1

Dupar, M., & Oates, N. (2012). *Getting to grips with the water-energy-food 'nexus.'* Climate & Development Knowledge Network. https://cdkn.org/2012/04/getting-to-grips-with-the-water-energy-food-nexus/?loclang=en_gb

Elecaustro. (2011). *Electro generadora del austro - elecaustro s.a.* -.

Elecaustro. (2014). *Central Hidroeléctrica Saymirín V Descripción de las Obras de la Central*.

Entholzner, A., & Reeve, C. (2016). Building Climate Resilience through Virtual Water and Nexus Thinking in the Southern African Development Community. In C. Entholzner, A and Reeve (Ed.), *BUILDING CLIMATE RESILIENCE THROUGH VIRTUAL WATER AND NEXUS THINKING IN THE SOUTHERN AFRICAN DEVELOPMENT COMMUNITY* (pp. 1–215). SPRINGER. https://doi.org/10.1007/978-3-319-28464-4

Environmental Software and Services. (1995). *WaterWare: water resources management information system*.

ESA. (2015). *Retrieved from Climate Change Initiative*. https://www.esa-landcover-cci.org/

Fallis, A. G. (2013). Transportation. In *Journal of Chemical Information and Modeling* (Vol. 53, Issue 9). https://doi.org/10.1017/CBO9781107415324.004

FAO. (2017). *Estimates of Water Flow*. FAO Training. http://www.fao.org/fishery/docs/CDrom/FAO_Training/FAO_Training/General/x6705e/x6705e03.htm

Fick, S. E., & Hijmans, R. J. (2017). WorldClim 2: new 1km spatial resolution climate surfaces for global land areas. *International Journal of Climatology*, *37*(12), 4302–4315.

Freire-González, J., Decker, C. A., & Hall, J. W. (2018). A linear programming approach towater allocation during a drought. *Water (Switzerland)*, *10*(4), 1–14. https://doi.org/10.3390/w10040363

Frizzone, J. A., Coelho, R. D., Dourado-Neto, D., & Soliani, R. (1997). Linear programming model to optimize the water resource use in irrigation projects: an application to the Senator Nilo Coelho Project. *Scientia Agricola*, *54*(spe). https://doi.org/10.1590/S0103-90161997000300016

Galelli, S., Goedbloed, A., Schwanenberg, D., & van Overloop, P.-J. (2014). Optimal Real-Time Operation of Multipurpose Urban Reservoirs: Case Study in Singapore. *Journal of Water Resources Planning and Management*, *140*(4), 511–523. https://doi.org/10.1061/(ASCE)WR.1943-5452.0000342

Galizia Tundisi, J. (2018). Reservoirs: New challenges for ecosystem studies and environmental management. *Water Security*, *4–5*(June 2017), 1–7. https://doi.org/10.1016/j.wasec.2018.09.001

Gambella, C., Ghaddar, B., & Naoum-Sawaya, J. (2021). Optimization problems for machine learning: A survey. In *European Journal of Operational Research* (Vol. 290, Issue 3, pp. 807–828). Elsevier B.V. https://doi.org/10.1016/j.ejor.2020.08.045

Ghosh, S., Ibarrarán, M. E., Willett, K. D., & Sanchez Torres Esqueda, G. (2017). Water allocation and management along the Santa Cruz border region. *Water Resources and Economics*, *19*(September), 1–17. https://doi.org/10.1016/j.wre.2017.09.004

Giupponi, C., Mysiak, J., Fassio, A., & Cogan, V. (2004). MULINO-DSS: A computer tool for sustainable use of water resources at the catchment scale. *Mathematics and Computers in Simulation*, *64*(1), 13–24. https://doi.org/10.1016/j.matcom.2003.07.003

Google. (2007). *Google Earth User Guide Getting to Know Google Earth*. https://earth.google.com/intl/ar/userguide/v4/index.htm

Grigg, N. S. (2016). *Integrated water resource management* (1st ed.). Springer Nature.

Gurobi, O. (2015). *Gurobi Optimization Documentation*. http://www.gurobi.com/index

Ha, M., & Gao, Z. (2017). Optimization of water allocation decisions under uncertainty: the case of option contracts. *Journal of Ambient Intelligence and Humanized Computing*, *8*(5), 809–818. https://doi.org/10.1007/s12652-017-0551-z

Häberle, J., & Kilger, C. (2015). Strategic Network Design in the Chemical Industry. *Supply Chain Management and Advanced Planning (Third Edition): Concepts, Models, Software and Case Studies*, 139–157. https://doi.org/10.1007/b106298

Hanasaki, N., Kanae, S., & Oki, T. (2006). A reservoir operation scheme for global river routing models. *Journal of Hydrology*, *327*(1–2), 22–41. https://doi.org/10.1016/j.jhydrol.2005.11.011

Hargreaves, G., Hargreaves, H., & Riley, P. (1985). Agricultural Benefits for Senegal River Basin. *Journal of Irrigation and Drainage Engineering*, *111*(2), 113–124. https://doi.org/10.1061/(ASCE)0733-9437(1985)111:2(113)

Harris, I., Jones, P. D., Osborn, T. J., & Lister, D. H. (2014). Updated high-resolution grids of monthly climatic observations - the CRU TS3.10 Dataset. *International Journal of Climatology*, *34*(3), 623–642. https://doi.org/10.1002/joc.3711

HassanzadehFard, H., & Jalilian, A. (2016). A novel objective function for optimal DG allocation in distribution systems using meta-heuristic algorithms. *International Journal of Green Energy*, *13*(15), 1624–1634. https://doi.org/10.1080/15435075.2016.1212355

Hastenrath, S., Polzin, D., & Mutai, C. (2011). Circulation mechanisms of kenya rainfall anomalies. *Journal of Climate*, *24*(2), 404–412. https://doi.org/10.1175/2010JCLI3599.1

Her, Y., Frankenberger, J., Chaubey, I., & Srinivasan, R. (2015). Threshold effects in HRU definition of the soil and water assessment tool. *Transactions of the ASABE*, *58*(2), 367–378. https://doi.org/10.13031/trans.58.10805

Herrera, I., & Carrera, P. (2017). Environmental flow assessment in Andean rivers of Ecuador, case study: Chanlud and El Labrado dams in the Machángara River. *Ecohydrology and Hydrobiology*, *17*(2), 103–112. https://doi.org/10.1016/j.ecohyd.2017.01.002

Heydari, M., Othman, F., Qaderi, K., Noori, M., & Parsa, A. S. (2015). Introduction to linear programming as a popular tool in optimal reservoir operation, a review. *Advances in Environmental Biology*, *9*(3), 906–917. https://doi.org/10.5281/zenodo.18254

Hoff, H. (2011). *Understanding the Nexus. Background Paper for the Bonn2011 Conference: The Water, Energy and Food Security Nexus*. *November*.

Holweg, M., Disney, S., Holmström, J., & Småros, J. (2005). Supply chain collaboration: Making sense of the strategy continuum. *European Management Journal*, *23*(2), 170–181. https://doi.org/10.1016/j.emj.2005.02.008

Horne, A., Kaur, S., Szemis, J., Costa, A., Webb, J. A., Nathan, R., Stewardson, M., Lowe, L., & Boland, N. (2017). Using optimization to develop a “designer” environmental flow regime. *Environmental Modelling and Software*, *88*, 188–199. https://doi.org/10.1016/j.envsoft.2016.11.020

Horne, A., Szemis, J. M., Kaur, S., Webb, J. A., Stewardson, M. J., Costa, A., & Boland, N. (2016). Optimization tools for environmental water decisions: A review of strengths, weaknesses, and opportunities to improve adoption. *Environmental Modelling and Software*, *84*, 326–338. https://doi.org/10.1016/j.envsoft.2016.06.028

Howells, M., & Rogner, H.-H. (2014). Assessing integrated systems. *Nature Climate Change*, *4*, 246.

Hu, Z., Chen, Y., Yao, L., Wei, C., & Li, C. (2016). Optimal allocation of regional water resources: From a perspective of equity-efficiency tradeoff. *Resources, Conservation and Recycling*, *109*, 102–113. https://doi.org/10.1016/j.resconrec.2016.02.001

IBM. (2020). *IBM ILOG CPLEX Optimization Studio CPLEX User ' s Manual*.

INEC. (2010). Resultados del Censo 2010 de población y vivienda en el Ecuador. Fascículo provincial Los Ríos. *Inec*, 8.

Jacobsen, D., & Encalada, A. (2016). The macroinvertebrate fauna of Ecuadorian highland streams in the wet and dry season. *Fundamental and Applied Limnology*, *142*(1), 53–70. https://doi.org/10.1127/archiv-hydrobiol/142/1998/53

Jafarzadegan, K., Abed-Elmdoust, A., & Kerachian, R. (2014). A stochastic model for optimal operation of inter-basin water allocation systems: A case study. *Stochastic Environmental Research and Risk Assessment*, *28*(6), 1343–1358. https://doi.org/10.1007/s00477-013-0841-8

Jamshid Mousavi, S., Anzab, N. R., Asl-Rousta, B., & Kim, J. H. (2017). Multi-Objective Optimization-Simulation for Reliability-Based Inter-Basin Water Allocation. *Water Resources Management*, *31*(11), 3445–3464. https://doi.org/10.1007/s11269-017-1678-6

Jerves-Cobo, R., Everaert, G., Iñiguez-Vela, X., Córdova-Vela, G., Díaz-Granda, C., Cisneros, F., Nopens, I., & Goethals, P. L. M. (2017). A methodology to model environmental preferences of EPT taxa in the Machangara River Basin (Ecuador). In *Water (Switzerland)* (Vol. 9, Issue 3). https://doi.org/10.3390/w9030195

Kadigi, R. M. J., Mdoe, N. S. Y., Ashimogo, G. C., & Morardet, S. (2008). Water for irrigation or hydropower generation?-Complex questions regarding water allocation in Tanzania. *Agricultural Water Management*, *95*(8), 984–992. https://doi.org/10.1016/j.agwat.2008.03.008

Kamski, B. (2016). The Kuraz Sugar Development Project (KSDP) in Ethiopia: between 'sweet visions' and mounting challenges. *Journal of Eastern African Studies*, *10*(3), 568–580. https://doi.org/10.1080/17531055.2016.1267602

Karimi, P., Bastiaanssen, W. G. M., Sood, A., Hoogeveen, J., Peiser, L., Bastidas-Obando, E., & Dost, R. J. (2015). Spatial evapotranspiration, rainfall and land use data in water accounting - Part 2: Reliability of water acounting results for policy decisions in the Awash Basin. *Hydrology and Earth System Sciences*, *19*(1), 533–550. https://doi.org/10.5194/hess-19-533-2015

Kermani, M., Périn-Levasseur, Z., Benali, M., Savulescu, L., & Maréchal, F. (2017). A novel MILP approach for simultaneous optimization of water and energy: Application to a Canadian softwood Kraft pulping mill. *Computers & Chemical Engineering*, *102*, 238–257. https://doi.org/10.1016/j.compchemeng.2016.11.043

Kilger, C. (2015a). Computer Assembly. *Supply Chain Management and Advanced Planning (Third Edition): Concepts, Models, Software and Case Studies*, 139–157. https://doi.org/10.1007/b106298

Kilger, C. (2015b). The Definition of a Supply Chain Project. *Supply Chain Management and Advanced Planning (Third Edition): Concepts, Models, Software and Case Studies*, 139–157. https://doi.org/10.1007/b106298

Kneis, D., Förster, S., & Bronstert, A. (2009). Simulation of water quality in a flood detention area using models of different spatial discretization. *Ecological Modelling*, *220*(13–14), 1631–1642. https://doi.org/10.1016/j.ecolmodel.2009.04.006

Kolb, O., Morsi, A., Lang, J., & Martin, A. (2012). *Nonlinear and Mixed Integer Linear Programming*. 55–65. https://doi.org/10.1007/978-3-0348-0436-3

Kondolf, G., Rubin, Z., & Minear, J. (2014). Dams on the Mekong: Cumulative sediment starvation. *Water Resources Research*, *51*(6), 294–299. https://doi.org/10.1002/2013WR014651.Received

Kulat, M. I., Mohtar, R. H., & Olivera, F. (2019). Holistic Water-Energy-Food Nexus for Guiding Water Resources Planning: Matagorda County, Texas Case. *Frontiers in Environmental Science*, *7*(February), 1–13. https://doi.org/10.3389/fenvs.2019.00003

Kuo, P., & Shih, S. (2015). *Determining water depth of detention wetlands from aspect of hydraulic efficiency*. *January 2013*.

Kurian, M. (2017). The water-energy-food nexus: Trade-offs, thresholds and transdisciplinary approaches to sustainable development. *Environmental Science and Policy*, *68*, 97–106. https://doi.org/10.1016/j.envsci.2016.11.006

Labadie, J. W. (2004). Optimal Operation of Multireservoir Systems: State-of-the-Art Review. *Journal of Water Resources Planning and Management*, *130*(2), 93–111. https://doi.org/10.1061/(ASCE)0733-9496(2004)130:2(93)

Labadie, J. W. (2006). MODSIM : Decision Support System for Integrated River Basin Management. *Summit on Environmental Modelling and Software the International Environmental Modelling and Software Society*, 1518–1524.

Lagacherie, P., Rabotin, M., Colin, F., Moussa, R., & Voltz, M. (2010). Geo-MHYDAS: A landscape discretization tool for distributed hydrological modeling of cultivated areas. *Computers and Geosciences*, *36*(8), 1021–1032. https://doi.org/10.1016/j.cageo.2009.12.005

Lalehzari, R., Boroomand Nasab, S., Moazed, H., & Haghighi, A. (2016). Multiobjective management of water allocation to sustainable irrigation planning and optimal cropping pattern. *Journal of Irrigation and Drainage Engineering*, *142*(1), 1–10. https://doi.org/10.1061/(ASCE)IR.1943-4774.0000933

Lautenschläger, M. (2015). Event-Based Planning for Standard Polymer Products. *Supply Chain Management and Advanced Planning (Third Edition): Concepts, Models, Software and Case Studies*, 139–157. https://doi.org/10.1007/b106298

le Goulven P, Ruf T, & Ribadeneira H. (1987). *Presentación del Proyecto INERHI (Instituto Ecuatoriano de Recursos Hidraulicos, Decadal oscillations in rainfall and air temperature 281 Author's personal copy Ecuador*.

Leck, H., Conway, D., Bradshaw, M., & Rees, J. (2015). Tracing the Water-Energy-Food Nexus: Description, Theory and Practice. *Geography Compass*, *9*(8), 445–460. https://doi.org/10.1111/gec3.12222

Li, W., Jiao, K., Bao, Z., Xie, Y., Zhen, J., Huang, G., & Fu, L. (2017). Chance-constrained dynamic programming for multiple water resources allocation management associated with risk-aversion analysis: A case study of Beijing, China. *Water (Switzerland)*, *9*(8). https://doi.org/10.3390/w9080596

Liang, X., Lettenmaier, D. P., Wood, E. F., & Burges, S. J. (1994). A simple hydrologically based model of land surface water and energy fluxes for general circulation models. *Journal of Geophysical Research: Atmospheres*, *99*(D7), 14415–14428. https://doi.org/10.1029/94JD00483

Lingo. (2006). *Optimization Modeling with LINGO*. *312*, 617.

Liu, W., Liu, L., & Tong, F. (2017). Least Squares Support Vector Machine for Ranking Solutions of Multi-Objective Water Resources Allocation Optimization Models. *Water*, *9*(4), 257. https://doi.org/10.3390/w9040257

Lu, Dr. D. (2011). *Fundamentals of Supply Chain Management*. Dr. Dawei Lu & Ventus Publishing ApS. https://doi.org/10.1007/978-3-540-24816-3_1

Mao, J., Zhang, P., Dai, L., Dai, H., & Hu, T. (2016). Optimal operation of a multi-reservoir system for environmental water demand of a river-connected lake. *Hydrology Research*, *47*, 206–224. https://doi.org/10.2166/nh.2016.043

Martin, A., Klamroth, K., Lang, J., Leugering, G., Morsi, A., Oberlack, M., Ostrowski, M., & Rosen, R. (2012). Mathematical optimization of water networks. In *Mathematical Optimization of Water Networks*. Springer-Verlag. https://doi.org/10.1007/978-3-0348-0436-3

Matute, V. (2014). *Análisis De Factibilidad De Generación Eléctrica A Pie De La Presa De Chanlud*. Universidad de Cuenca.

McEntee, F. (2019). *How green is hydropower?* https://www.sustaineurope.com/how-green-is-hydropower-20180229.html

Md. Azamathulla, H., Wu, F.-C., Ghani, A. A., Narulkar, S. M., Zakaria, N. A., & Chang, C. K. (2008). Comparison between genetic algorithm and linear programming approach for real time operation. *Journal of Hydro-Environment Research*, *2*(3), 172–181. https://doi.org/10.1016/j.jher.2008.10.001

Merkuryeva, G., Merkuryev, Y., Sokolov, B. V., Potryasaev, S., Zelentsov, V. A., & Lektauers, A. (2015). Advanced river flood monitoring, modelling and forecasting. *Journal of Computational Science*, *10*, 77–85. https://doi.org/10.1016/j.jocs.2014.10.004

Merrick, B. (2018). *The power of hydrology in the Omo-Gibe River Basin:*

Meyr, H., & Roitsch, M. (2015). Oil Industry. *Supply Chain Management and Advanced Planning (Third Edition): Concepts, Models, Software and Case Studies*, 139–157. https://doi.org/10.1007/b106298

Michigan State University. (2019). *Omo-Turkana Research Network*. https://www.canr.msu.edu/oturn/

Monteith, J. (1965). *Evaporation and Environment. Symposia of the Society for Experimental Biology*. *19*, 205–234.

Mora, D. E., Campozano, L., Cisneros, F., Wyseure, G., & Willems, P. (2014). Climate changes of hydrometeorological and hydrological extremes in the Paute basin, Ecuadorean Andes. *Hydrology and Earth System Sciences*, *18*(2), 631–648. https://doi.org/10.5194/hess-18-631-2014

Moridi, A., & Yazdi, J. (2017). Optimal Allocation of Flood Control Capacity for Multi-Reservoir Systems Using Multi-Objective Optimization Approach. *Water Resources Management*, *31*(14), 4521–4538. https://doi.org/10.1007/s11269-017-1763-x

Morsi, A., Geißler, B., & Alexander, M. (2012). Mixed Integer Optimization of Water Supply Networks. In *Mathematical Optimization of Water Networks* (pp. 55–65). https://doi.org/10.1007/978-3-0348-0436-3

Mula, J., Peidro, D., Díaz-Madroñero, M., & Vicens, E. (2010). Mathematical programming models for supply chain production and transport planning. *European Journal of Operational Research*, *204*(3), 377–390. https://doi.org/10.1016/j.ejor.2009.09.008

Namany, S., Al-Ansari, T., & Govindan, R. (2019). Sustainable energy, water and food nexus systems: A focused review of decision-making tools for efficient resource management

and governance. *Journal of Cleaner Production*, *225*, 610–626. https://doi.org/10.1016/j.jclepro.2019.03.304

Neitsch, S. L., Arnold, J. G., Kiniry, J. R., & Williams., J. R. (2005). Soil and Water Assessment Tool User's Manual Version 2005. *Diffuse Pollution Conference Dublin*, 494.

Neitsch, S. L., Arnold, J. G., Kiniry, J. R., & Williams, J. R. (2009). *Theoretical documentation SWAT*.

Nguyen, D. C. H., Maier, H. R., Dandy, G. C., & Ascough, J. C. (2016). Framework for computationally efficient optimal crop and water allocation using ant colony optimization. *Environmental Modelling & Software*, *76*, 37–53. https://doi.org/10.1016/j.envsoft.2015.11.003

Nyabe, I., Kalumba, M., Dondeyne, S., & Kleinschroth, F. (2017). *Quarrels over water in the Lunsemfwa catchment* (Issue July).

Olofintoye, O., Otieno, F., & Adeyemo, J. (2016). Real-time optimal water allocation for daily hydropower generation from the Vanderkloof dam, South Africa. *Applied Soft Computing Journal*, *47*, 119–129. https://doi.org/10.1016/j.asoc.2016.05.018

Pasumarthy, R., Ambati, V. R., & van der Schaft, A. J. (2012). Port-Hamiltonian discretization for open channel flows. *Systems and Control Letters*, *61*(9), 950–958. https://doi.org/10.1016/j.sysconle.2012.05.003

Pearce, F. (2014a). Dam nation. *New Scientist*, *222*(2974), 42–45. https://doi.org/https://doi.org/10.1016/S0262-4079(14)61218-5

Pearce, F. (2014b). *Publications, reports and video's of Wetlands International*. https://www.wetlands.org/publications/downstream-voices/

Perera, B. J. C., James, B., & Kularathna, M. D. U. (2005). Computer software tool REALM for sustainable water allocation and management. *Journal of Environmental Management*, *77*(4), 291–300. https://doi.org/10.1016/j.jenvman.2005.06.014

Pittock, J., Hussey, K., & McGlennon, S. (2013). Australian Climate, Energy and Water Policies: Conflicts and synergies. *Australian Geographer*, *44*(1), 3–22. https://doi.org/10.1080/00049182.2013.765345

Priestley, C., & Taylor, R. (1972). On the Assessment of Surface Heat Flux and Evaporation Using Large-Scale Parameters. *Monthly Weather Review*, *100*(February), 81–92. https://doi.org/10.1175/1520-0493(1972)100<0081:OTAOSH>2.3.CO;2

PROMAS. (2019). *Programa para el Manejo del Agua y el Suelo*. http://promas.ucuenca.edu.ec/Promas/

Qiao, J., Jeong, D., Lawley, M., Richard, J.-P. P., Abraham, D. M., & Yih, Y. (2007). Allocating security resources to a water supply network. *IIE Transactions*, *39*(1), 95–109. https://doi.org/10.1080/07408170600865400

Rasul, G., & Sharma, B. (2016). The nexus approach to water–energy–food security: an option for adaptation to climate change. *Climate Policy*, *16*(6), 682–702. https://doi.org/10.1080/14693062.2015.1029865

Rathjens, H., & Oppelt, N. (2012). SWATgrid: An interface for setting up SWAT in a grid-based discretization scheme. *Computers and Geosciences*, *45*, 161–167. https://doi.org/10.1016/j.cageo.2011.11.004

Reca, J., Roldán, J., Alcaide, M., López, R., & Camacho, E. (2001). Optimisation model for water allocation in deficit irrigation systems I. Description of the model. *Agricultural Water Management*, *48*(2), 103–116. https://doi.org/10.1016/S0378-3774(00)00126-8

Refsgaard, J. C., & Storm, B. (1996). Construction, Calibration And Validation of Hydrological Models. In M. B. Abbott & J. C. Refsgaard (Eds.), *Distributed Hydrological Modelling* (pp. 41–54). Springer Netherlands. https://doi.org/10.1007/978-94-009-0257-2_3

Renewables First. (2018). *How much hydropower power could I generate from a hydro turbine?* https://www.renewablesfirst.co.uk/hydropower/

Ringler, C., Bhaduri, A., & Lawford, R. (2013). The nexus across water, energy, land and food (WELF): Potential for improved resource use efficiency? In *Current Opinion in Environmental Sustainability* (Vol. 5, Issue 6, pp. 617–624). https://doi.org/10.1016/j.cosust.2013.11.002

Ritchie, H., & Roser, M. (2019). *Energy Production & Changing Energy Sources*. Our World In Data. https://ourworldindata.org/energy-production-and-changing-energy-sources

Roozbahani, R., Abbasi, B., & Schreider, S. (2017). Determining Location and Capacity of Dams through Economic and Environmental Indicators. *Water Resources Management*, *31*(14), 4539–4556. https://doi.org/10.1007/s11269-017-1764-9

Roozbahani, R., Abbasi, B., Schreider, S., & Iversen, J. (2021). Dam Location-Allocation under Multiple Hydrological Scenarios. *Water Resources Management*, *35*(3), 993–1009. https://doi.org/10.1007/s11269-021-02765-y

Roth, V., & Lemann, T. (2016). Comparing CFSR and conventional weather data for discharge and soil loss modelling with SWAT in small catchments in the Ethiopian Highlands. *Hydrology and Earth System Sciences*, *20*(2), 921–934. https://doi.org/10.5194/hess-20-921-2016

Royal Meteorological Societ. (2019). *Inter Tropical Convergence Zone (ITCZ) - SKYbrary Aviation Safety*. https://www.skybrary.aero/index.php/Inter_Tropical_Convergence_Zone_(ITCZ)

Sarkis, J. (2012). A boundaries and flows perspective of green supply chain management. *Supply Chain Management: An International Journal*, *17*(2), 202–216. https://doi.org/10.1108/13598541211212924

Sechi, G. M., & Zucca, R. (2015). Water Resource Allocation in Critical Scarcity Conditions: A Bankruptcy Game Approach. *Water Resources Management*, *29*(2), 541–555. https://doi.org/10.1007/s11269-014-0786-9

SENPLADES. (2019). *Zona de Planificación 1 – Norte – Secretaría Nacional de Planificación y Desarrollo*. https://www.planificacion.gob.ec/zona-de-planificacion-6-austro/

Serdarasan, S. (2013). A review of supply chain complexity drivers. *Computers and Industrial Engineering*, *66*(3), 533–540. https://doi.org/10.1016/j.cie.2012.12.008

Shafroth, P. B., Wilcox, A. C., Lytle, D. A., Hickey, J. T., Andersen, D. C., Beauchamp, V. B., Hautzinger, A., McMullen, L. E., & Warner, A. (2010). Ecosystem effects of environmental flows: Modelling and experimental floods in a dryland river. *Freshwater Biology*, *55*(1), 68–85. https://doi.org/10.1111/j.1365-2427.2009.02271.x

Shahid, S. (2010). Rainfall variability and the trends of wet and dry periods in Bangladesh. *International Journal of Climatology*, *30*(15), 2299–2313. https://doi.org/10.1002/joc.2053

Shahid, S. (2011). Impact of climate change on irrigation water demand of dry season Boro rice in northwest Bangladesh. *Climatic Change*, *105*(3–4), 433–453. https://doi.org/10.1007/s10584-010-9895-5

Shimizu, F., Akinaga, M., Matsuyoshi, Y., & Tanaka, K. (2019). Flow characteristics of water delivery piping system and its effective flow area at discharge branches. *IOP Conference*

Series: Earth and Environmental Science, *240*(6). https://doi.org/10.1088/1755-1315/240/6/062034

Shourian, M., Mousavi, S. J., & Tahershamsi, A. (2008). Basin-wide water resources planning by integrating PSO algorithm and MODSIM. *Water Resources Management*, *22*(10), 1347–1366. https://doi.org/10.1007/s11269-007-9229-1

Singh, A. (2017). Optimal allocation of water and land resources for maximizing the farm income and minimizing the irrigation-induced environmental problems. *Stochastic Environmental Research and Risk Assessment*, *31*(5), 1147–1154. https://doi.org/10.1007/s00477-016-1326-3

Smajgl, A., Ward, J., & Pluschke, L. (2016). The water-food-energy Nexus - Realising a new paradigm. *Journal of Hydrology*, *533*, 533–540. https://doi.org/10.1016/j.jhydrol.2015.12.033

Srivastava, S. K. (2007). Green supply-chain management: A state-of-the-art literature review. *International Journal of Management Reviews*, *9*(1), 53–80. https://doi.org/10.1111/j.1468-2370.2007.00202.x

Stadtler, H. (2015). Supply Chain Management: An Overview. *Supply Chain Management and Advanced Planning (Third Edition): Concepts, Models, Software and Case Studies*, 139–157. https://doi.org/10.1007/b106298

Sugar Corporation. (2019). *Omo Kuraz Sugar Development Project*. http://www.ethiopiansugar.com/

Sun, S., Cao, Z., Zhu, H., & Zhao, J. (2020). A Survey of Optimization Methods from a Machine Learning Perspective. *IEEE Transactions on Cybernetics*, *50*(8), 3668–3681. https://doi.org/10.1109/TCYB.2019.2950779

Syme, G. J., Nancarrow, B. E., & McCreddin, J. A. (1999). Defining the components of fairness in the allocation of water to environmental and human uses. *Journal of Environmental Management*, *57*(1), 51–70. https://doi.org/10.1006/jema.1999.0282

Tesfa, B. C. (2013). Benefit of Grand Ethiopian Renaissance Dam Project (GERDP) for Sudan and Egypt. *EIPSA Communicating Article: Energy, Water, Environment \& Economic*, *1*(1), 1–12.

Texas A&M University. (2009). *ArcSWAT | Soil and Water Assessment Tool*. https://swat.tamu.edu/software/arcswat/

Texas A&M University. (2018). *Global Weather Data for SWAT*. https://globalweather.tamu.edu/

The World Bank. (2017, September 20). *Water Resources Management Overview: Development news, research, data | World Bank*. https://www.worldbank.org/en/topic/waterresourcesmanagement#2

Thevs, N., Peng, H., Rozi, A., Zerbe, S., & Abdusalih, N. (2015). Water allocation and water consumption of irrigated agriculture and natural vegetation in the Aksu-Tarim river basin, Xinjiang, China. *Journal of Arid Environments*, *112*(PA), 87–97. https://doi.org/10.1016/j.jaridenv.2014.05.028

Tinoco, V., Willems, P., Wyseure, G., & Cisneros, F. (2014). Modelamiento de operación de embalses para el proyecto integral de riego en la cuenca del río Macul. *MASKANA*, *5*(1), 59–71.

Tinoco, V., Willems, P., Wyseure, G., & Cisneros, F. (2016). Evaluation of reservoir operation strategies for irrigation in the Macul Basin, Ecuador. *Journal of Hydrology: Regional Studies*, *5*, 213–225. https://doi.org/10.1016/j.ejrh.2015.12.063

Trenberth, K. E., Dai, A., Schrier, G. Van Der, Jones, P. D., Barichivich, J., Briffa, K. R., & Sheffield, J. (2014). *Global warming and changes in drought*. *4*(December 2013), 3–8. https://doi.org/10.1038/NCLIMATE2067

Tseng, Y. (2005). The role of transportation in logistics chain. *Proceedings of the Eastern Asia Society for Transportation Studies*, *5*, 1657–1672.

Türkeş, M., Turp, M., An, T., Ozturk, N., & Kurnaz, M. L. (2020). Water Resources of Turkey. In *Water Resources of Turkey* (Vol. 2). https://doi.org/10.1007/978-3-030-11729-0

Turral, H., Burke, J., Faures, J. M., & Faures, J. M. (2011). Climate change, water and food security. *Rome: Food and Agriculture Organization of the United Nations.*, 204. https://doi.org/ISSN 1020-1203

UNEP. (2013). *Ethiopia's Gibe III Dam: its Potential Impact on Lake Turkana Water Levels (A case study using hydrologic modeling and multi-source satellite data). Nairobi, Kenya: Division of Early Warning and Assessment, United Nations Environment Programme.*

Vaghefi, S. A., Srinivasan, R., Abbaspour, K., Faramarzi, M., & Chen, L. (2018). *Integrated Soil and Water Management: Selected Papers from 2016 International SWAT Conference*. MDPI - Multidisciplinary Digital Publishing Institute.

Van Orshoven, J., Sinclair, S., Giuliani, M., Castelletti, A., Bertoni, F., Micotti, M., & Zaniolo, M. (2018). *Baseline Scenario: Deleverable D2.1.* (Issue 690268).

Veintimilla-Reyes, J., Cattrysse, D., Meyer, A. De, & Orshoven, J. Van. (2016a). Mixed Integer Linear Programming (MILP) approach to deal with spatio-temporal water allocation. *Procedia Engineering*, *162*, 221–229. https://doi.org/10.1016/j.proeng.2016.11.045

Veintimilla-Reyes, J., Cattrysse, D., Meyer, A. De, & Orshoven, J. Van. (2016b). Mixed Integer Linear Programming (MILP) approach to deal with spatio-temporal water allocation. *2nd EWaS International Conference: "Efficient & Sustainable Water Systems Management toward Worth Living Development,"* 1–9.

Veintimilla-Reyes, J., De Meyer, A., Cattrysse, D., & Van Orshoven, J. (2017). A linear programming approach to optimise the management of water in dammed river systems for meeting demands and preventing floods. *Water Science and Technology: Water Supply*.

Veintimilla-Reyes, J., De Meyer, A., Cattrysse, D., & Van Orshoven, J. (2018). A linear programming approach to optimise the management of water in dammed river systems for meeting demands and preventing floods. *Water Science and Technology: Water Supply*, *18*(2), 713–722. https://doi.org/10.2166/ws.2017.144

Veintimilla-Reyes, J., Meyer, A. De, Cattrysse, D., & Orshoven, J. Van. (2018). From Linear Programming Model to Mixed Integer Linear Programming Model for the Simultaneous Optimisation of Water Allocation and Reservoir Location in River Systems. *Proceedings*, *2*(11), 594. https://doi.org/10.3390/proceedings2110594

Vreugdenhil, D. (2018). *NATIONAL PARKS OF ETHIOPIA*. https://www.nationalparks-worldwide.com/ethiopia.htm

Wagner, M., & Kilger, C. (2015). Demand Planning. *Supply Chain Management and Advanced Planning (Third Edition): Concepts, Models, Software and Case Studies*, 139–157. https://doi.org/10.1007/b106298

Wagner, M., & Meyr, H. (2015). Food and Beverages. *Supply Chain Management and Advanced Planning (Third Edition): Concepts, Models, Software and Case Studies*, 139–157. https://doi.org/10.1007/b106298

Walsh, S. J., Page, P. H., McKnight, S. A., Yao, X., & Morrissey, T. P. (2015). A reservoir siting tool for North Carolina: System design & operations for screening and evaluation. *Applied Geography*, *60*, 139–149. https://doi.org/10.1016/j.apgeog.2015.03.015

Wang, T., Fang, G., Xie, X., Liu, Y., & Ma, Z. (2017). A Multi-Dimensional Equilibrium Allocation Model of Water Resources Based on a Groundwater Multiple Loop Iteration Technique. *Water*, *9*(9), 718. https://doi.org/10.3390/w9090718

Wang, Z., Yang, J., Deng, X., & Lan, X. (2015). Optimal Water Resources Allocation under the Constraint of Land Use in the Heihe River Basin of China. *Sustainability*, *7*(2), 1558–1575. https://doi.org/10.3390/su7021558

WHO. (2015). *The right to water*. WHO; World Health Organization. https://www.who.int/gender-equity-rights/knowledge/right-to-water/en/

Winston, W., & Goldberg, J. (1994). Operations research. In *Operations Research* (Issue February). THOMSON. https://doi.org/10.1038/222304c0

World Bank. (2016). *Access to electricity (% of population) | Data*. https://data.worldbank.org/indicator/eg.elc.accs.zs

World Commission on Dams. (2001). Dams and development : a new framework for decision-making : overview of the report by the World Commission on Dams. *Issue Paper (Drylands Programme) ; No. 108*, *December*, 17 p.

Yan, D., Ludwig, F., Huang, H. Q., & Werners, S. E. (2017). Many-objective robust decision making for water allocation under climate change. *Science of the Total Environment*, *607–608*, 294–303. https://doi.org/10.1016/j.scitotenv.2017.06.265

Yates, D., Sieber, J., Purkey, D., & Huber-Lee, A. (2005). WEAP21 - A demand-, priority-, and preference-driven water planning model. Part 1: Model characteristics. *Water International*, *30*(4), 487–500. https://doi.org/10.1080/02508060508691893

Yeomans, J. S., & Gunalay, Y. (2008). Water resource planning under uncertanty using simulation optimization.pdf. *Applied Operation Research*, 286–295.

Yeomans, J. S., & Gunalay, Y. (2009). Using simulation optimization techniques for water resources planning. *Journal of Applied Operational Research*, *1*, 2–14.

Yewhalaw, D., Legesse, W., Van Bortel, W., Gebre-Selassie, S., Kloos, H., Duchateau, L., & Speybroeck, N. (2009). Malaria and water resource development: The case of Gilgel-Gibe hydroelectric dam in Ethiopia. *Malaria Journal*, *8*(1), 1–10. https://doi.org/10.1186/1475-2875-8-21

Zagona, E. A. (2001). RiverWare Model and Analysis Tools for River System Planning and Management. *Water*.

Zhang, C., Chen, X., Li, Y., Ding, W., & Fu, G. (2018). Water-energy-food nexus: Concepts, questions and methodologies. *Journal of Cleaner Production*.

Zhang, Z., Jiang, Y., Zhang, S., Geng, S., Wang, H., & Sang, G. (2014). An adaptive particle swarm optimization algorithm for reservoir operation optimization. *Applied Soft Computing Journal*, *18*, 167–177. https://doi.org/10.1016/j.asoc.2014.01.034

List of publications

Articles in (inter)nationally reviewed academic journals

Veintimilla-Reyes J., De Meyer A., Cattrysse D., Tacuri E., Vanegas P., Cisneros F., Van Orshoven J. Veintimilla Reyes JE. (joint first author), Van Orshoven J. (joint last author) (2019). MILP for Optimizing Water Allocation and Reservoir Location: A Case Study for the Machángara River Basin, Ecuador. Water, 11 (5), Art.No. 1011, doi: 10.3390/w11051011.

Veintimilla-Reyes J., De Meyer A., Cattrysse D., Van Orshoven J. (2018). A linear programming approach to optimise the management of water in dammed river systems for meeting demands and preventing floods. Water Science and Technology-water Supply, 18 (2), Art.No. ws2017144, 713-722. doi: 10.2166/ws.2017.144.

Veintimilla-Reyes J., Vanegas P., Estrella R. (2018). Application of standard web services for the automatic hydrometeorology monitoring, integrating information from diverse sensors using ontologies. ENFOQUE UTE, 9 (1), 34-42. doi: 10.29019/enfoqueute.v9n1.239.

Muñoz L., Medina J., Guillermo J., Veintimilla Reyes JE. (2017). Arquitectura para una red de sensores web basada en SWE (Sensor Web Enablement): Caso de estudio para la implementación en sensores hidrometeorológicos. Maskana, 1 (2016), 129-138.

Veintimilla-Reyes J., Tacuri E., Pino J., Cisneros F. (2016). Análisis y diseño de una red de comunicación para transmitir información de alerta temprana. Caso de estudio: Proyecto de control de inundaciones Bulubulu-Cañar-Naranjal. Revista Tecnológica ESPOL, 29 (1), 184-195.

Veintimilla-Reyes J., Ávila F. (2015). Análisis e implementación de una Infraestructura de Datos Espaciales (IDE). Revista Tecnológica ESPOL, 28 (2), 79-99.

Veintimilla-Reyes J., Cisneros F. (2015). Predicción de Caudales Basados en Redes Neuronales Artificiales (RNA) para Períodos de Tiempo Sub Diarios. Revista Politécnica (Quito), 35 (2), 42-49.

Veintimilla-Reyes J., Capelo P., Cisneros F. (2014). Diseño e implementación de un datalogger para la transmisión de información de sensores remotos de lluvia por medio de una red GSM o GPRS. Revista Tecnológica ESPOL, 27 (2), 55-66.

Veintimilla-Reyes J., Cisneros F. (2014). Redes Neuronales Artificiales (RNA) aplicadas en la predicción de caudales para intervalos de tiempo horarios. Revista Tecnológica ESPOL, 27 (2), 37-49.

Veintimilla-Reyes J., Espinoza M., Cisneros F. (2014). Estudio y selección de una arquitectura orientada a servicios (SOA) que permita la integración de sistemas informáticos legados. Revista Tecnológica ESPOL, 27 (1), 14-21.

Oral or poster presentations at (inter)national scientific conferences

Veintimilla-Reyes J., De Meyer A., Cattrysse D., Van Orshoven J. (2018). From Linear Programming Model to Mixed Integer Linear Programming Model for the Simultaneous Optimisation of Water Allocation and Reservoir Location in River Systems. In: proceedings: vol. 2 (11) (594-594). Presented at the 3rd EWaS International Conference on "Insights on the Water-Energy-Food Nexus", Lefkada Island, Greece, 27 Jun 2018-30 Jun 2018. doi: 10.3390/proceedings2110594.

Veintimilla-Reyes J., Guillermo J., Vanegas P., Estrella R. (2018). SWE sensor integration for controlling remote sensors applied to hidrometeorological sensing. In: Proceedings - 2017 International Conference on Information Systems and Computer Science, INCISCOS 2017: vol. 2017-November (212-216). ISBN: 9781538626443. doi: 10.1109/INCISCOS.2017.30.
Veintimilla Reyes, J., Cattrysse, D., & Van Orshoven, J. (2017). An NFO-LP-model to optimise water allocation in dammed river systems. Communications in Aagricultural and Applied Biological Sciences, 162, 2016.

Veintimilla-Reyes J., Cisneros F., Vanegas P. (2016). Artificial Neural Networks Applied to Flow Prediction: A Use Case for the Tomebamba River. In: Procedia Engineering: vol. 162 (2016) (153-161). Presented at the 2nd International Conference on Efficient and Sustainable Water Systems Management toward Worth Living Development (EWaS), Platanias, greece, 01 Jun 2016-04 Jun 2016. doi: 10.1016/j.proeng.2016.11.031.

Veintimilla-Reyes J., Cattrysse D., De Meyer A., Van Orshoven J. (2016). Mixed Integer Linear Programming (MILP) approach to deal with spatio-temporal water allocation. In: Kanakoudis V., Karatzas G., Keramaris E. (Eds.), Procedia Engineering (Eds.): vol. 162 (Paper No. ID053) (221-229). Presented at the EWaS: Efficient & Sustainable Water Systems Management toward Worth Living Development, Chania-Greece, 01 Jun 2016-04 Jun 2016. doi: 10.1016/j.proeng.2016.11.04